Initially-stressed hyperelastic materials : Modeling, mechanical and numerical analysis of singular problems and identification of residual stress

Fahmi Grine

INSA INSTITUT NATIONAL DES SCIENCES APPLIQUÉES LYON

N d'ordre NNT: 2021LYSEI060

THÈSE de DOCTORAT DE L'UNIVERSITÉ DE LYON

préparée au sein de

l'Institut National des Sciences Appliquées de Lyon

En cotutelle internationale avec

L'École Nationale d'Ingénieurs de Tunis

École Doctorale 162

Mécanique, Énergétique, Génie civil, Acoustique

Spécialité de doctorat

MÉCANIQUE GÉNIE CIVIL

Soutenue publiquement le 29/09/2021 par:

Fahmi Grine

Ingénieur en Mécanique

Initially-stressed hyperelastic materials: modeling, mechanical and numerical analysis of singular problems and identification of residual stress.

Devant le jury composé de:

Martine Ben Amar	Professeure des universités (Sorbonne Université/ENS)	Rapporteur
Stéphane Pagano	Directeur de Recherche CNRS (Université Montpellier 2)	Rapporteur
Evelyne Toussaint	Professeure des universités (Université Clermont Auvergne)	Examinatrice
Frédéric Lebon	Professeur des universités (Université d'Aix-Marseille)	Examinateur
Makrem Arfaoui	Maitre de Conférences (ENI de Tunis)	Directeur
Yves Renard	Professeur des universités (INSA de Lyon)	Directeur
Giuseppe Saccomandi	Professeur des universités (Università di Perugia)	Encadrant
Mohamed Trifa	Maitre Assistant (ENI de Tunis)	Encadrant

Département FEDORA – INSA Lyon - Ecoles Doctorales – Quinquennal 2016-2020

SIGLE	ECOLE DOCTORALE	NOM ET COORDONNEES DU RESPONSABLE
CHIMIE	**CHIMIE DE LYON** **http://www.edchimie-lyon.fr** Sec. : Renée EL MELHEM Bât. Blaise PASCAL, 3e étage **secretariat@edchimie-lyon.fr** INSA : R. GOURDON	M. Stéphane DANIELE Institut de recherches sur la catalyse et l'environnement de Lyon IRCELYON-UMR 5256 Équipe CDFA 2 Avenue Albert EINSTEIN 69 626 Villeurbanne CEDEX **directeur@edchimie-lyon.fr**
E.E.A.	**ÉLECTRONIQUE, ÉLECTROTECHNIQUE, AUTOMATIQUE** **http://edeea.ec-lyon.fr** Sec. : M.C. HAVGOUDOUKIAN **ecole-doctorale.eea@ec-lyon.fr**	M. Gérard SCORLETTI École Centrale de Lyon 36 Avenue Guy DE COLLONGUE 69 134 Écully Tél : 04.72.18.60.97 Fax 04.78.43.37.17 **gerard.scorletti@ec-lyon.fr**
E2M2	**ÉVOLUTION, ÉCOSYSTÈME, MICROBIOLOGIE, MODÉLISATION** **http://e2m2.universite-lyon.fr** Sec. : Sylvie ROBERJOT Bât. Atrium, UCB Lyon 1 Tél : 04.72.44.83.62 INSA : H. CHARLES **secretariat.e2m2@univ-lyon1.fr**	M. Philippe NORMAND UMR 5557 Lab. d'Ecologie Microbienne Université Claude Bernard Lyon 1 Bâtiment Mendel 43, boulevard du 11 Novembre 1918 69 622 Villeurbanne CEDEX **philippe.normand@univ-lyon1.fr**
EDISS	**INTERDISCIPLINAIRE SCIENCES-SANTÉ** **http://www.ediss-lyon.fr** Sec. : Sylvie ROBERJOT Bât. Atrium, UCB Lyon 1 Tél : 04.72.44.83.62 INSA : M. LAGARDE **secretariat.ediss@univ-lyon1.fr**	Mme Emmanuelle CANET-SOULAS INSERM U1060, CarMeN lab, Univ. Lyon 1 Bâtiment IMBL 11 Avenue Jean CAPELLE INSA de Lyon 69 621 Villeurbanne Tél : 04.72.68.49.09 Fax : 04.72.68.49.16 **emmanuelle.canet@univ-lyon1.fr**
INFOMATHS	**INFORMATIQUE ET MATHÉMATIQUES** **http://edinfomaths.universite-lyon.fr** Sec. : Renée EL MELHEM Bât. Blaise PASCAL, 3e étage Tél : 04.72.43.80.46 **infomaths@univ-lyon1.fr**	M. Luca ZAMBONI Bât. Braconnier 43 Boulevard du 11 novembre 1918 69 622 Villeurbanne CEDEX Tél : 04.26.23.45.52 **zamboni@maths.univ-lyon1.fr**
Matériaux	**MATÉRIAUX DE LYON** **http://ed34.universite-lyon.fr** Sec. : Stéphanie CAUVIN Tél : 04.72.43.71.70 Bât. Direction **ed.materiaux@insa-lyon.fr**	M. Jean-Yves BUFFIÈRE INSA de Lyon MATEIS - Bât. Saint-Exupéry 7 Avenue Jean CAPELLE 69 621 Villeurbanne CEDEX Tél : 04.72.43.71.70 Fax : 04.72.43.85.28 **jean-yves.buffiere@insa-lyon.fr**
MEGA	**MÉCANIQUE, ÉNERGÉTIQUE, GÉNIE CIVIL, ACOUSTIQUE** **http://edmega.universite-lyon.fr** Sec. : Stéphanie CAUVIN Tél : 04.72.43.71.70 Bât. Direction **mega@insa-lyon.fr**	M. Jocelyn BONJOUR INSA de Lyon Laboratoire CETHIL Bâtiment Sadi-Carnot 9, rue de la Physique 69 621 Villeurbanne CEDEX **jocelyn.bonjour@insa-lyon.fr**
ScSo	**ScSo*** **http://ed483.univ-lyon2.fr** Sec. : Viviane POLSINELLI Brigitte DUBOIS INSA : J.Y. TOUSSAINT Tél : 04.78.69.72.76 **viviane.polsinelli@univ-lyon2.fr**	M. Christian MONTES Université Lyon 2 86 Rue Pasteur 69 365 Lyon CEDEX 07 **christian.montes@univ-lyon2.fr**

*ScSo : Histoire, Géographie, Aménagement, Urbanisme, Archéologie, Science politique, Sociologie, Anthropologie

Acknowledgments

I would like to thank my advisors, Professors Yves Renard (LAMCOS) and Makrem Arfaoui (LMAI) at ENIT-UTM and also my tutors Giuseppe Saccomandi (University of Perugia) and Mr Mohamed Trifa (LMAI), for their guiding advices and support on this project.

I would also express my gratitude for both organizations ASENIT and INSAVALOR also the Tunisian and Italian governments for their financial support within the different granted scholarships. My thanks goes also to the different institution ENIT, INSA Lyon and University of Perugia for all the assistance and words of encouragements which have positively impacted this PhD.

I will not forget to thank all the personnel, students and PhD students of the mechanical department of ENIT, ICJ-INSA-Lyon, LAMCOS and the university of Perugia for the pleasant time I spent with them. The Members of the Jury are also acknowledged. Their comments help to improve this PhD research Thesis.

Abstract

The presence of initial stress in natural and manufactured materials and structures has been known for a long term and it is experimentally well attested in diverse scopes from biomechanics, geophysics, to welded structures and manufacturing. This internal stress has a substantial effect on material and structural behaviour and can be the origin of heterogeneous and anisotropic behaviour. The modelling of initially-stressed materials goes back to Cauchy's work on the classical theory of linear elasticity in its most general form, considering the effect of an initial stress of arbitrary origin. This thesis aims to contribute to the development of different formulations and theoretical results in the theory of initially-stressed hyperelasticity. The development of constitutive models for initially stressed hyperelastic materials have permitted to identify the kind of anisotropy generated by the initial stress field based on the analogy with the constitutive formulation for fibrous materials. The exploitation of this analogy for linear transverse isotropic elasticity has provided some insight into the use of anisotropy and fibre orientation to design some elastic machines by coupling different deformation modes in a continuum boundary value problem. In addition, the identification of material parameters of an initially stressed linear elastic model and the residual stress are addressed and an analysis of the different parameters influencing the quality of the reconstructed fields is carried out. Focusing on singular problems, two boundary value problems are considered and analyzed. The first problem is dedicated to the rigidity contrast (discontinuity) influence on the asymptotic mechanical field near a crack tip subjected to an antiplane transformation. Whereas in the second one, a particular generalization of the three-dimensional Linear Elastic Fracture Mechanics (LEFM) to a model of initially-stressed hyperelastic materials is developed. A numerical analysis to the prior problem using an XFEM formulation is realized and a convergence-stability study is achieved.

List of Figures

List of Tables

Contents

General introduction

The presence of initial stress in natural and manufactured materials and structures has been known for a long time and it is experimentally well attested in diverse scopes, from biomechanics, plants, geophysics, geomechanics, to welded structures and manufacturing. By initial stress, one means stress field verifying the equilibrium equation in the reference configuration with a no homogeneous static boundary condition (no zero surface loads) and/or a body force.. Here, the term initial stress should be used in its general sense regardless of its origin. When this initial stress is accompanied by a pre-strain due to the applied load in the reference configuration, the term pre-stress is usually used. In the case of zero applied loads, the term residual stress is commonly adopted according to the definition of [Hoger 1986]. This internal stress has a substantial effect on material and structural behaviour. It affects strength, fatigue life, and dimensional stability and can be the origin of inhomogeneous and anisotropic behaviour. Perhaps the most known initially stressed bodies due to gravity are the Earth and historical buildings from the Babylonians, Mayas, Egyptians, Romans, and other civilizations. In his book "Imaging the Cheops Pyramid" [Bui 2011], for example, H.D. Bui analyzed the effect of this internal stress on the presence of cracks near the King's Chamber of the Cheops Pyramid. In geophysics and during earthquakes, initial stress, developed below the Earth's surface, is generated by gravity and processes such as burying, heating, cooling, and prior tectonic events and its rotations along strike can generate significant changes in rupture speed as well as distinctive patterns in slip distribution and peak ground motion [Dunham 2003, Duan 2010]. For arteries, residual stress, a consequence of growth and remodelling, reduces the stress gradient distribution and decreases the peak stress [Cardamone 2009]. It prevents dissection and potential rupture of the aorta, which is a serious cardio-vascular disease [Humphrey 2012, Wang 2017]. In multi-network polymers, scission and reformation of networks give rise to initial stress [Rajagopal 1992, Wineman 1990, Huntley 1996]. Through all these problems, the initial stress can have detrimental and/or positive effects on the materials and structures, which need to be better understood, determined and quantified. It is the challenge of this thesis concerned with the modelling and the identification of initially stressed hyperelastic behaviour with the analysis of some continuum and singular boundary value problems.

Following Truesdell [Truesdell 1952], there are three approaches, from the born of continuum modelling due to Euler, Cauchy and Green (see [Truesdell 1952]), to model initially

stressed elastic material behaviour. Recall that these initial stresses are caused by microstructural misfits and rearrangement of matter, which can occur as a result of plastic deformations (for example, in metals), thermal processes (for example, rapid solidification in glass), or growth within biological tissues. The first method focuses on the modelling of the entire process, from the initial unstressed natural state, that creates initial and service stresses in the body. This methodology is popular in the manufacturing scientific community, particularly for modeling metallic products fabrication and life service. Nevertheless, the existence of this hypnotically initial unstressed natural state is a theoretical assumption and all materials and structures contain initial stresses. Thus, the second approach aims to model material behaviour from the initial stressed state where the stress-free configuration is not known. Indeed, the removal of this initial stress by cutting the body is not feasible without destroying the material continuity. Nonetheless, this stress-free configuration is assumed to exist, which is the basis of the concept of natural configuration as discussed by [Rajagopal 1998] by assuming a multiplicative decomposition of the deformation gradient, from the unstressed free configuration, into two contributions: a residual deformation describing the inelastic change of shape induced by the microstructural rearrangement of the matter and a deformation accounting for the elastic deformation of the body [Lee 1969, Haupt 1992, Rodriguez 1994]. Thus, the material response is governed by the deformation from the initially stressed configuration to the current one and the residual deformation from the unstressed configuration to the initially stressed one. This stress-free configuration is also called the virtual stress-free state by Hoger and her co-workers, who developed a constitutive representation from the stressed reference configuration to the current one by inverting the constitutive model response between the virtual unstressed configuration and the stressed one [Hoger 1997, Johnson 1995, Johnson 1998, Saravanan 2008, Agosti 2018]. To do this, challenging calculations are needed and rarely yield an analytic explicit model, unless great simplifications are assumed. The main drawback of the methodology described below is that it requires prior information about the natural stress-free configuration, which is not always physically accessible. Indeed, from an experimental standpoint, it would necessitate infinite cuts to relieve all initial stress [Chuong 1986, Ciarletta 2016a]. Although this technique has been successful in simple system models [Amar 2005]. It is ineffective when evaluating the effect of a generic condition of initial stress on the material response.

In the third approach, the problem of the choice of a virtual stress-free configuration is over-

come by developing a constitutive theory that includes explicitly the spatial distribution of initial stresses. This is done by the initially-stressed theory, which goes back to Cauchy's work on the classical theory of elasticity in its most general form, linking stress as a function of deformation and an initial stress of arbitrary origin (see [Truesdell 2012]). Another way to define initially stressed elasticity was given by Green [Truesdell 2012] in which stress is a derivative with respect to a deformation of a strain energy function of a deformation and an initial stress. These two methods of defining elasticity with initial stress were misunderstood, and the nineteenth-century scientific community reported them in a hazy or even erroneous manner, as pointed by [Truesdell 1952], who presented the proper theory long later with other authors [Truesdell 1952, Gurtin 1982, Biot 1965]. Early other contributors who made a significant contribution to the field including [Hadamard 1903, Love 2013]...

In the context of modern continuum mechanics [Truesdell 2004], it was only after the paper [Hoger 1986] on the determination of residual stress in an elastic body that the theory of elasticity with initial stress received considerable attention. This paper came after another fundamental paper [Hoger 1985] where it was shown that the conditions of the equilibrium equation and boundary condition of zero traction satisfied by the residual stress, coupled with those implied by material symmetry [Truesdell 2012, Coleman 1964], restrict the class of possible residual stresses in an elastic body. The work of Anne Hoger in this scope is so powerful that it touches all the aspects of modelling and the identification of initially stressed hyperelastic materials. The first such contribution is made in [Hoger 1993a, Johnson 1995], assuming the existence of hyperelastic potential depending on both the deformation and the initial stress, despite the fact that this hasn't always been properly acknowledged. The question of the uniqueness of solution for boundary value problems associated with initially stressed hyperelastic models is also addressed by analyzing the tangent elasticity tensors in different configurations [Hoger 1993b, Hoger 1994, Johnson 1993]. In fact, the resolution of the boundary value problems depends essentially on the form of the strain energy. Since no restrictions have been imposed on the nature of this function, it may be questionable whether the predicted response caused by the constitutive behaviour is physically reasonable and whether the solution to the initial stressed finite elasticity problem exists and is unique. This is the so-called Truesdell-Haupt problem and is concerned with stability, thermodynamics, and some mathematical conditions. The most known requirements for strain energy are those of Baker-Ericksen inequality, the Coleman-Noll inequality, and ellipticity condition, polyconvexity condition,

etc [Ogden 1997]. To this end, some restrictions have been developed to ensure reasonable physical response of initially stressed material and the existence of minimizers: initial stress compatibility (ISC), initial stress symmetry (ISS) and initial stress reference independence (ISRI) [Shams 2011, Gower 2015, Gower 2017, Riccobelli 2019]. Recall that restrictions on constitutive models are probably only those arising from frame indifference and material symmetry, as was mentioned in [Saccomandi 2004].

For the development of constitutive laws for initially stressed elastic materials, the determination of the model's parameters and the initial stress are of paramount importance. This is an inverse problem as mentioned in [Bui 2007]. From an experimental viewpoint, non-invasive techniques like X-ray diffraction, semi-invasive techniques like incremental center hole drilling and deep hole drilling, and fully destructive methods like slotting, contour, and inherent strain can all be used to determine the residual stress at surface and/or body points. Due to the cost, time commitment, and dispersion of the measured data, only discrete points of stress in sections are normally measured. In initial stressed linear elasticity theory, all the constitutive models of the first half of the twentieth century, presented in [ZP 1971], have the same algebraic structure as the model of [Hoger 1986]. This latter model depends on an unknown tangent elasticity tensor function of the initial stress. Different forms and identification methodologies of this elasticity tensor have been proposed [Hoger 1986, Man 1987, Man 1994]. A general form was proposed recently in [Gower 2015, Gower 2017]. The identification of the initial stress (or residual stress) can be done by an analytical (or semi-) method determined from its equilibrium equation and its boundary conditions for specific geometries [Hoger 1986, Sburlati 1992, Faghidian 2014]. In addition to its practical importance, determining residual stresses raises a number of difficult mathematical issues. In fact, several forms of the inverse problem of unique residual stress determination were investigated, utilizing several model equations for residual stress and various methods of measurements. The central questions here are those of stability and uniqueness [Man 1994, Rachele 2003, Ivanov 2005, Isakov 2007, Isakov 2008]. In large deformations and for initially residually hyperelastic materials, only the reconstruction of the residual stress is addressed in [Gou 2014] for a specific geometry and a particular form of the residual stress function.

Suppose now that the constitutive law of an initially stressed hyperelastic material is explicitly known and its parameters are determined. Thus, boundary value problems can

be formulated to analyze the effect of this initial stress on mechanical fields and material symmetry. To this end, the semi-inverse method [Truesdell 1952], which is based on heuristic ad hoc assumptions and ansatzes on the analytical form of elastostatic fields, is generally used. The effect of initial stress (and residual stress) on elastostatic fields has been analyzed theoretically for continuum problems by [Merodio 2013a, Merodio 2016, Ciarletta 2016a, Ciarletta 2016b, Gower 2015, Gower 2017, Riccobelli 2018, Agosti 2018, Du 2018, Du 2019a, Du 2019b, Liu 2020a, Liu 2020b, Mukherjee 2021, Melnikov 2021]. To our knowledge, the singular boundary value problem associated with initially stressed hyperelastic cracked solids has not been theoretically analyzed.

After this narrative overview to describe the scientific context of our work, it is now necessary to fix the objective of this thesis concerned with the modelling and the identification of initially stressed hyperelastic behaviour with the analysis of some continuum and singular boundary value problems. First, the modelling of an initially stressed hyperelastic material should be concisely unified and summarized based on the work of [Gower 2015, Gower 2017] and new results and interpretations will be presented, particularly the link between anisotropy and the initial stress effect. Secondly, the effect of anisotropic behaviour should be analyzed through a continuum and singular problems. Thirdly, the identification of the general initially stressed linear elastic model presented by [Gower 2015, Gower 2017] should be addressed theoretically and numerically. Finally, asymptotic and X-FEM analysis should be done for an initially stressed hyperelastic three-dimensional cracked solid.

The thesis plan will be presented in the following:
The first chapter is an overview on the finite transformation scope.Focusing on hyperelastic behaviour, a brief recall is made for the mathematical tools for the modeling of such mechanical behaviour.

The second chapter is dedicated for the initially-stressed hyperelastic materials modeling. The first part of this chapter is like a survey on the different approaches to model the initial stress on hyperelastic structures within two classes of materials: initially stressed and initially-strained materials. Multiple theoretical formulations and results are revisited in a different way. On the other hand, the second chapter presents the most explicit general model for an initially-stressed linear elastic material which is isotropic in the natural con-

figuration, and a generalization of the Airy stress function is performed. Also, this chapter discussed the anisotropy generated by the initial stress presence based on an analogy with fibrous materials.

Since the initial stress can be a source of anisotropy, then by considering a simple boundary value problem for an isotropic transverse cylinder a new kinematic coupling is discussed in the third chapter. The presence of fibers permits a coupling between the axial shear and the fibers rotation. Such coupling is analyzed in order to exploit it for the design of new devices that we have called elastic machines. In the same chapter, an analogous coupling is obtained using a simple form of initial stress field.

The fourth chapter is devoted to a set of inverse problems in the case of initially stressed linear elastic materials. This chapter presents multiple stability estimates. Focusing not only on the theoretical results, the fourth chapter provides an efficient direct approach for the identification of the residual stress field and the material parameters. Exploiting multiple perturbed displacement fields, a parametric analysis is performed to point out the influence of the different variants of this approach on the quality of the identified fields.

The fifth chapter discussed the influence of a constant initial stress field on a singular problem of a cracked hyperelastic material. An asymptotic analysis is made for the different mechanical fields near the crack tip considering a three dimensional transformation. Focusing on the plane problem, a numerical analysis for the singular problem using the XFEM method is done for different choices of elements formulations and crack-tip enrichment functions.

The idea behind the last chapter is the same as the third one. In fact, the final chapter treats an antiplane transformation within hyperelastic bimaterial. This chapter gives an asymptotic analysis on the rigidity gap and the geometrical configuration on the different mechanical fields near the crack tip. An analogy with the case of initially stressed materials is pointed out again.

Chapter 1

Introduction to finite elasticity

Contents

1.1 Kinematics

Let consider a body which occupies initially a reference configuration $\mathcal{B}_0$. The prior configuration is a collection of material particles whose $\vec{X} = (X_1, X_2, X_3)$ is the position vector in the undeformed configuration . The body is transformed at an instant t into a new

deformed configuration $\mathcal{B}_t$ where the position vector of the generic material particle is denoted $\vec{x} = (x_1, x_2, x_3)$ as it is illustrated in figure (1.1). This motion can be described by a mapping vector function χ and it can be expressed mathematically as:

$$\chi(\vec{X}, t) = \vec{X} + \vec{u}(\vec{X}, t) \tag{1.1}$$

$\vec{u}$ is the displacement field which characterize the deformation χ between the initial and the current configurations. Each point of the reference configuration $\mathcal{B}_0$ has a unique image in the current configuration $\mathcal{B}_t$ and vice-versa. Thus the deformation χ must be a one-to-one function (i.e bijective vectorial function). It is essential to distinguish the fields based on the configuration where they are defined. Since, the deformation function ϕ is defined on the undeformed configuration, such a kinematic approach is called a material or Lagrangian description. Although, when it is referred to the current configuration, then it is called a spatial or Eulerian description.

1.1.1 Deformation gradient

For the sake of local behaviour studying, the mapping function must be a smooth function and have suitable differentiability properties. Then, the deformation gradient field can be defined as:

$$\boldsymbol{F}(\vec{X}, t) = \mathrm{Grad}\chi(\vec{X}, t) = \mathbf{1} + \boldsymbol{H}, \quad \boldsymbol{H} = \mathrm{Grad}\vec{u}, \quad [F_{ij}] = \frac{\partial x_i}{\partial X_j}, \tag{1.2}$$

where $\mathbf{1}$ denotes the identity tensor and Grad is the gradient operator relative to the coordinates of the undeformed configuration. The deformation gradient tensor must avoid the singular values for the local invertibility of the mapping function. Now, we can similarly define the inverse deformation gradient tensor as:

$$\boldsymbol{F}^{-1}(\vec{X}, t) = \mathrm{grad}\chi(\vec{X}, t), \qquad [F^{-1}_{ij}] = \frac{\partial X_i}{\partial x_j}, \tag{1.3}$$

with grad is the gradient operator relative to the coordinates in the current configuration. In the following, the dependence on the time variable will be omitted unless it is necessary. The deformation gradient plays an important role in the finite elasticity formulation since it relies the transportation of an infinitesimal vector in the reference configuration to the

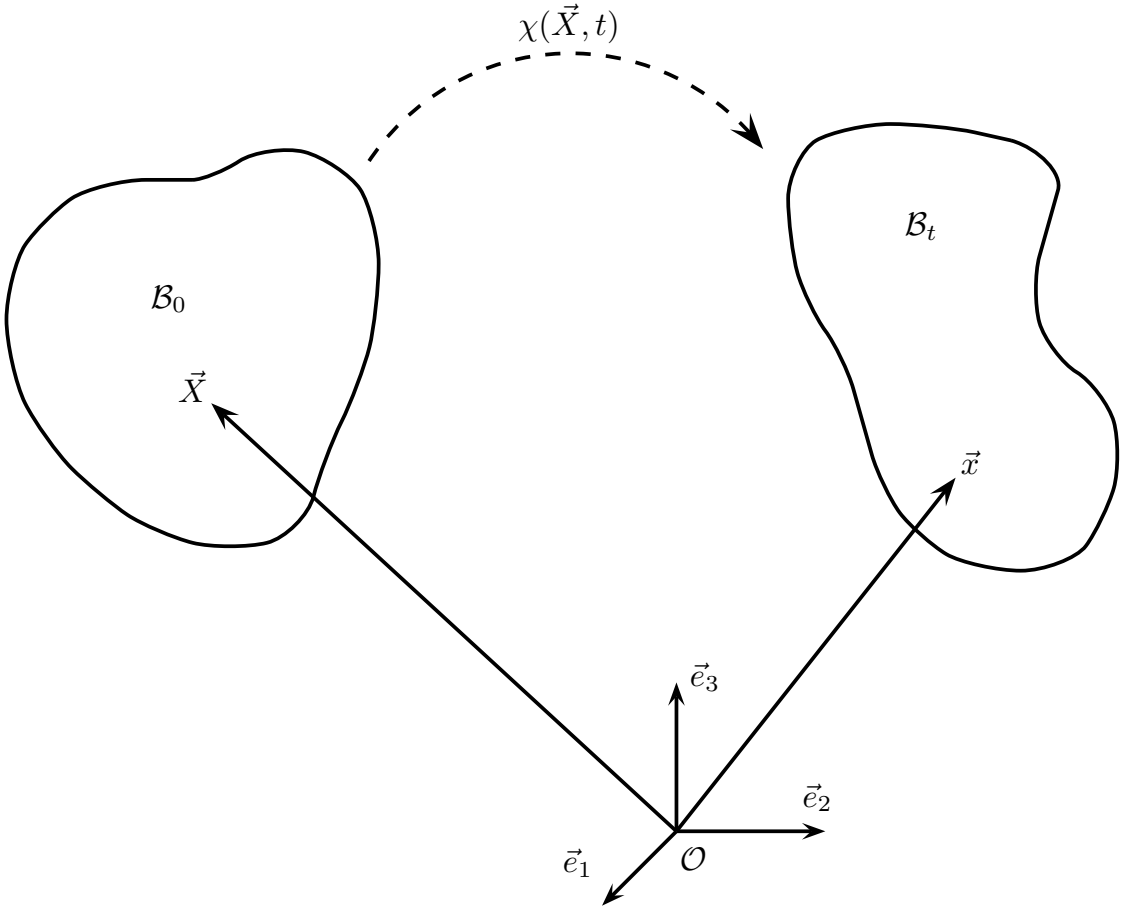

Figure 1.1: The reference and the current configurations

corresponding one in the current configuration in the following way:

$$d\vec{x} = \boldsymbol{F} d\vec{X} \tag{1.4}$$

Exploiting the bijectivity of the deformation function, the invertibility of the deformation gradient tensor is ensured and it can be considered as a point-to-point tensor relating two different configurations. Using the relation (2.4), with some easy algebraic manipulation, an information can be derived about the volume change and hence a relation between the infinitesimal volume respectively in the material and spatial configurations, so we can

write:

$$J = det(\boldsymbol{F}) = \frac{dv}{dV}, \tag{1.5}$$

with *det* is the determinant operator for second order tensors. Since the infinitesimal volume is a positive quantity, consequently a necessary condition that has to be satisfied by the deformation gradient tensor is:

$$J > 0. \tag{1.6}$$

J is also called the jacobian. As it is explained figure (1.2), another relation involving $\boldsymbol{F}$

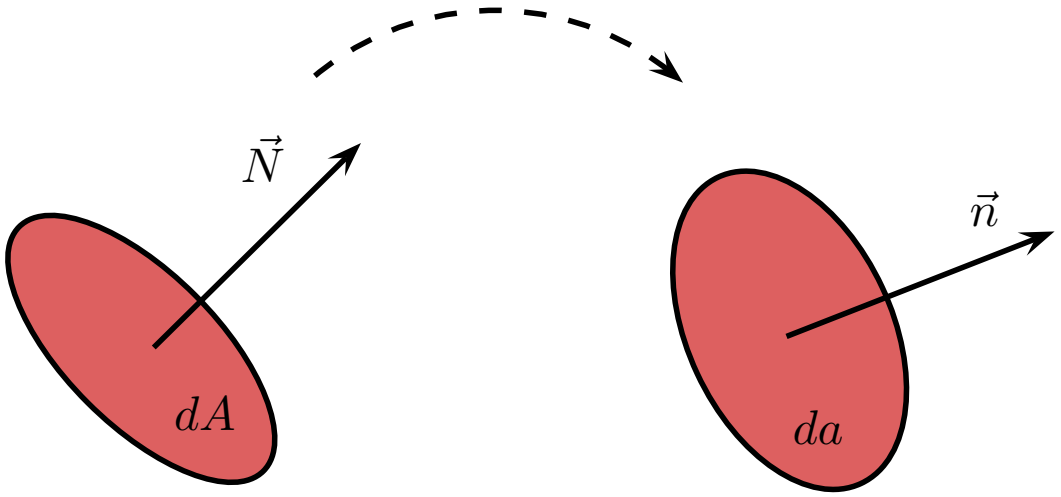

Figure 1.2: Deformation of an infinitesimal element of surface

can be obtained relying the surface element in the initial configuration to the corresponding surface element in the current configuration (Nanson formula) :

$$\vec{n}da = J\boldsymbol{F}^{-T}\vec{N}dA. \tag{1.7}$$

Returning to the point of volume change, a considered deformation can be splitted into volumetric and isochoric or distortional parts. Hence, the gradient deformation tensor can be decomposed as:

$$\boldsymbol{F} = \tilde{\boldsymbol{F}}\boldsymbol{F}^{v} = \boldsymbol{F}^{v}\tilde{\boldsymbol{F}} \tag{1.8}$$

where the isochoric part verifies:

$$\det(\tilde{\boldsymbol{F}}) = 1 \tag{1.9}$$

and they can be expressed in function of the original deformation gradient tensor like:

$$\tilde{\boldsymbol{F}} = J^{-\frac{1}{3}}\boldsymbol{F}, \quad \boldsymbol{F}^{v} = J^{\frac{1}{3}}\mathbf{1}. \tag{1.10}$$

The prior two equations hold in 2D space by replacing "3" by "2". Such decomposition is essential in material modeling to distinguish the effect of every part of the deformation especially when we are dealing with nearly-incompressible materials.

1.1.2 Polar decomposition

The polar decomposition has a great utility in the continuum mechanics. Such result is the decomposing of the gradient deformation tensor into a stretch tensor and a rotation one. It can be expressed mathematically in the reference configuration as:

$$\boldsymbol{F} = \boldsymbol{R}\boldsymbol{U}, \tag{1.11}$$

where $\boldsymbol{R}$ is an orthogonal tensor i.e $\boldsymbol{R}\boldsymbol{R}^T = \boldsymbol{R}^T\boldsymbol{R} = \mathbf{1}$ and it represents the rotation tensor. Whereas $\boldsymbol{U}$ is a definite symmetric tensor and it is usually called the material stretch tensor (or the right stretch tensor). equivalently, the polar decomposition has the following form in the current configuration:

$$\boldsymbol{F} = \boldsymbol{V}\boldsymbol{R}, \tag{1.12}$$

with $\boldsymbol{V}$ is a definite symmetric tensor and it can be regarded as the spatial stretch tensor (or the left stretch tensor). Since $\boldsymbol{U}$ and $\boldsymbol{V}$ are both symmetric tensors, then using the spectral theorem, it can be derived that they share the same principal values. Consequently, the two stretch tensor can be presented in theirs following spectral forms:

$$\boldsymbol{U} = \sum_{i=1}^{3} \lambda_i \vec{u}^{(i)} \otimes \vec{u}^{(i)}, \quad \boldsymbol{V} = \sum_{i=1}^{3} \lambda_i \vec{v}^{(i)} \otimes \vec{v}^{(i)}, \tag{1.13}$$

and for the rotation tensor:

$$\boldsymbol{R} = \sum_{i=1}^{3} \vec{v}^{(i)} \otimes \vec{u}^{(i)}, \tag{1.14}$$

where $\{\lambda_i, \quad i = 1..3\}$ are the common principal values (or principal stretch), while $\{\vec{u}^{(i)}, \quad i = 1..3\}$ and $\{\vec{v}^{(i)}, \quad i = 1..3\}$ are respectively the principal unitary orthogonal vectors for $\boldsymbol{U}$ and $\boldsymbol{V}$ i.e $\vec{u}^{(i)}.\vec{u}^{(j)} = \vec{v}^{(i)}.\vec{v}^{(j)} = \delta_{ij}$. For the sake of a brief demonstration of the polar decomposition theorem, let us consider a second order tensor $\boldsymbol{A}$. The demonstration will be restricted to the case of invertible tensors. Using the singular spectral theorem (the generalization of the spectral theorem), the tensor $\boldsymbol{A}$ can be decomposed as the following:

$$\boldsymbol{A} = \tilde{\boldsymbol{U}}\boldsymbol{\Sigma}\tilde{\boldsymbol{V}}^T, \tag{1.15}$$

where $\tilde{\boldsymbol{U}}$ and $\tilde{\boldsymbol{V}}$ are both orthogonal unitary tensors i.e $\tilde{\boldsymbol{U}}\tilde{\boldsymbol{U}}^T = \tilde{\boldsymbol{V}}\tilde{\boldsymbol{V}}^T = \boldsymbol{1}$, and $\boldsymbol{\Sigma}$ is an invertible diagonal second order tensor. This decomposition is unique because $\boldsymbol{A}$ is invertible. Then, it can be derived:

$$\boldsymbol{A}\boldsymbol{A}^T = \tilde{\boldsymbol{U}}\boldsymbol{\Sigma}\boldsymbol{\Sigma}^T\tilde{\boldsymbol{U}}^T, \quad \boldsymbol{A}^T\boldsymbol{A} = \tilde{\boldsymbol{V}}\boldsymbol{\Sigma}^T\boldsymbol{\Sigma}\tilde{\boldsymbol{V}}^T. \tag{1.16}$$

Then using the above equations, we can rewrite the tensor $\boldsymbol{A}$ as:

$$\boldsymbol{A} = \boldsymbol{A}(\boldsymbol{A}^T\boldsymbol{A})^{-\frac{1}{2}}(\boldsymbol{A}^T\boldsymbol{A})^{\frac{1}{2}} = (\boldsymbol{A}\boldsymbol{A}^T)^{\frac{1}{2}}(\boldsymbol{A}\boldsymbol{A}^T)^{-\frac{1}{2}}\boldsymbol{A} \tag{1.17}$$

Hence, it is easy to derive that:

$$\boldsymbol{A}(\boldsymbol{A}^T\boldsymbol{A})^{-\frac{1}{2}} = (\boldsymbol{A}\boldsymbol{A}^T)^{-\frac{1}{2}}\boldsymbol{A} \tag{1.18}$$

is a unitary orthogonal tensor which represents the rotation tensor, while $(\boldsymbol{A}^T\boldsymbol{A})^{\frac{1}{2}}$ and $(\boldsymbol{A}\boldsymbol{A}^T)^{\frac{1}{2}}$ denote respectively the right and left stretch tensors. The unicity of the polar decomposition is inherited by the unicity of the singular-value decomposition in the case of invertible tensors.

1.1.3 Incompressibility

The incompressibility is a material behaviour property that can be defined by the aptitude of accepting only an isochoric deformations i.e $J = 1$. In other words, the incompressibility characterizes the non changing in volume when the material is under a prescribed deformation. Such property is ensured by the presence of pressure force inside the material resisting the volume change. The rubber-like materials and the tissues in biomechanics are usually considered as incompressible materials. But, sometimes this hypothesis is relaxed with an asymptotic expansion in the stress-strain law which leads to the construction of the class of quasi-incompressible materials.

1.1.4 Strain

To study the shape change of a considered body, defining a measure of deformation is necessary. The deformation tensors serve to analyse the length and angle variation. To clear up this point let consider two infinitesimal material vectors $\delta\vec{X}_1$ and $\delta\vec{X}_2$ which are transformed respectively in the current configuration to $\delta\vec{x}_1$ and $\delta\vec{x}_2$. Then the stretch or the length change of the both considered infinitesimal vectors defined on the undeformed configuration can be calculated as:

$$||\delta\vec{x}_i||^2 = \delta\vec{X}_i \boldsymbol{C} \delta\vec{X}_i, \quad i \in \{1, 2\} \tag{1.19}$$

where $\boldsymbol{C}$ is called the right Cauchy-Green tensor and its is defined as:

$$\boldsymbol{C} = \boldsymbol{F}^T \boldsymbol{F} \tag{1.20}$$

We can proceed inversely, similarly to the above calculation, to obtain:

$$||\delta\vec{X}_i||^2 = \delta\vec{x}_i \boldsymbol{B} \delta\vec{x}_i, \quad i \in \{1, 2\} \tag{1.21}$$

where $\boldsymbol{B}$ is called the left Cauchy-Green tensor and it is mathematically expressed as:

$$\boldsymbol{B} = \boldsymbol{F}\boldsymbol{F}^T \tag{1.22}$$

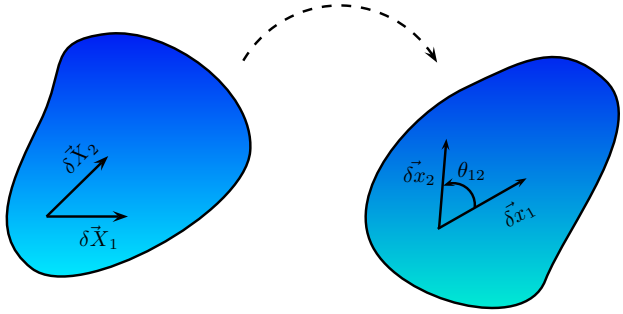

Figure 1.3: Transporting of infinitesimal vectors from the initial configuration to the current one

Whereas for the angle change (see figure (1.3)), we can exploit the scalar product to obtain:

$$\cos(\theta_{12}) = \frac{1}{\sqrt{\delta\vec{X}_1.\boldsymbol{C}.\delta\vec{X}_1}\sqrt{\delta\vec{X}_2.\boldsymbol{C}.\delta\vec{X}_2}}\delta\vec{X}_1\boldsymbol{C}\delta\vec{X}_2 \tag{1.23}$$

with θ_{12} denotes the angle between the two deformed infinitesimal vectors in the current configuration. Exploiting the polar decomposition of the deformation gradient $\boldsymbol{F}$, the left and right Cauchy-Green tensors can be rewritten like:

$$\boldsymbol{B} = \boldsymbol{V}^2, \quad \boldsymbol{C} = \boldsymbol{U}^2 \tag{1.24}$$

Therefore $\boldsymbol{B}$ and $\boldsymbol{V}$ are two measures of deformation in the spatial configuration $\mathcal{B}_t$ while $\boldsymbol{C}$ and $\boldsymbol{U}$ represents two measures of deformation defined on the material configuration $\mathcal{B}_0$. Using (2.11-2.14) and (2.24), it is easy to derive that both the left and right Cauchy-Green tensors have the same principal values and which leads to:

$$\boldsymbol{C} = \sum_{i=1}^{3} \lambda_i^2 \vec{u}^{(i)} \otimes \vec{u}^{(i)}, \quad \boldsymbol{B} = \sum_{i=1}^{3} \lambda_i^2 \vec{v}^{(i)} \otimes \vec{v}^{(i)} \tag{1.25}$$

The Cauchy-Green and both of the stretch tensors represent the basis elements for the definitions of the different class of deformation tensors. For example, the Green-Lagrange tensor $\boldsymbol{E}$ can be defined in $\mathcal{B}_0$ as:

$$\boldsymbol{E} = \frac{1}{2}(\boldsymbol{C} - \boldsymbol{1}) = \frac{1}{2}(\boldsymbol{F}^T\boldsymbol{F} - \boldsymbol{1}) \tag{1.26}$$

Similarly, the Euler-Almansi tensor is defined by:

$$\mathcal{A} = \frac{1}{2}(\mathbf{1} - \boldsymbol{B}^{-1}) = \boldsymbol{F}^{-T}\boldsymbol{E}\boldsymbol{F}^{-1} \tag{1.27}$$

Also, using the right stretch tensor $\boldsymbol{U}$ we can define the class of Lagrangian strain tensor by:

$$\begin{cases} \boldsymbol{E}^{(m)} & = \frac{1}{m}(\boldsymbol{U}^m - \mathbf{1}), \quad m \in \mathbb{N}^* \\ \boldsymbol{E}^{(0)} & = ln(\boldsymbol{U}), \quad m = 0. \end{cases} \tag{1.28}$$

1.2 Stress and equilibrium equations

If we consider a material particle with a surface element da in the spatial configuration, then the force $d\vec{F}$ associated to the contact with the adjacent rest of the material (cohesion internal force) or related to the loading devices can be expressed in the spatial configuration as:

$$d\vec{F} = \vec{t}da, \tag{1.29}$$

where $\vec{t}$ is called the traction force vector, and it is related to the Cauchy stress tensor $\boldsymbol{\sigma}$ in the following way:

$$\vec{t} = \boldsymbol{\sigma}\vec{n} \tag{1.30}$$

where $\vec{n}$ denotes the unit normal vector for the surface element da. In the case of small deformations, the material and spatial configuration are the same. Although, in the case of large deformations, it is necessary to transform the Cauchy stress tensor and the equilibrium equations to the reference configuration. That is why, the First Piola Kirchhof stress tensor $\boldsymbol{S}$ will be defined and associated to the same internal force $d\vec{F}$ as:

$$d\vec{F} = \boldsymbol{S}\vec{N}dA \tag{1.31}$$

where $\vec{N}$ denotes the unit normal vector of the surface element dA corresponding to the surface element da in the reference configuration. By means of the Nanson formula (2.7), a relation between the first Piola Kirchhoff and Cauchy stress tensors can be conducted:

$$\boldsymbol{S} = J\boldsymbol{\sigma}\boldsymbol{F}^{-T} \tag{1.32}$$

The nominal stress tensor denoted by $\boldsymbol{\pi}$ is related to the First Piola Kirchhof stress tensor by:

$$\boldsymbol{\pi} = \boldsymbol{S}^T \tag{1.33}$$

Consider ρ and ρ_0 as the mass density respectively in the current and reference configuration. hence the local equation of the mass conservation leads to:

$$dm = \rho_0 dV = \rho dv, \tag{1.34}$$

then using the equation (2.5) describing the volume change, an interesting relation can be derived:

$$\rho_0 = J\rho \tag{1.35}$$

Let $\boldsymbol{f}$ denote the massic density of external forces. Thus the weak equilibrium equation for the considered body in either the reference configuration $\mathcal{B}_0$ or the current one $\mathcal{B}_t$ will be:

$$\int_{\partial\mathcal{B}_t} \boldsymbol{\sigma}\vec{n}da + \int_{\mathcal{B}_t} \rho\vec{f}dv = \int_{\mathcal{B}_t} \rho\vec{\gamma}dv, \tag{1.36}$$

$$\int_{\partial\mathcal{B}_0} \boldsymbol{S}\vec{N}dA + \int_{\mathcal{B}_0} \rho_0\vec{f}dV = \int_{\mathcal{B}_0} \rho_0\vec{\gamma}dV, \tag{1.37}$$

where $\vec{\gamma}$ represents the acceleration vector and it is related to the displacement field by:

$$\vec{\gamma} = \frac{\partial^2\chi(\vec{X},t)}{\partial t^2} \tag{1.38}$$

we notice that in the definition of the acceleration vector in the prior equation , the displacement field was considered as Langrangian field (depending of the reference position vector $\vec{X}$ and the time t) to avoid the complicated expression in the case of the Eulerian formalism. Using the divergence theorem (or Green identity) the integrated form of the equilibrium equations yields to:

$$div\boldsymbol{\sigma} + \rho\vec{f} = \rho\vec{\gamma}, \tag{1.39}$$

$$Div\boldsymbol{S} + \rho_0\vec{f} = \rho_0\vec{\gamma}. \tag{1.40}$$

Div and *div* are the divergence operators respectively to the current and the reference configurations, and using the Einstein sum convention, they can be defined as:

$$[div\boldsymbol{\sigma}]_i = \frac{\partial \sigma_{ij}}{\partial x_j}, \quad [div\boldsymbol{S}]_i = \frac{\partial S_{ij}}{\partial X_j} \tag{1.41}$$

Additionally, the balance of the moment implies the symmetry of the Cauchy stress tensor i.e $\boldsymbol{\sigma} = \boldsymbol{\sigma}^T$. In consequence, such the prior result can be expressed in terms of the First Piola Kirchhoff stress tensor as:

$$\boldsymbol{F}\boldsymbol{S}^T = \boldsymbol{S}\boldsymbol{F}^T \tag{1.42}$$

Contrary to the Cauchy stress tensor, the First Piola Kirchhoff stress tensor is not necessarily symmetric. Another stress tensor which is usually used in the finite elasticity formalism is the second Piola Kirchhoff stress tensor denoted by $\boldsymbol{P}$, which is relied to the Cauchy and first Piola Kirchhoff stress tensors as:

$$\boldsymbol{P} = J\boldsymbol{F}^{-1}\boldsymbol{\sigma}\boldsymbol{F}^{-T} = \boldsymbol{F}^{-1}\boldsymbol{S}. \tag{1.43}$$

If we define $\tilde{\vec{t}}$ as the fictive traction vector in the initial configuration, then the following relations can be deduced:

$$\vec{t} = \boldsymbol{F}\tilde{\vec{t}}, \quad \tilde{\vec{t}} = \boldsymbol{P}\vec{N} \tag{1.44}$$

Now, the equation of the virtual work done by both the surface and volume forces combined with the virtual motion $\delta\vec{x}$ in the spatial configuration, can be obtained using the equilibrium equation (2.40) and the divergence theorem as the following:

$$\int_{\partial\mathcal{B}_0} (\boldsymbol{S}\vec{N}).\delta\vec{x}dA + \int_{\mathcal{B}_0} \rho_0\vec{f}.\delta\vec{x}dV = \int_{\mathcal{B}_0} \rho_0\vec{\gamma}.\delta\vec{x}dV + \int_{\mathcal{B}_0} \boldsymbol{S} : \boldsymbol{\delta F}dV \tag{1.45}$$

with $\boldsymbol{\delta F} = Grad\delta\vec{x}$ and ":" denotes the scalar product defined in the space of the second order tensors which can be defined mathematically as $\boldsymbol{A}_1 : \boldsymbol{A}_2 = tr(\boldsymbol{A}_1^T\boldsymbol{A}_2)$ where tr is the trace operator. Considering the prior virtual equation, the work done by the external loadings (in the left side of the equation (2.45)) to which the considered body is subjected, is transformed to a cinetic work and deformation one in the bulk (right side of the equation (2.45)). The term $tr(\boldsymbol{S} : \boldsymbol{\delta F})$ represents the volumetric density of of deformation work

and by definition the First Piola Kirchhoff stress tensor is called the conjugate tensor to the deformation tensor $\boldsymbol{F}$. Moreover, a stress tensor can be defined for any measure of the deformation field. For example, in the case of Lagrangian deformation tensor $\boldsymbol{E}^m$ defined in (2.28) , a stress tensor $\boldsymbol{T}^m$ can be defined as:

$$\boldsymbol{S} : \boldsymbol{\delta F} = \boldsymbol{T}^{(m)} : \boldsymbol{\delta E}^{(m)}. \tag{1.46}$$

In the particular case where $m = 1$ (i.e $\boldsymbol{E}^{(1)} = \boldsymbol{U} - \boldsymbol{1}$), the corresponding stress measure denoted by $\boldsymbol{T}^{(1)}$ is called the Biot stress tensor and it can be defined as:

$$\boldsymbol{T}^{(1)} = \frac{1}{2}(\boldsymbol{S}^T\boldsymbol{R} + \boldsymbol{R}^T\boldsymbol{S}) \tag{1.47}$$

1.3 Hyperelastic materials

An elastic material is defined to be a material where every measure of stress $\boldsymbol{T}$ can be described by a function depending only on the deformation gradient tensor $\boldsymbol{F}$ as:

$$\boldsymbol{T} = \tilde{\boldsymbol{T}}(\boldsymbol{F}). \tag{1.48}$$

$\tilde{\boldsymbol{T}}$ is called the response function associated to the stress tensor $\boldsymbol{T}$ and it depends on the choice of the reference configuration $\mathcal{B}_0$. $\mathcal{B}_0$ is called the natural configuration, when the stress tensor $\boldsymbol{T}$ vanishes in the reference configuration which means:

$$\tilde{\boldsymbol{T}}(\boldsymbol{1}) = \boldsymbol{0}. \tag{1.49}$$

In the case of initially-stressed materials, the prior relation does not hold (see chapter 3 for more details). A material is called hyperelastic, when the work relative to the deformation of the body shape in the bulk can be associated with a considered energy potential W. Referring to the equation (2.45), an infinitesimal variation of the volumetric density of energy W can be expressed as:

$$\delta W = \boldsymbol{S} : \boldsymbol{\delta F} \tag{1.50}$$

W is also called the strain energy function. Henceforth, the first Piola Kirchhof can be related to the strain energy as:

$$\boldsymbol{S} = \frac{\partial W}{\partial \boldsymbol{F}}. \quad S_{ij} = \frac{\partial W}{\partial F_{ij}}. \tag{1.51}$$

Using the equations relating the Cauchy and the second Piola Kirhoff stress tensors to the first Piola Kirchhoff stress tensor, a similar result can be obtained:

$$J\boldsymbol{\sigma} = \frac{\partial W}{\partial \boldsymbol{F}}\boldsymbol{F}. \quad \boldsymbol{P} = \boldsymbol{F}^{-1}\frac{\partial W}{\partial \boldsymbol{F}}. \tag{1.52}$$

The strain energy W is usually required to fulfill some physical requirements that can be summarized into the following points:

- $W(\mathbf{1}) = 0$ to ensure that the strain energy is relative to the reference configuration.
- $\frac{\partial W}{\partial \boldsymbol{F}} = \mathbf{0}$ in the case where the reference configuration is not initially-stressed.
- $W(\boldsymbol{F})$ increases with the deformation based on physical observations.
- $W(\boldsymbol{F}) \to +\infty$ when $J \to +\infty$ or $J \to 0$: It is called the growth conditions. Otherwise speaking, the strain energy must diverge in the case of extreme strain.

1.3.1 Objectivity

Consider a rigid deformation:

$$\vec{x}^* = \boldsymbol{Q}\vec{X} + \vec{c}. \tag{1.53}$$

which can be decomposed into a rotation motion represented by the orthogonal tensor $\boldsymbol{Q}$ i.e $\boldsymbol{Q}\boldsymbol{Q}^T = \mathbf{1}$ and translation motion by the mean of the constant vector $\boldsymbol{c}$. Now, if the considered rigid deformation is superimposed to the deformation $\vec{x} = \chi(\vec{X})$ whose the deformation gradient is denoted by $\boldsymbol{F}$, then the total deformation gradient becomes:

$$\boldsymbol{F}^* = \boldsymbol{Q}\boldsymbol{F} \tag{1.54}$$

The strain energy has to verify the objectivity principle or what is usually denoted as the frame indifference. Such principle means that the strain energy has to be independent or unchanged under any superimposed rigid motion. This principle can be translated

mathematically into:

$$W(\boldsymbol{F}^{*}) = W(\boldsymbol{QF}) = W(\boldsymbol{F}), \quad \forall \boldsymbol{Q} \in Orth, \tag{1.55}$$

where $Orth$ is the space including the orthogonal tensors. Now, bearing in mind the relations of the Cauchy and first piola Kirchhoff stress tensor to the strain energy function, the objectivity property can be expressed in another way into:

$$\tilde{\boldsymbol{S}}(\boldsymbol{QF}) = \boldsymbol{Q}\tilde{\boldsymbol{S}}(\boldsymbol{F}), \quad \tilde{\boldsymbol{\sigma}}(\boldsymbol{QF}) = \boldsymbol{Q}\tilde{\boldsymbol{\sigma}}(\boldsymbol{F})\boldsymbol{Q}^{T}, \quad \forall \boldsymbol{Q} \in Orth. \tag{1.56}$$

1.3.2 Material symmetry

The group of symmetry (usually denoted by $\mathcal{G}$) of a considered material is a set of transformations represented by a proper orthogonal tensor $\boldsymbol{Q'}$ conserving the strain energy which leads to:

$$W(\boldsymbol{FQ}^{'}) = W(\boldsymbol{F}), \quad \forall \boldsymbol{Q}^{'} \in \mathcal{G} \subset Orth^{+}, \tag{1.57}$$

with $Orth^{+}$ is the proper orthogonal tensors space. In terms of the different stress measures, the prior relation of the material symmetry is equivalent to:

$$\tilde{\boldsymbol{\sigma}}(\boldsymbol{FQ}^{'}) = \tilde{\boldsymbol{\sigma}}(\boldsymbol{F}), \quad \tilde{\boldsymbol{S}}(\boldsymbol{FQ}^{'}) = \tilde{\boldsymbol{S}}(\boldsymbol{F})\boldsymbol{Q}^{'}, \quad \tilde{\boldsymbol{P}}(\boldsymbol{FQ}^{'}) = \boldsymbol{Q}^{'T}\tilde{\boldsymbol{P}}(\boldsymbol{F})\boldsymbol{Q}^{'}, \quad \forall \boldsymbol{Q}^{'} \in Orth^{+}. \tag{1.58}$$

1.3.3 Internal constraints

An internal constraint is usually a kinematic condition that must be fulfilled by the gradient deformation tensor, and it can be represented by the following form:

$$\mathcal{C}(\boldsymbol{F}) = 0. \tag{1.59}$$

Among the most common internal constraint, the incompressibility and the inextensibility in a chosen direction $\vec{M}$ are equivalent respectively to:

$$\mathcal{C}(\boldsymbol{F}) = det(\boldsymbol{F}) - 1 = 0, \quad \mathcal{C}(\boldsymbol{F}) = \vec{M}.\boldsymbol{C}.\vec{M} - 1 = 0 \tag{1.60}$$

In presence of an internal constraint, the Cauchy and the first Piola Kirchhoff stress tensors can be written as:

$$\boldsymbol{\sigma} = \frac{\partial W}{\partial \boldsymbol{F}}\boldsymbol{F}^T + q\frac{\partial \mathcal{C}}{\partial \boldsymbol{F}}\boldsymbol{F}^T, \quad \boldsymbol{S} = \frac{\partial W}{\partial \boldsymbol{F}} + q\frac{\partial \mathcal{C}}{\partial \boldsymbol{F}}, \tag{1.61}$$

where q is a Lagrange multiplier associated with the internal constraint $\mathcal{C}$. It is important to notice that the stress part related to the internal constraint does not work i.e $\frac{\partial \mathcal{C}}{\partial \boldsymbol{F}} : \delta\boldsymbol{F} = 0$.

1.3.4 Isotropic materials

1.3.4.1 Constitutive equations

In the case of isotropic materials, whether the response function or the strain energy do not depend on the direction of the loading and henceforth there is no preferential direction. Thus the symmetry group in this case is the entire group of proper orthogonal tensors. So, by combinating the both objectivity and group symmetry properties then we get:

$$W(\boldsymbol{Q}\boldsymbol{F}\boldsymbol{Q}^{'}) = W(\boldsymbol{F}), \quad \forall \boldsymbol{Q}, \boldsymbol{Q}^{'} \in Orth^{+}. \tag{1.62}$$

Bearing in mind the polar decomposition of the deformation gradient in equation (1.62) and by choosing $\boldsymbol{Q} = \boldsymbol{R}^T$ & $\boldsymbol{Q}^{'} = \boldsymbol{1}$ or $\boldsymbol{Q} = \boldsymbol{1}$ & $\boldsymbol{Q}^{'} = \boldsymbol{R}^T$, we derive:

$$W(\boldsymbol{F}) = W(\boldsymbol{U}) = W(\boldsymbol{V}) \tag{1.63}$$

Using similar arguments, it is easy to prove that the strain energy is an isotropic function of the right and left stretch tensors which is equivalent to:

$$W(\boldsymbol{Q}\boldsymbol{U}\boldsymbol{Q}^T) = W(\boldsymbol{U}), \quad W(\boldsymbol{Q}\boldsymbol{V}\boldsymbol{Q}^T) = W(\boldsymbol{V}), \quad \forall \boldsymbol{Q} \in Orth^{+}. \tag{1.64}$$

Then by using the theorem of invariant (or isotropic functions) as it is described in [Boehler 1987a], the strain energy depends on the common invariant of the both right and left stretch tensor which leads to:

$$W(\boldsymbol{U}) = W(\boldsymbol{V}) = W(i_1, i_2, i_3), \tag{1.65}$$

with the different invariant of the stretches tensors are defined as:

$$\begin{cases} i_1 &= tr(\boldsymbol{U}) = tr(\boldsymbol{V}), \\ i_2 &= \frac{1}{2}((tr(\boldsymbol{U}))^2 - tr(\boldsymbol{U}^2)) = \frac{1}{2}((tr(\boldsymbol{V}))^2 - tr(\boldsymbol{V}^2)), \\ i_3 &= det(\boldsymbol{U}) = det(\boldsymbol{V}). \end{cases} \tag{1.66}$$

Using the uniqueness of square root tensor for positive symmetric one, thus we can define similarly a strain energy density depending of the left or the right Cauchy strain tensor which leads to:

$$W(\boldsymbol{U}) = \tilde{W}(\boldsymbol{C}) = \tilde{W}(\boldsymbol{B}). \tag{1.67}$$

Thus the isotropy of the strain energy function W implies the isotropy of both $\tilde{W}$ and $\hat{W}$. Thus using the invariants theory, it leads to:

$$\tilde{W}(\boldsymbol{C}) = \tilde{W}(\boldsymbol{B}) = \tilde{W}(I_1, I_2, I_3), \tag{1.68}$$

with the new set of invariants which are the same for the left and right Cauchy-Green strain tensors and they are defined as:

$$\begin{cases} I_1 &= tr(\boldsymbol{C}) = tr(\boldsymbol{B}), \\ I_2 &= \frac{1}{2}((tr(\boldsymbol{C}))^2 - tr(\boldsymbol{C}^2)) = \frac{1}{2}((tr(\boldsymbol{B}))^2 - tr(\boldsymbol{B}^2)), \\ I_3 &= det(\boldsymbol{C}) = det(\boldsymbol{B}). \end{cases} \tag{1.69}$$

Considering a strain energy as the one in equation (2.67), then the Cauchy and the First Piola Kirchhoff stress tensors can be explicitly expressed as:

$$\boldsymbol{S} = 2\tilde{W}_1\boldsymbol{F} + 2\tilde{W}_2(I_1\mathbf{1} - \boldsymbol{B})\boldsymbol{F} + 2I_3\tilde{W}_3\boldsymbol{F}^{-T}, \quad J\boldsymbol{\sigma} = 2\tilde{W}_1\boldsymbol{B} + 2\tilde{W}_2(I_1\boldsymbol{B} - \boldsymbol{B}^2) + 2I_3\tilde{W}_3\mathbf{1}, \tag{1.70}$$

with $\tilde{W}_i = \frac{\partial \tilde{W}}{\partial I_i}, \quad i \in \{1, 2, 3\}$. In the case of incompressible materials $I_3 = J = 1$. Thus based on the results in the prior section relative to the internal constraint of incompressibility, the Cauchy and the First Piola stress tensors becomes:

$$\boldsymbol{S} = 2\tilde{W}_1\boldsymbol{F} + 2\tilde{W}_2(I_1\mathbf{1} - \boldsymbol{B})\boldsymbol{F} - p\boldsymbol{F}^{-T}, \quad \boldsymbol{\sigma} = 2\tilde{W}_1\boldsymbol{B} + 2\tilde{W}_2(I_1\boldsymbol{B} - \boldsymbol{B}^2) - p\mathbf{1}, \tag{1.71}$$

where p is the Lagrange multiplier associated with the constraint of incompressibility.

1.3.4.2 Examples of strain energy models

Incompressible materials

Ogden model: This model can be seen as a generalized form of the incompressible isotropic hyperelastic material. It was developed by Ogden for the modeling of rubber-like materials (rubber, biomechanical tissues...). The strain energy is a function of the principal stretches and it can be presented in the following mathematical form:

$$W(\lambda_1, \lambda_2, \lambda_3) = \sum_{i=1}^{N} \frac{\mu_i}{\alpha_i}(\lambda_1^{\alpha_i} + \lambda_2^{\alpha_i} + \lambda_3^{\alpha_i} - 3), \quad \lambda_1\lambda_2\lambda_3 = 1, \tag{1.72}$$

where the shear modulus μ can be expressed as:

$$\sum_{i=1}^{N} \mu_i\alpha_i = 2\mu. \tag{1.73}$$

Polynomial form: Inspired by the model of Mooney, Rivlin has a proposed a more general form for the strain energy as a polynomial expansion of the left Cauchy-Green tensor invariants as:

$$\tilde{W}(I_1, I_2, I_3) = \sum_{i,j=1}^{N} C_{ij}(I_1 - 3)^i(I_2 - 3)^j \tag{1.74}$$

where C_{ij} are material parameters and $C_{00} = 0$. Another form can be obtained for the strain energy if we replace the invariant of the Cauchy-Green strain tensors by those of the stretch tensors.

Mooney Rivlin model: As a special case of the polynomial form presented above, the Monney-Rivlin model is a linear combination of the involved invariants for an isochoric deformation. Thus the potential in this case becomes:

$$W = C_1(I_1 - 3) + C_2(I_2 - 3), \tag{1.75}$$

with C_1 and C_2 are two material parameters and they depend on temperature. This model is usually used for moderate levels of deformations.

NeoHookean model: Considered as one of the most simple models in finite elasticity, the NeoHookean model is usually used for many analyses in the literature. It is the result of the statistical mechanics if a gaussian distribution is considered for the particles interactions in the microscopic level. the mathematical form of the strain energy relative to this model is:

$$W = \frac{\mu}{2}(I_1 - 3), \tag{1.76}$$

Here μ is denoted as the infinitesimal modulus shear.

Compressible materials

In the case of compressible materials, usually the energy is decoupled into volumetric and distortion parts. For a strain energy depending on the Cauchy-Green strain tensor invariants, its generalization for the compressible materials can be in the following form:

$$\tilde{W}(I_1, I_2, I_3) = \tilde{W}(I_1, I_2)) + \tilde{W}_{vol}(I_3). \tag{1.77}$$

In this way, we can generalize the above polynomial class of strain energy forms. one of the classical form of the volumetric strain energy is the one proposed by Ogden:

$$\tilde{W}_{vol}(J) = \kappa\beta^2(\beta ln(J) + J^{-\beta} - 1), \tag{1.78}$$

where κ denotes the bulk modulus and β is an empirical coefficient. Moreover, the model of Ogden may be generalized for compressible materials to take the following form:

$$\tilde{W}(\lambda_1, \lambda_2, \lambda_3) = W_{vol}(J) + W(\bar{\lambda_1}, \bar{\lambda_2}, \bar{\lambda_3}), \quad \bar{\lambda_i} = J^{-\frac{1}{3}}\lambda_i, \quad i \in \{1, 2, 3\}. \tag{1.79}$$

Blatz-Ko model Developed by Blatz and Ko in [Blatz 1962], this model was proposed to model the foam behaviour. It is considered one of the few models characterized by the coupling between the isochoric and volumetric parts. The strain energy function for this model is given by:

$$\tilde{W}(I_1, I_2, I_3) = f\frac{\mu}{2}[(I_1 - 3) + \frac{1}{\beta}(I_3^{-\beta} - 1)] + (1 - f)\frac{\mu}{2}[(\frac{I_2}{I_3} - 3) + \frac{1}{\beta}(I_3^{\beta} - 1)] \tag{1.80}$$

with μ and β denotes respectively the shear modulus and a positive coefficient, whereas f is considered as an interpolation parameter defined in $[0, 1]$.

1.3.5 Anisotropic materials

1.3.5.1 Constitutive equations

Isotropic transverse material: Let $\vec{M}$ be a unit vector denoting the preferential direction in the reference configuration $\mathcal{B}_0$. An isotropic transverse material is a material presenting a single family of fibers whose orientation is described by the vector $\vec{M}$. The material behaviour is unchanged by any rotation around the fiber direction i.e $\boldsymbol{Q}\vec{M} = \pm\vec{M}$. The strain energy depends in this case not only on the deformation gradient tensor but also on the fiber direction $\vec{M}$ i.e $W = W(\boldsymbol{F}, \vec{M})$. Using the objectivity of the strain energy implies:

$$W(\boldsymbol{QF}, \vec{M}) = W(\boldsymbol{F}, \vec{M}), \quad \forall \boldsymbol{Q} \in Orth^{+}. \tag{1.81}$$

If we consider that the deformation χ related to the deformation gradient $\boldsymbol{F}$ is superimposed to a rotation represented by the proper orthogonal $\boldsymbol{Q}'$, then we can deduce:

$$W(\boldsymbol{FQ}', \boldsymbol{Q}'^{T}\vec{M}) = W(\boldsymbol{F}, \vec{M}), \quad \forall \boldsymbol{Q}' \in Orth^{+}. \tag{1.82}$$

As done in the case of isotropic materials above, by choosing $\boldsymbol{Q} = \boldsymbol{R}$ in equation (2.81), which signify:

$$W(\boldsymbol{F}, \vec{M}) = W(\boldsymbol{U}, \vec{M}) = \tilde{W}(\boldsymbol{C}, \vec{M}). \tag{1.83}$$

Now by coupling the equations (2.81-2.83), the isotropy of the strain energy is guaranteed:

$$W(\boldsymbol{QUQ}^{T}, \boldsymbol{Q}\vec{M}) = \tilde{W}(\boldsymbol{QCQ}^{T}, \boldsymbol{Q}\vec{M}) = W(\boldsymbol{U}, \vec{M}) = \tilde{W}(\boldsymbol{C}, \vec{M}) \tag{1.84}$$

Hence, the theory of invariants requires that the strain energy $\tilde{W}$ depends on five invariants: I_1 , I_2, I_3 as they are defined in (2.69) added to two supplementary invariants namely I_4 and I_5 which can be expressed as:

$$I_4 = \vec{M}.\boldsymbol{C}.\vec{M}, \quad I_5 = \vec{M}.\boldsymbol{C}^2.\vec{M}. \tag{1.85}$$

Therefore, the resulting Cauchy stress tensor becomes:

$$J\boldsymbol{\sigma} = 2\tilde{W}_1\boldsymbol{B} + 2\tilde{W}_2(I_1\boldsymbol{B} - \boldsymbol{B}^2) + 2I_3\tilde{W}_3\mathbf{1} + 2\tilde{W}_4\vec{m}\otimes\vec{m} + 2\tilde{W}_5(\boldsymbol{B}.\vec{m}\otimes\vec{m} + \vec{m}\otimes\boldsymbol{B}.\vec{m}), \tag{1.86}$$

with $\vec{m} = \boldsymbol{F}.\vec{M}$ and $W_i = \frac{\partial\tilde{W}}{\partial I_i}$ for $i = 1, 2..5$. For isotropic materials, we recover the same form of the Cauchy stress by putting $\tilde{W}_4 = \tilde{W}_5 = 0$. For incompressible materials ($J = I_3 = 1$), then the formula (2.86) is replaced by:

$$\boldsymbol{\sigma} = 2\tilde{W}_1\boldsymbol{B} + 2\tilde{W}_2(I_1\boldsymbol{B} - \boldsymbol{B}^2) - p\mathbf{1} + 2\tilde{W}_4\vec{m}\otimes\vec{m} + 2\tilde{W}_5(\boldsymbol{B}.\vec{m}\otimes\vec{m} + \vec{m}\otimes\boldsymbol{B}.\vec{m}). \tag{1.87}$$

Orthotropic material: In this case the material in its reference configuration $\mathcal{B}_0$ presents two preferred directions associated to two unitary vectors $\vec{M}$ and $\vec{M}'$. The material behaviour is independent of all the rotation unchanging one of the two vectors or its reverse. Then the symmetry group is the set of the rotations around $\vec{M}$ or $\vec{M}'$. Then using the same argument type, we can prove that the strain energy is an isotropic function of: $\boldsymbol{C}$ or $\boldsymbol{U}$, $\vec{M}$ and $\vec{M}'$. Consequently, there are more invariants to which the strain energy must depend:

$$I_6 = \vec{M}'.\boldsymbol{C}.\vec{M}', \quad I_7 = \vec{M}'.\boldsymbol{C}^2.\vec{M}', \quad I_8 = \vec{M}'.\boldsymbol{C}.\vec{M}, \quad I_9 = \vec{M}'.\vec{M}, \quad I_{10} = \vec{M}'.\boldsymbol{C}^2.\vec{M}. \tag{1.88}$$

Since, the last invariant I_{10} can be expressed in terms of the rest of the invariants (see appendix C for the demonstration), the strain energy is considered as a function only of the first 9 invariants. Henceforth, the Cauchy stress in the case an unconstrained orthotropic hyperelastic material is given by:

$$\begin{aligned} J\boldsymbol{\sigma} = {} & 2\tilde{W}_1\boldsymbol{B} + 2\tilde{W}_2(I_1\boldsymbol{B} - \boldsymbol{B}^2) + 2I_3\tilde{W}_3\mathbf{1} + 2\tilde{W}_4\vec{m}\otimes\vec{m} + 2\tilde{W}_5(\boldsymbol{B}.\vec{m}\otimes\vec{m} + \vec{m}\otimes\boldsymbol{B}.\vec{m}) \\ & + 2\tilde{W}_6\vec{m'}\otimes\vec{m'} + 2\tilde{W}_7(\boldsymbol{B}.\vec{m'}\otimes\vec{m'} + \vec{m'}\otimes\boldsymbol{B}.\vec{m'}) + 2\tilde{W}_8(\vec{m'}\otimes\vec{m} + \vec{m}\otimes\vec{m'}), \end{aligned} \tag{1.89}$$

where $\vec{m'} = \boldsymbol{F}\vec{M'}$ and $\tilde{W}_i = \frac{\partial \tilde{W}}{\partial I_i}$ for $i = 1..8$. However, when the incompressibility constraint holds, the prior equation is replaced by:

$$\boldsymbol{\sigma} = 2\tilde{W}_1\boldsymbol{B} + 2\tilde{W}_2(I_1\boldsymbol{B} - \boldsymbol{B}^2) - p\mathbf{1} + 2\tilde{W}_4\vec{m}\otimes\vec{m} + 2\tilde{W}_5(\boldsymbol{B}.\vec{m}\otimes\vec{m} + \vec{m}\otimes\boldsymbol{B}.\vec{m}) \tag{1.90}$$

$$+ 2\tilde{W}_6\vec{m'}\otimes\vec{m'} + 2\tilde{W}_7(\boldsymbol{B}.\vec{m'}\otimes\vec{m'} + \vec{m'}\otimes\boldsymbol{B}.\vec{m'}) + 2\tilde{W}_8(\vec{m'}\otimes\vec{m} + \vec{m}\otimes\vec{m'}). \tag{1.91}$$

1.3.5.2 Examples of strain energy models

Usually in the literature for fiber reinforced hyperelastic materials modeling, the volumetric and isochoric parts are decoupled. So in the following we will present only the isochoric part of the strain energy.

polynomial form: Inspired by the polynomial strain energy function for incompressible materials, a polynomial expansion for the volumetric energy density can be given as:

$$\tilde{W}(I_1, I_2, I_4, I_5, I_6, I_7, I_8) = \sum_{j_1,\ldots,j_8} C_{j_1 j_2 j_4 j_5 j_6 j_7 j_8}(I_1-3)^{j_1}(I_2-3)^{j_2}(I_4-1)^{j_4}(I_5-1)^{j_5}(I_6-1)^{j_6} \times(I_7-1)^{j_7}(I_8-1)^{j_8} \tag{1.92}$$

Humphrey and Yin model: based on the assumption of the non-interacting families of fibers in soft tissues, Humphrey and Yin proposed in [Humphrey 1987] a model where the isotropic and anisotropic parts of the strain energy are decoupled and it can be presented in the following mathematical form:

$$W(I_1, I4)) = c[exp(b(I_1-3)) - 1] + A[exp(a(\sqrt{I_4}-1)^2) - 1], \tag{1.93}$$

with A, a , b and c are material parameters.

Holzapfel model: For the sake of multilayered arterial wall presenting two connected families or fibers, Holzapfel and al in [Holzapfel 2000] have proposed the following form for

the strain energy:

$$W(I_1, I_4, I_6) = \frac{\mu}{2}(I_1 - 3) + \frac{k_1}{2k_2} \sum_{i=4,6} \{exp(k_2(I_i - 1)^2) - 1\}. \tag{1.94}$$

Here, μ, k_1 and k_2 are positive material constants.

1.3.6 Strong ellipticity

The equilibrium equation in the reference configuration as it is mentioned in equation (2.40) can be rewritten as:

$$\mathcal{A}^1_{kilj} \frac{\partial^2 x_j}{\partial X_k \partial X_l} + \rho_0 f_i = \rho_0 \frac{\partial^2 x_i}{\partial t^2} \tag{1.95}$$

whereas in the case of incompressible materials the equilibrium equation (2.95) is transformed to:

$$\mathcal{A}^1_{kilj} \frac{\partial x_j}{\partial X_k \partial X_l} - \frac{\partial p}{\partial x_i} + \rho_0 f_i = \rho_0 \frac{\partial^2 x_i}{\partial t^2} \tag{1.96}$$

with the different components of the fourth order tensor $\mathcal{A}^1$ in both cases are defined as:

$$\mathcal{A}^1_{kilj} = \mathcal{A}^1_{ljki} = \frac{\partial^2 W}{\partial F_{ik} \partial F_{jl}}. \tag{1.97}$$

The components $\mathcal{A}^1_{kilj}$ are in general nonlinear functions of the deformation gradient tensor components. In other words, the nonlinearity of the prior partial differential equation is controlled by the fourth order tensor $\mathcal{A}^1$. The equation (2.95) is said to be strong elliptic if and only if:

$$\mathcal{A}^1_{kilj} m_i m_j N_k N_l > 0 \tag{1.98}$$

for all non zero vectors $\vec{m}$ and $\vec{N}$. In the case of incompressible materials, the equation (2.98) holds for the following restriction:

$$\vec{m}.\vec{n} = 0, \tag{1.99}$$

where $\vec{n}$ is considered as the push forward of $\vec{N}$ and they are related together as:

$$\vec{N} = \boldsymbol{F}^T \vec{n}. \tag{1.100}$$

The strong ellipticity condition is used essentially initially to guarantee the propagation of plane waves (the celerity of the plane wave is real). Then, this condition was added to the constraints discussed above that must be fulfilled by the strain energy for a general deformation field.

1.3.7 Linear elasticity

In the scope of small deformations, the displacement field and its gradient tensor are sufficiently small i.e:

$$||\boldsymbol{H}|| << 1, \quad |u| << L, \tag{1.101}$$

so that the reference and current configurations are usually considered as the same. $||.||$ and $|.|$ denote respectively two norms for tensor and vector functions, whereas L is a characteristic length for the studied body. If the reference configuration is natural, then all the stress measures presented above are the same. In linear elasticity, the fourth order incremental elastic tensor denoted by $\mathcal{C}$ is relied to the fourth order tensor $\mathcal{A}^1$, defined above, as:

$$\mathcal{C}_{ijkl} = \mathcal{A}^1_{ijkl} = \frac{\partial^2 W}{\partial \varepsilon_{ij} \partial \varepsilon_{kl}}, \tag{1.102}$$

where $\boldsymbol{\varepsilon}$ is the infinitesimal strain tensor and it is defined as:

$$\boldsymbol{\varepsilon} = \frac{1}{2}(\boldsymbol{H} + \boldsymbol{H}^T). \tag{1.103}$$

The Cauchy stress tensor can be expressed as:

$$\boldsymbol{\sigma} = \frac{\partial W}{\partial \boldsymbol{\varepsilon}}. \tag{1.104}$$

and the strain energy can be considered as quadratic function of the infinitesimal strain tensor which is equivalent to:

$$W = \frac{1}{2}\boldsymbol{\varepsilon} : \mathcal{C} : \boldsymbol{\varepsilon} = \frac{1}{2}\mathcal{C}_{ijkl}\varepsilon_{ij}\varepsilon_{kl}. \tag{1.105}$$

Using the symmetry of both the strain and Cauchy stress tensors and the expression of the strain energy in equation (2.105), thus the incremental elastic tensor $\mathcal{C}$ posses the full symmetries i.e :

$$\mathcal{C}_{ijkl} = \mathcal{C}_{klij} = \mathcal{C}_{jikl}. \tag{1.106}$$

Isotropic linear elasticity: For isotropic materials the elastic tensor in the natural configuration becomes:

$$\mathcal{C}_{ijkl} = 2\mu(\delta_{ik}\delta_{jl} + \delta_{il}\delta_{jk}) + \lambda\delta_{ij}\delta_{kl} \tag{1.107}$$

with μ and λ denote the Lamé coefficients and δ is the Kroneker operator. Thus the Cauchy stress tensor can be expressed as:

$$\boldsymbol{\sigma} = 2\mu\boldsymbol{\varepsilon} + \lambda\mathrm{tr}(\boldsymbol{\varepsilon})\mathbf{1} \tag{1.108}$$

and the linearized strong ellipticity condition leads to:

$$\mu > 0, \quad \lambda \geq 0, \tag{1.109}$$

Isotropic transverse material:
When there is one family of fibers and the fibers direction is represented by the unitary vector $\vec{M}$, then the stress-strain relation becomes:

$$\begin{aligned}\boldsymbol{\sigma} = {} & (\lambda tr(\boldsymbol{\varepsilon}) + \alpha\vec{M}.\boldsymbol{\varepsilon}.\vec{M})\mathbf{1} + (\alpha tr(\boldsymbol{\varepsilon}) + \beta\vec{M}.\boldsymbol{\varepsilon}.\vec{M})\vec{M}\otimes\vec{M} + 2\mu_T\boldsymbol{\varepsilon} \\ & + 2(\mu_L - \mu_T)[\boldsymbol{\varepsilon}.\vec{M}\otimes\vec{M} + \vec{M}\otimes\boldsymbol{\varepsilon}.\vec{M}],\end{aligned} \tag{1.110}$$

where λ, α, β, μ_T and μ_L are material parameters.

Orthotropic material:
When the material symmetry become orthotropic which is equivalent to the presence of two families of fibers whose the direction is represented by the unitary vectors $\vec{M}$ and $\vec{M}'$,

then in case of orthogonal fibers, the expression of Cauchy stress tensor is simplified to:

$$\begin{aligned}\boldsymbol{\sigma} &= (\lambda tr(\boldsymbol{\varepsilon}) + \alpha_1 \vec{M}.\boldsymbol{\varepsilon}.\vec{M} + \alpha_2 \vec{M}'.\boldsymbol{\varepsilon}.\vec{M}')\mathbf{1} + (\alpha_1 tr(\boldsymbol{\varepsilon}) + \beta_1 \vec{M}.\boldsymbol{\varepsilon}.\vec{M} + \beta_3 \vec{M}'.\boldsymbol{\varepsilon}.\vec{M}')\vec{M} \otimes \vec{M} \\ &+ (\alpha_2 tr(\boldsymbol{\varepsilon}) + \beta_3 \vec{M}.\boldsymbol{\varepsilon}.\vec{M} + \beta_2 \vec{M}'.\boldsymbol{\varepsilon}.\vec{M}')\vec{M}' \otimes \vec{M}' + 2\mu\boldsymbol{\varepsilon} + 2\mu_1[\boldsymbol{\varepsilon}.\vec{M} \otimes \vec{M} + \vec{M} \otimes \boldsymbol{\varepsilon}.\vec{M}] \\ &+ 2\mu_2[\boldsymbol{\varepsilon}.\vec{M}' \otimes \vec{M}' + \vec{M}' \otimes \boldsymbol{\varepsilon}.\vec{M}'], \end{aligned} \tag{1.111}$$

Although for the more general case, a tension-shear coupling take in place and the stress-strain relation becomes more complicated (see the work of Spencer in [Spencer 1984a] for more details)

1.3.8 Linearization of the hyperelastic models

The linear elasticity theory can be whether constructed mathematically with the choice of quadratic form for the strain energy or by the linearization of the hyperelastic model in the finite elasticity. In this section, we intend to rely the hyperelastic models to the linear stress-strain relation by Linearization. For the sake of generality, the hyperelastic model for orthotropic material is considered and the case of isotropic and isotropic transverse materials can be then deduced. The infinitesimal or the Linearized Cauchy stress tensor becomes:

$$\begin{aligned}\boldsymbol{\sigma} &= [2\tilde{W}_1^L + 4\tilde{W}_2^L + 2\tilde{W}_3^L + tr(\boldsymbol{\varepsilon})(4\tilde{W}_1^0 + 4\tilde{W}_3^0)]\mathbf{1} + 4(\tilde{W}_1^0 + \tilde{W}_3^0)\boldsymbol{\varepsilon} + [2\tilde{W}_4^L + 4\tilde{W}_5^L]\vec{M} \otimes \vec{M} \\ &+ [2\tilde{W}_6^L + 4\tilde{W}_7^L]\vec{M}' \otimes \vec{M}' + 4\tilde{W}_5^0[\boldsymbol{\varepsilon}\vec{M} \otimes \vec{M} + \vec{M} \otimes \boldsymbol{\varepsilon}\vec{M}] + 4\tilde{W}_7^0[\boldsymbol{\varepsilon}\vec{M}' \otimes \vec{M}' + \vec{M}' \otimes \boldsymbol{\varepsilon}\vec{M}'] \\ &+ \tilde{W}_8^L[\vec{M}' \otimes \vec{M} + \vec{M} \otimes \vec{M}'] \end{aligned} \tag{1.112}$$

with

$$\begin{aligned}\tilde{W}_i^L &= (2\tilde{W}_{i1} + 4\tilde{W}_{i2} + 2\tilde{W}_{i3})tr(\boldsymbol{\varepsilon}) + (2\tilde{W}_{i4} + 4\tilde{W}_{i5})\vec{M}.\boldsymbol{\varepsilon}.\vec{M} \\ &+ (2\tilde{W}_{i6} + 4\tilde{W}_{i7})\vec{M}'.\boldsymbol{\varepsilon}.\vec{M}' + 2\tilde{W}_{i8}\vec{M}'.\boldsymbol{\varepsilon}.\vec{M}, \quad \forall i \in \{1..8\}, \end{aligned} \tag{1.113}$$

where $\tilde{W}_{ij} = \partial^2\tilde{W}/\partial I_i \partial I_j$, $i, j = 1..8$. To ensure that the reference configuration is a natural one which is equivalent to the absence of an initial stress field, then the following

condition must hold:

$$\tilde{W}_1^0 + 2\tilde{W}_2^0 + \tilde{W}_3^0 = 0 \tag{1.114}$$
$$\tilde{W}_4^0 + 2\tilde{W}_5^0 = 0 \tag{1.115}$$
$$\tilde{W}_6^0 + 2\tilde{W}_7^0 = 0 \tag{1.116}$$
$$\tilde{W}_8^0 = 0, \tag{1.117}$$

where the index $.^0$ in the terms W_i^0 refers to express these terms in the reference configuration which is equivalent to:

$$W_i^0 = W_i(I_1 = 3, I_2 = 3, I_3 = 1, I_4 = 1, I_5 = 1, I_6 = 1, I_7 = 1, I_8 = I_9) \tag{1.118}$$

When the internal constraint of incompressibility is taken into consideration, thus the linearized stress strain relation becomes:

$$\begin{aligned}\boldsymbol{\sigma} = &-p\mathbf{1} + 4(\tilde{W}_1^0 + \tilde{W}_3^0)\boldsymbol{\varepsilon} + [2\tilde{W}_4^L + 4\tilde{W}_5^L]\vec{M}\otimes\vec{M} \\ &+ [2\tilde{W}_6^L + 4\tilde{W}_7^L]\vec{M}'\otimes\vec{M}' + 4\tilde{W}_5^0[\boldsymbol{\varepsilon}\vec{M}\otimes\vec{M} + \vec{M}\otimes\boldsymbol{\varepsilon}\vec{M}] + 4\tilde{W}_7^0[\boldsymbol{\varepsilon}\vec{M}'\otimes\vec{M}' + \vec{M}'\otimes\boldsymbol{\varepsilon}\vec{M}'] \\ &+ \tilde{W}_8^L[\vec{M}'\otimes\vec{M} + \vec{M}\otimes\vec{M}']\end{aligned} \tag{1.119}$$

with p is the Lagrange multiplier relative to the incompressibility condition which is equivalent to:

$$tr(\boldsymbol{\epsilon}) = 0 \tag{1.120}$$

and to guarantee the vanishing of any type of initial stress field the following conditions are transformed to:

$$\tilde{W}_1^0 + 2\tilde{W}_2^0 - p_0 = 0 \tag{1.121}$$
$$\tilde{W}_4^0 + 2\tilde{W}_5^0 = 0 \tag{1.122}$$
$$\tilde{W}_6^0 + 2\tilde{W}_7^0 = 0 \tag{1.123}$$
$$\tilde{W}_8^0 = 0, \tag{1.124}$$

where p_0 is the value of the Lagrange multiplier field in the reference configuration.

1.4 Conclusion

In this chapter, the formalism of finite transformations is presented focusing on the special case of hyperelastic materials. Through the previous sections, a set of multiple theoretical concepts are presented and discussed like the principle of frame indifference or the strong ellipticity. Such concepts or principles are necessary for the materials behaviour modeling. Centering our attention on the case of hyperelastic initially-stressed materials, the behaviour modeling of such class of materials is a real challenge. As well as, more mathematical constraints than the ones presented above are established to be more coherent with the physical behaviour of such materials as we will see in detail in the next chapter.

Chapter 2

Modeling of initially-stressed hyperelastic materials

Contents

2.1 Introduction

Materials sciences were and still considered one of the pillars of industrial and scientific development in the last two centuries. The technological advancements in different areas play the role of driven force behind the evolution in such scientific scope. Despite the long

steps made in the modeling of material behaviors, many fundamental foundations remain raising a lot of questions. One of the first fundamental columns, on which is based on the materials sciences, is the theory of elasticity whose the spark idea was coming from Robert Hook in the 17th century. Despite the development of many new complex non-linear theories for materials modeling involving many class of behaviors like plasticity, viscosity and damage, the elasticity still essential for pre-sizing structure and in some sciences like fracture mechanics or fatigue, remains one of the basis.

Among the biggest challenges that the theory of elasticity in particular and the material science in general are facing is the modeling of residual stress which is defined as the remaining stress inside a considered body in a chosen configuration in absence of all exterior loadings. The residual stress can be involved in various examples and scopes. The residual stress plays a key role in the propagations of cracks by fatigue. It is shown in [Nelson 1982] that the nature and the amount of the residual stress have direct effects on the threshold of fatigue, it can be advantageous to the material especially in high cycle regime when the residual stress is of compressive type leading to the brake of the crack propagation and so the delay of failure, and it could be disastrous in the opposite case. In biomechanics many works like [Fung 1991, Holzapfel 2014] cleared out the contribution of residual stress in self-regulation properties of stress and strains in the different types of arteries inside various organs in the objective to preserve the ideal mechanical conditions for tissues functions. In geophysics, It is shown that residual stress can possibly affect not only the direction of crack propagation through the stones [Holzhausen 1979, Friedman 1970] and the changement of tectonic plates topography [Savage 1986], but also the dynamic properties of seismic waves [Tolstoy 1982]. In the oil and gas industry many techniques are based on the scope of elastodynamics are still used for identifying the oil fields or even stimulating and influencing the reservoir for better recuperation [Roberts 2003]. But since it is shown the impact of residual stress on wave propagation [Guz 2002], it is necessary to take into account the presence of internal stress and its consequences.

The residual stress origins can be multiple, varying from the heterogeneity of the material to the way of loading the structure to even the in-vivo mechanisms. In metals, the residual stress essentially is due to the high gradient of loading like welding process [Deng 2008], multiple manufacturing processes invoking plastic deformations (rolling...)[Treuting 1951] and thermal or surface treatments [Withers 2001]. In composite structures, focusing on

the meso-scale, the difference of thermal expansivity, rigidity or any other material property of different parts of the composite structure leads to the residual stress presence near the boundary between the matrix and inclusions or fibers. In arteries, residual stress is a result of non-uniform growth and remodeling [Fung 1991] due to the physiological functions. More explicitly, the disorganization of fragmentation and the fibrous constituents of tissues ,mainly collagens and protein elastin, leads to the presence of residual stress to preserve the mechanical integrity and the optimal functions of the body parts in vivo state [Cardamone 2009].

Since the concept of residual stress touches almost all the areas, the development of a model taking into account the influence of such a field on the behaviour of the material is necessary. Also, this concept could be used to have a better physical understanding and explanation to the different complex phenomena in material sciences.

In the litterature, the modeling of residual stress began inside a more general category of stress fields, the one of initial stress or in presence of dead loads defined as a non changed loadings in both amplitude and direction. Based on the investigation of Bazant in [ZP 1971], many formulations as constitutive relations in presence of pre-stress were found by many authors in some special cases like Southwell, Biezeno and Hencky, Trefftz, and Biot. But essentially, to our knowledge, the first studies focusing specifically on the residual stress were managed by Colman and Noll: One of the interesting properties, they found in [Coleman 1964] the commutation of the residual stress tensor with the tensors elements of the symmetry group. This property was exploited by Anne Hoger to propose the possible form of residual stress within different classes of symmetry [Hoger 1985]. Then, Hoger established in [Hoger 1986] one of the most general constitutive stress-strain relations in presence of residual stress for compressible materials in the scope of small deformation. The same formulation was extended to the case of arbitrary rotations and small strains in [Hoger 1993b], and was generalized by Marlow in [Marlow 1992] to take account of the possible constraints in the material. Jonshon and Hoger in [Johnson 1993], supposing that the residual stress is due to prior elastic deformations, they derived a general stress-strain constitutive relation in the presence of pre-stress for isotropic materials, in the same paper considering a small deformation superimposed to a large one, they found an explicit linearized form of the constitutive relation unlike the relation found by Hoger in [Hoger 1986] where the elastic tensor operator is unknown. Inspired by experimental protocols used to

release the residual stress from arteries, Johnson and Hoger presented a method for modeling the materials behaviour affected by the residual stress using the concept of virtual configuration where the material could be relieved from all its internal stress [Johnson 1995] and it was generalized in [Hoger 1997] to study the influence of material symmetry on the previous formulation. The determination of the response function invert in explicit form and the identification of the virtual configuration are among the biggest challenges for the use of the prior method. Far from these constraints, an interesting idea is to consider the strain energy as a function of both the deformation gradient tensor and the residual stress. In the scope of finite transformations, this idea was introduced in [Hoger 1993a] to focus on the case of isotropic transverse symmetry and later in [Shams 2014] in the objective of studying the wave propagation. The only difference between the introduced formulations is that the first one is expressed in function of the right Cauchy strain and residual stress tensors and in the second one the strain measure used is the right Cauchy-Green deformation tensor. Recently, Gower et al in [Gower 2015, Gower 2017] developed two new restrictions on the prior presented strain energy potential. The first one is based on the symmetry of the response function for both the Cauchy and residual stresses tensors, and is called the initial stress symmetry (ISS). This restriction was made to preclude the influence of the reference configuration choice on the strain energy. A set of mathematical conditions was proposed to be verified by the potential of energy to satisfy the ISS restriction. The second restriction, named initial stress reference independence (ISRI), focuses on the energy conservation property. Then a linearized form for the density of energy was deduced.

Introduced by Morgan in [Morgan 1966], and developed recently by the group of Rajagopal, the implicit theory could be one of the promising attempts to extend the limits of classical theory of elasticity. It is shown that the implicit theory characterizes a wider class of reversible elastic materials than the Cauchy materials [Rajagopal 2003]. Focusing on the scope of small deformations, Bustamante and Rajagopal through examples of some proposed implicit relations studied the response of such material models to a set of chosen known transformations. Later they studied a special subclass where the strain tensor is derived from the derivation of a strain energy potential relative to the stress tensor [Bustamante 2016, Bustamante 2015]. Recently, the implicit theory was exploited to derive a new formulation for the modeling of residual stress influence on an elastic solids [Bustamante 2018].

Here in this chapter, we propose a new formulation to take account of the influence of residual stress on elastic behaviour proposing a general explicit form of elastic tensor without making any hypothesis on the residual stress source. Also a study for different formulations proposed in the litterature for the same objective, are presented as a review. Also, the different restrictions that were derived recently (ISS and ISRI) are presented in a detailed way and we show that they are equivalent although the different arguments used for each one. On the other hand, it is well known the strong link between the initial stress field presence and the anisotropy. That's why, in this chapter a detailed study illuminates an explicit analogy between the initially-stressed hyperelastic materials behaviour and the behaviour of some symmetry classes for fibrous hyperelastic materials.

In the other hand, the plane deformations and/or plane stress hypothesis are among the most used scopes in order to simplify the analysis of complex boundary values problems in mechanics. In both cases, it has been shown that equilibrium equations can be reduced to a single partial differential equation on a scalar potential field based on the compatibility of the deformation field. Such type of formulations like the one invoking the Airy stress function is essential for many problems in mechanics: for example, to derive the asymptotic form of the different mechanical fields near a crack tip in an isotropic material, the use of such function was primordial. That is why the third section will be dedicated to the establishment of plane deformations formulation in the case of constant initial stress field.

2.2 Preliminary equations

Let us consider a body B in a reference configuration denoted by $\mathcal{B}_0 \subset \mathbb{R}^3$. Consider a one-to-one mapping vector-valued function $\boldsymbol{\phi}$ that transforms a point $\boldsymbol{X}$ in $\mathcal{B}_0$ into $\boldsymbol{x} = \boldsymbol{\phi}(\boldsymbol{X})$ in the actual configuration denoted as $\mathcal{B}_t$. Besides, we can define the deformation gradient tensor as:

$$\boldsymbol{F} = \boldsymbol{\nabla}_X \boldsymbol{\phi}, \tag{2.1}$$

where $\boldsymbol{\nabla}_X$ is the gradient operator relative to the coordinates system of the reference configuration, and $\boldsymbol{F}$ has to satisfy $J = \det(\boldsymbol{F}) > 0$ for admissible mathematical transformations. Thus, the deformation measures subsequently denoted as Left and Right Cauchy-Green

deformation tensors can be defined as the following:

$$\boldsymbol{B} = \boldsymbol{F}\boldsymbol{F}^T, \quad \boldsymbol{C} = \boldsymbol{F}^T\boldsymbol{F}. \tag{2.2}$$

The First Piola-Kirchhoff stress tensor $\boldsymbol{S} = \hat{\boldsymbol{S}}(\boldsymbol{F})$ is related to the Cauchy stress tensor $\boldsymbol{\sigma} = \hat{\boldsymbol{\sigma}}(\boldsymbol{F})$, which is defined on the actual configuration, as:

$$\boldsymbol{S} = J\boldsymbol{\sigma}\boldsymbol{F}^{-T}. \tag{2.3}$$

If we denote by Orth^+ the set of proper orthogonal tensors, then the observer independence for both Cauchy stress tensor $\boldsymbol{\sigma}$ and the first Piola-Kirchhoff tensor $\boldsymbol{S}$ is equivalent to:

$$\boldsymbol{\sigma}(\boldsymbol{Q}\boldsymbol{F}) = \boldsymbol{Q}\boldsymbol{\sigma}(\boldsymbol{F})\boldsymbol{Q}^T, \quad \boldsymbol{S}(\boldsymbol{Q}\boldsymbol{F}) = \boldsymbol{Q}\boldsymbol{S}(\boldsymbol{F}), \quad \forall \boldsymbol{Q} \in \mathrm{Orth}^+. \tag{2.4}$$

The equilibrium equations in presence of a mass density of forces denoted as $\boldsymbol{f}$ and in its static form for both stress measures are:

$$\boldsymbol{\nabla}_X.\boldsymbol{S} + \rho_0\boldsymbol{f} = \boldsymbol{0}, \quad \boldsymbol{\nabla}_x.\boldsymbol{\sigma} + \rho\boldsymbol{f} = \boldsymbol{0}, \tag{2.5}$$

where the indexations by $_x$ and $_X$ denote the coordinate systems relative to what the derivation of the divergence operator is made. ρ_0 and ρ represent the mass density respectively for the reference and actual configurations.

2.3 Modeling of initially-stressed hyperelastic materials

Residual stress can be defined as the remaining stress in a considered body in absence of any external forces. Such kind of internal stress is regarded as a critical and potential phenomenon that can affect the material behaviour. This influence may touch the mechanical parameters, the heterogeneity or the anisotropy of the material or it can even change the constitutive equation describing the material behaviour itself. In the following the residual stressed bodies will be studied in a more general class denoted by the initially-stressed materials where the stress field in the chosen configuration is usually called initial stress or initial stress and it is equilibrated not necessarily in absence of external loadings.

Now, we define the initial stress field $\boldsymbol{\tau}$ as the Cauchy stress in the reference configuration. This definition is usually denoted by the initial stress compatibility condition ISC (It will

be used in almost the following presentations of the different constitutive formulations). Thus it must be symmetric, and it has to satisfy:

$$\boldsymbol{\nabla}_X.\boldsymbol{\tau} = \vec{0}. \tag{2.6}$$

In the special case where:

$$\boldsymbol{\tau}.\vec{N} = \vec{0}, \tag{2.7}$$

where $\vec{N}$ is the unit outward normal vector to the body B in the reference configuration $\mathcal{B}_0$, then $\boldsymbol{\tau}$ is called residual stress: the remaining internal stress when all the external loadings are removed. Based on the theorem of average of Signorini (see [Hoger 1986]), the residual stress is heterogeneous inside the material body, and so the presence of such a field inside the structure leads to an inhomogeneity in the mechanical behaviour. Considering equation (2.7) implies that the residual stress depends on the shape of the studied structure. The modeling of the residual stress influence on the material behaviour was initiated with Coleman and Noll in [Coleman 1964] where they discussed the possible initial stress based on the symmetry group of a material. So far multiple formulations were derived in different ways to model such internal stress affecting the constitutive equations of the material behaviour.

2.3.1 Hyperelastic model based on the theory of invariants

In finite elasticity, the modeling of initially-stressed hyperelastic materials has begun to our knowledge with the work of Shams et al in [Shams 2011] where the strain energy is a function of the deformation gradient $\boldsymbol{F}$ and the initial stress field $\boldsymbol{\tau}$ so we can write:

$$W = W(\boldsymbol{F}, \boldsymbol{\tau}). \tag{2.8}$$

To ensure that the energy is independent of the rigid deformations, the strain energy W must satisfy:

$$W(\boldsymbol{Q}\boldsymbol{F}, \boldsymbol{\tau}) = W(\boldsymbol{F}, \boldsymbol{\tau}), \quad \forall \boldsymbol{Q} \in \mathrm{Orth}^+. \tag{2.9}$$

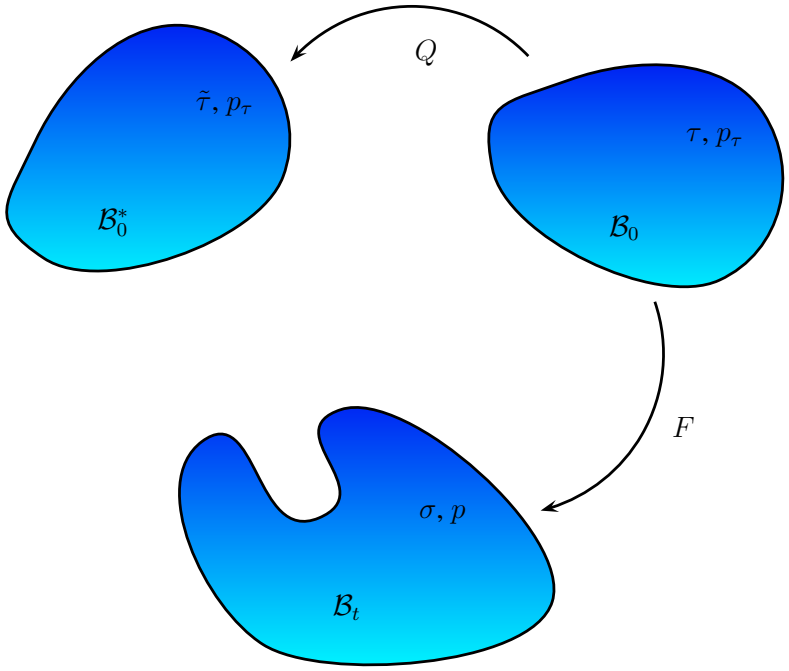

Figure 2.1: The different configurations for the formulation proof of the initially-stressed hyperelastic model based on the invariants theory

Bearing in mind the polar decomposition of the deformation gradient tensor $\boldsymbol{F} = \boldsymbol{RU}$ and by choosing $\boldsymbol{Q} = \boldsymbol{R}^T$, the prior equation leads to:

$$W(\boldsymbol{F}, \boldsymbol{\tau}) = W(\boldsymbol{U}, \boldsymbol{\tau}), \tag{2.10}$$

Since the right Cauchy-Green strain tensor $\boldsymbol{C}$ is a definite positive, consequently, the stretch tensor $\boldsymbol{U}$ which represents the square root tensor of $\boldsymbol{C}$ is unique. Hence, the strain energy W depends on $\boldsymbol{F}$ through the right Cauchy-Green strain tensor $\boldsymbol{C}$. That is why, a new strain energy function $\tilde{W}$ can be defined as:

$$\tilde{W}(\boldsymbol{C}, \boldsymbol{\tau}) = W(\boldsymbol{F}, \boldsymbol{\tau}) = W(\boldsymbol{U}, \boldsymbol{\tau}). \tag{2.11}$$

Consider the configuration $\mathcal{B}_0^*$ as the result of a rotation of the initial configuration $\mathcal{B}_0$ as it is shown in figure (2.1). The rotation is defined by a proper orthogonal tensor $\boldsymbol{Q}$. Focusing on figure (2.1) and exploiting the outcomes of the objectivity principle on the Cauchy stress tensor illustrated in equation (2.4) and the invariance of the strain energy

under superimposed rigid rotations, we derive:

$$\tilde{\boldsymbol{\tau}} = \hat{\boldsymbol{\sigma}}(\boldsymbol{Q}) = \boldsymbol{Q}\boldsymbol{\tau}\boldsymbol{Q}^T, \quad W(\boldsymbol{F}\boldsymbol{Q}^T, \tilde{\boldsymbol{\tau}}) = W(\boldsymbol{F}, \boldsymbol{\tau}) \tag{2.12}$$

As a conclusion, using equation (2.11-2.12), we can deduce that the strain energy $\tilde{W}$ (or W) is an isotropic function of the right Cauchy-Green strain tensor and the initial stress tensor $\boldsymbol{\tau}$ i.e :

$$\tilde{W}(\boldsymbol{Q}\boldsymbol{C}\boldsymbol{Q}^T, \boldsymbol{Q}\boldsymbol{\tau}\boldsymbol{Q}^T) = \tilde{W}(\boldsymbol{C}, \boldsymbol{\tau}), \quad \forall \boldsymbol{Q} \in \mathrm{Orth}^+ \tag{2.13}$$

Thus, using the theory of invariants and based on the works of Spence and Bohler [Spencer 1971, Boehler 1987a], we can get finally an explicit justification for the formulation established by Shams and al [Shams 2011] where the strain energy W is a function of the following invariants:

$$I_1 = \mathrm{tr}(\boldsymbol{C}), \quad I_2 = \frac{1}{2}(\mathrm{tr}(\boldsymbol{C}^2) - \mathrm{tr}(\boldsymbol{C})^2), \quad I_3 = \det(\boldsymbol{C}), \tag{2.14}$$

$$I_1^\tau = \mathrm{tr}(\boldsymbol{\tau}), \quad I_2^\tau = \frac{1}{2}(\mathrm{tr}(\boldsymbol{\tau}^2) - \mathrm{tr}(\boldsymbol{\tau})^2), \quad I_3^\tau = \det(\boldsymbol{\tau}), \tag{2.15}$$

$$I_4 = \mathrm{tr}(\boldsymbol{C}\boldsymbol{\tau}), \quad I_5 = \mathrm{tr}(\boldsymbol{C}^2\boldsymbol{\tau}), \quad I_6 = \mathrm{tr}(\boldsymbol{C}\boldsymbol{\tau}^2), \quad I_7 = \mathrm{tr}(\boldsymbol{C}^2\boldsymbol{\tau}^2). \tag{2.16}$$

So, we can deduce the Cauchy stress tensor expression as:

$$\begin{aligned} J\boldsymbol{\sigma} = {} & 2W_1\boldsymbol{B} + 2W_2(I_1\boldsymbol{B} - \boldsymbol{B}^2) + 2I_3W_3\mathbf{1} + 2W_4\boldsymbol{F}\boldsymbol{\tau}\boldsymbol{F}^T + 2W_5\boldsymbol{F}(\boldsymbol{C}\boldsymbol{\tau} + \boldsymbol{\tau}\boldsymbol{C})\boldsymbol{F}^T \\ & + 2W_6\boldsymbol{F}\boldsymbol{\tau}^2\boldsymbol{F}^T + 2W_7\boldsymbol{F}(\boldsymbol{C}\boldsymbol{\tau} + \boldsymbol{\tau}\boldsymbol{C})\boldsymbol{F}^T, \end{aligned} \tag{2.17}$$

with $W_i = \partial W/\partial I_i$ for $i = 1..7$. In case of incompressible materials, the expression of Cauchy stress tensor is modified to be:

$$\begin{aligned} \boldsymbol{\sigma} = {} & 2W_1\boldsymbol{B} + 2W_2(I_1\boldsymbol{B} - \boldsymbol{B}^2) - p\mathbf{1} + 2W_4\boldsymbol{F}\boldsymbol{\tau}\boldsymbol{F}^T + 2W_5\boldsymbol{F}(\boldsymbol{C}\boldsymbol{\tau} + \boldsymbol{\tau}\boldsymbol{C})\boldsymbol{F}^T \\ & + 2W_6\boldsymbol{F}\boldsymbol{\tau}^2\boldsymbol{F}^T + 2W_7\boldsymbol{F}(\boldsymbol{C}\boldsymbol{\tau} + \boldsymbol{\tau}\boldsymbol{C})\boldsymbol{F}^T, \end{aligned} \tag{2.18}$$

where p is the Lagrange multiplier relative to the incompressibility condition.

2.3.2 Constitutive equation based on the concept of virtual configuration

In biomechanics, there are different methods to estimate qualitatively or quantitatively the residual stress field inside the ex-vivo organs or parts of them. Focusing on the destructive and semi-destructive methods, among the most popular and commonly used approaches to measure the residual stress, we find cutting body into seperate parts, hole drilling, surface grinding and ring coring [Hauk 1997]. For the sake of introducing a constitutive equation modeling the influence of the residual stress on elastic behaviour and inspired by these different experimental approaches, Johnsen and Hoger in [Johnson 1995] have introduced the concept of virtual configuration. The virtual configuration denotes the stress free configuration which may be attainable by a sequence of sectioning and cutting the considered body to release all the residual stress. To clarify the approach of virtual configuration,

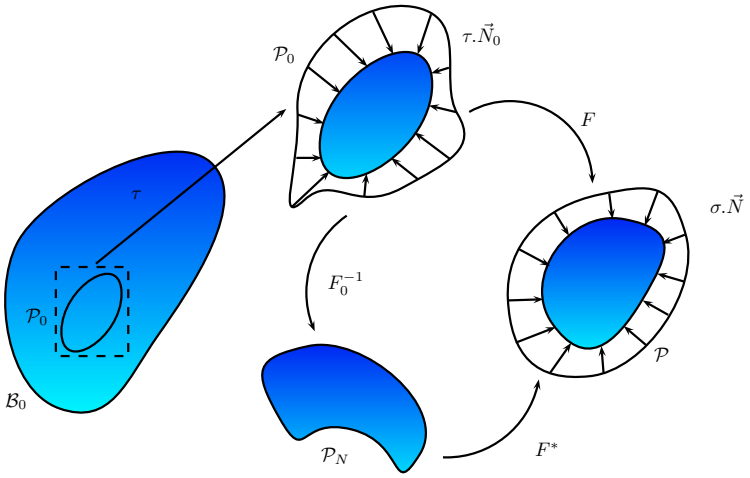

Figure 2.2: The different configurations for the virtual configuration concept

the reference configuration will be denoted as $\mathcal{B}_0$. Let consider $\mathcal{P}_0$ as a material part of the considered body in the reference configuration. Through the deformation gradient $\boldsymbol{F}$, the reference configuration $\mathcal{B}_0$ is mapped into a current configuration denoted by $\mathcal{B}$ and in particular the material part $\mathcal{P}_0$ is transformed into $\mathcal{P}$ as it is illustrated in the figure (2.2). By examining the work of [Johnson 1995], the derivation of the constitutive equation for residual stressed bodies is based on the idea that "for each infinitesimal neighborhood in

the residual stressed body there exists a corresponding stress free configuration". To simplify the derivation of the constitutive equation, Johnson and Hoger have treated first the class of initially-stressed material that can be cut in finite volume to release the residual stress. Let consider the material part $\mathcal{P}$ as one of these parts that will be stress free when it is separated from the rest of the material body. Thus, implicitly, this implies the existence of gradient deformation tensor denoted by $\boldsymbol{F}_0$ that describes the transformation of $\mathcal{P}_0$ into a stress free part denoted by $\mathcal{P}_N$. $\boldsymbol{F}_0$ can be either incompatible tensor in the case of residual stress field presence in the reference configuration or compatible when the internal stress is nothing but a regular elastic initial stress equilibrated by some external tension loadings. Let consider that material body has an elastic behaviour for both transformation from $\mathcal{P}_0$ to $\mathcal{P}$ and from $\mathcal{P}_N$ to $\mathcal{P}_0$. Therefore, the Cauchy stress tensor $\boldsymbol{\sigma}$ in the current configuration and the residual stress $\boldsymbol{\tau}$ defined in the reference configuration become:

$$\boldsymbol{\sigma} = \tilde{\mathcal{T}}(\boldsymbol{F}^*, \vec{X}), \quad \boldsymbol{\tau} = \tilde{\mathcal{T}}(\boldsymbol{F}_0, \vec{X}) \tag{2.19}$$

with $\tilde{\mathcal{T}}$ represents the response function and $\boldsymbol{F}^*$ is the resulting deformation gradient tensor obtained from the transformation of $\mathcal{P}_N$ into $\mathcal{P}$:

$$\boldsymbol{F}^* = \boldsymbol{F}\boldsymbol{F}_0 \tag{2.20}$$

In the rest of this chapter, the dependence of the response function $\tilde{\mathcal{T}}$ through the position will not be shown explicitly unless it is necessary. If the response function is invertible, then the deformation measure $\boldsymbol{F}_0$ can be expressed in function of the residual stress as:

$$\boldsymbol{F}_0 = \tilde{\mathcal{T}}^{-1}(\boldsymbol{\tau}), \tag{2.21}$$

and consequently by using the elastic constitutive equation (2.20-2.21), the constitutive equation describing the residual stress influence on the elastic behaviour can be described through the following constitutive relation:

$$\boldsymbol{\sigma} = \tilde{\mathcal{T}}(\boldsymbol{F}\tilde{\mathcal{T}}^{-1}(\boldsymbol{\tau}), \vec{X}). \tag{2.22}$$

It is important to notice that the prior constitutive equation is independent of the history of the process source of the residual stress field presented in the material. Also, the natural configuration has not to be reachable or known.

Since, the hypothesis of releasing the residual stress field by cutting the material body into finite parts can not stands for the residually stressed materials, in [Johnson 1995], the same constitutive equation (2.22) can be derived reasoning on the infinitesimal neighborhood of a material point and the same way of Cauchy tetrahedron argument. In this case, every material point in the reference configuration has a corresponding material point in the stress free configuration. The latter will be the sum of all these points which are not necessarily the one near the other. The stress free configuration in this case is just a mathematical concept. That's why the term "virtual" was employed to denote this method.

2.4 Restrictions in initially-stressed materials modeling

2.4.1 Initial stress symmetry (ISS)

The model based on the theory of invariants illustrated above is quite general without any physical restriction. That is why, in this section and the following one, we will present the different mathematical conditions based on some physical restrictions that specify more the proposed formulation above. The first restriction is based on the work of Gower and al in [Gower 2015] and it is denoted initial Stress Symmetry (ISS). If we consider the response function $\hat{\boldsymbol{\xi}}$, then the ISS condition can be expressed as:

$$\boldsymbol{\sigma} = \hat{\boldsymbol{\xi}}(\boldsymbol{F}, \boldsymbol{\tau}), \quad \boldsymbol{\tau} = \hat{\boldsymbol{\xi}}(\boldsymbol{F}^{-1}, \boldsymbol{\sigma}), \quad \forall \boldsymbol{F}, \forall \boldsymbol{\tau}, \tag{2.23}$$

whereas in the case of incompressible materials this conditions is equivalent to:

$$\boldsymbol{\sigma} = \hat{\boldsymbol{\xi}}(\boldsymbol{F}, \boldsymbol{\tau}, p), \quad \boldsymbol{\tau} = \hat{\boldsymbol{\xi}}(\boldsymbol{F}^{-1}, \boldsymbol{\sigma}, p_\tau), \tag{2.24}$$

$$p = \hat{p}(\boldsymbol{\sigma}, \boldsymbol{F}, \boldsymbol{\tau}), \quad p_\tau = \hat{p}(\boldsymbol{\tau}, \boldsymbol{F}, \boldsymbol{\sigma}), \tag{2.25}$$

with $\hat{p}$ is the response function relative to the Lagrange multiplier associated to the incompressibility condition and p_τ is the Lagrange multiplier defined on the reference configuration $\mathcal{B}_0$. The ISS condition is based on the symmetry of the response function and implies that the behaviour modeling is independent of the reference configuration choice. If the equations in (2.23-2.25) are rewritten in a way where they are incorporated one in the other, then the ISS restriction implies:

$$\boldsymbol{\tau} = \hat{\boldsymbol{\xi}}(\boldsymbol{F}^{-1}, \hat{\boldsymbol{\xi}}(\boldsymbol{F}, \boldsymbol{\tau}, \hat{p}(\boldsymbol{\sigma}, \boldsymbol{F}, \boldsymbol{\tau})), p_\tau), \quad \forall \boldsymbol{F}, \quad \forall \boldsymbol{\tau}. \tag{2.26}$$

Hence, based on some compulsory algebraic calculations, the prior condition can be summarized into nine mathematical equations that must be satisfied by the strain energy W (for more details, see [Gower 2015] and the relative electronic supplementary material).

2.4.2 Initial stress reference indifference (ISRI)

Whereas the ISRI restriction is based on the reversibility of the response function, Gower and al in [Gower 2017] have added a new restriction based on the energy conservation (or decomposition) and it has been denoted as ISRI which stands for the initial stress reference indifference. In other words this supplementary condition is established to ensure that the stress-strain relation in the presence of an initial stress field is independent of the choice of the reference configuration where the initial stress field is defined. Based on energetic perspective, the ISRI restriction can be formulated in terms of the strain energy W which must fulfill:

$$W(\hat{\boldsymbol{F}}\bar{\boldsymbol{F}}, \boldsymbol{\tau}) = \det(\bar{\boldsymbol{F}}) W(\hat{\boldsymbol{F}}, \tilde{\boldsymbol{\sigma}}(\bar{\boldsymbol{F}}, \boldsymbol{\tau})), \quad \forall \boldsymbol{\tau}, \quad \forall \{\bar{\boldsymbol{F}}, \hat{\boldsymbol{F}}\}, \tag{2.27}$$

where $\boldsymbol{\tau}$ is the Cauchy stress tensor in a chosen reference configuration and $\tilde{\boldsymbol{\sigma}}(\bar{\boldsymbol{F}}, \boldsymbol{\tau})$ denotes

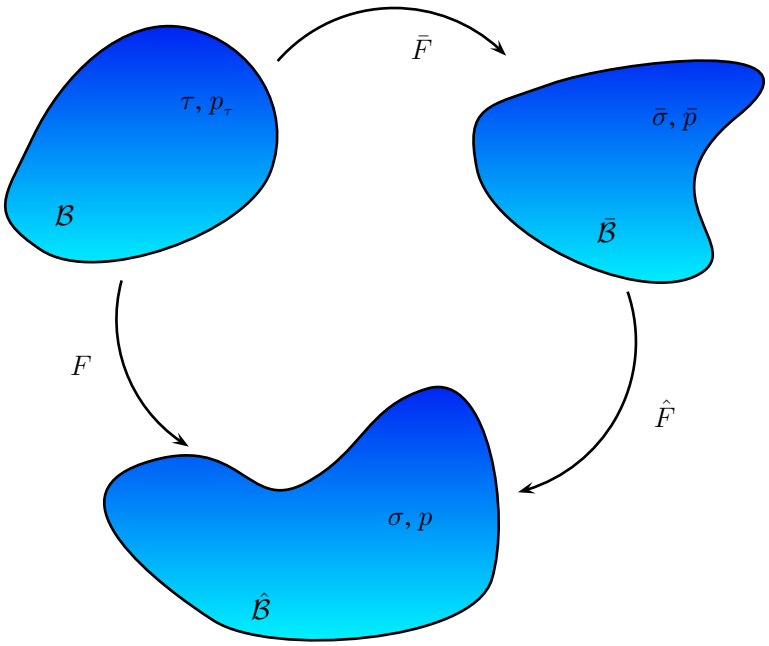

Figure 2.3: The different configurations illustrating the ISRI restriction.

the Cauchy stress tensor defined on a new configuration result of the transformation of the configuration, where the stress tensor $\boldsymbol{\tau}$ is defined, by a transformation relative to the gradient transformation tensor $\bar{\boldsymbol{F}}$. The ISRI condition (2.27) is a result of the conservation of the strain energy which can be illustrated through the following equation:

$$\int_{\mathcal{B}_0} W(\hat{\boldsymbol{F}}\bar{\boldsymbol{F}}, \boldsymbol{\tau}) dV = \int_{\bar{\mathcal{B}}} W(\hat{\boldsymbol{F}}, \boldsymbol{\sigma}(\bar{\boldsymbol{F}}, \boldsymbol{\tau})) d\bar{V}, \tag{2.28}$$

where $\mathcal{B}_0$ is the reference configuration where the initial stress field $\boldsymbol{\tau}$ is defined, and $\bar{\mathcal{B}}$ is the image of the configuration $\mathcal{B}_0$ by the mapping transformation relied to the transformation gradient tensor $\bar{\boldsymbol{F}}$. Thus the infinitesimal volume elements in the two configurations are connected by:

$$d\bar{V} = \det(\bar{\boldsymbol{F}}) dV. \tag{2.29}$$

By considering the strong form of equation (2.28) , the ISRI condition illustrated through equation (2.27) is easily obtained. The condition (2.27) can be expressed in terms of the Cauchy stress response function as the following:

$$\tilde{\boldsymbol{\sigma}}(\hat{\boldsymbol{F}}\bar{\boldsymbol{F}}, \boldsymbol{\tau}) = \tilde{\boldsymbol{\sigma}}(\hat{\boldsymbol{F}}, \tilde{\boldsymbol{\sigma}}(\bar{\boldsymbol{F}}, \boldsymbol{\tau})), \quad \forall \boldsymbol{\tau}, \quad \forall \hat{\boldsymbol{F}} \text{ and } \forall \bar{\boldsymbol{F}}. \tag{2.30}$$

Proof: If we consider the decomposition of the transformation gradient tensor as it is illustrated in the figure (2.3), then it leads to

$$\boldsymbol{F} = \hat{\boldsymbol{F}}\bar{\boldsymbol{F}}, \tag{2.31}$$

and by consequence, the ratio of volume change can be expressed in function of the same ratios defined between the different configurations as:

$$J = \det(\boldsymbol{F}) = \det(\hat{\boldsymbol{F}})\det(\bar{\boldsymbol{F}}) = \hat{J}\bar{J}. \tag{2.32}$$

Now, the Cauchy stress tensor defined in the configuration $\hat{\mathcal{B}}$ can be expressed in terms of the strain energy relatively to both the configurations $\mathcal{B}_0$ and $\bar{\mathcal{B}}$ in the following way:

$$J\tilde{\boldsymbol{\sigma}}(\hat{\boldsymbol{F}}\bar{\boldsymbol{F}}, \boldsymbol{\tau}) = \frac{\partial W}{\partial \boldsymbol{F}}(\boldsymbol{F}, \boldsymbol{\tau})\boldsymbol{F}^T, \tag{2.33}$$

$$\hat{J}\tilde{\boldsymbol{\sigma}}(\hat{\boldsymbol{F}}, \tilde{\boldsymbol{\sigma}}(\bar{\boldsymbol{F}}, \boldsymbol{\tau})) = \frac{\partial W}{\partial \hat{\boldsymbol{F}}}(\hat{\boldsymbol{F}}, \tilde{\boldsymbol{\sigma}}(\bar{\boldsymbol{F}}, \boldsymbol{\tau}))\hat{\boldsymbol{F}}^T. \tag{2.34}$$

Using the ISRI restriction illustrated by equation (2.27) and exploiting the definition of the Cauchy stress tensor in equation (2.34) side to side with some calculus properties for the tensor fields, it leads to:

$$J\tilde{\boldsymbol{\sigma}}(\hat{\boldsymbol{F}}\bar{\boldsymbol{F}}, \boldsymbol{\tau}) = \bar{J}\frac{\partial W}{\partial \hat{\boldsymbol{F}}}(\hat{\boldsymbol{F}}, \tilde{\boldsymbol{\sigma}}(\bar{\boldsymbol{F}}, \boldsymbol{\tau}))\bar{\boldsymbol{F}}^{-T}\boldsymbol{F}^T = J\tilde{\boldsymbol{\sigma}}(\hat{\boldsymbol{F}}, \tilde{\boldsymbol{\sigma}}(\bar{\boldsymbol{F}}, \boldsymbol{\tau})). \tag{2.35}$$

Hence, the equivalent form of the ISRI restriction illuminated by equation (2.30) is finally obtained.

In the incompressible case, the ISRI condition expressed in terms of the Cauchy stress response function and illustrated by equation (2.30) (like it was done in [Gower 2017]), needs to be adapted to take account of the Lagrange multiplier compatibility. Hence, following figure (2.2), it becomes:

$$\tilde{\boldsymbol{\sigma}}(\hat{\boldsymbol{F}}\bar{\boldsymbol{F}}, \boldsymbol{\tau}, p) = \tilde{\boldsymbol{\sigma}}(\hat{\boldsymbol{F}}, \tilde{\boldsymbol{\sigma}}(\bar{\boldsymbol{F}}, \boldsymbol{\tau}, \bar{p}), p), \quad \forall\boldsymbol{\tau}, \quad \forall\hat{\boldsymbol{F}} \text{ and } \forall\bar{\boldsymbol{F}}, \tag{2.36}$$

$$p = \tilde{p}(\boldsymbol{\sigma}, \hat{\boldsymbol{F}}\bar{\boldsymbol{F}}, \boldsymbol{\tau}) = \tilde{p}(\boldsymbol{\sigma}, \hat{\boldsymbol{F}}, \bar{\boldsymbol{\sigma}}), \quad \forall\boldsymbol{\tau}, \quad \forall\hat{\boldsymbol{F}} \text{ and } \forall\bar{\boldsymbol{F}}, \tag{2.37}$$

with

$$\bar{p} = \tilde{p}(\bar{\boldsymbol{\sigma}}, \bar{\boldsymbol{F}}, \boldsymbol{\tau}), \tag{2.38}$$

$$\bar{\boldsymbol{\sigma}} = \tilde{\boldsymbol{\sigma}}(\bar{\boldsymbol{F}}, \boldsymbol{\tau}, \bar{p}). \tag{2.39}$$

The ISS and ISRI restrictions are based each one on a different perspective: the first one comes from the reversibility of the response function and its symmetry, whereas the prior restriction is based on energetic constraint decomposition. Although the two restrictions seem to be justified with different arguments, they are indeed equivalent. The proof of such a property is trivial if we consider the decomposition as it is illustrated in the figure (2.2), and the similarity of the two stress Cauchy response functions $\boldsymbol{\xi}$ and $\tilde{\boldsymbol{\sigma}}$ i.e $(\xi(.,.,.) \equiv \tilde{\boldsymbol{\sigma}}(.,.,.))$.

2.5 Link between the initial stress field and the anisotropy

The presence of the initial stress field can be both a source of anisotropy and heterogeneity. To treat such a point, in the litterature, to our knowledge, Noll and Colemann were the first to investigate the possible residual stress form in an elastic body with a particular material symmetry [Coleman 1964]. Such investigation was based on an interesting property: the initial stress tensor commutes with the elements of the symmetry group of the considered material i.e

$$\boldsymbol{\tau}\boldsymbol{Q} = \boldsymbol{Q}\boldsymbol{\tau}, \quad \forall \boldsymbol{Q} \in \mathcal{G}, \tag{2.40}$$

where $\mathcal{G}$ denotes the group of symmetry elements relative to the considered material body. Based on the work of Coleman and Noll [Coleman 1964], Anne Hoger in [Hoger 1985] exploited the equilibrium equation and the boundary conditions for a residual stress field, to get more specific properties about the form of the residual stress tensor for some classes of material symmetries. Conversely, in this section, based on the initial stress spectral form, we intend to study its influence on the generated anisotropy for an isotropic material in the natural configuration which is defined as the configuration where the initial stress field vanishes. Since the initial stress field is defined to be the Cauchy stress tensor in the reference configuration, then it has to be symmetric and by using the spectral theorem, we

get:

$$\boldsymbol{\tau} = \tau_1 \vec{L}_1 \otimes \vec{L}_1 + \tau_2 \vec{L}_2 \otimes \vec{L}_2 + \tau_3 \vec{L}_3 \otimes \vec{L}_3, \tag{2.41}$$

with

$$\vec{L}_1 \otimes \vec{L}_1 + \vec{L}_2 \otimes \vec{L}_2 + \vec{L}_3 \otimes \vec{L}_3 = \mathbf{1}, \quad \vec{L}_i.\vec{L}_j = \delta_{ij}, \quad i,j = 1,2,3 \tag{2.42}$$

where $(\tau_i, i = 1..3)$ and $(\vec{L}_i, i = 1..3)$ are respectively the eigenvalues and the relative eigenvectors of the initial stress field $\boldsymbol{\tau}$ and δ denotes the Kronecker symbol. Based on the theory of invariants as it was illustrated above, added to the isotropic invariants (I_1, I_2, I_3) and the invariants of the initial stress field $(I_1^\tau, I_2^\tau, I_3^\tau)$, the strain energy depends also on the following set of invariants which can be expressed differently as:

$$I_4 = (\tau_1 - \tau_3)\tilde{I}_4 + (\tau_2 - \tau_3)\tilde{I}_6 + \tau_3 \tilde{I}_1, \tag{2.43}$$
$$I_5 = (\tau_1 - \tau_3)\tilde{I}_5 + (\tau_2 - \tau_3)\tilde{I}_7 + \tau_3(\tilde{I}_1^2 - 2\tilde{I}_2), \tag{2.44}$$
$$I_6 = (\tau_1^2 - \tau_3^2)\tilde{I}_4 + (\tau_2^2 - \tau_3^2)\tilde{I}_6 + \tau_3^2 \tilde{I}_1, \tag{2.45}$$
$$I_7 = (\tau_1^2 - \tau_3^2)\tilde{I}_5 + (\tau_2^2 - \tau_3^2)\tilde{I}_7 + \tau_3^2(\tilde{I}_1^2 - 2\tilde{I}_2) \tag{2.46}$$

with

$$\tilde{I}_1 = I_1, \quad \tilde{I}_2 = I_2, \quad \tilde{I}_3 = I_3, \tag{2.47}$$
$$\tilde{I}_4 = \vec{L}_1.\boldsymbol{C}.\vec{L}_1, \quad \tilde{I}_5 = \vec{L}_1.\boldsymbol{C}^2.\vec{L}_1, \tag{2.48}$$
$$\tilde{I}_6 = \vec{L}_2.\boldsymbol{C}.\vec{L}_2, \quad \tilde{I}_7 = \vec{L}_2.\boldsymbol{C}^2.\vec{L}_2. \tag{2.49}$$

Thus the strain energy which depends previously on the 10 different invariants as expressed in the section related to the modeling of hyperelastic initially-stressed materials, can be formulated as function of a new set of invariants equivalent to the previous ones, so we can write:

$$W(I_1, I_2, ..., I_7, I_1^\tau, I_2^\tau, I_3^\tau) = \tilde{W}(\tilde{I}_1, ..., \tilde{I}_7, \tau_1, \tau_2, \tau_3). \tag{2.50}$$

It is clear that the new set of invariants are analogous to those of the orthotropic material where the fibers directions are described by 2 eigenvectors of the initial stress field and the invariant relative to the shear between the two families of fibers is neglected. Thus, based

on the new set of invariants and theirs relations with the previous ones, we can deduce the following different material symmetries for a initially-stressed hyperelastic material where the material body is considered to be isotropic in the natural configuration:

- If $\boldsymbol{\tau}$ is spherical tensor (i.e $\boldsymbol{\tau} = \tau\mathbf{1}$), then the initially-stressed material has an isotropic behaviour and in the reference configuration the material body is subject to the pressure field τ.

- if $\boldsymbol{\tau}$ has only two different eigenvalues (i.e $\boldsymbol{\tau} = \tau_1\vec{L}_1\otimes\vec{L}_1+\tau_2(\vec{L}_2\otimes\vec{L}_2+\vec{L}_3\otimes\vec{L}_3)$), then the initially-stressed material has an analogous behaviour to an isotropic transverse material where the fibers direction is parallel to the eigenvector $\vec{L}_1$ and they are subjected to the tension or compression stress τ_1 along the fibers orientation in the reference configuration.

- if the initial stress field $\boldsymbol{\tau}$ has three different eigenvalues, the initially-stressed material has an analogous behaviour to an orthotropic material where the two families of fibers are described by two among the three eigenvectors and the shear invariant (I_9) influence is neglected. Besides that, in the reference configuration every fiber is subjected to the tension stress equal to the corresponding eigenvalue of the initial stress field.

The new formulation of the initially-stressed hyperelastic materials gives more physical sense to the different invariants and presents a clear analogy between the behaviour of both anisotropic fibrous materials and the initially-stressed hyperelastic ones. Thus using the new strain energy $\tilde{W}$, the Cauchy stress tensor becomes:

$$\begin{aligned} J\boldsymbol{\sigma} = {} & 2\tilde{W}_1\boldsymbol{B} + 2\tilde{W}_2(\tilde{I}_1\boldsymbol{B} - \boldsymbol{B}^2) - p\mathbf{1} + 2\tilde{W}_4\vec{l_1}\otimes\vec{l_1} + 2\tilde{W}_5(\boldsymbol{B}\vec{l_1}\otimes\vec{l_1} + \vec{l_1}\otimes\boldsymbol{B}\vec{l_1}) \\ & + 2\tilde{W}_6\vec{l_2}\otimes\vec{l_2} + 2\tilde{W}_7(\boldsymbol{B}\vec{l_2}\otimes\vec{l_2} + \vec{l_2}\otimes\boldsymbol{B}\vec{l_2}), \end{aligned} \tag{2.51}$$

with

$$\vec{l_i} = \boldsymbol{F}\vec{L}_i, \quad i = 1..2, \tag{2.52}$$

and where $\tilde{W}_i = \partial\tilde{W}/\partial I_i, i = 1..7$ and $p = -2\tilde{W}_3\tilde{I}_3$ for compressible materials whereas it represents the Lagrange multiplier when the incompressibility condition holds. To ensure the compatibility of the initial stress tensor definition, some conditions on the strain energy

must be satisfied:

$$2\tilde{W}_1^\circ + 4\tilde{W}_2^\circ - p_\tau = \tau_3, \tag{2.53}$$

$$2\tilde{W}_4^\circ + 4\tilde{W}_5^\circ = \tau_1 - \tau_3, \tag{2.54}$$

$$2\tilde{W}_6^\circ + 4\tilde{W}_7^\circ = \tau_2 - \tau_3, \tag{2.55}$$

where $\tilde{W}_i^\circ$ represents the different derivatives of the strain energy $\tilde{W}$ evaluated in the reference configuration.

2.6 Anne Hoger formulation

In the scope of small deformation the linearization of the dependence of both Cauchy and First Piola-Kirchhoff stress tensors relative to the displacement gradient tensor leads to:

$$\boldsymbol{\sigma} = \hat{\boldsymbol{\sigma}}(\boldsymbol{F}) = \hat{\boldsymbol{\sigma}}(\mathbf{1} + \boldsymbol{H}) = \boldsymbol{\tau} + \mathcal{L}[\boldsymbol{H}] + o(\boldsymbol{H}), \quad \mathcal{L}[\boldsymbol{H}] = \frac{\partial \hat{\boldsymbol{\sigma}}}{\partial \boldsymbol{H}}(\mathbf{1})[\boldsymbol{H}], \tag{2.56}$$

$$\boldsymbol{S} = \hat{\boldsymbol{S}}(\boldsymbol{F}) = \hat{\boldsymbol{S}}(\mathbf{1} + \boldsymbol{H}) = \boldsymbol{\tau} + \mathcal{C}[H] + o(\boldsymbol{H}), \quad \mathcal{C}[H] = \frac{\partial \hat{\boldsymbol{S}}}{\partial \boldsymbol{H}}(\mathbf{1})[\boldsymbol{H}], \tag{2.57}$$

where $\mathcal{L}$ and $\mathcal{C}$ are called the elasticity tensors relative respectively to the stress measures $\boldsymbol{\sigma}$ and $\boldsymbol{S}$, whereas $\boldsymbol{H}$ denotes the displacement gradient tensor. With the linearization of (2.3) and using equations (2.56-2.57), we can deduce:

$$\mathcal{C}[H] = -\boldsymbol{\tau}\boldsymbol{H}^T + \mathrm{tr}(\boldsymbol{H})\boldsymbol{\tau} + \mathcal{L}[H] + o(\boldsymbol{H}) \tag{2.58}$$

Both of the two elastic tensors depend on the residual stress and they are not equal contrary to the case of classic theory of linear elasticity in absence of residual stress. Based on some results of Gurtin in [Gurtin 1982], Hoger in [Hoger 1985] deduced the following mathematical properties of the elastic tensor relative to the first Piola-Kirchhoff stress tensor:

$$\mathcal{C}[\boldsymbol{W}] = \boldsymbol{W}\boldsymbol{\tau}, \quad \forall \boldsymbol{\omega} \in \mathrm{Skw(Lin)}, \tag{2.59}$$

$$\mathrm{skw}\ \ \mathcal{C}[\boldsymbol{\epsilon}] = \frac{1}{2}[\boldsymbol{\epsilon}\boldsymbol{\tau} - \boldsymbol{\tau}\boldsymbol{\epsilon}], \quad \forall \boldsymbol{\epsilon} \in \mathrm{Sym(Lin)}, \tag{2.60}$$

$$\mathcal{C}[\boldsymbol{Q}\boldsymbol{H}\boldsymbol{Q}^T] = \boldsymbol{Q}\mathcal{C}[H]\boldsymbol{Q}^T, \quad \forall \boldsymbol{H} \in \mathrm{Lin}, \quad \forall \boldsymbol{Q} \in \mathcal{G}, \tag{2.61}$$

where Lin denotes the second order tensor space, Skw(Lin) and Sym(Lin) are respectively the space of skew-symmetric and symmetric second order tensors spaces. If the material is hyperelastic, then we get the fourth property:

$$\mathcal{C}[\boldsymbol{H}_2] : \boldsymbol{H}_1 = \mathcal{C}[\boldsymbol{H}_1] : \boldsymbol{H}_2^T, \quad \forall \boldsymbol{H}_1, \boldsymbol{H}_2 \in \text{Lin}, \tag{2.62}$$

where the operator ':' stands for the double contraction of second order tensors which satisfies:

$$\boldsymbol{H}_2 : \boldsymbol{H}_1 = \text{tr}(\boldsymbol{H}_2^T \boldsymbol{H}_1), \quad \forall \boldsymbol{H}_1, \boldsymbol{H}_2 \in \text{Lin}. \tag{2.63}$$

Using the previous properties of the elastic tensor mentioned above, then the linearized form of the first Piola Kirchhoff stress tensor becomes:

$$\boldsymbol{S} = \boldsymbol{\tau} + \boldsymbol{H}\boldsymbol{\tau} - \frac{1}{2}(\boldsymbol{\tau}\boldsymbol{\epsilon} + \boldsymbol{\epsilon}\boldsymbol{\tau}) + \boldsymbol{L}[\boldsymbol{\epsilon}] + o(\boldsymbol{H}), \tag{2.64}$$

where $\boldsymbol{L}[.]$ is called by Hoger the "incremental elastic operator" and it is defined as:

$$\boldsymbol{L}[\boldsymbol{H}] = \text{sym} \ \ \mathcal{C}[H], \quad \forall \boldsymbol{H} \in \text{Lin}. \tag{2.65}$$

It is important to notice that there is no general explicit form for the operator $\boldsymbol{L}[.]$ in the scope of small deformations. Hoger proposed in [Hoger 1986] a simple form for the incremental elastic operator like the one for isotropic material in absence of residual stresses, so we can write:

$$\boldsymbol{L}[\boldsymbol{\epsilon}] = 2\mu\boldsymbol{\epsilon} + \lambda \text{tr}(\boldsymbol{\epsilon})\boldsymbol{1}, \tag{2.66}$$

where μ and λ are the Lamé coefficients. In the objective to derive a more general form for the Hartig law, Man in [Man 1998] has proposed the following stress-strain relation:

$$\begin{aligned}\boldsymbol{S} = \boldsymbol{\tau} + \boldsymbol{H}\boldsymbol{\tau} + \beta_1 \text{tr}(\boldsymbol{\epsilon})\text{tr}(\boldsymbol{\tau})\boldsymbol{1} + \beta_2 \text{tr}(\boldsymbol{\tau})\boldsymbol{\epsilon} + \beta_3(\text{tr}(\boldsymbol{\epsilon})\boldsymbol{\tau} + \text{tr}(\boldsymbol{\epsilon}\boldsymbol{\tau})\boldsymbol{1}) \\ + \beta_4(\boldsymbol{\tau}\boldsymbol{\epsilon} + \boldsymbol{\epsilon}\boldsymbol{\tau}) + 2\mu\boldsymbol{\epsilon} + \lambda \text{tr}(\boldsymbol{\epsilon})\boldsymbol{1}.\end{aligned} \tag{2.67}$$

Respecting the formulation introduced in equation (2.64), Robertson has proposed a more simple model in [Robertson 1997] where the stress-strain relation can be expressed as:

$$\boldsymbol{S} = \boldsymbol{\tau} + \boldsymbol{H}\boldsymbol{\tau} + 2\mu\boldsymbol{\epsilon} + \lambda \mathrm{tr}(\boldsymbol{\epsilon})\mathbf{1}. \tag{2.68}$$

As illustrated above, multiple tentatives took place for the sake of initially-stressed materials modeling in the scope of small deformations. Despite the generality of Anne Hoger formulation, we still need to look for a more general explicit form for the incremental elastic operator which will be the subject of the next section.

2.7 General model for linear elastic initially-stressed material

Here, in this section, our objective is to give a more explicit general model for linear elastic initially-stressed material. Returning to the formulation established by Hoger in equation (2.64) let's define:

$$\boldsymbol{G}[E] = -\frac{1}{2}(\boldsymbol{\tau}\boldsymbol{\epsilon} + \boldsymbol{\epsilon}\boldsymbol{\tau}) + \boldsymbol{L}[\boldsymbol{\epsilon}]. \tag{2.69}$$

Then exploiting the concept of polynomial isotropic tensor function defined by Spencer [Boehler 1987b], a possible representation of the operator $\boldsymbol{G}[.]$ in the first order on $\boldsymbol{\epsilon}$ could be as a function of:

$$\mathbf{1}, \quad \boldsymbol{\tau}, \quad \boldsymbol{\epsilon}, \quad \boldsymbol{\tau}\boldsymbol{\epsilon} + \boldsymbol{\epsilon}\boldsymbol{\tau}, \quad \boldsymbol{\tau}\boldsymbol{\epsilon}\boldsymbol{\tau}, \quad \boldsymbol{\tau}^2\boldsymbol{\epsilon} + \boldsymbol{\epsilon}\boldsymbol{\tau}^2, \quad \boldsymbol{\tau}^2\boldsymbol{\epsilon}\boldsymbol{\tau} + \boldsymbol{\tau}\boldsymbol{\epsilon}\boldsymbol{\tau}^2, \quad \boldsymbol{\tau}^2\boldsymbol{\epsilon}\boldsymbol{\tau}^2, \tag{2.70}$$

and of the invariants:

$$I_1^{\tau}, \quad I_2^{\tau}, \quad I_3^{\tau}, \quad \mathrm{tr}(\boldsymbol{\epsilon}), \quad \mathrm{tr}(\boldsymbol{\epsilon}\boldsymbol{\tau}), \quad \mathrm{tr}(\boldsymbol{\epsilon}\boldsymbol{\tau}^2), \tag{2.71}$$

where

$$I_1^{\tau} = \mathrm{tr}(\boldsymbol{\tau}), \quad I_2^{\tau} = \frac{1}{2}((I_1^{\tau})^2 - \mathrm{tr}(\boldsymbol{\tau}^2)), \quad I_3^{\tau} = \det(\boldsymbol{\tau}). \tag{2.72}$$

Such representation implies implicitly the isotropic behaviour of the material in the natural configuration. In this section, we would like to exploit the work of Gower et al in [Gower 2017] being more consistent to derive a more general explicit form for the elastic tensor taking account of the initial stress influence.

If we consider a second order tensor $\boldsymbol{A}$, then using the theorem of Cayley Hamilton, $\boldsymbol{A}$ must satisfy:

$$\boldsymbol{A}^3 - I_1^A \boldsymbol{A}^2 + I_2^A \boldsymbol{A} - I_3^A \mathbf{1} = \mathbf{0}, \tag{2.73}$$

with

$$I_1^A = \mathrm{tr}(\boldsymbol{A}), \quad I_2^A = \frac{1}{2}((I_1^A)^2 - \mathrm{tr}(\boldsymbol{A}^2)), \quad I_3^A = \det(\boldsymbol{A}). \tag{2.74}$$

Expressing the tensor $A = \gamma\boldsymbol{\tau} + \boldsymbol{\epsilon}$, then using the identities of Cayley Hamilton in equation (2.73), for the order γ^2 the same equation as it is mentioned in [Gower 2017] is obtained:

$$\begin{aligned}\boldsymbol{\tau}\boldsymbol{\epsilon}\boldsymbol{\tau} = &-[\boldsymbol{\tau}^2\boldsymbol{\epsilon} + \boldsymbol{\epsilon}\boldsymbol{\tau}^2] + I_1^\tau[\boldsymbol{\tau}\boldsymbol{\epsilon} + \boldsymbol{\epsilon}\boldsymbol{\tau}] - I_2^\tau\boldsymbol{\epsilon} - [I_1^\tau \mathrm{tr}(\boldsymbol{\epsilon} - \mathrm{tr}(\boldsymbol{\epsilon}\boldsymbol{\tau})]\boldsymbol{\tau} - \mathrm{tr}(\boldsymbol{\epsilon})\boldsymbol{\tau}^2 \\ &+ [\mathrm{tr}(\boldsymbol{\epsilon}\boldsymbol{\tau}^2) - I_1^\tau \mathrm{tr}(\boldsymbol{\epsilon}\boldsymbol{\tau}) + I_2^\tau \mathrm{tr}(\boldsymbol{\epsilon})]\mathbf{1} + \boldsymbol{o}(\boldsymbol{\epsilon}).\end{aligned} \tag{2.75}$$

Exploiting the prior equation (2.75) and the theorem of Cayley Hamilton for the initial stress tensor $\boldsymbol{\tau}$, we can derive:

$$\begin{aligned}\boldsymbol{\tau}^2\boldsymbol{\epsilon}\boldsymbol{\tau} + \boldsymbol{\tau}\boldsymbol{\epsilon}\boldsymbol{\tau}^2 &= I_1^\tau\boldsymbol{\tau}\boldsymbol{\epsilon}\boldsymbol{\tau} - I_3^\tau\boldsymbol{\epsilon} + [\mathrm{tr}(\boldsymbol{E}\boldsymbol{\tau}) - I_1^\tau \mathrm{tr}(\boldsymbol{E})]\boldsymbol{\tau}^2 \\ &\quad + [\mathrm{tr}(\boldsymbol{E}\boldsymbol{\tau}^2) - I_1^\tau \mathrm{tr}(\boldsymbol{E}\boldsymbol{\tau}) + I_2^\tau \mathrm{tr}(\boldsymbol{E})]\boldsymbol{\tau}, \qquad (2.76) \\ \boldsymbol{\tau}^2\boldsymbol{\epsilon}\boldsymbol{\tau}^2 &= I_2^\tau\boldsymbol{\tau}\boldsymbol{\epsilon}\boldsymbol{\tau} - I_3^\tau[\boldsymbol{E}\boldsymbol{\tau} + \boldsymbol{\tau}\boldsymbol{E}] \\ &\quad + [\mathrm{tr}(\boldsymbol{E}\boldsymbol{\tau}) - I_1^\tau \mathrm{tr}(\boldsymbol{E})][I_1^\tau\boldsymbol{\tau}^2 - I_2^\tau\boldsymbol{\tau} + I_3^\tau\mathbf{1}] \\ &\quad + [\mathrm{tr}(\boldsymbol{E}\boldsymbol{\tau}^2) - I_1^\tau \mathrm{tr}(\boldsymbol{E}\boldsymbol{\tau}) + I_2^\tau \mathrm{tr}(\boldsymbol{E})]\boldsymbol{\tau}^2. \qquad (2.77)\end{aligned}$$

Contrary to what is said in [Gower 2017], using equation (2.75), we can not express $\mathrm{tr}(\boldsymbol{E}\boldsymbol{\tau}^2)$ as a function of the rest of invariant in equation (2.71). Consequently, the second order linear operator $\boldsymbol{G}[.]$ can be explicitly expressed as:

$$\begin{aligned}\boldsymbol{G}[\boldsymbol{E}] = &[\alpha_1 \mathrm{tr}(\boldsymbol{E}) + \alpha_2 \mathrm{tr}(\boldsymbol{E}\boldsymbol{\tau}) + \alpha_3 \mathrm{tr}(\boldsymbol{E}\boldsymbol{\tau}^2)]\mathbf{1} + [\alpha_4 \mathrm{tr}(\boldsymbol{E}) + \alpha_5 \mathrm{tr}(\boldsymbol{E}\boldsymbol{\tau}) + \alpha_6 \mathrm{tr}(\boldsymbol{E}\boldsymbol{\tau}^2)]\boldsymbol{\tau} \\ &+ [\alpha_7 \mathrm{tr}(\boldsymbol{E}) + \alpha_8 \mathrm{tr}(\boldsymbol{E}\boldsymbol{\tau}) + \alpha_9 \mathrm{tr}(\boldsymbol{E}\boldsymbol{\tau}^2)]\boldsymbol{\tau}^2 + \alpha_{10}(\boldsymbol{\epsilon}\boldsymbol{\tau} + \boldsymbol{\tau}\boldsymbol{\epsilon}) + \alpha_{11}(\boldsymbol{\epsilon}\boldsymbol{\tau}^2 + \boldsymbol{\tau}^2\boldsymbol{\epsilon}) \\ &+ \alpha_{12}\boldsymbol{\epsilon} + \boldsymbol{o}(\boldsymbol{E}),\end{aligned} \tag{2.78}$$

where $\{\alpha_i, \quad i \in [1..12]\}$ are all functions of the initial stress invariants (I_1^τ, I_2^τ, I_3^τ). It is clear that the new tensorial function $\boldsymbol{G}[.]$ has to satisfy the same property of $\mathcal{C}[.]$ in

equation (2.62) for hyperelastic material, and hence it must verify:

$$\alpha_2 = \alpha_4, \quad \alpha_3 = \alpha_7, \quad \alpha_6 = \alpha_8. \tag{2.79}$$

As a conclusion for this section the first Piola Kirchhoff stress tensor can be expressed in more general explicit form:

$$\begin{aligned}\boldsymbol{S} = \boldsymbol{\tau} + \boldsymbol{H}\boldsymbol{\tau} + [\alpha_1 \mathrm{tr}(\boldsymbol{E}) + \alpha_2 \mathrm{tr}(\boldsymbol{E}\boldsymbol{\tau}) + \alpha_3 \mathrm{tr}(\boldsymbol{E}\boldsymbol{\tau}^2)]\mathbf{1} \\ + [\alpha_2 \mathrm{tr}(\boldsymbol{E}) + \alpha_5 \mathrm{tr}(\boldsymbol{E}\boldsymbol{\tau}) + \alpha_6 \mathrm{tr}(\boldsymbol{E}\boldsymbol{\tau}^2)]\boldsymbol{\tau} \\ + \alpha_{12}\boldsymbol{\epsilon} + [\alpha_3 \mathrm{tr}(\boldsymbol{E}) + \alpha_6 \mathrm{tr}(\boldsymbol{E}\boldsymbol{\tau}) + \alpha_9 \mathrm{tr}(\boldsymbol{E}\boldsymbol{\tau}^2)]\boldsymbol{\tau}^2 \\ + \alpha_{10}(\boldsymbol{\epsilon}\boldsymbol{\tau} + \boldsymbol{\tau}\boldsymbol{\epsilon}) + \alpha_{11}(\boldsymbol{\epsilon}\boldsymbol{\tau}^2 + \boldsymbol{\tau}^2\boldsymbol{\epsilon}) + \boldsymbol{o}(\boldsymbol{E}).\end{aligned} \tag{2.80}$$

Now, we can recover the model established by Man (see equation (22) in [Man 1998]) when the only non vanishing parameters α_i are set to:

$$\alpha_1 = \beta_1 I_1^{\tau} + \lambda, \quad \alpha_2 = \beta_3, \quad \alpha_{10} = \beta_4, \quad \alpha_{12} = \beta_2 I_1^{\tau} + 2\mu. \tag{2.81}$$

Strong ellipticity is one of the well known mathematical constraints used to make restrictions on the different models in the scope of hyperelasticity. In fact, such a condition is a sufficient one to guarantee that the celerity for plane waves must remain real, otherwise there will be a dissipation of energy which must not exist in such an elastic medium. The strong ellipticity can be presented through the following mathematical condition:

$$\vec{a} \otimes \vec{b} : \frac{\partial \boldsymbol{S}}{\partial \boldsymbol{F}} : \vec{a} \otimes \vec{b} > 0, \quad \forall \vec{a} \neq \vec{0} \ \text{ and } \ \vec{b} \neq \vec{0}. \tag{2.82}$$

Without loss of generality, we can suppose that $\vec{a}$ and $\vec{b}$ are unit vectors. In the scope of small deformation $\boldsymbol{S} - \boldsymbol{\tau}$ is a linear tensor function of the displacement gradient tensor $\boldsymbol{H}$. Therefore, the strong ellipticity condition becomes:

$$\vec{a} \otimes \vec{b} : (\boldsymbol{S} - \boldsymbol{\tau}) : \vec{a} \otimes \vec{b} > 0, \quad \forall \vec{a} \neq \vec{0} \ \text{ and } \ \vec{b} \neq \vec{0}. \tag{2.83}$$

A sufficient condition to preserve equation (2.83) is to hold:

$$\begin{aligned}\min_{\vec{X}\in\mathcal{B}_0}\frac{1}{2}\alpha_{12} > max_{\vec{X}\in\mathcal{B}_0}\{&|\alpha_1| + (|\alpha_2| + |\alpha_4| + 2|\alpha_{10}|)||\boldsymbol{\tau}|| + |\alpha_5|||\boldsymbol{\tau}||^2 \\ &+ (|\alpha_3| + |\alpha_7| + 2|\alpha_{11}|)||\boldsymbol{\tau}^2|| + |\alpha_9|||\boldsymbol{\tau}^2||^2 \\ &+ (|\alpha_6| + |\alpha_8|)||\boldsymbol{\tau}||||\boldsymbol{\tau}^2||\}. \end{aligned} \tag{2.84}$$

For the weak formulation of the equilibrium equation in a initially-stressed material, an analogous inequality has been obtained for the case of Man's model presented in equation (2.63) in the objective to ensure the coercivity of the derived bilinear form[Robertson 1998].

2.8 Plane deformations

Plane deformation and/or plane stress are still one of the most used hypotheses for the analysis of many boundary values problems using analytic solutions. In such a case, the equilibrium equation will be reduced to a single partial differential equation on a scalar function, and the different stress components and strain components can be expressed in function of this potential. In other words, the potential or the scalar function we are talking about is the generalization of the Airy stress function (used for isotropic materials) to the class of initially-stressed material in the case of infinitesimal deformations. Since this section will be devoted to the case of plane deformations, then the displacement field will be in the following form:

$$u = u(X_1, X_2), \quad v = v(X_1, X_2), \quad w = 0. \tag{2.85}$$

u, v and w are the displacement field components in the cartesian coordinate system.

2.8.1 Sufficient conditions to sustain plane deformations

It is clear that independently of the material parameters α_i presented above, the vanishing of the antiplane shear components of the initial stress field (τ_{13} and τ_{23}) is a sufficient condition to obtain plane deformations. Thus, using the displacement field form in equation (2.85) and the constitutive relation in equation (2.80), the explicit form of the different

components of the first Piola-Kirchhoff stress tensor can be presented as:

$$S_{11} = \tau_{11} + \tau_{11}u_{,1} + \tau_{12}u_{,2} + G_{11}[\boldsymbol{E}], \tag{2.86}$$
$$S_{12} = \tau_{12} + \tau_{12}u_{,1} + \tau_{22}u_{,2} + G_{12}[\boldsymbol{E}], \tag{2.87}$$
$$S_{21} = \tau_{12} + \tau_{11}v_{,1} + \tau_{12}v_{,2} + G_{12}[\boldsymbol{E}], \tag{2.88}$$
$$S_{22} = \tau_{22} + \tau_{12}v_{,1} + \tau_{22}v_{,2} + G_{22}[\boldsymbol{E}], \tag{2.89}$$
$$S_{13} = S_{31} = S_{23} = S_{32}, \tag{2.90}$$
$$S_{33} = \tau_{33}. \tag{2.91}$$

where $G_{ij}[.]$ denotes the component ij of the tensorial operator $\boldsymbol{G}$ i.e $G_{ij}[\boldsymbol{E}] = [G_{ij}[\boldsymbol{E}]]_{ij}$. Now, by the vanishing of the components τ_{13} and τ_{23}, the equilibrium equation is transformed into two partial differential equations:

$$(\tau_{11}u_{,1} + \tau_{12}u_{,2} + G_{11}[\boldsymbol{E}])_{,1} + (\tau_{12}u_{,1} + \tau_{22}u_{,2} + G_{12}[\boldsymbol{E}])_{,2} = 0, \tag{2.92}$$
$$(\tau_{11}v_{,1} + \tau_{12}v_{,2} + G_{12}[\boldsymbol{E}])_{,1} + (\tau_{12}v_{,1} + \tau_{22}v_{,2} + G_{22}[\boldsymbol{E}])_{,2} = 0. \tag{2.93}$$

Without any hypothesis, it is easy to show that the vanishing of the antiplane shear components and the depending of the initial stress field on only the plane-coordinates of the deformation field i.e

$$\boldsymbol{\tau} = \boldsymbol{\tau}(X_1, X_2) \tag{2.94}$$

are sufficient conditions to permit sustaining a plane deformation.

2.8.2 Potential formulation for constant initial stress field

The objective of this section is to generalize the concept of Airy stress function. In fact, in the case of singular problems (crack ..) the displacement gradient becomes singular and the linearization of the relation between the Cauchy and the first Piola Kirchhoff stress tensors has no meaning. Thus the constitutive relation can only be expressed in function of the First PIola Kirchhoff stress tensor. Since the latter stress measure is non symmetric in general, the definition of the classical stress Airy function has to be modified for the formulation of the plane deformation problem within an initially-stressed linear elastic material.

In this section, we will suppose that the initial stress field $\boldsymbol{\tau}$ is constant. Even with this simplification, this case is still a curious and interesting situation, since the presence of a constant initial stress creates certain classes of symmetries and consequently an anisotropic behaviour. In the following, we will consider the cartesian coordinates (Y_1, Y_2, Y_3) respectively to the orthonormal basis $(\vec{L}_1, \vec{L}_2, \vec{L}_3)$. Then the planar displacement field will be considered in the following form:

$$\tilde{u} = \tilde{u}(Y_1, Y_2), \quad \tilde{v} = \tilde{u}(Y_1, Y_2), \quad \tilde{w} = w = 0. \tag{2.95}$$

Thus the different components of the stress tensor $\boldsymbol{S}$ can be simplified to:

$$\tilde{S}_{11} = \tau_1 + \tau_1 \tilde{u}_{,1} + G_{11}[\tilde{\boldsymbol{E}}], \tag{2.96}$$
$$\tilde{S}_{12} = \tau_2 \tilde{u}_{,2} + G_{12}[\tilde{\boldsymbol{E}}], \tag{2.97}$$
$$\tilde{S}_{21} = \tau_1 \tilde{v}_{,1} + G_{12}[\tilde{\boldsymbol{E}}], \tag{2.98}$$
$$\tilde{S}_{22} = \tau_2 + \tau_2 \tilde{v}_{,2} + G_{22}[\tilde{\boldsymbol{E}}], \tag{2.99}$$
$$\tilde{S}_{13} = \tilde{S}_{23} = \tilde{S}_{31} = \tilde{S}_{32} = 0, \tag{2.100}$$
$$\tilde{S}_{33} = \tau_3, \tag{2.101}$$

where $f_{,1}$ and $f_{,2}$ denotes the derivatives of a function f relative to the new cartesian system (Y_1, Y_2, Y_3). Using the diagonal spectral form of the initial stress field then we can derive:

$$\mathrm{tr}(\tilde{\boldsymbol{E}}) = \tilde{u}_{,1} + \tilde{v}_{,2}, \quad \mathrm{tr}(\tilde{\boldsymbol{E}}\boldsymbol{\tau}) = \tau_1 \tilde{u}_{,1} + \tau_2 \tilde{v}_{,2}, \quad \mathrm{tr}(\tilde{\boldsymbol{E}}\boldsymbol{\tau}^2) = \tau_1^2 \tilde{u}_{,1} + \tau_2^2 \tilde{v}_{,2}, \tag{2.102}$$

$$\tilde{\boldsymbol{E}}\boldsymbol{\tau} + \boldsymbol{\tau}\tilde{\boldsymbol{E}} = \begin{bmatrix} 2\tau_1 \tilde{u}_{,1} & \frac{1}{2}(\tilde{u}_{,2} + \tilde{v}_{,1})(\tau_1 + \tau_2) & 0 \\ \frac{1}{2}(\tilde{u}_{,2} + \tilde{v}_{,1})(\tau_1 + \tau_2) & 2\tau_2 \tilde{v}_{,2} & 0 \\ 0 & 0 & 0 \end{bmatrix}, \tag{2.103}$$

$$\tilde{\boldsymbol{E}}\boldsymbol{\tau}^2 + \boldsymbol{\tau}^2\tilde{\boldsymbol{E}} = \begin{bmatrix} 2\tau_1^2 \tilde{u}_{,1} & \frac{1}{2}(\tilde{u}_{,2} + \tilde{v}_{,1})(\tau_1^2 + \tau_2^2) & 0 \\ \frac{1}{2}(\tilde{u}_{,2} + \tilde{v}_{,1})(\tau_1^2 + \tau_2^2) & 2\tau_2^2 \tilde{v}_{,2} & 0 \\ 0 & 0 & 0 \end{bmatrix} \tag{2.104}$$

Now, the equilibrium equation (2.5) for the first Piola-Kirchhoff stress tensor in absence of volumetric forces leads to:

$$\tau_1\tilde{u}_{,11} + (G_{11}[\tilde{\boldsymbol{E}}])_{,1} + \tau_2\tilde{u}_{,22} + (G_{12}[\tilde{\boldsymbol{E}}])_{,2} = 0, \tag{2.105}$$

$$\tau_1\tilde{v}_{,11} + (G_{12}[\tilde{\boldsymbol{E}}])_{,1} + \tau_2\tilde{v}_{,22} + (G_{22}[\tilde{\boldsymbol{E}}])_{,2} = 0. \tag{2.106}$$

Let us define the following stress quantities:

$$\hat{S}_{11} = \tau_1 + \tau_1(\tilde{u}_{,1} - \tilde{v}_{,2}) + G_{11}[\tilde{\boldsymbol{E}}], \tag{2.107}$$

$$\hat{S}_{12} = \tau_2\tilde{u}_{,2} + \tau_1\tilde{v}_{,1} + G_{12}[\tilde{\boldsymbol{E}}], \tag{2.108}$$

$$\hat{S}_{22} = \tau_2 + \tau_2(\tilde{v}_{,2} - \tilde{u}_{,1}) + G_{22}[\tilde{\boldsymbol{E}}]. \tag{2.109}$$

So we can express the planar components of the initial stress field in the new coordinates system as:

$$\tilde{S}_{11} = \hat{S}_{11} + \tau_1\tilde{v}_{,2}, \tag{2.110}$$

$$\tilde{S}_{12} = \hat{S}_{12} - \tau_1\tilde{v}_{,1}, \tag{2.111}$$

$$\tilde{S}_{21} = \hat{S}_{12} - \tau_2\tilde{u}_{,2}, \tag{2.112}$$

$$\tilde{S}_{22} = \hat{S}_{22} + \tau_2\tilde{u}_{,1}. \tag{2.113}$$

Exploiting the equilibrium equation (2.5) and the new defined quantities in equations (2.107-2.109), then it leads to:

$$\hat{S}_{11,1} + \hat{S}_{12,2} = 0, \tag{2.114}$$

$$\hat{S}_{12,1} + \hat{S}_{22,2} = 0, \tag{2.115}$$

which implies the existence of a potential function ψ such that:

$$\hat{S}_{11} = \psi_{,22}, \quad \hat{S}_{22} = \psi_{,11}, \quad \hat{S}_{12} = -\psi_{,12}. \tag{2.116}$$

Using the general form of the operator $\boldsymbol{G}[.]$ mentioned in equation (2.78) and bearing in mind all equations (2.102-2.109), we can show that:

$$\hat{S}_{11} = \beta_{11} u_{,1} + \beta_{12} v_{,2}, \tag{2.117}$$

$$\hat{S}_{22} = \beta_{21} u_{,1} + \beta_{22} v_{,2}, \tag{2.118}$$

$$\hat{S}_{12} = \beta_{31} u_{,2} + \beta_{32} v_{,1}, \tag{2.119}$$

with β_{ij} are functions of the defined parameters α_k involved in the stress-strain relation in the previous section. Therefore, we can deduce:

$$u_{,1} = \frac{1}{\beta_{22}\beta_{11} - \beta_{21}\beta_{12}} [\beta_{22}(\psi_{,22} - \tau_1) - \beta_{12}(\psi_{,11} - \tau_2)], \tag{2.120}$$

$$v_{,2} = \frac{1}{\beta_{22}\beta_{11} - \beta_{21}\beta_{12}} [\beta_{11}(\psi_{,11} - \tau_2) - \beta_{21}(\psi_{,22} - \tau_1)]. \tag{2.121}$$

Then by making the derivative of equation (2.119) relatively to Y_1 and Y_2, and by using equations (2.116,2.120,2.121), a partial differential equation on the unknown potential function ψ is deduced the following way:

$$\gamma_1 \psi_{,2222} + \gamma_2 \psi_{,2211} + \gamma_3 \psi_{,1111} = 0, \tag{2.122}$$

where we can express the constants γ_1, γ_2 and γ_3 as:

$$\gamma_1 = \frac{1}{\beta_{22}\beta_{11} - \beta_{12}\beta_{21}} \beta_{31}\beta_{22}, \tag{2.123}$$

$$\gamma_2 = \frac{-1}{\beta_{22}\beta_{11} - \beta_{12}\beta_{21}} (\beta_{12}\beta_{31} + \beta_{32}\beta_{21}), \tag{2.124}$$

$$\gamma_3 = \frac{1}{\beta_{22}\beta_{11} - \beta_{12}\beta_{21}} \beta_{32}\beta_{11}. \tag{2.125}$$

In absence of residual stress, the stress-strain relation in equation (2.76) is transformed into the classical constitutive equation for isotropic materials, and hence the potential ψ satisfies the classical biharmonic partial differential equation:

$$\Delta\Delta\psi = 0. \tag{2.126}$$

2.9 Concluding remarks

In the beginning of this chapter, some theoretical results about the initially-stressed materials are discussed. Moreover, to widen and enrich the class of models describing the behaviour of initially-stressed materials, we have proposed a more general linear elastic model compared to the existing ones in the literature. Also, we have analyzed explicitly the link between initial stress field presence and the generated anisotropy. Using a reformulation of the different invariants involved in the formulation based on the theory of invariant, we have shown the analogy between such class of initially-stressed hyperelastic materials behaviour and the one of hyperelastic anisotropic fibrous materials. The last part of this chapter is dedicated to the establishment of a simple formulation for the case of plane deformations in initially-stressed solids. Generalizing the concept of Airy stress function, we have succeeded to transform equilibrium equations into one single differential partial equation on a scalar potential.

Chapter 3

Elastic Machines : a non standard use of the axial shear of linear transversely isotropic elastic cylinders.

Contents

3.1 Introduction

Most materials behaviour exhibit moderate to high anisotropy in macroscopic mechanical properties due to the dependence of their microstructure to one or more preferred directions. This feature is present in many biomaterials, polycrystals, fiber-reinforced materials and composites which are usually sorted on the basis of their anisotropic behaviour,

i.e., the symmetry elements of the underlying microstructure [Finger 1983, Ting 1996b, Ting 1996a]. As elasticity is concerned in this work, symmetry considerations reduce the number of mechanical properties to a range from 3 (cubic system) to 21 (triclinic system) [Gurtin 1972] and classify the elastic energy into 8 categories [Forte 1996]. Material anisotropy emerged as an important aspect of material sciences, and it becomes necessary to use the knowledge of this behaviour to design better products. Otherwise, recent design requirements and constraints of mass reduction cannot be easily fulfilled. To this end, numerical approaches are usually used. However, analytic methods provide exact solutions for some idealized problems which enable us to have an overall picture of the anisotropy influence on local and global mechanical fields [Vannucci 2018].

Analysis of the boundary value problems associated to anisotropic elasticity has been often tedious due to the complexity of the constitutive behaviour models. In linear anisotropic elasticity, two stress and displacement based formalisms, due to Lekhnitskii [Lekhnitskii 1950, Lekhnitskii 1963] and Stroh [Stroh 1958, Stroh 1962], are the most used techniques to find numerical and, if possible, analytical solutions when the mechanical fields depend on only two spatial coordinates. These two formalisms, which have been shown to be equivalent [Barnett 1997], have been applied to study anisotropic solids, for example, in [Horgan 1996, Ting 1996a, Tings 1999, Ting 1996b, Ting 2000]. In anisotropic elasticity coupling general loadings with in-plane and anti-plane deformations, is quite complex.

Let us consider an isotropic linearly elastic cylinder subject to a prescribed axial traction field on its outer curved boundary whose only nonzero component is axial and which does not vary in the axial direction. In absence of body force, the infinitesimal deformation corresponding to this surface traction field is an *anti-plane* shear deformation, where the word *plane* denotes here the cylinder's cross section plane.

On the other hand, it is well known that not all arbitrary anisotropic cylinders can sustain an anti-plane shear deformation when they are subject to axial tractions. Necessary and sufficient conditions on the elastic moduli which do allow an anti-plane shear deformation in anisotropic materials have been obtained by Horgan and Miller [HORGAN 1994] who proved that, when the cross-section is circular, the most general elastic symmetry consistent with such a deformation is that with only one plane of symmetry (monoclinic material with 13 elastic moduli).

The result by Horgan and Miller suggests that an anisotropic hollow elastic cylinder cannot undergo an anti-plane shear deformation when it is subject to axial tractions on its outer curved boundary.

Anti-plane shear deformations of isotropic elastic materials have been the subject of several studies (see [Horgan 1995b] and references therein for a review on the subject). Some recent results on this problem in isotropic nonlinear elasticity are contained in [Pucci 2013b, Pucci 2015a]. In the framework of the linear theory of elasticity, anti-plane shear deformation is much less studied. In the isotropic case, the linear elastic problem is reduced to a single linear partial differential equation. In the framework of anisotropic elastic materials, some explicit solutions based on the anti-plane shear deformation are given and/or summarised in the book by Ting [Ting 1996b]. Among the works devoted to the study of deformations coupling in the framework of linear anisotropic materials we can cite [Blouin 1989, Crossley 2003] where extension-torsion and bending-flexure respectively are considered. These two fields of deformation are different from the ones that will be studied in the following of this chapter.

Here, we consider an infinite cylindrical hollow tube with inner radius a and outer radius b in the reference configuration Ω. In cylindrical coordinates $r \in [a, b], \theta \in [0, 2\pi]$, $z \in [-\infty, \infty]$. This cylinder is composed by a fiber reinforced elastic material (i.e. transversely isotropic) and is subject to the following tension boundary conditions:

$$(\vec{\sigma}\vec{n})\,|_{r=b} = T\vec{e}_z, \tag{3.1}$$

and

$$\vec{u}(a) = \vec{0}. \tag{3.2}$$

In this case, the equations of linear elasticity, under the usual standard requirements, admit a unique solution. For isotropic elasticity, this solution can be easily determined by considering just an *axial* shear deformation and solving an ordinary differential equation. In the anisotropic case, this is possible only for special arrangements of the fibers, while in the general case, a more complex deformation is produced by the given tension field on the boundary.

Clearly, the symmetry of geometry and boundary conditions simplifies the problem and makes it solvable by using the semi-inverse method. With this approach, we show that the general solution consists in a superposition to the anti-plane axial shear of an in-plane deformation composed by a radial deformation and an azimuthal shear.

Using this solution, it is possible to show how to *control* the various deformation modes via their coupling [1]. This fact might be used to create new kinds of actuators that we call *elastic machines* able to exploit anisotropy to convert forces into moments or vice versa.

The plan of the chapter is as follows. In the next Section, we introduce the basic equations. Section 3 is dedicated to the study of the pure axial shear and the fiber arrangements compatible with such deformation. In Section 4, we prove that in the most general setting, the equilibrium configuration is a superposition of anti-plane and in-plane deformations. The superposition of an in-plane deformation is a necessary and sufficient condition for an anti-plane deformation to be sustainable by a transversely isotropic elastic tube with any arrangement of fibers. The coupling between the various deformation modes is studied in details via an asymptotic procedure for the compressible materials. In Section 5, some optimisation problems are presented. The sixth section treats the analogy between the initially-stressed and the isotropic transverse elastic materials through the solutions of the studied boundary value problem. The last Section is devoted to some concluding remarks.

[1] This coupling should not be confused with the Poynting effect [Poynting 1909] for two reasons. First, the Poynting effect is a non-linear effect. Then, in the Poynting effect, the twist and the extension are coupled [Atkin 2005]. Although, here the coupling is between two shear modes (azimuthal and axial shear). The composition of these two modes is also denoted as helical shear and it has been studied into details in non-linear elasticity (see for example [Horgan 2003a]). In wire ropes (see [Costello 1997]) that are structures and not materials, a coupling between bending and twist deformations is usual.

3.2 Basic Equations

The constitutive equation for the Cauchy stress tensor $\vec{\sigma}$ for a linear elastic transversely isotropic material with a preferred direction $\vec{M}$ (the fiber direction) has the form [Spencer 1984b]:

$$\begin{aligned}\vec{\sigma} &= (\lambda \mathrm{tr}\vec{\epsilon} + \alpha\epsilon_f)\vec{I} + 2\mu_T\vec{\epsilon} + (\alpha \mathrm{tr}\vec{\epsilon} + \beta\epsilon_f)\vec{M}\otimes\vec{M} \\ &+ 2(\mu_L - \mu_T)\left(\vec{M}\otimes\epsilon\vec{M} + \epsilon\vec{M}\otimes\vec{M}\right),\end{aligned} \tag{3.3}$$

where $\vec{I}$ is the identity tensor, $\vec{\epsilon}$ is the infinitesimal strain tensor, $\epsilon_f = \mathrm{tr}(\epsilon\vec{M}\otimes\vec{M})$ is the strain in the fiber direction and $\lambda, \alpha, \beta, \mu_T, \mu_L$ are the constitutive parameters. Clearly, μ_T and μ_L are the infinitesimal shear modulus in the transverse and longitudinal direction relative to the preferred direction. The connection of all these parameters with the longitudinal and transverse Young's modulus can be found in [Spencer 1984b]. From (3.3), the isotropic case can be recovered considering $\alpha = \beta = 0$ and $\mu_L = \mu_T$.

In the case of *incompressible* materials, only isochoric deformations are admissible (i.e. $\mathrm{tr}\vec{\epsilon} = 0$) and the constitutive equation is given by [Spencer 1984b]:

$$\begin{aligned}\vec{\sigma} &= -p\vec{I} + 2\mu_T\vec{\epsilon} + \beta\epsilon_f\vec{M}\otimes\vec{M} \\ &+ 2(\mu_L - \mu_T)\left(\vec{M}\otimes\epsilon\vec{M} + \epsilon\vec{M}\otimes\vec{M}\right),\end{aligned} \tag{3.4}$$

where p is the arbitrary Lagrange multiplier associated with the constraint of incompressibility. To guarantee the uniqueness of the boundary value problem's solution, the strong ellipticity is a sufficient and necessary condition [Marsden 1994], i.e.:

$$\mu_L > 0, \quad \mu_T > 0, \quad 2\mu_L + \lambda > 0, \quad 2\alpha + \beta + \lambda + 4\mu_l - 2\mu_T > 0 \tag{3.5}$$

and

$$|\mu_L + \alpha + \lambda| < \mu_L + \sqrt{(2\mu_T + \lambda)(2\alpha + \beta + \lambda + 4\mu_l - 2\mu_T)}. \tag{3.6}$$

For the incompressible materials, the above strong ellipticity conditions are replaced by:

$$\mu_L > 0, \quad \mu_T > 0, \quad \beta + 4\mu_L - 2\mu_T > 0. \tag{3.7}$$

We now assume that the displacement field is a function only of the radial coordinate and the domain is a circular cylinder. Therefore, in the absence of body forces, the three scalar equilibrium equations become:

$$\frac{d}{dr}(r\sigma_{rr}) = \sigma_{\theta\theta}, \quad \frac{d}{dr}\left(r^2\sigma_{r\theta}\right) = 0, \quad \frac{d}{dr}(r\sigma_{rz}) = 0. \tag{3.8}$$

3.3 Axial Shear

The axial shear problem is a trivial problem in the framework of the theory of linear isotropic elasticity and for this reason, it is usually not considered into details in the classical textbooks (see for example [Horgan 1995b]). The objective of this section is to identify the possible fibers arrangements that can sustain the axial shear deformation.

Considering an axial anti-plane deformation field $\vec{u}^{ap}$ whose components are:

$$u_r^{ap} = 0, \quad u_\theta^{ap} = 0, \quad u_z^{ap} = w(r), \tag{3.9}$$

the strain tensor relative to the displacement field mentioned in (3.9) becomes:

$$\bar{\epsilon}^{ap} = \frac{1}{2}w'(\vec{e}_r \otimes \vec{e}_z + \vec{e}_z \otimes \vec{e}_r), \tag{3.10}$$

where $w' = dw/dr$. To preclude any confusion in the following, we notice here that $\vec{M}$ is not assumed to be aligned with z-axis of the considered cylinder. Also, the anti-plane nature of the displacement field $\vec{u}^{ap}$ is relevant to the tube geometry i.e: $\vec{u}^{ap}$ is perpendicular to the cross section of the cylinder and it is not necessarily in the same direction of the vector $\vec{M}$.

In the isotropic case, the only non zero component of the Cauchy stress tensor is the axial shear stress σ_{rz} and the balance equations (3.8) are reduced to a single differential equation: $(r\sigma_{rz})' = 0$. The boundary conditions, (1.1) and (1.2), to append to this equation are: $\sigma_{rz}(b) = T$, $w(a) = 0$.

Therefore, the solution of our problem in the isotropic case is given by:

$$w(r) = \frac{Tb}{\mu} \ln\left(\frac{r}{a}\right), \tag{3.11}$$

where μ is the isotropic infinitesimal shear modulus.

3.3.1 Compressible transversely isotropic materials

In the absence of any internal constraints in a transversely isotropic material, the use of equation (3.10) leads to:

$$\mathrm{tr}\bar{\epsilon}^{ap} = 0, \quad \epsilon_f^{ap} = w' M_r M_z. \tag{3.12}$$

Thus, the explicit form of the stress field components corresponding to (3.9) is:

$$\sigma_{rr}^{ap} = \left[\alpha M_r M_z + \beta M_r^3 M_z + 2(\mu_L - \mu_T) M_r M_z\right] w', \tag{3.13}$$

$$\sigma_{\theta\theta}^{ap} = \left[\alpha M_r M_z + \beta M_r M_\theta^2 M_z\right] w', \tag{3.14}$$

$$\sigma_{zz}^{ap} = \left[\alpha M_r M_z + \beta M_r M_z^3 + 2(\mu_L - \mu_T) M_r M_z\right] w', \tag{3.15}$$

$$\sigma_{r\theta}^{ap} = \left[\beta M_r^2 M_\theta M_z + (\mu_L - \mu_T) M_\theta M_z\right] w', \tag{3.16}$$

$$\sigma_{rz}^{ap} = \left[\mu_T + \beta M_r^2 M_z^2 + (\mu_L - \mu_T)(M_r^2 + M_z^2)\right] w', \tag{3.17}$$

$$\sigma_{\theta z}^{ap} = \left[\beta M_r M_\theta M_z^2 + (\mu_L - \mu_T) M_r M_\theta\right] w'. \tag{3.18}$$

In this case, the three balance equilibrium equations (3.8) compose an *overdetermined* system where the only unknown is the anti-plane displacement field $w = w(r)$. The boundary conditions relative to this overdetermined system are:

$$\sigma_{rr}(b) = 0, \quad \sigma_{r\theta}(b) = 0, \quad \sigma_{rz}(b) = T, \quad w(a) = 0. \tag{3.19}$$

One important question is to establish when a *non-trivial* (i.e. $w(r)$ non constant) solution for such a system exists.

Using (3.8-2) and the corresponding boundary condition $\sigma_{r\theta}(b) = 0$ leads to the vanishing of the azimuthal shear stress component i.e $\sigma_{r\theta}(r) = 0$.

Assuming that the components of $\boldsymbol{M}$ with respect to the fundamental basis associated with the cylindrical coordinate system are constants, equation (3.19-2) reduces to:

$$\left[\beta M_r^2 + \mu_L - \mu_T\right] M_\theta M_z w' = 0. \tag{3.20}$$

Considering only non-trivial solutions, we get:

$$\text{i)}\, M_\theta = 0, \quad \text{ii)}\, M_z = 0, \quad \text{iii)}\, \beta M_r^2 + \mu_L - \mu_T = 0. \tag{3.21}$$

Equation (3.8-3) and the corresponding boundary conditions are:

$$\sigma_{rz}(b) = T, \quad w(a) = 0, \tag{3.22}$$

and therefore the axial displacement field is:

$$w(r) = \left[\mu_T + \beta M_r^2 M_z^2 + (\mu_L - \mu_T)(M_r^2 + M_z^2)\right]^{-1} Tb \ln\left(\frac{r}{a}\right), \tag{3.23}$$

in case i) and

$$w(r) = \left[\mu_T + (\mu_L - \mu_T) M_r^2\right]^{-1} Tb \ln\left(\frac{r}{a}\right), \tag{3.24}$$

in the remaining cases ii) and iii).

When the axial field is defined by (3.23) or (3.24), it is remarkable that $(r\sigma_{rr})' = 0$ and therefore (3.8-1) reduces to $\sigma_{\theta\theta} = 0$. In so doing, we distinguish three possibilities:

i) $M_r = M_\theta = 0$ (figure (3.1.c)) and

$$w(r) = \frac{Tb}{\mu_L} \ln\left(\frac{r}{a}\right). \tag{3.25}$$

ii) $M_z = 0$ (figures (3.1.a), (3.1.b) and (3.1.d)) and

$$w(r) = \left[\mu_T + (\mu_L - \mu_T)M_r^2\right]^{-1} Tb \ln\left(\frac{r}{a}\right). \tag{3.26}$$

iii) $M_r^2 = (\mu_T - \mu_L)/\beta$ and $M_\theta^2 = -\alpha/\beta$. Therefore, $M_z^2 = 1 + \frac{\alpha}{\beta} + \frac{\mu_L - \mu_T}{\beta}$. In this case, once again, the axial displacement component could be written as in in (3.26) (figure (3.1.g)).

Case iii) introduces a link among fiber direction of the material and the constitutive parameters. It is necessary to check if this link is compatible with the strong ellipticity condition and the conditions:

$$(\mu_T - \mu_L)/\beta \geq 0, \quad -\alpha/\beta \geq 0.$$

3.3.2 Incompressible transversely isotropic materials

Considering the isochoric displacement (3.9), it is interesting to note what happens when the incompressibility constraint is in force. For incompressible materials, the first equilibrium equation (3.8-1) is used to determine the pressure field $p = p(r)$ and therefore the previous classification is simplified as follows:

i) $M_\theta = 0$ (figures (3.1.a), (3.1.c) and (3.1.e)) and the axial shear is defined by (3.25).

ii) $M_z = 0$ (figures (3.1.a), (3.1.b) and (3.1.d)) and the axial shear is defined by (3.26).

iii) $M_r^2 = (\mu_T - \mu_L)/\beta$, $M_\theta^2 + M_z^2 = 1 + (\mu_L - \mu_T)/\beta$, and once again the axial shear is defined by (3.26) (figure (3.1.g)).

3.4 Coupling the In-Plane and Anti-Plane Deformations

The possibility to have a transverse isotropic material in an anti-plane deformation without restrictions on the fiber direction relies on the presence of an *in-plane* special deformation field $\vec{u}^{ip}$ whose components are:

$$u_r^{ip} = f(r), \quad u_\theta^{ip} = g(r), \quad u_z^{ip} = 0. \tag{3.27}$$

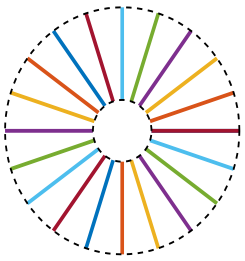

(a) $M_r = 1$

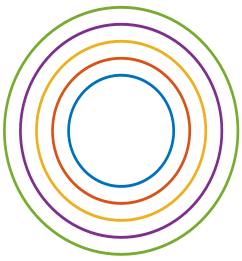

(b) $M_\theta = 1$

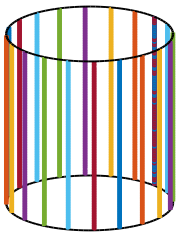

(c) $M_z = 1$

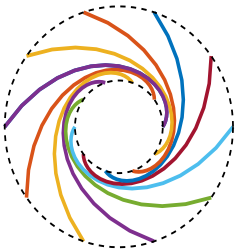

(d) $M_r \neq 0, M_\theta \neq 0, M_z = 0$

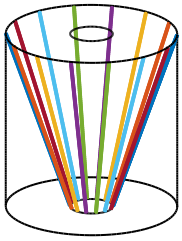

(e) $M_r \neq 0, M_\theta = 0, M_z \neq 0$

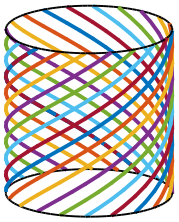

(f) $M_r = 0, M_\theta \neq 0, M_z \neq 0$

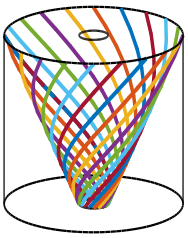

(g) $M_r \neq 0, M_\theta \neq 0, M_z \neq 0$

Figure 3.1: Possible fibers arrangements

Indeed, in this case the corresponding strain tensor field has the following form:

$$[\vec{\epsilon}^{ip}]_{ij} = \frac{1}{2}\begin{bmatrix} 2f' & rg' & 0 \\ rg' & 2\frac{f}{r} & 0 \\ 0 & 0 & 0 \end{bmatrix}. \tag{3.28}$$

Then, the volumetric dilatation and the stretch in the fiber direction, corresponding to the

in-plane deformation field, can both be expressed as:

$$\mathrm{tr}\vec{\epsilon}^{ip} = f' + \frac{f}{r}, \tag{3.29}$$

$$\epsilon_f = f' M_r^2 + \frac{f}{r} M_\theta^2 + r g' M_r M_\theta. \tag{3.30}$$

Consequently, the stress distribution relative to the in-plane deformation is given by:

$$\begin{aligned}\sigma_{rr}^{ip} &= (M_r^4\beta + (4\mu_L - 4\mu_T + 2\alpha)M_r^2 + 2\mu_T + \lambda)f' \\ &\quad + [(M_\theta^2\beta + \alpha)M_r^2 + M_\theta^2\alpha + \lambda]\frac{f}{r} + M_rM_\theta(M_r^2\beta + \alpha + 2\mu_L - 2\mu_T)rg',\end{aligned} \tag{3.31}$$

$$\begin{aligned}\sigma_{\theta\theta}^{ip} &= [(M_r^2\beta + \alpha)M_\theta^2 + M_r^2\alpha + \lambda]f' \\ &\quad + [M_\theta^4\beta + (4\mu_L - 4\mu_T + 2\alpha)M_\theta^2 + 2\mu_T + \lambda]\frac{f}{r} \\ &\quad + M_rM_\theta(M_\theta^2\beta + \alpha + 2\mu_L - 2\mu_T)rg',\end{aligned} \tag{3.32}$$

$$\begin{aligned}\sigma_{zz}^{ip} &= \left[(M_r^2 + M_z^2)\alpha + M_r^2M_z^2\beta + \lambda\right] f' \\ &\quad + [(M_\theta^2 + M_z^2)\alpha + M_\theta^2M_z^2\beta + \lambda]\frac{f}{r} + M_rM_\theta(M_z^2\beta + \alpha)rg',\end{aligned} \tag{3.33}$$

$$\begin{aligned}\sigma_{r\theta}^{ip} &= \left[(M_r^2\beta + \alpha + 2\mu_L - 2\mu_T)f' + (M_\theta^2\beta + \alpha + 2\mu_L - 2\mu_T))\frac{f}{r}\right] M_rM_\theta \\ &\quad + [(M_r^2\beta + \mu_L - \mu_T)M_\theta^2 + (\mu_L - \mu_T)M_r^2 + \mu_T]rg',\end{aligned} \tag{3.34}$$

$$\begin{aligned}\sigma_{rz}^{ip} &= \left[(M_r^2\beta + \alpha + 2\mu_L - 2\mu_T)f' + (M_\theta^2\beta + \alpha)\frac{f}{r}\right] M_rM_z \\ &\quad + M_\theta M_z(M_r^2\beta + \mu_L - \mu_T)rg',\end{aligned} \tag{3.35}$$

$$\begin{aligned}\sigma_{\theta z}^{ip} &= \left[(M_r^2\beta + \alpha)f' + (M_\theta^2\beta + \alpha + 2\mu_L - 2\mu_T)\frac{f}{r}\right] M_\theta M_z \\ &\quad + (M_\theta^2\beta + \mu_L - \mu_T)M_rM_zrg'.\end{aligned} \tag{3.36}$$

.

Taking advantage of the linearity of the constitutive equation, the composition of the in-plane and anti-plane deformation fields implies:

$$\vec{\sigma} = \vec{\sigma}^{ap} + \vec{\sigma}^{ip}, \tag{3.37}$$

where the boundary conditions are:

$$\sigma_{rr}(b) = 0, \quad \sigma_{r\theta}(b) = 0, \quad \sigma_{rz}(b) = T, \tag{3.38}$$

and

$$w(a) = 0, \quad f(a) = 0, \quad g(a) = 0. \tag{3.39}$$

Bearing in mind that $\left(r^2\sigma_{r\theta}\right)' = 0$ and $\sigma_{r\theta}(b) = 0$, it must be $\sigma_{r\theta}(r) \equiv 0$ i.e.

$$\left[\tilde{\Gamma}_1 f' + \tilde{\Gamma}_2 \frac{f}{r}\right] M_r M_\theta + \tilde{\Gamma}_3 r g' + \tilde{\Gamma}_4 M_z M_\theta w' = 0. \tag{3.40}$$

On the other hand, from $(r\sigma_{rz})' = 0$ and $\sigma_{rz}(b) = T$, the axial shear stress component must be $\sigma_{rz}(r) = Tb/r$, i.e.

$$\left[\tilde{\Gamma}_1 f' + (M_\theta^2\beta + \alpha)\frac{f}{r}\right] M_r M_z + \tilde{\Gamma}_4 M_\theta M_z r g' + \tilde{\Gamma}_5 w' = \frac{bT}{r}, \tag{3.41}$$

with

$$\begin{cases} \tilde{\Gamma}_1 = M_r^2\beta + \alpha + 2(\mu_L - \mu_T), \quad \tilde{\Gamma}_2 = M_\theta^2\beta + \alpha + 2(\mu_L - \mu_T) \\ \tilde{\Gamma}_3 = (M_r^2\beta + \mu_L - \mu_T)M_\theta^2 + (\mu_L - \mu_T)M_r^2 + \mu_T, \\ \tilde{\Gamma}_4 = M_r^2\beta + \mu_L - \mu_T, \\ \tilde{\Gamma}_5 = (M_r^2\beta + \mu_L - \mu_T)M_z^2 + (\mu_L - \mu_T)M_r^2 + \mu_T. \end{cases} \tag{3.42}$$

From (3.40) and (3.41), when

$$\tilde{\Gamma}_3\tilde{\Gamma}_5 - \tilde{\Gamma}_4^2 M_\theta M_z \neq 0, \tag{3.43}$$

it is possible to determine g' and w' and then to reduce (3.8-1) to a second order linear differential equation in the unknown $f(r)$. The boundary conditions for such a differential equation are provided by $\sigma_{rr}(b) = 0$ and $f(a) = 0$.

Once the solution for the radial displacement has been provided, the azimuthal and axial shear components are determined from (3.40) and (3.41) imposing $g(a) = 0$ and $w(a) = 0$.

This means that our boundary value problem is well determined and this is for any di-

rection of the fibers. Moreover, because the system is linear, it is possible to implement its resolution in a numerical code. Instead to pursue this general solution, which is just a simple numerical computation, two special cases are examined: an asymptotic solution in the case of the compressible behaviour and the incompressible case.

3.4.1 An asymptotic solution for the compressible case

When $M_z = 1$ and $M_r = M_\theta = 0$, the anti-plane shear deformation can be sustained. We now rewrite the fiber direction M in spherical coordinates as:

$$\vec{M} = \sin(\varphi)\cos(\psi)\vec{e}_r + \sin(\varphi)\sin(\psi)\vec{e}_\theta + \cos(\varphi)\vec{e}_z \tag{3.44}$$

and assume that the fibers have a small deviation from the $z-$direction i.e.:

$$\begin{cases} M_r = \varepsilon\cos(\psi) + \mathcal{O}(\varepsilon^3), \\ M_\theta = \varepsilon\sin(\psi) + \mathcal{O}(\varepsilon^3), \\ M_z = 1 - \frac{1}{2}\varepsilon^2 + \mathcal{O}(\varepsilon^3), \end{cases} \tag{3.45}$$

where the polar angle $\varphi = \epsilon << 1$.

We perform a perturbation analysis of the field equations with respect to the small parameter ε introducing:

$$\begin{cases} f(r) = \varepsilon f_1(r) + \varepsilon^2 f_2(r) + \mathcal{O}(\varepsilon^3), \\ g(r) = \varepsilon g_1(r) + \varepsilon^2 g_2(r) + \mathcal{O}(\varepsilon^3), \\ w(r) = w_0(r) + \varepsilon w_1(r) + \varepsilon^2 w_2(r) + \mathcal{O}(\varepsilon^3). \end{cases} \tag{3.46}$$

To the leading order, the solution of our problem is clearly given by:

$$w_0(r) = \frac{Tb}{\mu_L}\ln\left(\frac{r}{a}\right). \tag{3.47}$$

At order $\mathcal{O}(\varepsilon)$, we have:

$$\sigma_{r\theta} = \varepsilon\left[\mu_T r g_1' + (\mu_L - \mu_T)\sin(\psi)w_0'\right] + \mathcal{O}(\varepsilon^2). \tag{3.48}$$

From the balance equation (3.8-2) and the corresponding stress boundary condition, we obtain $\sigma_{r\theta} = 0$. Solving (3.48) imposing $g_1(a) = 0$ it is:

$$g_1(r) = \frac{\mu_L - \mu_T}{\mu_T} \sin(\psi) \frac{bT}{a\mu_L} \frac{a-r}{r}. \tag{3.49}$$

From (3.8-1), we obtain:

$$r^2 f_1'' + r f_1' - f_1 = \frac{\alpha b T \cos(\psi)}{\mu_L(\lambda + 2\mu_T)}, \tag{3.50}$$

whose exact solution is:

$$f_1 = k_{11} r + \frac{k_{12}}{r} - \frac{\alpha b T \cos(\psi)}{\mu_L(\lambda + 2\mu_T)}, \tag{3.51}$$

where k_{11} and k_{12} are integration constants fixed by the boundary conditions $f_1(a) = 0$ and $\sigma_{rr}(b) = 0$ as:

$$k_{11} = \frac{\{[2\mu_T^2 + (-2\mu_L - \alpha + \lambda)\mu_T - \lambda\mu_L]b + \mu_T a\alpha\} bT\cos(\psi)}{(2\mu_T + \lambda)\mu_L(a^2\mu_T + b^2\lambda + b^2\mu_T)}, \tag{3.52}$$

$$k_{12} = \frac{\{[-2\mu_T^2 + (2\mu_L + \alpha - \lambda)\mu_T + \lambda\mu_L]a + b\alpha(\mu_T + \lambda)\} ab^2 T\cos(\psi)}{(2\mu_T + \lambda)\mu_L(a^2\mu_T + b^2\lambda + b^2\mu_T)}. \tag{3.53}$$

On the other hand, the use of equation of (3.8-3), i.e. $\sigma_{rz}(r) = Tb/r$, implies:

$$w_1 = 0.$$

In conclusion at order $\mathcal{O}(\epsilon)$ the effect of a dispersion of the fibers out of the $z-$direction like in (3.45) produces an in-plane deformation given by (3.49) and (3.51), but it will not change the anti-plane deformation field. To outline the effect of the fibers dispersion on the anti-plane shear deformation mode, it is necessary to consider $\mathcal{O}(\varepsilon^2)$ terms.

In this case, the second order of the asymptotic expansion relative to the axial displacement component w is obtained as it follows:

$$w_2 = \frac{k_{23}}{k_{21}} \ln\left(\frac{a}{r}\right) + \frac{k_{24}}{a k_{21}} \left(\frac{a-r}{r}\right) + \frac{k_{22}}{k_{21}}(a-r), \tag{3.54}$$

with

$$k_{21} = \mu_L^2(2\mu_T + \lambda)\mu_T[(a^2 + b^2)\mu_T + b^2\lambda], \tag{3.55}$$

$$k_{22} = 2b\{2b\mu_T^2 + [(-2\mu_L - \alpha + \lambda)b + a\alpha]\mu_T - b\lambda\mu_L\}\cos(\psi)^2 \times (\alpha + \mu_L - \mu_T)\mu_T T, \tag{3.56}$$

$$k_{23} = \{[2(\beta - \mu_L)\mu_T^2 + ((\beta - \mu_L)\lambda + 2\mu_L^2 - \alpha^2)\mu_T + \lambda\mu_L^2]\cos(\psi)^2 - (2\mu_T + \lambda)(\mu_L - \mu_T)\mu_L\}bT[(a^2 + b^2)\mu_T + b^2\lambda], \tag{3.57}$$

$$k_{24} = \{-4a\mu_T^2 + [(4\mu_L + 2\alpha - 2\lambda)a + 2b\alpha]\mu_T + 2\lambda(a\mu_L + \alpha b)\} \times (\mu_T - \mu_L)\mu_T b^2 aT\cos(\psi)^2, \tag{3.58}$$

which introduces the direction of the fibers influence on the anti-plane shear component of the displacement. This situation is similar to what happens to the same problem in non-linear isotropic elasticity [Pucci 2013a].

3.4.2 Incompressible case

In the incompressible case a radial displacement is not admissible (i.e $f \equiv 0$) and the computations are simplified because the displacement field is directly determined from (3.40) and (3.41). The remaining equilibrium equation in (3.8) must be used to determine the pressure field and a simple and complete exact solution is derived.

We set:

$$\begin{cases} \Gamma_1 = \hat{\mu} + \hat{\beta}M_r^2M_\theta^2 + (1 - \hat{\mu})(M_r^2 + M_\theta^2), \\ \Gamma_2 = \left[\hat{\beta}M_r^2 + (1 - \hat{\mu})\right] M_\theta M_z \\ \Gamma_3 = \hat{\mu} + \hat{\beta}M_r^2M_z^2 + (1 - \hat{\mu})(M_r^2 + M_z^2). \end{cases} \tag{3.59}$$

So, we can write (3.40) and (3.41) as:

$$\Gamma_1\hat{r}g' + \Gamma_2\hat{w}' = 0, \quad \Gamma_2\hat{r}g' + \Gamma_3\hat{w}' = \frac{\hat{T}}{\hat{r}}, \tag{3.60}$$

where the dimensionless variables and parameters are defined as:

$$\hat{\mu} = \mu_T/\mu_L, \quad \hat{\beta} = \beta/\mu_L, \quad \hat{r} = r/b, \quad \hat{w} = w/b, \quad \hat{T} = T/\mu_L. \tag{3.61}$$

The solutions of this system, subject to the boundary conditions $g(a/b) = 0$, $w(a/b) = 0$, are given by:

$$\hat{w}(\hat{r}) = \frac{\Gamma_1}{\Gamma_1\Gamma_3 - \Gamma_2^2}\hat{T}\ln\left(\frac{b}{a}\hat{r}\right), \quad g(\hat{r}) = \frac{\Gamma_2}{\Gamma_1\Gamma_3 - \Gamma_2^2}\hat{T}\left(\frac{1}{\hat{r}} - \frac{b}{a}\right). \tag{3.62}$$

This means that the axial shear deformation is always coupled with an anti-clockwise azimuthal shear.

3.5 Optimisation Problems

There are several interesting aspects about the coupling between the in-plane and the anti-plane deformations in the anisotropic setting. First of all, by using an axial deformation, it is possible to generate an azimuthal shear (or the converse). This fact allows to create the concept of some simple *elastic machines* that may be very useful in some frameworks.

The other aspect of this framework is given by the possibility to arrange the fibers in such a way that it is possible to optimise some quantities of mechanical interest.

It is well known that in the isotropic case, the moment associated with an anti-plane shear, given by:

$$\mathcal{M} = \int_0^{2\pi}\int_a^b r^2\sigma_{\theta z}drd\theta, \tag{3.63}$$

is null because $\sigma_{\theta z} = 0$. But, in the anisotropic case the situation is completely different.

For example, in case ii) where the distribution of the fibers is as in figure (3.1.d), using (3.26), the moment expression is found to be:

$$\hat{\mathcal{M}} = \frac{(1-\hat{\mu})M_rM_\theta}{\hat{\mu} + (1-\hat{\mu})M_r^2}\hat{T}\pi\left(1 - \frac{a^2}{b^2}\right), \tag{3.64}$$

where

$$\hat{\mu} = \frac{\mu_T}{\mu_L}, \quad \hat{\mathcal{M}} = \frac{\mathcal{M}}{b^3\mu_L}, \quad \hat{T} = \frac{T}{\mu_L}. \tag{3.65}$$

Therefore, a rectilinear surface traction generates a moment which is a function:

$$\hat{\mathcal{M}} : S^1 \to \mathbb{R}.$$

Since S^1 (defined as the unit circle in the plane (M_r, M_θ): $M_r^2 + M_\theta^2 = 1$) is a compact set and $\hat{\mathcal{M}}$ is a continuous function, the Weierstrass extreme value theorem guarantees the existence of *optimal* arrangements of fibers that maximise and minimize the moment. Parametrising $\vec{M}$ as:

$$M_r = \cos(\tilde{\theta}), \quad M_\theta = \sin(\tilde{\theta}), \tag{3.66}$$

the optimal arrangements are attained when:

$$\tilde{\theta}_1 = \arccos\left(\sqrt{\frac{\hat{\mu}}{\hat{\mu}+1}}\right), \quad \tilde{\theta}_2 = \pi - \arccos\left(\sqrt{\frac{\hat{\mu}}{\hat{\mu}+1}}\right). \tag{3.67}$$

If $\hat{\mu} < 1$, $\tilde{\theta}_1$ is a maximum and $\tilde{\theta}_2$ a minimum. The converse situation occurs if $\hat{\mu} > 1$.

A general treatment of these problems is quite involved. In the incompressible case the solution is known in an explicit form and results in closed form can be obtained.

Indeed, in this case (see subsection 3.2) the torsion stress component $\sigma_{\theta z}$ is given explicitly by:

$$\sigma_{\theta z} = \left(\beta M_\theta^2 + \mu_L - \mu_T\right) M_r M_z r g' + \left[\beta M_z^2 + \mu_L - \mu_T\right] M_r M_\theta w' \tag{3.68}$$

and therefore:

$$\begin{aligned}\mathcal{M} = \pi(b^2 - a^2)&\frac{b\hat{T} M_r}{\Gamma_1\Gamma_3 - \Gamma_2^2} \\ &\times [\Gamma_1 M_\theta(\beta M_z^2 + \mu_L - \mu_T) - \Gamma_2 M_z(\beta M_\theta^2 + \mu_L - \mu_T)].\end{aligned} \tag{3.69}$$

Introducing the dimensionless variable $\hat{r} = r/b \in [a/b, 1]$, the maximum amount of the azimuthal shear is obtained on the external mantle of the cylinder as:

$$g(1) = \left(\frac{\Gamma_2}{\Gamma_1\Gamma_3 - \Gamma_2^2}\right)\hat{T}\left(1 - \frac{b}{a}\right). \tag{3.70}$$

Reading $g(1)$ as a function:

$$g(1) : S^2 \to \mathbb{R},$$

where S^2 is the unit sphere (defined by $M_r^2 + M_\theta^2 + M_z^2 = 1$), it is possible to search for arrangements of the fibers that optimise the azimuthal displacement, once again, using the classical extreme value theorem of real analysis.

To compute the extrema of the rotation field g, the following Lagrangian is introduced:

$$\mathcal{L} = \frac{\Gamma_2}{\Gamma_1\Gamma_3 - \Gamma_2^2} - \Lambda(M_r^2 + M_\theta^2 + M_z^2 - 1), \tag{3.71}$$

and therefore, the following system must be solved:

$$\begin{cases} M_\theta \frac{\partial \mathcal{L}}{\partial M_r} - M_r \frac{\partial \mathcal{L}}{\partial M_\theta} = 0, \\ \\ M_z \frac{\partial \mathcal{L}}{\partial M_\theta} - M_\theta \frac{\partial \mathcal{L}}{\partial M_z} = 0, \\ \\ M_r^2 + M_\theta^2 + M_z^2 - 1 = 0. \end{cases} \tag{3.72}$$

From $(5.10)_2$:

$$(\hat{\beta} M R^2 + 1 - \hat{\mu})(M_z^2 - M_\theta^2) = 0 \tag{3.73}$$

and since we require $\Gamma_2 \neq 0$, otherwise $g \equiv 0$, we obtain:

$$M_r^2 = 1 - 2M_z^2, \quad M_\theta^2 = M_z^2. \tag{3.74}$$

Using this assumption, it is possible to find a general solution of (5.10) given by:

$$M_r = 0, \quad M_\theta = \pm\frac{1}{\sqrt{2}}, \tag{3.75}$$

see figure (3.1.f).

Another solution to (5.10) can be obtained only for special values of $\hat{\mu}$ and $\hat{\beta}$, if the

algebraic equation:

$$16\hat{\beta}^2(\hat{\mu}-1)M_z^8+16\hat{\beta}(\hat{\mu}-1)(\hat{\mu}-\hat{\beta}-1)M_z^6$$
$$-4\hat{\beta}(\hat{\mu}-1)(\hat{\mu}-\hat{\beta}-3)M_z^4+4\hat{\beta}M_z^2+\hat{\mu}-\hat{\beta}-1=0, \tag{3.76}$$

admits a solution $M_z^2 \in]0,1[$.

It is possible to determine the zone of existence or non-existence of solutions of (5.10) in the $\hat{\alpha},\hat{\beta}-$plane by a direct numerical method see the left plot of figure (3.2).

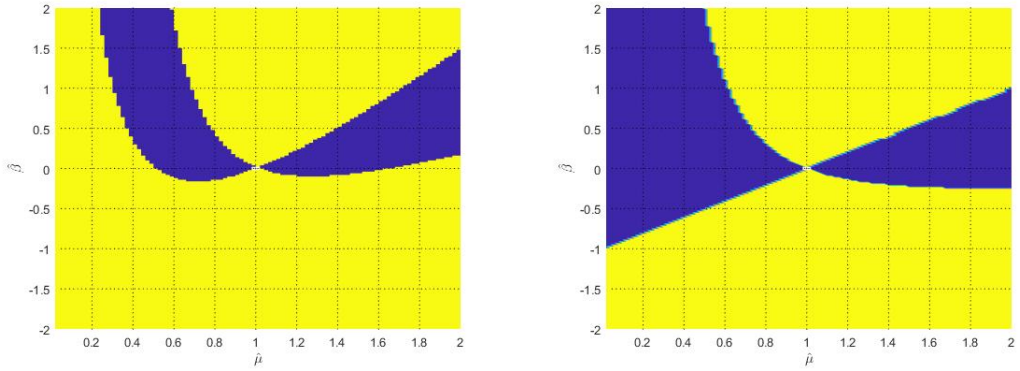

(a) Shear's optimisation (b) Moment's optimisation

Figure 3.2: Number of the optimal fibers arrangements depending on the material parameters (yellow color: existence of two admissible solutions, blue color: existence of unique general solution).

Another optimisation problem can be studied if the moment in (5.7) is considered as a function:

$$\mathcal{M}: S^2 \to \mathbb{R}.$$

Now the Lagrangian of interest is:

$$\hat{\mathcal{L}} = \mathcal{M} - \Lambda((M_r^2+M_\theta^2+M_z^2-1)), \tag{3.77}$$

and the equations to be solved have the same formal structure of (5.10):

$$\begin{cases} M_\theta \frac{\partial \hat{\mathcal{L}}}{\partial M_r} - M_r \frac{\partial \hat{\mathcal{L}}}{\partial M_\theta} = 0, \\ \\ M_z \frac{\partial \hat{\mathcal{L}}}{\partial M_\theta} - M_\theta \frac{\partial \hat{\mathcal{L}}}{\partial M_z} = 0, \\ \\ M_r^2 + M_\theta^2 + M_z^2 - 1 = 0. \end{cases} \tag{3.78}$$

A first solution of (5.16), valid for any value of the constitutive parameters, is:

$$M_z = 0, M_r = \pm\sqrt{\frac{\hat{\mu}}{\hat{\mu}+1}}, M_\theta = \pm\sqrt{\frac{1}{\hat{\mu}+1}}. \tag{3.79}$$

Solving $(5.16)_2$ we obtain the following relation:

$$M_\theta^2 = \frac{[2\hat{\mu}^2 - (\hat{\beta}+4)\hat{\mu} + 2]M_r^2 - 2\hat{\mu}^2 + (\hat{\beta}+3)\hat{\mu} - 1}{3\hat{\beta}(\hat{\mu}-1)M_r^2 - 6\hat{\mu}^2 + 3(\hat{\beta}+4)\hat{\mu} - 6}, \tag{3.80}$$

and introducing it in $(5.16)_{1,3}$, we reduce the problem of the additional solution determination to the search of real roots of a fifth order polynomial equation (see Appendix A for details). The existence of this additional solution depends on the values of constitutive parameters (see the right plot of figure (3.2)).

3.6 Analogy with initially-stressed materials

As illustrated in chapter 2, the presence of an initial stress leads in general to the material anisotropy. That is why the objective of this section is to point out in a different way the analogy between initially-stressed and fibrous materials behaviours. Let consider that the material cylinder is subjected to a constant initial tensor $\boldsymbol{\tau}$ which satisfies:

$$\begin{cases} \text{div}\boldsymbol{\tau} = \vec{0}, \text{ in } \Omega, \\ \boldsymbol{\tau}.\vec{n} = \vec{t}, \text{ on } \partial\Omega, \end{cases} \tag{3.81}$$

where $\vec{n}$ denotes the outward normal to the boundary $\partial\Omega$, whereas $\vec{t}$ is the traction force imposed on the boundary $\partial\Omega$ to equilibrate the initial stress field $\boldsymbol{\tau}$.
In analogy with what is discussed above, suppose that the material cylinder is subjected

to an initial stress field denoted by $\boldsymbol{\tau}$ which is in the following form:

$$\boldsymbol{\tau} = \alpha_\tau \mathbf{1} + \beta_\tau \vec{L} \otimes \vec{L} \tag{3.82}$$

where α_τ, β_τ are constant and the components of the vector $\vec{L}$ components in the cylindrical coordinates are constant. The Cauchy stress can be divided into two parts as:

$$\boldsymbol{\sigma} = \boldsymbol{\tau} + \boldsymbol{\delta\sigma}, \tag{3.83}$$

with $\boldsymbol{\delta\sigma}$ is a linear tensorial operator depending on the displacement gradient. Then, if we choose the same boundary conditions for the unstressed material in the previous sections with a slight changes as:

$$\begin{cases} (\boldsymbol{\delta\sigma}\vec{n})\,|_{r=b} = T\vec{e}_z, \\ \vec{u}(r=a) = \vec{0}. \end{cases} \tag{3.84}$$

The same structure of the partial differential equations related to the equilibrium equation are obtained for both compressible and incompressible transformations discussed above. Hence, analogous couplings to the ones studied above can be enlightened in the case of initially-stressed materials. It is important to notice, that in the incompressible case, the radial displacement component vanishes and the equilibrium equation leads to an overdetermined partial differential equations system which needs to be studied in detail for the possible existence of non-trivial solutions.

3.7 Concluding Remarks

Using a simple, but non trivial example, we have illustrated some interesting couplings of the various modes of deformation in a transverse isotropic material. This kind of couplings shows the inherent complexity of anisotropic elasticity and can be exploited to create some elastic actuators.

Arranging the anisotropy of the material, for example, it is possible to turn an axial displacement into an azimuthal deformation and vice versa. A very interesting property to design *elastic machines*, but also to understand the arrangement of the fibers in some biological materials. In the bio-framework, it is possible that these coupling effects have been optimised for the best efficiency of the different organs functions. Therefore, our

findings shed a new light on the structure of some fiber-reinforced biomaterials.

The different couplings studied in this chapter for an anisotropic material can be in an analogous form in the case of initially-stressed materials. Such fact highlights in a different way, the analogy between initially-stressed and anisotropic materials behaviours. A generalization of our approach, in presence of nonlinear deformations and residual stresses, is a necessary step to adapt our results for realistic applications in biomechanics.

Chapter 4

Identification of linear elastic initially-stressed material parameters

Contents

4.1 Introduction

For the development of constitutive laws for initially stressed elastic materials, the determination of the model's parameters and the initial stress are of paramount impor-

tance. This is an inverse problem as mentioned in [Bui 2007]. From an experimental viewpoint, non-invasive techniques like X-ray diffraction, semi-invasive techniques like incremental center hole drilling and deep hole drilling, and fully destructive methods like slotting, contour, and inherent strain can all be used to determine the residual stress at surface and/or body points. Due to the cost, time commitment, and dispersion of the measured data, only discrete points of stress in sections are normally measured. In initial stressed linear elasticity theory, all the constitutive models of the first half of the twentieth century, presented in [ZP 1971], have the same algebraic structure as the model of [Hoger 1986]. This latter model depends on an unknown tangent elasticity tensor function of the initial stress. Different forms and identification methodologies of this elasticity tensor have been proposed [Hoger 1986, Man 1987, Man 1994]. A general form was proposed recently in [Gower 2015, Gower 2017]. The identification of the initial stress (or residual stress) can be done by an analytical (or semi-) method determined from its equilibrium equation and its boundary conditions for specific geometries [Hoger 1986, Sburlati 1992, Faghidian 2014]. The stress function method [Faghidian 2012] and the inverse eigenstrain technique [Jun 2010] have been developed to date in order to reconstruct residual stress fields. This avoids modelling the mechanisms that cause residual stresses. Both approaches are utilized only when the stress or strain distributions can be stated using a parametric equation, such as when the distribution varies in one direction [Korsunsky 2007], due to the complexity of the hypothesis and debugging of the stress or strain function. In [Ballard 1994], an approximate inverse method to build a residual stress field is used. These methods, however, do not guarantee that the distributions satisfy the equilibrium and boundary requirements due to a lack of knowledge about additional and significant constraints.

In addition to its practical importance, determining residual stresses raises a number of difficult mathematical issues. In fact, several forms of the inverse problem of unique residual stress determination were investigated, utilizing several model equations for residual stress and various methods of measurements [Bonnet 2005]. The central questions here are those of stability and uniqueness [Man 1994, Robertson 1997, Robertson 1998, Rachele 2003, Ivanov 2005, Isakov 2007, Isakov 2008] . For the residually stressed linear elastic model proposed by [Hoger 1986], some basic properties for the associated boundary value problem have been established particularly Carleman estimates, which lead to the Cauchy problem's uniqueness and stability [Lin 2003, Isakov 2007].

The objective of this chapter is to study some inverse problems in the scope of initially-stressed linear elastic materials whose constitutive formulation is presented by [Hoger 1986]. This chapter can be divided into two main parts. The first part includes section 2 and 3 and focuses on the general constitutive relation for initially stressed linear elastic materials with a three-dimensional material body. Whereas the second part gathers the remaining sections and treats a simple behaviour model in the scope of plane deformations with a different reconstruction approach. In fact, The second section is devoted to the reformulation of the general constitutive relation established by [Hoger 1986]. Based on the new form of the constitutive relation established in the second section, the third section illustrates a reconstruction approach for the different material parameters and a stability estimate is obtained. Moreover, section 4 presents the theoretical formulation of the direct approach that will be used for the material parameters identification in the case of the considered simplified model. The next section provides a stability estimate for the special case of residual stress reconstruction. The remaining sections detail the numerical aspect of the used approach and show the influence of multiple parameters on the quality of the different fields reconstruction.

4.2 Preliminary equations

First, we will denote by $M_3(\mathbb{R})$ the vector space of 3×3 real matrices endowed with the scalar product $A : B = \mathrm{tr}(A^T B)$. The space $M_3(\mathbb{R})$ can be decomposed with respect to the defined scalar product as $M_3(\mathbb{R}) = S_3(\mathbb{R}) \oplus A_3(\mathbb{R})$, where $S_3(\mathbb{R})$ and $A_3(\mathbb{R})$ denote respectively the spaces of symmetric and skew-symmetric matrices. Let consider $\Omega \subset \mathbb{R}^3$ as a bounded domain with smooth boundary. If we suppose that the material body has a linear elastic behaviour relative to a reference configuration free of any residual stress which is defined geometrically by the domain Ω, then the material behaviour can be formulated through a stress-strain relation usually denoted by Hooke's law and it can be exhibit as:

$$\boldsymbol{\sigma} = \boldsymbol{\mathcal{C}} : \boldsymbol{\epsilon} \tag{4.1}$$

with

$$\boldsymbol{\epsilon} = \frac{1}{2}(\boldsymbol{\nabla}\vec{u} + \boldsymbol{\nabla}\vec{u}^T) = \boldsymbol{\nabla}^s\vec{u} \tag{4.2}$$

where $\boldsymbol{\sigma}$ and $\boldsymbol{\epsilon}$ denote respectively the Cauchy stress tensor and the strain tensor whereas $\boldsymbol{\mathcal{C}}$ is a fourth order tensor and represents the elastic tensor in absence of any initial stress. $\boldsymbol{\mathcal{C}}$ satisfies the following symmetries:

$$\mathcal{C}_{ijkl} = \mathcal{C}_{jikl}, \quad \mathcal{C}_{ijkl} = \mathcal{C}_{klij} \quad 1 \leq i, j, k, l \leq 3, \tag{4.3}$$

Hence, the linear elastic behaviour represented through the fourth order tensor $\boldsymbol{\mathcal{C}}$ is characterized by a 21 independent scalar material parameters instead of 81.

Based on the Voigt representation, the elasticity tensor $\boldsymbol{\mathcal{C}}$ can be represented by a symmetric matrix valued function $\boldsymbol{C}$ in $S_6(\mathbb{R})$. The components of the $\boldsymbol{C}$ matrix is constructed via the double index mapping:

$$\gamma = \begin{cases} 11 & \to 1, \\ 22 & \to 2, \\ 33 & \to 3, \\ 32, 23 & \to 4, \\ 13, 31 & \to 5, \\ 12, 21 & \to 6. \end{cases} \tag{4.4}$$

in a way that we can define the matrix $\boldsymbol{C}$ in function of the elasticity tensor $\boldsymbol{\mathcal{C}}$ as:

$$C_{mn} = \mathcal{C}_{ijkl}, \quad \text{with } m = \gamma(ij) \text{ and } n = \gamma(kl). \tag{4.5}$$

Using Voigt representation, the Hooke's law presented above in equation (4.1), can be reformulated as:

$$\boldsymbol{\sigma}_V = \boldsymbol{C}\boldsymbol{\epsilon}_V \tag{4.6}$$

with

$$\begin{cases} \boldsymbol{\sigma}_V & = [\sigma_{11}, \sigma_{22}, \sigma_{33}, \sigma_{23}, \sigma_{13}, \sigma_{12}], \\ \boldsymbol{\epsilon}_V & = [\epsilon_{11}, \epsilon_{22}, \epsilon_{33}, 2\epsilon_{23}, 2\epsilon_{13}, 2\epsilon_{12}]. \end{cases} \tag{4.7}$$

In the case of initially-stressed material, the elastic material behaviour is not any more a simple relation between the Cauchy stress tensor and the strain tensor, but a more complex relation, although it is linear, involving the displacement gradient field $\boldsymbol{\nabla}\vec{u}$. Now, we

suppose that the reference configuration Ω is subjected to an initial stress field denoted by $\boldsymbol{\tau}$ which is defined as the Cauchy stress tensor in the reference configuration. Consequently, $\boldsymbol{\tau}$ is symmetric and it satisfies the equilibrium equation:

$$\text{Div}\boldsymbol{\tau} = \vec{0}, \quad \text{in } \Omega \tag{4.8}$$

and the boundary conditions:

$$\boldsymbol{\tau}.\vec{N} = \vec{t_0}, \quad \text{on } \partial\Omega, \tag{4.9}$$

where Div is the divergence operator defined relatively to the reference configuration Ω, $\vec{N}$ denotes the outward unit normal to the boundary of Ω whereas $\vec{t_0}$ denotes the exterior force vector needed for the equilibrium of the material body in the presence of the initial stress field $\boldsymbol{\tau}$. When $\vec{t_0}$ vanishes, $\boldsymbol{\tau}$ is called a residual stress (auto-equilibrated initial stress field in absence of any exterior loadings). The behaviour of such material can be characterized as a mathematical formulation relating the first Piola Kirchhof stress tensor $\boldsymbol{S}$ and the displacement gradient tensor $\boldsymbol{\nabla}\vec{u}$ as:

$$\boldsymbol{S} = \boldsymbol{\tau} + (\boldsymbol{\nabla}\vec{u})\boldsymbol{\tau} + \boldsymbol{\mathcal{L}} : \boldsymbol{\epsilon} \tag{4.10}$$

with $\boldsymbol{\mathcal{L}}$ is a fourth order tensor having the same symmetry properties of the standard elastic tensor $\boldsymbol{\mathcal{C}}$ (see equation (4.3)) and it is depending of the initial stress field $\boldsymbol{\tau}$. Similarly to the elastic tensor $\boldsymbol{\mathcal{C}}$, the initially-stressed elastic tensor $\boldsymbol{\mathcal{L}}$ can be represented by a symmetric matrix $\boldsymbol{L}$ in $S_6(\mathbb{R})$. To have an analogous form of the stress-displacement gradient relation as the one for the Hooke's law using Voigt representation, we will introduce the general vector representation of non symmetric tensors in $M_3(\mathbb{R})$ as:

$$\begin{cases} \boldsymbol{S}_G & = [S_{11}, S_{12}, S_{13}, S_{21}, S_{22}, S_{23}, S_{31}, S_{32}, S_{33}]^T, \\ (\boldsymbol{\nabla}\vec{u})_G & = [u_{1,1}, u_{1,2}, u_{1,3}, u_{2,1}, u_{2,2}, u_{2,3}, u_{3,1}, u_{3,2}, u_{3,3}]^T \\ & = [(\nabla u_1)^T, (\nabla u_2)^T, (\nabla u_3)^T]^T. \end{cases} \tag{4.11}$$

In the sake of pure simplification, the general vector representation of a tensor in $M_3(\mathbb{R})$ will be denoted in the following of this chapter as G-representation. Now, we can express the strain tensor (in Voigt representation) in function of the displacement gradient (in

G-representation) as:

$$\boldsymbol{\epsilon}_V = \boldsymbol{M}_{\epsilon H}(\boldsymbol{\nabla}\vec{u})_G \tag{4.12}$$

where $\boldsymbol{M}_{\epsilon H}$ is a constant matrix and it can be explicited as:

$$\boldsymbol{M}_{\epsilon H} = \begin{bmatrix} 1 & 0 & 0 & 0 & 0 & 0 & 0 & 0 & 0 \\ 0 & 0 & 0 & 0 & 1 & 0 & 0 & 0 & 0 \\ 0 & 0 & 0 & 0 & 0 & 0 & 0 & 0 & 1 \\ 0 & 0 & 0 & 0 & 0 & 1 & 0 & 1 & 0 \\ 0 & 0 & 1 & 0 & 0 & 0 & 1 & 0 & 0 \\ 0 & 1 & 0 & 1 & 0 & 0 & 0 & 0 & 0 \end{bmatrix} \tag{4.13}$$

Furthermore, the equivalence between the general vectorial and Voigt representations for the symmetric Cauchy stress tensor can be illuminated through the following equation:

$$\boldsymbol{\sigma}_G = \boldsymbol{M}_{S\sigma}\boldsymbol{\sigma}_V, \tag{4.14}$$

where the constant matrix $\boldsymbol{M}_{S\sigma}$ may be presented as:

$$\boldsymbol{M}_{S\sigma} = \begin{bmatrix} 1 & 0 & 0 & 0 & 0 & 0 \\ 0 & 0 & 0 & 0 & 0 & 1 \\ 0 & 0 & 0 & 0 & 1 & 0 \\ 0 & 0 & 0 & 0 & 0 & 1 \\ 0 & 1 & 0 & 0 & 0 & 0 \\ 0 & 0 & 0 & 1 & 0 & 0 \\ 0 & 0 & 0 & 0 & 1 & 0 \\ 0 & 0 & 0 & 1 & 0 & 0 \\ 0 & 0 & 1 & 0 & 0 & 0 \end{bmatrix} = \boldsymbol{M}_{\epsilon H}^T \tag{4.15}$$

In fact, the first Piola Kirchhoff stress tensor can be divided into two parts: a symmetric tensor $\boldsymbol{S}^{(1)}$ expressed in a similar way of the Hooke's law and a second part $\boldsymbol{S}^{(2)}$ depending explicitly on the the residual stress field $\boldsymbol{\tau}$, so we can write:

$$\begin{cases} \boldsymbol{S} & = \boldsymbol{S}^{(1)} + \boldsymbol{S}^{(2)}, \\ \boldsymbol{S}^{(1)} & = \boldsymbol{\mathcal{L}} : \boldsymbol{\epsilon}, \\ \boldsymbol{S}^{(2)} & = \boldsymbol{\tau} + \boldsymbol{\nabla}\vec{u}\boldsymbol{\tau}, \end{cases} \tag{4.16}$$

Using the G-representation, the different tensors $\boldsymbol{S}^{(1)}$ and $\boldsymbol{S}^{(2)}$ can be shown as:

$$\begin{cases} \boldsymbol{S}_G^{(1)} &= \boldsymbol{M}_{S\sigma}\boldsymbol{S}_V^{(1)} = \boldsymbol{M}_{S\sigma}\boldsymbol{L}\boldsymbol{M}_{S\sigma}^T(\boldsymbol{\nabla}\vec{u})_G, \\ \boldsymbol{S}_G^{(2)} &= \boldsymbol{\tau}_G + \boldsymbol{M}_\tau(\boldsymbol{\nabla}\vec{u})_G, \end{cases} \tag{4.17}$$

where the matrix $\boldsymbol{M}_\tau$ can be displayed in function of the initial stress tensor $\boldsymbol{\tau}$ as a block-matrix in the following form:

$$\boldsymbol{M}_\tau = \begin{bmatrix} \boldsymbol{\tau} & \boldsymbol{0} & \boldsymbol{0} \\ \boldsymbol{0} & \boldsymbol{\tau} & \boldsymbol{0} \\ \boldsymbol{0} & \boldsymbol{0} & \boldsymbol{\tau} \end{bmatrix} \tag{4.18}$$

Consequently, using equations (4.16-4.17) related to the decomposition of the first Piola Kirchhof stress tensor, we can derive the stress-displacement gradient formulation in the case of an initially-stressed material as:

$$\boldsymbol{S}_G = \boldsymbol{\tau}_G + \tilde{\boldsymbol{C}}(\boldsymbol{\nabla}\vec{u})_G, \tag{4.19}$$

where the matrix $\tilde{\boldsymbol{C}}$ can be written as:

$$\tilde{\boldsymbol{C}} = \boldsymbol{M}_{S\sigma}\boldsymbol{L}\boldsymbol{M}_{S\sigma}^T + \boldsymbol{M}_\tau, \tag{4.20}$$

It is important to notice that the term $\boldsymbol{\tau}_G$ is not involved in the equilibrium equation since the initial stress tensor $\boldsymbol{\tau}$ satisfies also the equilibrium equation (4.8). Also, it is clear that $\tilde{\boldsymbol{C}}$ is a symmetric matrix in a subspace of $S_9(\mathbb{R})$ which will be denoted by $\mathcal{V}(\mathbb{R})$ and can be defined as:

$$\mathcal{V}(\mathbb{R}) = \{\boldsymbol{M}_{S\sigma}\boldsymbol{L}\boldsymbol{M}_{S\sigma}^T + \boldsymbol{M}_\tau| \quad \boldsymbol{L} \in S_6(\mathbb{R}), \quad \boldsymbol{\tau} \in S_3(\mathbb{R})\} \subset S_9(\mathbb{R}). \tag{4.21}$$

Based on the form of the matrix $\tilde{\boldsymbol{C}}$ function of the matrces $\boldsymbol{\tau}$ (6 independents components) and $\boldsymbol{L}$ (21 parameters), we can deduce that $\dim(\mathcal{V}(\mathbb{R})) \leq 27$. Furthermore, using the explicit form of the matrix $\tilde{\boldsymbol{C}}$ in function of both $\boldsymbol{L}$ and $\boldsymbol{\tau}$ components, we can show that $\dim(\mathcal{V}(\mathbb{R})) = 27$ (see appendix D) and we can construct a basis for $\mathcal{V}(\mathbb{R})$ exploiting two chosen basis of $S_3(\mathbb{R})$ and $S_6(\mathbb{R})$ using the expression of $\tilde{\boldsymbol{C}}$ in equation (4.20).

Both Cauchy stress and the first Piola Kirchhoff stress tensors satisfy the following equi-

librium equations:

$$\mathrm{Div}\boldsymbol{S} = \vec{0}, \quad \mathrm{div}\boldsymbol{\sigma} = \vec{0}, \quad \text{in } \Omega \tag{4.22}$$

where Div and div are the divergence operator relative to respectively the reference and the current configurations. Since the scope of small deformations is considered, in the case of smooth deformation fields, as an approximation of first order, both the current and reference divergence operators can be considered as the same one.

Hypothesis 1: In the rest of this chapter we will assume that the initially-stressed elasticity tensor $\boldsymbol{\mathcal{L}}$ is pointwise stable over Ω as it is defined in [[Hughes 1983] Chap. 6, Def. 1.9] (for the standard elasticity tensor $\boldsymbol{\mathcal{C}}$) as the existence of a constant $\beta > 0$ such that

$$\boldsymbol{\epsilon} : \boldsymbol{\mathcal{L}} : \boldsymbol{\epsilon} > \beta \boldsymbol{\epsilon} : \boldsymbol{\epsilon}, \quad \forall \vec{X} \in \Omega, \quad \forall \boldsymbol{\epsilon} \in S_3(\mathbb{R}). \tag{4.23}$$

Lemma 1: Based on Hypothesis 1 illustrated through equation (4.23), and based on Lemma 2.1 in [Bal 2015], there exists a constant $\beta^{'}$ such that

$$det(\boldsymbol{L}) > \beta^{'}, \quad \forall \vec{X} \in \Omega. \tag{4.24}$$

4.3 Inverse problem for a generalized initially-stressed material

4.3.1 Reconstruction of the elasticity tensor

In this section we intend to present a methodology for the reconstruction of both the initially-stressed field and the initially-stressed elastic tensor $\boldsymbol{\mathcal{L}}$ which are both represented by the matrix $\tilde{\boldsymbol{C}}$. Based on this method, a set of stability results can be derived. First, let define the operator D_G related to the equilibrium equation satisfied by the First Piola Kirchhoff and the initial stress as:

$$D_G = \begin{bmatrix} \partial_1 & \partial_2 & \partial_3 & 0 & 0 & 0 & 0 & 0 & 0 \\ 0 & 0 & 0 & \partial_1 & \partial_2 & \partial_3 & 0 & 0 & 0 \\ 0 & 0 & 0 & 0 & 0 & 0 & \partial_1 & \partial_2 & \partial_3 \end{bmatrix} \tag{4.25}$$

where ∂_i denotes the partial derivative relative to the coordinate X_i defined in the reference configuration Ω.

In the following, to develop the idea whose the reconstruction of the matrix $\tilde{\boldsymbol{C}}$ is based on, we suppose the existence of $N+9$ displacement fields whose the first 9 fields satisfies the following hypothesis.

Hypothesis 2.
There exist nine solutions $\vec{u}^{(1)},...,\vec{u}^{(9)}$, whose gradient tensors form a basis of $M_3(\mathbb{R})$ at every $\vec{X}\in\Omega$. This condition can be summarized as:

$$inf_{\vec{X}\in\Omega} det((\boldsymbol{\nabla}\vec{u}^{(1)})_G,\dots,(\boldsymbol{\nabla}\vec{u}^{(9)})_G)\geq c_0>0, \quad \textit{for some constant } \ c_0. \tag{4.26}$$

In fact Hypothesis 2 is equivalent to assume that the first 9 displacement gradient fields construct a basis in $M_3(\mathbb{R})$, so we can express the rest of the gradient displacement fields in function of this basis elements as:

$$\boldsymbol{\nabla}\vec{u}^{(p)}(\vec{X})=\sum_{j=1}^{9}\mu_{pj}(\vec{X})\boldsymbol{\nabla}\vec{u}^{(j)}(\vec{X}), \quad \forall\vec{X}\in\Omega_0 \tag{4.27}$$

where μ_{pj} is the coordinate of $\boldsymbol{\nabla}\vec{u}^{(p)}$ relative to the basis element $\boldsymbol{\nabla}\vec{u}^{(j)}$. If we define the operator $\det_G$ as:

$$\det\nolimits_G(\boldsymbol{\nabla}\vec{u}^{(1)},\dots,\boldsymbol{\nabla}\vec{u}^{(9)})=\det((\boldsymbol{\nabla}\vec{u}^{(1)})_G,\dots,(\boldsymbol{\nabla}\vec{u}^{(9)})_G) \tag{4.28}$$

then the coordinates functions μ_{pj} can be explicitly defined as:

$$\mu_{pj}=\frac{det_G(\boldsymbol{\nabla}\vec{u}^{(1)},...,\overset{j}{\boldsymbol{\nabla}\vec{u}^{(p)}},...,\boldsymbol{\nabla}\vec{u}^{(9)})}{det_G(\boldsymbol{\nabla}\vec{u}^{(1)},...,\boldsymbol{\nabla}\vec{u}^{(9)})} \tag{4.29}$$

Now, exploiting the decomposition of the displacement gradient fields in equation (4.27) and bearing in mind that the initial stress field satisfies the equilibrium equation as it is illustrated in equation (4.8), then the equilibrium equation associated to the first Piola Kirchhoff stress presented in equation (4.22) can be reformulated for the set of displacement

fields data as:

$$\begin{aligned}\vec{0} = D_G(\tilde{\boldsymbol{C}}(\boldsymbol{\nabla}\vec{u}^{(p)})_G) &= \sum_{j=1}^{9} D_G(\mu_{pj}\tilde{\boldsymbol{C}}(\boldsymbol{\nabla}\vec{u}^{(j)})_G) \\ &= \sum_{j=1}^{9}(D_G\mu_{pj})\tilde{\boldsymbol{C}}(\boldsymbol{\nabla}\vec{u}^{(j)})_G + \mu_{pj}D_G(\tilde{\boldsymbol{C}}(\boldsymbol{\nabla}\vec{u}^{(j)})_G)\end{aligned} \tag{4.30}$$

$\boldsymbol{\nabla}\vec{u}^{(j)}$ is the gradient of the displacement field $\vec{u}^{(j)}$ solution of the equilibrium equation i.e $D_G(\tilde{\boldsymbol{C}}(\boldsymbol{\nabla}\vec{u}^{(j)})_G) = \vec{0}$ and hence the previous equations is reduced to:

$$\sum_{j=1}^{9}(D_G\mu_{pj})\tilde{\boldsymbol{C}}(\boldsymbol{\nabla}\vec{u}^{(j)})_G = \vec{0} \tag{4.31}$$

This last equation can be seen as three scalar orthogonality constraints on the tensor $\tilde{\boldsymbol{C}}$ in the inner product ":" structure of $\mathcal{V}(\mathcal{R})$, where the matrices that are orthogonal to $\tilde{\boldsymbol{C}}$ are directly known from the available measurements. For every single displacement field measurement $\vec{u}^{(p)}$, the prior equilibrium equation is equivalent to the following three scalar constraints:

$$\tilde{\boldsymbol{C}} : \boldsymbol{M}^{(p),1} = \tilde{\boldsymbol{C}} : \boldsymbol{M}^{(p),2} = \tilde{\boldsymbol{C}} : \boldsymbol{M}^{(p),3} = 0 \tag{4.32}$$

with

$$\begin{cases} \boldsymbol{M}^{(p),1} &= \sum_{j=1}^{9}(\partial_1\mu_{pj}, \partial_2\mu_{pj}, \partial_3\mu_{pj}, 0, 0, 0, 0, 0, 0) \otimes \boldsymbol{\nabla}\vec{u}^{(j)}, \\ \boldsymbol{M}^{(p),2} &= \sum_{j=1}^{9}(0, 0, 0, \partial_1\mu_{pj}, \partial_2\mu_{pj}, \partial_3\mu_{pj}, 0, 0, 0) \otimes \boldsymbol{\nabla}\vec{u}^{(j)}, \\ \boldsymbol{M}^{(p),3} &= \sum_{j=1}^{9}(0, 0, 0, 0, 0, 0, \partial_1\mu_{pj}, \partial_2\mu_{pj}, \partial_3\mu_{pj}) \otimes \boldsymbol{\nabla}\vec{u}^{(j)}. \end{cases} \tag{4.33}$$

Note that since $\tilde{\boldsymbol{C}}$ is orthogonal to $A_9(\mathbb{R})$, and $\mathcal{V}(\mathbb{R})$ is a subspace of $\mathcal{M}_9(\mathbb{R})$ one could replace the matrices $M^{(p),i}$ with the projection of their symmetrized versions on $\mathcal{V}(\mathbb{R})$.
If we have a rich enough set of displacement measurements, we can construct a set of linear constraints of the form (4.32) and then construct enough set of matrices as the ones presented in equation (4.33) to form a hyperplane in $\mathcal{V}(\mathbb{R})$ at every point $\vec{X}$ in Ω. Then, the matrix $\tilde{\boldsymbol{C}}$ which must be perpendicular to this hyperplane, can be reconstructed up to a multiplicative constant. The reconstruction procedure can be done via a generalization of the cross-product, as used, in [Monard 2013] for the material parameters identification in the context of the conductivity equation or in [Bal 2015] for the sake of the elastic tensor

identification.

Define by $\{\boldsymbol{m}_j\}_{j=1}^{27}$ a basis of $\mathcal{V}(\mathbb{R})$, and given set $M = \{\boldsymbol{M}_j\}_{j=1}^{20} \subset \mathcal{V}(\mathbb{R})$. Now, following [Bal 2015], we can define define the generalized version of the cross product operator denoted by $\mathcal{N} : \mathcal{V}(\mathbb{R})^{20} \to \mathcal{V}(\mathbb{R})$ as follows

$$[\mathcal{N}(M)]_i = \frac{1}{\det(\boldsymbol{m}_1, \ldots, \boldsymbol{m}_{27})} \begin{vmatrix} \boldsymbol{M}_1 : \boldsymbol{m}_1 & \cdots & \boldsymbol{M}_{26} : \boldsymbol{m}_1 & \\ \vdots & \ddots & \vdots & \boldsymbol{m}_i \\ \boldsymbol{M}_1 : \boldsymbol{m}_{27} & \cdots & \boldsymbol{M}_{26} : \boldsymbol{m}_{27} & \end{vmatrix}, \quad \forall 1 \leq i \leq 27. \tag{4.34}$$

Based on its expression in the last equation, $\mathcal{N}$ is a 26-linear, alternating map that does not depend on the choice of basis for $\mathcal{V}(R)$. $\mathcal{N}(M)$ is a vector that is normal to the hyperplane spanned by M when M is linearly independent; zero otherwise. In particular, if M is a family of matrices known to be orthogonal to a given matrix $\boldsymbol{m}'$, then $\mathcal{N}(M)$ is either zero (if $dim \;\; span \;\; M < 26$) or proportional to $\boldsymbol{m}'$ (if $dim \;\; span \;\; M = 26$).

In light of this last comment, and assuming that a rich enough set of solutions of the direct problem gives rise to a family of matrices M of the form (4.33), with cardinality greater than 26 and spanning a hyperplane of $\mathcal{V}(\mathbb{R})$ at a given point $\vec{X}_0 \in \Omega$, for any given 26-tuple $M' \subset M$,$\mathcal{N}(M')$ is either zero or proportional to $\tilde{\boldsymbol{C}}(\vec{X}_0)$.

Before going deeper in the details of the parameters reconstruction, we will show that we extract both the initially-stressed elastic matrix $\boldsymbol{L}$ and the initial stress tensor $\boldsymbol{\tau}$ from the matrix $\tilde{\boldsymbol{C}}$. To do so, based on equations (4.18,4.20), we can get the matrix $\tilde{\boldsymbol{C}}$ function of matrices $\boldsymbol{L}$ and $\boldsymbol{\tau}$ components as:

$$\tilde{\boldsymbol{C}} = \begin{bmatrix} L_{11}+\tau_{11} & L_{16}+\tau_{12} & L_{15}+\tau_{13} & L_{16} & L_{12} & L_{14} & L_{15} & L_{14} & L_{13} \\ L_{61}+\tau_{12} & L_{66}+\tau_{22} & L_{65}+\tau_{23} & L_{66} & L_{62} & L_{64} & L_{65} & L_{64} & L_{63} \\ L_{51}+\tau_{13} & L_{56}+\tau_{23} & L_{55}+\tau_{33} & L_{56} & L_{52} & L_{54} & L_{55} & L_{54} & L_{53} \\ L_{61} & L_{66} & L_{65} & L_{66}+\tau_{11} & L_{62}+\tau_{12} & L_{64}+\tau_{13} & L_{65} & L_{64} & L_{63} \\ L_{21} & L_{26} & L_{25} & L_{26}+\tau_{12} & L_{22}+\tau_{22} & L_{24}+\tau_{23} & L_{25} & L_{24} & L_{23} \\ L_{41} & L_{46} & L_{45} & L_{46}+\tau_{13} & L_{42}+\tau_{23} & L_{44}+\tau_{33} & L_{45} & L_{44} & L_{43} \\ L_{51} & L_{56} & L_{55} & L_{56} & L_{52} & L_{54} & L_{55}+\tau_{11} & L_{54}+\tau_{12} & L_{53}+\tau_{13} \\ L_{41} & L_{46} & L_{45} & L_{46} & L_{42} & L_{44} & L_{45}+\tau_{12} & L_{44}+\tau_{22} & L_{43}+\tau_{23} \\ L_{31} & L_{36} & L_{35} & L_{36} & L_{32} & L_{34} & L_{35}+\tau_{13} & L_{34}+\tau_{23} & L_{33}+\tau_{33} \end{bmatrix}$$

. (4.35)

Using the components of $\tilde{\boldsymbol{C}}$ expressed only function of $\boldsymbol{L}$ components we can extract directly the following quantities which can be sorted in two sets:
-mixed index components of $\boldsymbol{L}$: L_{ij} with $i \neq j$.
-L_{44}, L_{55}, L_{66}.

Next, using the first 3×3 block of $\tilde{\boldsymbol{C}}$, we can extract all the components of the initial stress field $\boldsymbol{\tau}$ except τ_{11}. Then, knowing $\tilde{C}_{44}$ we can get the value of τ_{11} since L_{66} is already determined. Hence, so far all the components of the initial stress field are determined and we can use the rest of the matrix $\tilde{\boldsymbol{C}}$ components to derive the rest of the matrix $\boldsymbol{L}$ components (which are L_{11}, L_{22} and L_{33}).

Since the extraction of the matrices $\boldsymbol{L}$ and $\boldsymbol{\tau}$ from $\tilde{\boldsymbol{C}}$ is feasible, we will denote by $\mathcal{K}_L$ and $\mathcal{K}_\tau$ the operators that extract respectively $\boldsymbol{L}$ and $\boldsymbol{\tau}$ from the generalized initially-elastic matrix $\tilde{\boldsymbol{C}}$.

Based on the Lemma 1 and as it was in the proof of Lemma 2.1 in [Bal 2015], the Hypothesis 1 implies that the components L_{11}, L_{22} and L_{33} must be strictly positive. Thus, to make the reconstruction operator of the matrix $\tilde{\boldsymbol{C}}$ unique, using the Lemma.1, we can define the final reconstructed matrix $\tilde{\boldsymbol{C}}^*$ by normalizing the matrix $\boldsymbol{L}$ enforcing the strict positivity of the components L_{11}, L_{22} and L_{33}. So we can define the reconstructed generalized

initially-stressed matrix as:

$$(\pm)_{M'}\mathcal{N}(M') = (\det(\mathcal{K}_L(\mathcal{N}(M'))))^{\frac{1}{6}}\tilde{\boldsymbol{C}}^*, \quad \forall \vec{X} \in \Omega, \tag{4.36}$$

for every 27-tuple $M' \subset M$, where $(\pm)_{M'}$ is the sign of the top-left entry of $\mathcal{K}_L(\mathcal{N}(M'))$. This equation is either trivial when M' is linearly dependent, or reconstructs $\tilde{\boldsymbol{C}}(\vec{X_0})$ otherwise.

Hypothesis 3 *Assuming hypothesis 2 is fulfilled, there exists N additional solutions $\vec{u}^{(9+1)}, ..., \vec{u}^{(9+N)}$ giving rise to a family M of $3N$ matrices, whose expressions are explicit in terms of ($\boldsymbol{\nabla}\vec{u}^{(i)}$, $\partial_j\boldsymbol{\nabla}\vec{u}^{(i)}$, $1 \leq i \leq 6+N$, $1 \leq j \leq 3$ (see equation (4.33)) and such that they span a hyperplane of $\mathcal{V}(\mathbb{R})$ at every $\vec{X} \in \Omega$. This condition can be summarized as*

$$inf_{\vec{X}\in\Omega} \sum_{M^{'}\subset M,\ \ \#M^{'}=20} \mathcal{N}(M^{'}) : \mathcal{N}(M^{'}) \geq c_1 > 0, \ \textit{for some constant } c_1. \tag{4.37}$$

The last hypothesis ensures that at least one subfamily M' is linearly independent, so we can sum the last equation over all subfamilies so we can establish the following formula

$$\tilde{\boldsymbol{C}}^* = \Big(\sum_{M^{'}\subset M,\ \ \#M^{'}=20} (\det(\mathcal{K}_L(\mathcal{N}(M'))))^{\frac{1}{6}}\Big)^{-1} \sum_{M^{'}\subset M,\ \ \#M^{'}=26} (\pm)_{M'}\mathcal{N}(M') \tag{4.38}$$

The reconstruction formula in equation (4.38) makes the stability of the problem straightforward to assess, because based on the hypothesis 3, one subfamily linearly independent exists at least, and hence by summution we can reconstruct the generalized initially-stressed elastic tensor up to a multiplicative constant and avoid the trivial null solution.

4.3.2 Stability results

In order to build up our reconstruction method, we have already developed our key hypothesis above. In fact, based on the different 3 hypotheses, the unknown generalized initially-stressed matrix is forced to lie on the orthogonal of a vector space constructed by a rich enough set of displacement measurements. And finally, both the couple initial stress and the initially-stressed elastic matrix can be reconstructed up to multiplicative constant. To follow this approach, $9+N$ displacement fields are needed. We should emphasize that N depends on the number of $\tilde{\boldsymbol{C}}$ unknown parameters. In other words, N depends on the anisotropy generated by both the initial stress $\boldsymbol{\tau}$ and the initially-stressed elastic matrix

$\boldsymbol{L}$. If we denote by d_{param} the number of scalar parameters in the matrix $\tilde{\boldsymbol{C}}$, then N must satisfy $N \geq \frac{d_{param}}{3}$, where the number 3 refers to the extra three constraints for every added displacement field measurement. In the most general case, $d_{param} = 21 + 6 = 27$ and hence we need to get $N + 9 = 18$ displacement data fields.

It should be highlighted that Hypotheses 2 and 3 are stable when the boundary conditions generating the displacement fields $\vec{u}^{(9+1)}, ..., \vec{u}^{(9+N)}$ are perturbed smoothly. This is because both of the latter hypotheses are expressed in terms of continuous functionals of their boundary conditions that rely polynomially on the components of displacement fields and their derivatives up to second order.

Theorem 1. *Suppose that over some open set $\Omega_0 \subset \Omega$, Hypothesis 2 and 3 hold for two families of displacement fields $\{\vec{u}^{(j)}\}_{j=1}^{9+N}$ and $\{\vec{u'}^{(j)}\}_{j=1}^{9+N}$ corresponding to the couple elastic tensor-residual stress fields $(\boldsymbol{L}^*, \boldsymbol{\tau}^*)$ and $(\boldsymbol{L}^{*'}, \boldsymbol{\tau}^{*'})$. Then $\tilde{\boldsymbol{C}}^*$ and $\tilde{\boldsymbol{C}}^{*'}$ each can be uniquely reconstructed over Ω_0 from knowledge of their corresponding solutions, with the following stability estimate:*

$$||\tilde{\boldsymbol{C}}^* - \tilde{\boldsymbol{C}}^{*'}||_{W^{p,\infty}(\Omega_0)} \leq K \sum_{j=1}^{N+9} ||\boldsymbol{\nabla}\vec{u}^{(j)} - \boldsymbol{\nabla}\vec{u'}^{(j)}||_{W^{p+1,\infty}(\Omega_0)} \tag{4.39}$$

where K is a constant ($K > 0$) and p is a fixed integer depending on the regularity of the displacement fields.

We express the latter stability inequality explicitly in terms of the initially-stressed elastic matrix $\boldsymbol{L}$ and the initial stress field $\boldsymbol{\tau}$ as:

$$||\boldsymbol{L}^* - \boldsymbol{L}^{*'}||_{W^{p,\infty}(\Omega_0)} + ||\boldsymbol{\tau}^* - \boldsymbol{\tau}^{*'}||_{W^{p,\infty}(\Omega_0)} \leq K \sum_{j=1}^{N+9} ||\boldsymbol{\nabla}\vec{u}^{(j)} - \boldsymbol{\nabla}\vec{u'}^{(j)}||_{W^{p+1,\infty}(\Omega_0)} \tag{4.40}$$

Proof:
Uniquness: Based on equation (4.38) , the matrix $\tilde{\boldsymbol{C}}$ gathering the initially-stressed elastic matrix $\boldsymbol{L}$ and the initial stress tensor $\boldsymbol{\tau}$ can be explicitly reconstructed up to multiplicative constant. Using the same refereed reconstruction formula, the uniqueness of the reconstructed matrix $\tilde{\boldsymbol{C}}^*$ is ensured by normalizing the matrix $\boldsymbol{L}$ and enforcing the positivity of the diagonal terms of the first3×3-block.

Stability : The reconstructed matrix $\tilde{\boldsymbol{C}}^*$ is a rational function of the displacement gradient components and their partial derivatives. Then if two sets of displacement measurements $\{\vec{u}^{(j)}\}_{j=1}^{9+N}$ and $\{\vec{u'}^{(j)}\}_{j=1}^{9+N}$ satisfies the hypotheses (2) and (3) over some smooth domain Ω, the denominator of the formula (4.38) never vanishes, and its rational expression function of displacement gradient components implies the following local estimate:

$$||\tilde{\boldsymbol{C}}^* - \tilde{\boldsymbol{C}}^{*'}||_{L^\infty(\Omega_0)} \leq K \sum_{j=1}^{N+9} ||\boldsymbol{\nabla}\vec{u}^{(j)} - \boldsymbol{\nabla}\vec{u}'^{(j)}||_{W^{1,\infty}(\Omega_0)} \tag{4.41}$$

for a positive constant K. Now, if the displacement gradient tensor components are in $W^{p+1,\infty}(\Omega_0)$ for some integer $p \geq 0$, then by differentiating the reconstruction equation (4.41) p times leads to the stability estimates in equation (4.38).

4.4 Inverse problem for a particular initially-stressed material

In the previous section, the reconstruction of the initial stress field and the material parameters represented by the generalized initially-stressed elastic matrix is done via a pointwise identification procedure. The motivation behind the analysis of such methods is to have an idea about the quantity of necessary data that can be needed for an elastic initially-stressed material characterization. On the other hand, it permits to obtain a stability result to analyze the regularity of the different reconstructed fields.

In practice, the equilibrium equation is always solved using weak formulations in the objective to obtain numerical solution. That is why, in the following of this chapter we will consider a direct method based on the weak formulation related to the equilibrium equation of the direct problem to reconstruct all the fields to be identified.

4.4.1 Weak formulation of the direct problem

This section will be dedicated to the development of the variational formulation of the direct problem. Let consider the static version of the equilibrium equation in presence of

a volumetric force density $\vec{f}$ as:

$$\text{Div}\boldsymbol{S} + \vec{f} = \vec{0}, \quad \text{in } \Omega. \tag{4.42}$$

To establish the equilibrium weak formulation, let consider the Sobolev space denoted by $H^1(\Omega)$ and defined as:

$$H^1(\Omega) = \{\boldsymbol{v} \in L^2(\Omega, \mathbb{R}^d), \nabla \boldsymbol{v} \in L^2(\Omega, \mathbb{R}^{d\times d})\}, \tag{4.43}$$

Using the definition of $H^1(\Omega)$ and the equilibrium equation (4.42) and bearing in mind the Green integral formula lead to:

$$\int_\Omega \boldsymbol{S} : \boldsymbol{\nabla v} d\Omega = \int_\Omega \boldsymbol{f}.\boldsymbol{v} d\Omega + \int_{\Gamma=\partial\Omega} (\boldsymbol{S}.\boldsymbol{N}).\boldsymbol{v} d\Gamma \quad , \forall \boldsymbol{v} \in H^1(\Omega). \tag{4.44}$$

Here we divide the boundary $\partial\Omega$ into two parts based on the type of boundary conditions:

- Γ_u: where *Dirichlet* conditions are imposed,
- Γ_t: where *Neuman* conditions are imposed,

with the compatibility constraint $\Gamma_u \cup \Gamma_t = \partial\mathcal{B}$ and measure$(\Gamma_u \cap \Gamma_t) = 0$. Now, the above boundary conditions can be explicitly presented as:

$$\begin{cases} \boldsymbol{S}.\vec{N} = \vec{t}, & \text{on } \Gamma_t, \\ \vec{u} = \vec{u}^d, & \text{on } \Gamma_u. \end{cases} \tag{4.45}$$

By defining the subspace $H_0^1(\Gamma_u, \Omega)$:

$$H_0^1(\Gamma_u, \Omega) = \{\vec{v} \in H_1(\Omega), \vec{v} = \vec{0} \ \text{ on } \ \Gamma_u\}, \tag{4.46}$$

the weak formulation presented in equation (4.44) can be transformed into:

$$\begin{cases} a(\vec{u}, \vec{v}) & = l(\vec{v}), \quad \forall \vec{v} \in H_0^1(\Gamma_u, \Omega), \\ \vec{u} & = \vec{u}^d \ \ on \ \ \Gamma_u, \end{cases} \tag{4.47}$$

and by considering the material behaviour asserted through equation (4.10), both the bilinear and linear operators introduced in the weak formulation (4.47) can be explicitly

presented as:

$$a(\vec{u},\vec{v}) = \int_\Omega [(\boldsymbol{\nabla}\vec{u})\boldsymbol{\tau} + \mathcal{L} : \boldsymbol{\nabla}\vec{u}] : \boldsymbol{\nabla}\vec{v} d\Omega, \quad \forall \tag{4.48}$$

$$vecv \in H_0^1(\Gamma_u,\Omega), \tag{4.49}$$

$$l(\vec{v}) = -\int_\Omega \boldsymbol{\tau} : \boldsymbol{\nabla}\vec{v} d\Omega + \int_\Omega \vec{f}.\vec{v} d\Omega + \int_{\Gamma_t} \vec{t}.\vec{v} d\Gamma, \quad \forall \vec{v} \in H_0^1(\Gamma_u,\Omega). \tag{4.50}$$

Let us define the Frobenius norm for a second order tensor $\boldsymbol{A}$ as $||\boldsymbol{A}|| = \sqrt{\sum A_{ij}^2}$ and the norm associated to the sobolev space $H^1(\Omega)$ as $||\vec{v}||_{H^1(\Omega)} = \sqrt{||\vec{v}||^2_{L^2(\Omega)} + ||\boldsymbol{\nabla}\vec{v}||^2_{L^2(\Omega)}}$. Hence, the continuity of both linear and bilinear operators involved in the weak formulation can be easily ensured since:

$$\begin{cases} |a(\vec{u},\vec{v})| & \leq (|||\mathcal{L}|||_\infty + ||\tau||_\infty)||\vec{u}||_{H^1(\Omega)}||\vec{v}||_{H^1(\Omega)}, \quad \forall \vec{u},\vec{v} \in H^1(\Omega), \\ |l(\vec{v})| & \leq (||\vec{g}||_{L^2(\Gamma_t)} + ||\vec{f}||_{L^2(\Omega)} + ||\boldsymbol{\tau}||_\infty)||\vec{v}||_{H^1(\Omega)}, \quad \forall \vec{v} \in H^1(\Omega), \end{cases} \tag{4.51}$$

with

$$\begin{cases} |||\mathcal{L}|||_\infty & = \mathrm{Sup}_\Omega |||\mathcal{L}|||, \\ |||\mathcal{L}||| & = \mathrm{Sup}_{\boldsymbol{A}\in M(\mathbb{R}^{d\times d})} \dfrac{||\mathcal{L} : \boldsymbol{A}||}{||\boldsymbol{A}||}, \\ ||\boldsymbol{\tau}||_\infty & = \mathrm{Sup}_\Omega ||\boldsymbol{\tau}||, \end{cases} \tag{4.52}$$

whereas the coercivity of the bilinear operator requires extra constraints involving the initial stress field and the initially-stressed elastic tensor $\mathcal{L}$. For example in the case where the elastic tensor $\mathcal{L}$ can be revealed explicitly in function of the residual stress field $\boldsymbol{\tau}$, to ensure the coercivity of the bilinear operator $a(.,.)$, a sufficient inequality have been found in [Robertson 1998]. In fact such constraint enforce the residual stress to be sufficiently small so it cannot perturbate the coercivity of the bilinear operator related to the standard elastic tensor $\boldsymbol{C}$.

To simplify the analysis of the proposed identification approach that will be presented in details in the following sections, we will consider a relatively simple model which was used by Anne Hoger in [Hoger 1986] in the objective to study the residual stress effect on an isotropic material in the free-configuration (the configuration free of any internal stresses). Such model can be described via the explicit formula for the initially-stressed

elastic tensor $\mathcal{L}$:

$$\mathcal{L} = 2\mu \boldsymbol{I} + \lambda \mathbf{1} \otimes \mathbf{1} + \mathcal{L}_\tau, \tag{4.53}$$

where $\boldsymbol{I}$ is the identity tensor for the fourth order tensor space, whereas $\mathcal{L}_\tau$ is a fourth order tensor depending explicitly on the residual stress field and whose components can be written as:

$$[\mathcal{L}_\tau]_{ijkl} = \tau_{ik}\delta_{jl} + \tau_{jl}\delta_{ik}, \tag{4.54}$$

with δ is the Kronecker symbol. Considering the explicit expression of the initially-stressed elastic operator, the First Piola Kirchhoff-displacement gradient tensor relation is transformed to:

$$\boldsymbol{S} = \boldsymbol{\tau} + \boldsymbol{\nabla}\vec{u}\boldsymbol{\tau} - \frac{1}{2}(\boldsymbol{\epsilon}\boldsymbol{\tau} + \boldsymbol{\tau}\boldsymbol{\epsilon}) + 2\mu\boldsymbol{\epsilon} + \lambda \mathrm{tr}(\boldsymbol{\epsilon})\mathbf{1} \tag{4.55}$$

The residual stress field $\boldsymbol{\tau}$ involved in the latter formulation is usually subjected to the mathematical constraint of strong ellipticity. Such constraint is not only a sufficient condition for the propagation of elastic plane waves, but also it is necessary for the uniqueness of the boundary value problem's strong solution. Such condition implies:

$$0 < \frac{\mu}{2} - ||\boldsymbol{\tau}|| \tag{4.56}$$

Whereas, using the mathematical constraint established in [Robertson 1998], to guarantee the coercivity of the bilinear form $a(.,.)$ a sufficient condition is:

$$\sup_{\vec{X}\in\Omega} ||\boldsymbol{\tau}|| < \inf_{\vec{X}\in\Omega} \frac{\mu}{2}. \tag{4.57}$$

Thus, using all the previous results above and exploiting the Theorem of Lax-Milgram, the existence and the uniqueness of the displacement solution of the weak problem (4.47) is ensured.

4.4.2 Formulation of the identification approach

Before presenting the reconstruction method, let us define the Sobolev space $H_0^1(\Omega) = H_0^1(\partial\Omega, \Omega)$. Considering only the internal part of the displacement data measurements, the weak formulation of the equilibrium equation is still valid in $H_0^1(\Omega)$, since $H_0^1(\Omega) \subset$

$H_0^1(\Gamma_u, \Omega)$. The equilibrium equation can be seen differently when we suppose the displacement field is known and both the initial stress and the initially-stressed elastic tensor $\boldsymbol{L}$ are unknown, and by consequence we introduce the following equivalence:

$$\begin{cases} a(\vec{u}, \vec{v}) = a_u(\begin{bmatrix} \mu & \lambda & \boldsymbol{\tau} \end{bmatrix}, \vec{v}) = l(\vec{v}) \quad \forall \vec{v} \in H_0^1(\Omega), \\ l(\vec{v}) = \int_\Omega \vec{f}.\vec{v} d\Omega, \quad \forall \vec{v} \in H_0^1(\Omega). \end{cases} \tag{4.58}$$

In order to remain in the Hilbert space framework relatively to the second equality sign in (4.57-1), we suppose that displacement gradient tensor $\boldsymbol{\nabla}\vec{u}$ is bounded. In the objective to formulate the identification approach on the set of scalar fields, we can rewrite the residual stress field as a projection on the canonical basis of symmetric matrices in $S_2(\mathbb{R})$ in the following form:

$$\boldsymbol{\tau} = \tau_{11}\boldsymbol{M}^{(11)} + \tau_{22}\boldsymbol{M}^{(22)} + \tau_{12}\boldsymbol{M}^{(12)}, \tag{4.59}$$

with

$$\boldsymbol{M}^{(11)} = \begin{bmatrix} 1 & 0 \\ 0 & 0 \end{bmatrix}, \quad \boldsymbol{M}^{(22)} = \begin{bmatrix} 0 & 0 \\ 0 & 1 \end{bmatrix}, \quad \boldsymbol{M}^{(12)} = \begin{bmatrix} 0 & 1 \\ 1 & 0 \end{bmatrix} \tag{4.60}$$

Hence, the weak formulation of the equilibrium equation (4.57) related to the measures $(\vec{u}, \vec{f})$, can be rewritten as the sum of separate terms related to every scalar field to be identified as:

$$\int_\Omega \boldsymbol{K}_u^{\boldsymbol{I}}(\mu).\vec{v} d\Omega + \int_\Omega \boldsymbol{K}_u^{\boldsymbol{1}\otimes\boldsymbol{1}}(\lambda).\vec{v} d\Omega + \sum_{i=1, i\leq j}^{2} \int_\Omega \boldsymbol{K}_u^{\boldsymbol{M}^{(ij)}}(\tau_{ij}).\vec{v} d\Omega = \int_\Omega \vec{f}.\vec{v} d\Omega, \quad \forall \vec{v} \in H_0^1(\Omega), \tag{4.61}$$

where the different stiffness-to-force operators involved above read:

$$\boldsymbol{K}_u^{\boldsymbol{I}}(\mu) = -\mathrm{Div}[\mu\boldsymbol{\epsilon}] \tag{4.62}$$

$$\boldsymbol{K}_u^{\boldsymbol{1}\otimes\boldsymbol{1}}(\lambda) = -\mathrm{Div}[\lambda \mathrm{Div}\vec{u}] \tag{4.63}$$

$$\boldsymbol{K}_u^{\boldsymbol{M}^{(ij)}}(\tau_{ij}) = -\mathrm{Div}(\tau_{ij}[\boldsymbol{\nabla}\vec{u}\boldsymbol{M}^{(ij)} - \frac{1}{2}(\boldsymbol{M}^{(ij)}\boldsymbol{\epsilon} + \boldsymbol{\epsilon}\boldsymbol{M}^{(ij)})]), \quad i, j \in \{1, 2\} \tag{4.64}$$

The general recovery problem with multiple measurements reads as the following system:

$$\boldsymbol{K}\begin{bmatrix}\mu & \lambda & \tau_{11} & \tau_{22} & \tau_{12}\end{bmatrix}^T = \boldsymbol{F}, \quad \text{in } H^{-1}(\Omega) \tag{4.65}$$

where the general stiffness-to-force and force operators related to the set of displacement and forces measures $\{(\vec{u}^{(i)}, \vec{f}_{(i)})\}_{i=1}^n$ can be presented as:

$$\boldsymbol{K} = \begin{bmatrix} \boldsymbol{K}^{\boldsymbol{I}}_{u^{(1)}} & \boldsymbol{K}^{\boldsymbol{1}\otimes\boldsymbol{1}}_{u^{(1)}} & \boldsymbol{K}^{\boldsymbol{M}^{(11)}}_{u^{(1)}} & \boldsymbol{K}^{\boldsymbol{M}^{(22)}}_{u^{(1)}} & \boldsymbol{K}^{\boldsymbol{M}^{(12)}}_{u^{(1)}} \\ \vdots & \vdots & \vdots & \vdots & \vdots \\ \boldsymbol{K}^{\boldsymbol{I}}_{u^{(n)}} & \boldsymbol{K}^{\boldsymbol{1}\otimes\boldsymbol{1}}_{u^{(n)}} & \boldsymbol{K}^{\boldsymbol{M}^{(11)}}_{u^{(n)}} & \boldsymbol{K}^{\boldsymbol{M}^{(22)}}_{u^{(n)}} & \boldsymbol{K}^{\boldsymbol{M}^{(12)}}_{u^{(n)}} \end{bmatrix}, \quad \boldsymbol{F} = \begin{bmatrix} \vec{f}^{(1)} \\ \vdots \\ \vec{f}^{(n)} \end{bmatrix} \tag{4.66}$$

4.5 Residual stress invertibility and stability

In this section we will focus on the reconstruction of the residual stress field knowing the Lamé coefficients and based on the displacement data fields. In fact, such simplification of the initial inverse problem can be encountered in special cases for the material or structures characterization. For example, we consider a material structure with an isotropic linear elastic behaviour already characterized with known Lamé fields. If the structure is subjected to a process leading to the appearance of a residual stress field. Then, in the objective to characterize the linear elastic behaviour of the initially-stressed structure, an extra task is to identify the residual stress field.

4.5.1 Reconstruction of the residual stress field

Let consider two data sets $(\vec{u}^{(1)}, \vec{f}^{(1)})$, $(\vec{u}^{(2)}, \vec{f}^{(2)})$. Now, if we consider that the Lamé coefficients are known everywhere in Ω, then using the following tensorial identities:

$$\mathrm{Div}(\boldsymbol{AB}) = (\boldsymbol{\nabla A}) : \boldsymbol{B} + \boldsymbol{A}.(\mathrm{Div}\boldsymbol{B}), \tag{4.67}$$

$$\boldsymbol{\nabla}(\alpha\boldsymbol{A}) = \boldsymbol{\nabla}(\boldsymbol{A}) + \boldsymbol{A} \otimes \vec{\nabla}\alpha, \tag{4.68}$$

$$\boldsymbol{A} \otimes \vec{c} : \boldsymbol{B} = \boldsymbol{AB}.\vec{c} \tag{4.69}$$

where $\boldsymbol{A}$ and $\boldsymbol{B}$ are two general 2×2 tensors, $\vec{c}$ is a vectorial function whereas α is a scalar function. Consequently, similarly to what is done in the reconstruction system of equations in [Bal 2014], the equilibrium equation in the reference configuration can be written as a differential partial system on the residual stress components similar to the

transport equation and which can be given as:

$$\boldsymbol{A}\begin{bmatrix}\nabla\tau_{11}\\ \nabla\tau_{22}\\ \nabla\tau_{12}\end{bmatrix}+\boldsymbol{B}\begin{bmatrix}\tau_{11}\\ \tau_{22}\\ \tau_{12}\end{bmatrix}=\boldsymbol{f} \tag{4.70}$$

with

$$\boldsymbol{A}=\begin{bmatrix}\boldsymbol{M}^{(11)}\boldsymbol{\epsilon}^{(1)} & \boldsymbol{M}^{(22)}\boldsymbol{\epsilon}^{(1)} & \boldsymbol{M}^{(12)}\boldsymbol{\epsilon}^{(1)}\\ \boldsymbol{M}^{(11)}\boldsymbol{\epsilon}^{(2)} & \boldsymbol{M}^{(22)}\boldsymbol{\epsilon}^{(2)} & \boldsymbol{M}^{(12)}\boldsymbol{\epsilon}^{(2)}\\ \boldsymbol{M}^{(11)} & \boldsymbol{M}^{(22)} & \boldsymbol{M}^{(12)}\end{bmatrix},\quad \boldsymbol{B}=\begin{bmatrix}\vec{b}^{(11)}_{u^{(1)}} & \vec{b}^{(22)}_{u^{(1)}} & \vec{b}^{(12)}_{u^{(1)}}\\ \vec{b}^{(11)}_{u^{(2)}} & \vec{b}^{(22)}_{u^{(2)}} & \vec{b}^{(12)}_{u^{(2)}}\\ \vec{0} & \vec{0} & \vec{0}\end{bmatrix},\quad \vec{f}=\begin{bmatrix}\vec{f}_{u^{(1)}}\\ \vec{f}_{u^{(2)}}\\ \vec{0}\end{bmatrix}, \tag{4.71}$$

and

$$\vec{b}^{(ij)}_{u^{(k)}}=\boldsymbol{\nabla}(\boldsymbol{\epsilon}^{(k)}-2\boldsymbol{\nabla}\vec{u}^{(k)}):\boldsymbol{M}^{(ij)}+\boldsymbol{M}^{(ij)}.\mathrm{Div}\boldsymbol{\epsilon}^{(k)}, \tag{4.72}$$

$$\vec{f}_{u^{(k)}}=\mathrm{Div}[4\mu\boldsymbol{\epsilon}^{(k)}+2\lambda\mathrm{Div}\vec{u}^{(k)}\mathbf{1}]. \tag{4.73}$$

In fact, the first two block-matrix rows are the origin of the equilibrium equation for the two force-displacement measures, whereas, the last one is a result of the equilibrium equation satisfied by the residual stress itself. To simplify the partial differential system in equation (4.69), we will suppose the invertibility of the matrix $\boldsymbol{A}$ which implies

$$\begin{bmatrix}\nabla\tau_{11}\\ \nabla\tau_{22}\\ \nabla\tau_{12}\end{bmatrix}+\boldsymbol{M}\begin{bmatrix}\tau_{11}\\ \tau_{22}\\ \tau_{12}\end{bmatrix}=\boldsymbol{f},\quad \boldsymbol{M}=\boldsymbol{A}^{-1}\boldsymbol{B} \tag{4.74}$$

Based on cumbersome algebraic calculation, we can show that the invertibility of the matrix $\boldsymbol{A}$ is equivalent to the following condition on the displacement data fields:

$$\det\boldsymbol{A}\neq 0\Leftrightarrow(u^{(1)}_{2,2}-u^{(1)}_{1,1})(u^{(2)}_{2,1}+u^{(2)}_{1,2})-(u^{(2)}_{2,2}-u^{(2)}_{1,1})(u^{(1)}_{2,1}+u^{(1)}_{1,2})\neq 0,\quad \forall\vec{X}\in\Omega. \tag{4.75}$$

The transformation of the system of equations (4.69) is not done for the sole sake of simplification, but also to avoid the attraction points to better reconstruct the initial stress field over the characteristic curves. That is why we will make the following assumption which will be used in the next section for the stability analysis of the residual stress reconstruction.

Hypothesis 3: *The displacement fields satisfy* $\vec{u}^{(n)} \in H^1(\Omega) \cap W^{1,\infty}(\Omega)$ *for* $n = 1, 2$ *and satisfy:*

$$(u^{(1)}_{2,2} - u^{(1)}_{1,1})(u^{(2)}_{2,1} + u^{(2)}_{1,2}) - (u^{(2)}_{2,2} - u^{(2)}_{1,1})(u^{(1)}_{2,1} + u^{(1)}_{1,2}) > c_0, \quad \forall \vec{X} \in \Omega \tag{4.76}$$

where c_0 *is a constant.*

4.5.2 ODE-based approach and stability estimate

Focusing only on the stability estimate, we will consider that the reconstruction of the initial stress field is based on a direct integration method of the differential system (4.73). So, suppose that Ω is a connected domain, and two points $\vec{X}_0$ and $\vec{X}_1$ which are related via the smooth curve γ. Such curve can be defined as:

$$\gamma : \begin{cases} [0 \;\; 1] & \to \tilde{\Omega} \\ t & \to \xi(t) \end{cases} \qquad \text{with } \gamma(0) = \vec{X}_0 \text{ and } \gamma(1) = \vec{X}_1. \tag{4.77}$$

Now, using the variable change $\vec{X} = \gamma(t)$ and the differentiation chain rule, the differential system (4.73) will take the following ODE form:

$$\frac{d\vec{\phi}_\gamma(t)}{dt} + \boldsymbol{M}_\gamma(t)\vec{\phi}_\gamma(t) = \vec{f}_\gamma(t), \quad \vec{\phi}_\gamma(t) = \begin{bmatrix} \tau_{11} \circ \gamma(t) \\ \tau_{22} \circ \gamma(t) \\ \tau_{12} \circ \gamma(t) \end{bmatrix} \text{ and } \vec{\phi}_\gamma(0) = \begin{bmatrix} \tau_{11}(\vec{X}_0) \\ \tau_{22}(\vec{X}_0) \\ \tau_{12}(\vec{X}_0) \end{bmatrix}. \tag{4.78}$$

Hence, if we know the values of the residual stress $\boldsymbol{\tau}$ components in a chosen starting point of the curve γ, by a direct integration of the ODE system illustrated in equation (4.77) and by varying the end point $\vec{X}$ of the curve γ we can reconstruct the residual stress field at any point of Ω. It is clear that the space of the ODE system in equation (4.77) is a vector space of dimension 3. Since the residual stress field satisfies equation (4.9) (with $\vec{t}_0 = \vec{0}$) on the boundary of the domain Ω, we can choose the end points of the curve γ on the boundary $\partial\Omega$ so that we obtain 4 scalar relations which can be sufficient (based on the choice of γ) to reconstruct the values the residual stress field components on the curve γ. After clarifying the reconstruction procedure, we can show that this approach is a stable so we can state the following theorem.

Theorem 2: *Consider that Ω is a convex domain and let suppose the existence of two $\mathcal{C}^2$ displacement data sets $(\vec{u}^{(1)}, \vec{u}^{(2)})$, $(\vec{u'}^{(1)}, \vec{u'}^{(2)})$ associated to two residual stress fields $\boldsymbol{\tau}$, $\boldsymbol{\tau}'$ with the same Lamé coefficients μ and λ. Supposing that the considered displacement field sets satisfy the criteria illustrated in hypothesis 3, then the residual stress fields $\boldsymbol{\tau}$ and $\boldsymbol{\tau}'$ can be determined uniquely over Ω using the data as:*

$$||\boldsymbol{\tau} - \boldsymbol{\tau}'||_{W^{1,\infty}(\Omega)} \leq K \sum_{i=1}^{2} ||\vec{u} - \vec{u'}||_{W^{2,\infty}(\Omega)} \tag{4.79}$$

where K is a positive constant.

Proof: Based on PicardâĂŞLindelöf theorem and Gronwall′s lemma for the error controlling along characteristic curves the proof of the theorem 2 can be established as it was done in [Bal 2014] in the context of isotropic elasticity and with detailed analysis in [Monard 2011] for multi physical problem, but it will be omitted here. The extra major difference at the proof level illustrated in the later 2 references is that in our context we have exploited the homogeneous boundary condition satisfied by the residual stress field.

4.6 Numerical approach

4.6.1 Direct problem and data generation

The displacement data are generated by computing the direct problem over the domain Ω using non structured triangular mesh and where the displacement field is interpolated on Lagrange polynomial functions $\mathcal{P}_2$. We suppose that the volumetric force density $\vec{f}$ vanishes. In the case of residual stress identification, for the sake of simplicity, we have chosen homogeneous constant fields for the Lamé parameters. Whereas in the case of the reconstruction of all the material parameters, continuous inhomogeneous Lamé fields are considered. The perturbation of the displacement measures is done by adding a noisy field to the direct problem solution. To ensure the repeatability of the results, as it is done in [Bal 2014], the noise field is represented by the following function:

$$\vec{u}_{noise} = \delta \frac{1}{Sup_{\vec{X}\in\Omega} f} \vec{f}_{\delta,m}(\vec{x}) \tag{4.80}$$

with

$$\vec{f}_{\delta,m}(\vec{X}) = \sum_{k=-m}^{m} \frac{|k|}{m} \chi(\frac{|k|}{m} \frac{\vec{X}}{\sqrt{\delta}}), \tag{4.81}$$

$$\vec{\chi}(\vec{X}) = \cos(2\pi \vec{X}.\vec{e}_1)\cos(2\pi \vec{X}.\vec{e}_2)(\vec{e}_1 + \vec{e}_2) \tag{4.82}$$

whereas δ denotes the noise amplitude and m is an integer parameter. The considered noise field illustrated in the prior equation is illustrated in figure (4.1).

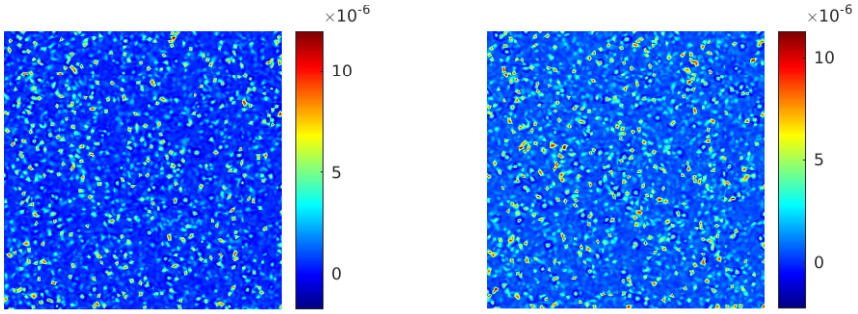

(a) u_x^{noise} (b) u_y^{noise}

Figure 4.1: Noise function components ($\delta = 10^{-5}$)

4.6.2 Discrete formulation of the inverse problem

Let suppose that the domain Ω admits an exact triangular mesh denoted by $\mathcal{T}_h$ for any mesh characteristic length denoted by h. Such hypothesis is to avoid the influence of the geometrical meshing on the fields reconstruction approach. Now let define the following finite element spaces:

- $\mathcal{P}^2(\mathcal{T}_h)$: the space of continuous scalar piecewise quadratic Lagrange functions associated to the mesh $\mathcal{T}_h$.
- $\mathcal{P}^2(\mathcal{T}_h, \mathbb{R}^2)$: the space of vector-valued $\mathcal{P}^2(\mathcal{T}_h)$ functions in $\mathbb{R}^2$.
- $\mathcal{P}^1(\mathcal{T}_h)$: the space of continuous scalar piecewise linear Lagrange functions associated to the mesh $\mathcal{T}_h$.

Let $\{\xi_k\}_{k=1}^{N_s}$ and $\{\vec{\phi}\}_{k=1}^{N^v}$ denote respectively the canonical basis of shape functions of $\mathcal{P}^1(\mathcal{T}_h)$ and $\mathcal{P}^2(\mathcal{T}_h, \mathbb{R}^2)$. Hence the displacement field and the scalar fields to be reconstructed can

be decomposed on the different above interpolation spaces as:

$$a(\vec{X}) = \sum_{i}^{N_s} a_k \xi_k(\vec{X}), \quad a = \tau_{11}, \quad \tau_{22}, \quad \tau_{12}, \quad \mu, \quad \lambda \tag{4.83}$$

$$\vec{u}(\vec{X}) = \sum_{i}^{N_v} u_k \vec{\phi}_k(\vec{X}), \tag{4.84}$$

where N_s and N_v denote respectively the degrees of freedom number for the scalar material parameters and the displacement field. In fact, the initial stress field components and the Lamé parameters are chosen to be projected in a continuous space of interpolation in the sake of the identification approach simplification. In general, the interpolation spaces for the fields to be identified may be chosen to be discontinuous to better account for the discontinuous character of the different material parameters that can be encountered (presence of inclusion ...).

Using the interpolation from for the different scalar fields as it is illustrated in equations (4.82-4.83), the discrete form of the partial differential system in equation (4.64), can be transformed into the following algebraic system:

$$\mathbb{K}\mathbb{V} = \mathbb{F}, \quad \mathbb{K} \in M(\mathbb{R}^{nN_v^{int} \times 5N_s}), \quad \mathbb{V} \in M(\mathbb{R}^{5N_s}), \quad \mathbb{F} \in M(\mathbb{R}^{nN_v^{int}}), \tag{4.85}$$

with N_v^{int} denotes the number of degree of freedom associated to the internal displacement field, and where $\mathbb{V}$ denotes the vector of the coordinates associated to the interpolation of the different scalar fields to be identified, whereas $\mathbb{F}$ and $\mathbb{K}$ are the discrete form of the operators $\boldsymbol{F}$ and $\boldsymbol{K}$ respectively. The matrices $\mathbb{K}$, $\mathbb{F}$ and $\mathbb{V}$ can be presented as:

$$\mathbb{K} = \begin{bmatrix} \mathbb{K}^{\boldsymbol{I}}_{u^{(1)}} & \mathbb{K}^{\boldsymbol{1}\otimes\boldsymbol{\mathbb{1}}}_{u^{(1)}} & \mathbb{K}^{\boldsymbol{M}^{(11)}}_{u^{(1)}} & \mathbb{K}^{\boldsymbol{M}^{(22)}}_{u^{(1)}} & \mathbb{K}^{\boldsymbol{M}^{(12)}}_{u^{(1)}} \\ \vdots & \vdots & \vdots & \vdots & \vdots \\ \mathbb{K}^{\boldsymbol{I}}_{u^{(n)}} & \mathbb{K}^{\boldsymbol{1}\otimes\boldsymbol{\mathbb{1}}}_{u^{(n)}} & \mathbb{K}^{\boldsymbol{M}^{(11)}}_{u^{(n)}} & \mathbb{K}^{\boldsymbol{M}^{(22)}}_{u^{(n)}} & \mathbb{K}^{\boldsymbol{M}^{(12)}}_{u^{(n)}} \end{bmatrix}, \quad \mathbb{F} = \begin{bmatrix} \mathbb{F}_{u^{(1)}} \\ \vdots \\ \mathbb{F}_{u^{(n)}} \end{bmatrix} \tag{4.86}$$

$$\mathbb{V} = \begin{bmatrix} (\mathbb{V}^{\mu})^T & (\mathbb{V}^{\lambda})^T & (\mathbb{V}^{\tau_{11}})^T & (\mathbb{V}^{\tau_{22}})^T & (\mathbb{V}^{\tau_{12}})^T \end{bmatrix}^T,$$
$$\mathbb{V}^{\mu} = [\mu], \quad \mathbb{V}^{\lambda} = [\lambda], \quad \mathbb{V}^{\tau_{ij}} = [\tau_{ij}], \quad i,j \in \{1,2\} \tag{4.87}$$

with $[a]$ are the vectors of the coordinates associated to the interpolation of the scalar field "a". The block-matrices involved in the expression of the general discrete form of the identification formulation in equation (4.85), can be expressed as:

$$[\mathbb{K}^{\boldsymbol{I}}_{u^{(l)}}]_{ij} = \int_\Omega \xi_j \boldsymbol{\nabla}^s \vec{u}^{(l)} : \boldsymbol{\nabla}\vec{\phi}_i d\Omega \tag{4.88}$$

$$[\mathbb{K}^{\mathbf{1}\otimes\mathbf{1}}_{u}]_{ij} = \int_\Omega \xi_j \mathrm{Div}\vec{u}^{(l)} \mathrm{Div}\vec{\phi}_i d\Omega \tag{4.89}$$

$$[\mathbb{K}^{\boldsymbol{M}^{(pq)}}_{u}]_{ij} = \int_\Omega \xi_j [\boldsymbol{\nabla}\vec{u}^{(l)}\boldsymbol{M}^{(pq)} - \frac{1}{2}(\boldsymbol{M}^{(pq)}\boldsymbol{\nabla}^s\vec{u}^{(l)} + \boldsymbol{\nabla}^s\vec{u}^{(l)}\boldsymbol{M}^{(pq)})] : \boldsymbol{\nabla}\vec{\phi}_i d\Omega, \tag{4.90}$$

$$i = 1..N_v^{int}, \quad j = 1..N_s, \quad l = 1..n \quad p,q = 1..2, \quad p \leq q.$$

4.6.3 Least squares approach and regularization

In practice, we compute the identifiable fields by minimizing a regularized mean squares functional of the form

$$J(\mathbb{V}) = ||\mathbb{K}\mathbb{V} - \mathbb{F}||_2^2 + R(\mathbb{V}) \tag{4.91}$$

where the regularization term $R(.)$ is a sum of multiple operators penalizing the variations of the Lamé coefficients and the divergence of the residual stress field as the following:

$$R(\mathbb{V}) = \alpha_\mu ||\boldsymbol{\nabla}\mu||^2_{L^2(\Omega)} + \alpha_\lambda ||\boldsymbol{\nabla}\lambda||^2_{L^2(\Omega)} + \alpha_{div} ||\mathrm{Div}\boldsymbol{\tau}||^2_{L^2(\Omega)}, \tag{4.92}$$

with α_μ, α_λ and α_{div} are 3 chosen scalar regularization parameters. In the case of Lamé coefficients and residual stress reconstruction, the optimization of the cost function J is subjected to the positivity of μ and λ and the boundary condition satisfied by the residual stress field as it is illustrated through equation (4.9) (with $\vec{t}_0 = \vec{0}$). Since the set of the constitutive parameters are determined to a multiplicative scalar, we can enforce in the optimization problem that $\min(\mu, \lambda) > \alpha_0 > 0$ where α_0 is a chosen constant or field to preclude the trivial null solution. Consider the matrix $\mathbb{L}$ such that $\mathbb{L}[[\tau_{11}][\tau_{22}][\tau_{12}]]$ gives the vector of the degree of freedom involved in the boundary condition ($\boldsymbol{\tau}.\vec{N} = \vec{0}$) for the different residual stress components. Consequently, the interpolation of the different fields to be reconstructed represented through $\mathbb{V}^{id}$ can be formulated as the following

optimization problem:

$$\begin{cases} \mathbb{V}^{id} & = \text{argmin}_{\mathbb{V}} \quad J(\mathbb{V}) \\ s.b.t & \mathbb{L}\mathbb{V}^{\tau} = [0] \quad \& \quad \mathbb{V}^{\mu} > \alpha_0 \quad \& \quad \mathbb{V}^{\lambda} > \alpha_0. \end{cases} \tag{4.93}$$

where $\mathbb{V}^{\tau}$ gathers all the degree of freedom associated to the residual stress components i.e

$$[\mathbb{V}^{\tau}]^T = [[\mathbb{V}^{\tau_{11}}]^T, [\mathbb{V}^{\tau_{22}}]^T, [\mathbb{V}^{\tau_{12}}]^T]. \tag{4.94}$$

Regarding the convexity character of the optimization problem, the minimization of (4.92) was carried out using the *cvxopt* Python module which is efficient for convex optimization problems under linear constraints.

To enhance the quality of the reconstructed fields, we may use a filter regularizing the perturbed displacement measurements. Two alternatives are studied:

-the classical elastic filter where the gradient of the displacement is penalized and the regularized displacement field denoted by $\vec{u}_f$ associated to the perturbed displacement measure $\vec{u}_p$ can be obtained as the solution of the following minimization problem:

$$\vec{u}_f = \text{argmin}_{\vec{u}}\{||\vec{u} - \vec{u}_d||^2_{L^2(\Omega)} + \alpha_{elas}||\boldsymbol{\nabla}\vec{u}||^2_{L^2(\Omega)}\} \tag{4.95}$$

where α_{elas} is a regularization scalar parameter.

-the displacement measurement carried out on the reference mesh $\mathcal{T}_{h_0}$ is L^2-projected on a coarse mesh $\mathcal{T}_h$ which decrease the noise influence on the displacement gradient field which will be regularized. Such filter was used in [Bal 2014] in the objective of the Lamé coefficients reconstruction. It can be characterized through the parameter $k_h = \dfrac{h}{h_0}$.

4.6.4 Numerical results

4.6.4.1 Reconstruction of the residual stress field

In this section, we focus on the numerical results of the residual stress field reconstruction. Before dealing with results, we introduce the used data. In fact, we have exploited two displacement fields resulting from the direct problem associated with different boundary conditions: the first one is a simple tensile test, whereas the second data is the result of a

simple shear test. The two displacement measurements are presented in the figure (4.2). A

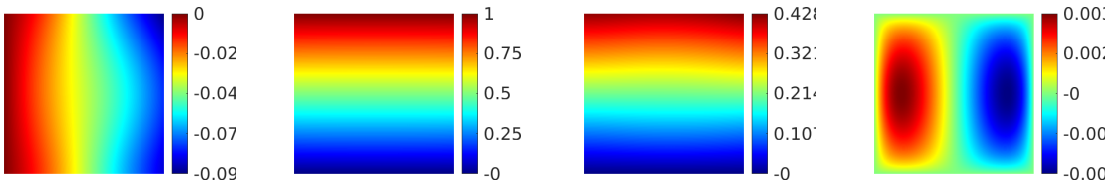

(a) $u_x^{(1)}$ (b) $u_x^{(2)}$ (c) $u_y^{(1)}$ (d) $u_y^{(2)}$

Figure 4.2: Displacement fields data

numerical check of the residual stress identifiability criteria illuminated in equation (4.75) is done for the displacement data and it is shown over all the domain Ω in the figure (4.3) which ensures that the chosen displacement fields shown in figure (4.2) are sufficient for the reconstruction of the residual stress field. Both the proposed two filtering approach:

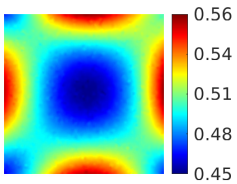

Figure 4.3: Criteria on the displacement fields data for the identification of the initial stress field)

filtering by mesh projection or elastic filter are tested on the displacement data to choose the best one. H_1 error norm for all the filtered displacement data are carried out using the two filters as it is shown in figure (4.4). In fact the H_1-norm measure is used here to quantify the error measure because simply the displacement field is involved in the reconstruction formulation through its gradient. For the mesh-projection filter there is always an optimal parameter k_h depending on the noise level (see figure (4.4-b) where the optimal values for k_h are $(3, 6)$ for the noise levels respectively 10^{-5}, 10^{-4}). However, this filter has a limitation, when the noise amplitude is very small, the quality of the filtered displacement field can not be enhanced like it is shown in figure (4.4-b) for the case $\delta = 10^{-7}$. Whereas, the elastic filter is not ameliorating the error of the filtered displacement data relative to the exact solution. Such result does not mean that the elastic filter is not useful but it precludes that it is less performant compared to the mesh projection filter at least in the regularization of the used data fields. That is why, only the mesh-projection filtering

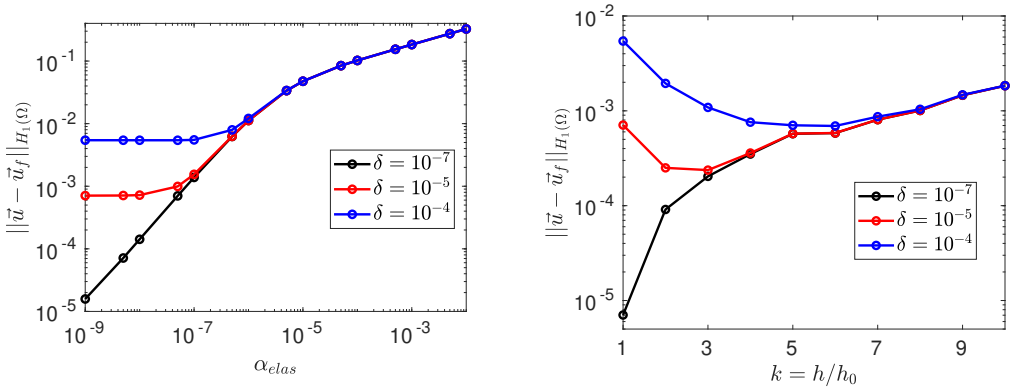

(a) Elastic filter

(b) Mesh projection filter

Figure 4.4: H_1-norm error for the set of the filtered displacement data

approach will be considered in the residual stress reconstruction method.

Similarly to the above analysis reserved to the filtering parameter k_h, we have examined the regularization parameter α_{div} influence on the reconstruction quality of the residual stress field. This investigation is done for different noise levels but using the optimal k_h for every noise amplitude δ in the objective to eliminate the filtering influence. In fact, the α_{div} impact on the reconstruction approach is inspected based on three error measures: L_2-relative error, H_1-relative error and an error measure on the divergence of the residual stress field. The divergence of the residual stress field can be represented in the discrete form by:

$$f_{div}(\mathbb{V}^\tau) = \sum_{i=1, i\leq j} \mathbb{K}_0^{\boldsymbol{M}^{(ij)}} \mathbb{V}^{\tau_{ij}}, \tag{4.96}$$

with $\mathbb{K}_0^{\boldsymbol{M}^{(ij)}} = \mathbb{K}_u^{\boldsymbol{M}^{(ij)}}$ if $\vec{u} = \vec{0}$. Then the prior error measure related to the divergence of the reconstructed residual stress field can be defined mathematically as:

$$Err_{div}(\mathbb{V}^\tau) = ||f_{div}(\mathbb{V}^{\tau^{exact}}) - f_{div}(\mathbb{V}^{\tau^{id}})||_2 \tag{4.97}$$

where $\mathbb{V}^{\tau^{exact}}$ and $\mathbb{V}^{\tau^{id}}$ denote respectively the discrete coordinates of the exact and the identified residual stress field. Based on figures-set (4.5), it is clear that for every noise level, there is always an optimal value for the regularization parameter α_{div} to get the lower

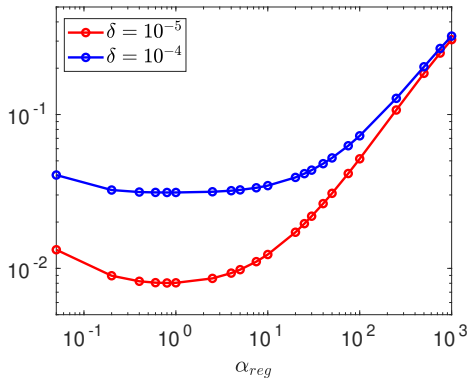

(a) Relative L_2-norm error for the residual stress reconstruction function of the regularization parameter α_{reg}

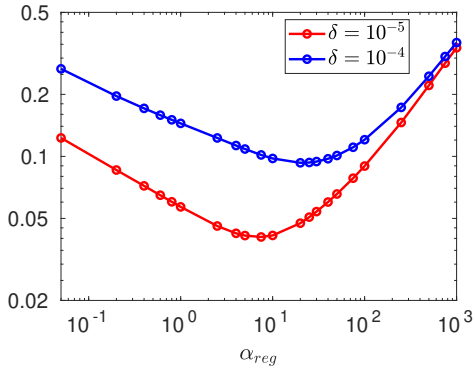

(b) Relative L_2-norm error for the residual stress reconstruction function of the regularization parameter α_{reg}

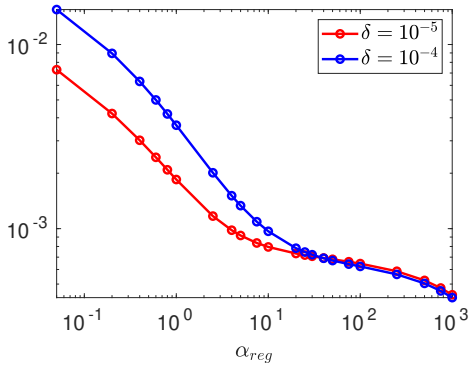

(c) Evaluation of Div $\boldsymbol{\tau}$ reconstruction function of the regularization parameter α_{reg}

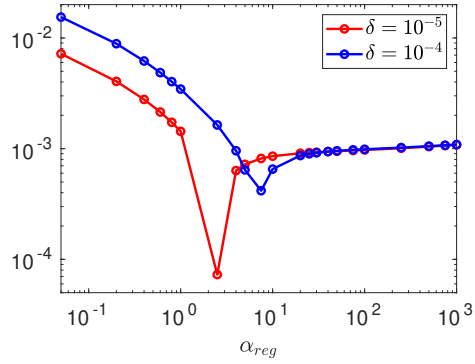

(d) Error measure for the Div $\boldsymbol{\tau}$ reconstruction function of the regularization parameter α_{reg}

Figure 4.5: Influence of the regularization parameter α_{reg} on the residual stress recontruction

error. Fixing the noise level, it is remarkable that the optimal regularization parameter value differs slightly from an error measure to another. In fact, the regularization can be seen as a penalty parameter for the equilibrium equation satisfied by the residual stress. Hence no wonder to the decreasing of the divergence measure of the residual stress if α_{div} become greater and greater like it is illustrated in figure (4.5-c). Also, a stability analysis

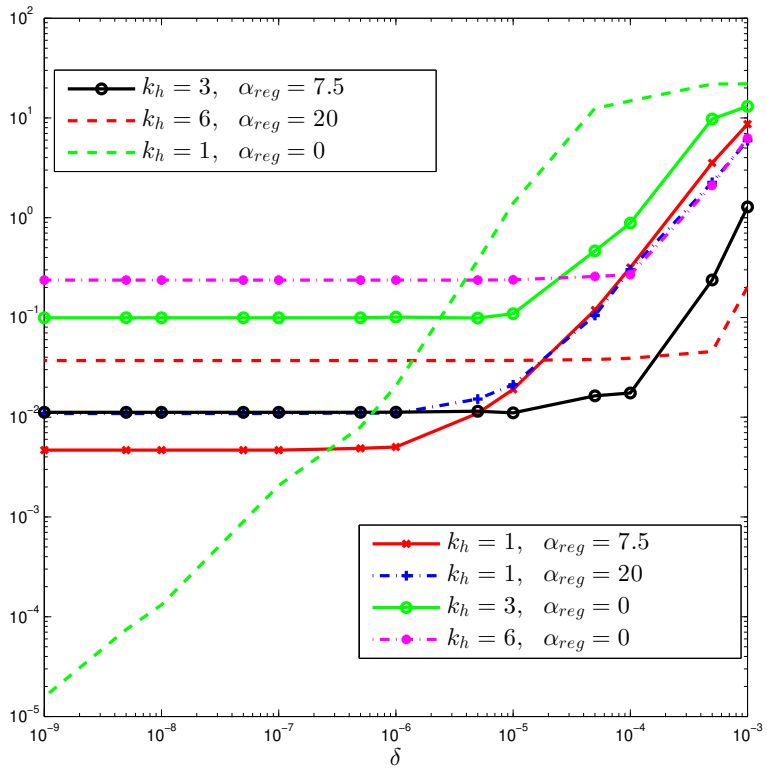

(a) Relative L_2-norm error for the residual stress reconstruction function of the noise amplitude δ

Figure 4.6: Influence of the parameters k_h and α_{reg} on the stability of the residual stress recontruction

is performed with a different set of regularization and filtering parameters as it is presented in figures-set (4.6), where different measures of error are plotted in function of the noise level. In fact, in absence of any regularization or filtering techniques (i.e $k_h = 1, \quad \alpha_{reg} = 0$), the identified residual stress converges to the predefined field as the noise level decreases relatively to the different measures of error. Based on figures-set (4.6), it is clear that for every noise level there exists an optimal filtering and regularization parameter. But also fixing these both parameters to different values than ($k_h = 1, \quad \alpha_{reg} = 0$ implies that the error of the reconstruction method converges to a limit value and by consequence it creates a limitation on the reconstruction approach accuracy.

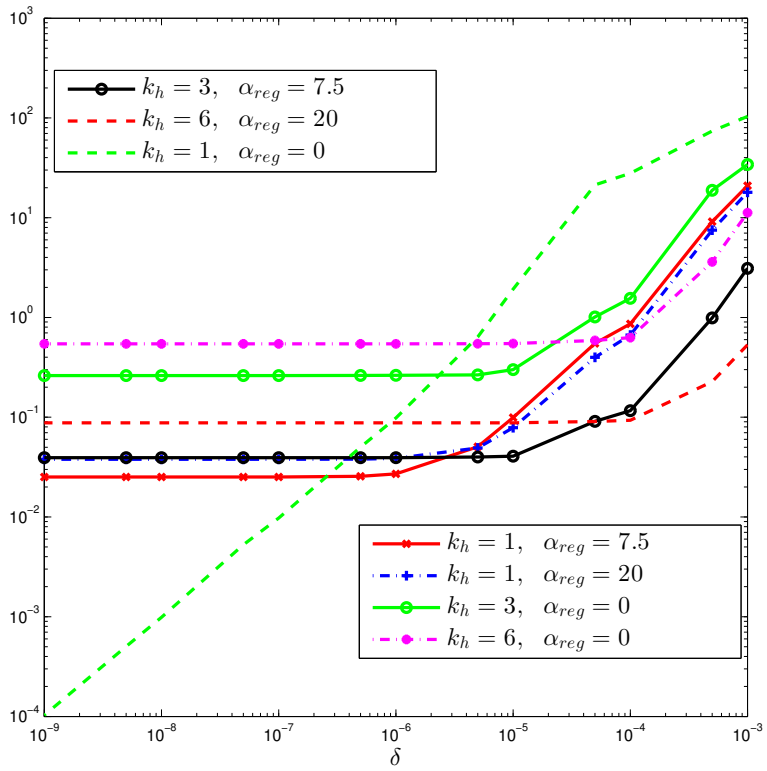

(b) Relative H_1-norm error for the residual stress reconstruction function of the noise amplitude δ

Figure 4.6: Influence of the parameters k_h and α_{reg} on the stability of the residual stress recontruction

In the remaining part of this section, we present a set of the reconstruction approach results for different scenarios by binary game considering-omitting the filtering and the regularization terms.

Such choice of analysis is considered to emphasize the importance of both filtering and regularization terms in enhancing the quality of the reconstructed residual stress field. The parameters couple $(k_h = 6, \alpha_{div} = 20)$ guarantees a quasi-optimal reconstruction of the

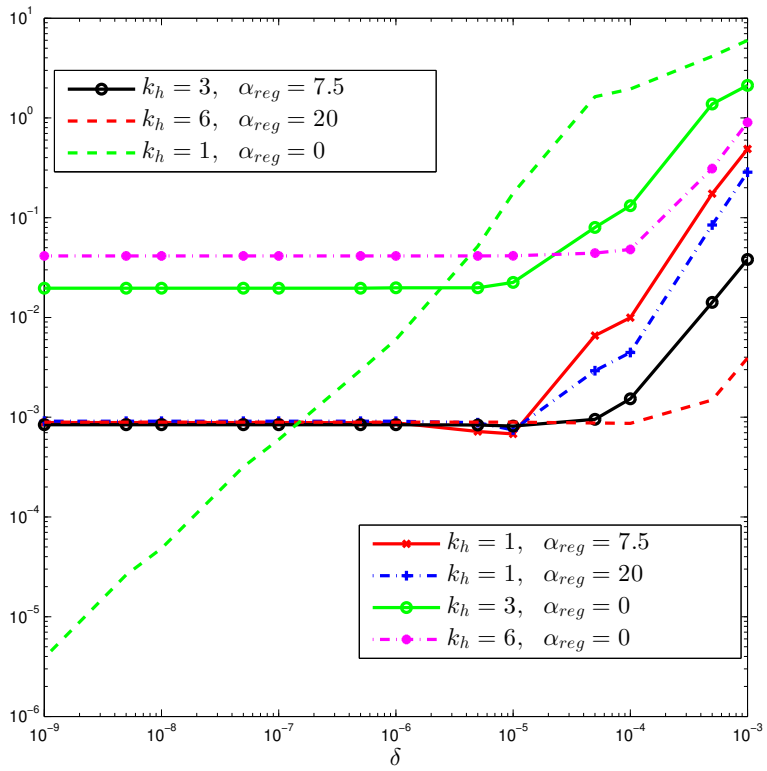

(c) Error measure for the Div $\boldsymbol{\tau}$ reconstruction function of the noise amplitude δ

Figure 4.6: Influence of the parameters k_h and α_{reg} on the stability of the residual stress recontruction

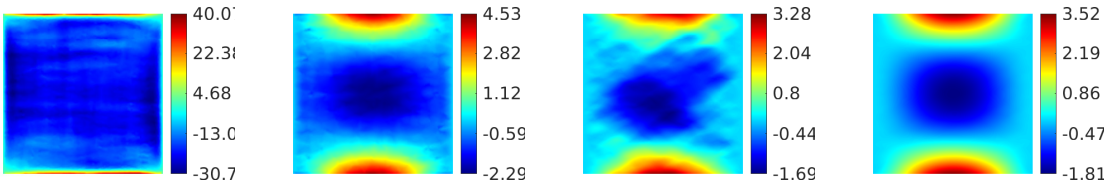

(a) $k_h = 1$, $\alpha_{div} = 0$ (b) $k_h = 6$, $\alpha_{div} = 0$ (c) $k_h = 1$, $\alpha_{div} = 20$ (d) $k_h = 6$, $\alpha_{div} = 20$

Figure 4.7: Reconstruction of τ_{11}, $\delta = 10^{-4}$

residual stress components when the noise amplitude is chosen to be $\delta = 10^{-4}$. Focusing on the figures set (4.10), we remark that the ellipticity criteria is verified when at least

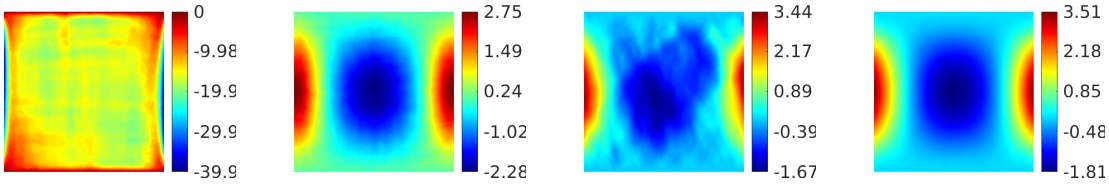

(a) $k_h = 1$, $\alpha_{div} = 0$ (b) $k_h = 6$, $\alpha_{div} = 0$ (c) $k_h = 1$, $\alpha_{div} = 20$ (d) $k_h = 6$, $\alpha_{div} = 20$

Figure 4.8: Reconstruction of τ_{22}, $\delta = 10^{-4}$

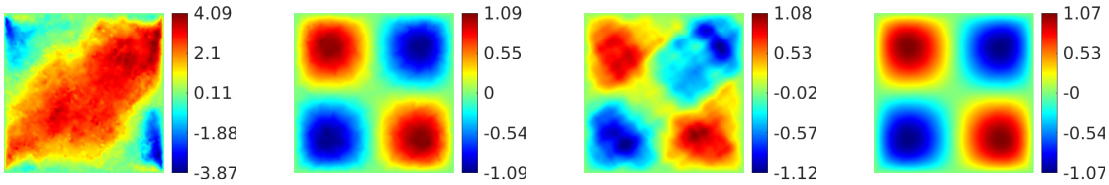

(a) $k_h = 1$, $\alpha_{div} = 0$ (b) $k_h = 6$, $\alpha_{div} = 0$ (c) $k_h = 1$, $\alpha_{div} = 20$ (d) $k_h = 6$, $\alpha_{div} = 20$

Figure 4.9: Reconstruction of τ_{12}, $\delta = 10^{-4}$

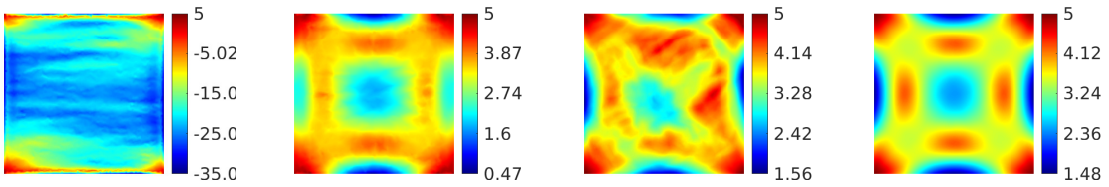

(a) $k_h = 1$, $\alpha_{div} = 0$ (b) $k_h = 6$, $\alpha_{div} = 0$ (c) $k_h = 1$, $\alpha_{div} = 20$ (d) $k_h = 6$, $\alpha_{div} = 20$

Figure 4.10: Checking of the ellipticity condition for the reconstructed initial stress field, $\delta = 10^{-4}$

one or both of the filtering and regularization procedures are considered. But, we cannot guarantee that such restrictions can be satisfied if the noise level increases. As a solution we can add an extra constraint to the optimization problem to satisfy the ellipticity criteria. However, such a solution implies the non-linearity of the added inequality-constraint which will complicate the optimization procedure.

4.6.4.2 Reconstruction of residual stress field and the material parameters

In the case of all parameters reconstruction, we have chosen continuous Lamé coefficients fields and the same residual stress as the one considered in the previous section. Regarding

the Lamé representation in figures (4.12-d) and (4.12-e), their fields can represent an inclusion presence in a heterogeneous material but with a smooth material rigidity variation to avoid the discontinuity character of the problem. Again, the ellipticity criteria presented in equation (4.55) is checked through figure (4.12-f). In this section we have used 6 displacement fields that are again results of direct problem solutions perturbation using different Dirichlet boundary conditions. To ensure that the noise function has the same influence on the different displacement fields, these measures are chosen to have the same displacement maximum which is fixed to the unity value. The number 6 here is a full arbitrary choice. Indeed, following the same ODE approach used in section 4.5, we have shown algebraically that five displacement fields are in general not sufficient for the reconstruction of all the parameters. So, to present our reconstruction method in an efficient way, we have thinked of using a relatively small number of data measures but higher than five. This is why, we have chosen six displacements fields.

Since the residual stress field and the Lamé coefficients are determined to a multiplicative constant, in the following results we have considered the reconstructed fields as L_2-projection of the identified parameters-vector field on the exact predefined one. In the first step to ensure the efficiency of the exploited chosen displacement fields, a stability analysis is done. Through this analysis, without using nor filtering nor regularization terms, we have shown that both relative L_2, H_1-norms errors and the residual stress divergence error converges to zero as the noise amplitude decreases as it is illustrated in figures-set (4.11).

Proceeding by the same way as in the previous section, multiple possible cases by changing the filtering and regularization parameters to show they are both necessary to obtain a good reconstruction of the different material parameters as it is shown in figures (4.13-4.17) with an amplitude level $\delta = 10^{-}4$. In addition, the ellipticity criteria is checked also for this inverse problem as it is presented in figures-set (4.18). In short, the ellipticity criteria is satisfied for the optimal reconstructed fields. Similarly to what proposed in the previous section, we can enforce the strong ellipticity restriction in the optimization problem. However, the added inequality constraint is not only non linear but is also non convex.

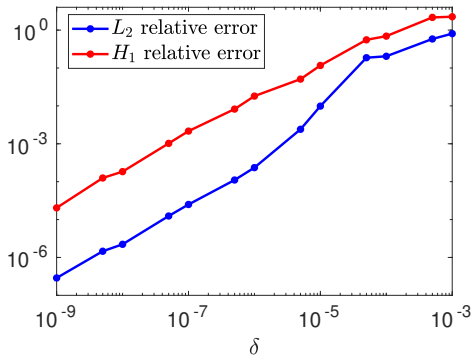

(a) Relative H_1 and L_2 norms of all the identified parameters vector

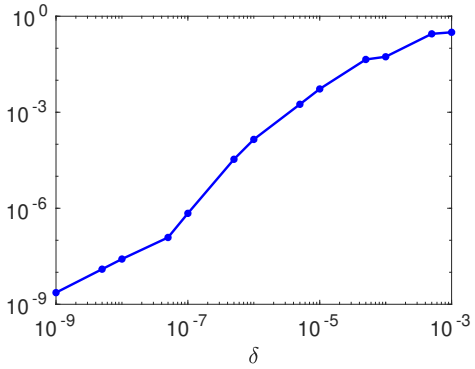

(b) Stability of the Div $\boldsymbol{\tau}$ reconstruction

Figure 4.11: Stabilty of the parameters reconstruction method

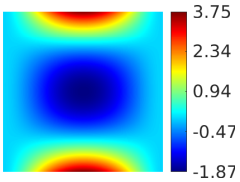

(a) τ_{11}

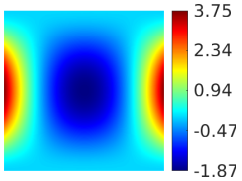

(b) τ_{22}

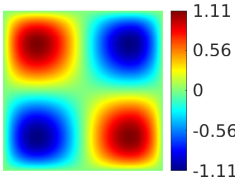

(c) τ_{12}

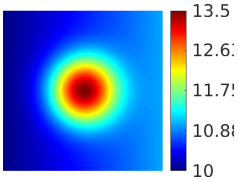

(d) μ

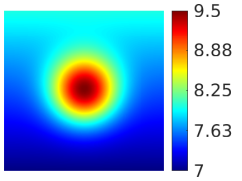

(e) λ

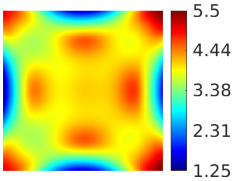

(f) ellipticity criteria

Figure 4.12: Reconstruction of λ, $\delta = 10^{-4}$

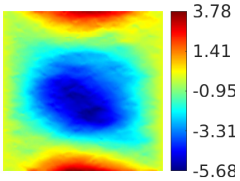

(a) $k_h = 1$, $\alpha_{div} = 0$, $\alpha_L = 0$

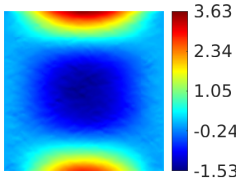

(b) $k_h = 3$, $\alpha_{div} = 0$, $\alpha_L = 0$

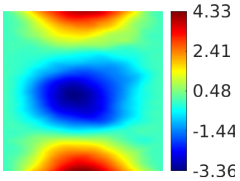

(c) $k_h = 1$, $\alpha_{div} = 100$, $\alpha_L = 10^{-4}$

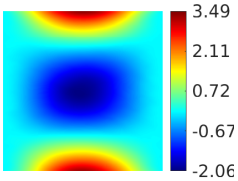

(d) $k_h = 3$, $\alpha_{div} = 100$, $\alpha_L = 10^{-4}$

Figure 4.13: Reconstruction of τ_{11}, $\delta = 10^{-4}$

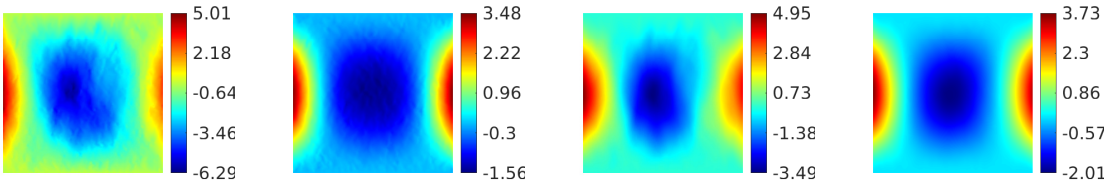

(a) $k_h = 1$, $\alpha_{div} = 0$, $\alpha_L = 0$ (b) $k_h = 3$, $\alpha_{div} = 0$, $\alpha_L = 0$ (c) $k_h = 1$, $\alpha_{div} = 100$, $\alpha_L = 10^{-4}$ (d) $k_h = 3$, $\alpha_{div} = 100$, $\alpha_L = 10^{-4}$

Figure 4.14: Reconstruction of τ_{22}, $\delta = 10^{-4}$

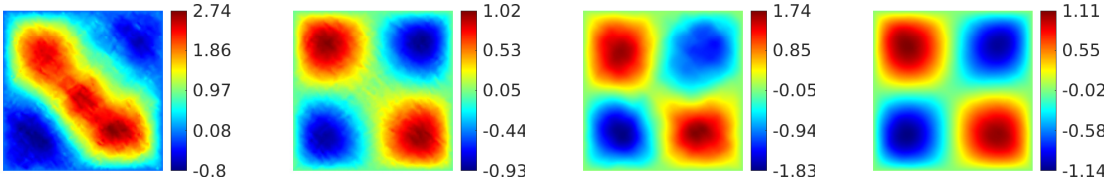

(a) $k_h = 1$, $\alpha_{div} = 0$, $\alpha_L = 0$ (b) $k_h = 3$, $\alpha_{div} = 0$, $\alpha_L = 0$ (c) $k_h = 1$, $\alpha_{div} = 100$, $\alpha_L = 10^{-4}$ (d) $k_h = 3$, $\alpha_{div} = 100$, $\alpha_L = 10^{-4}$

Figure 4.15: Reconstruction of τ_{12}, $\delta = 10^{-4}$

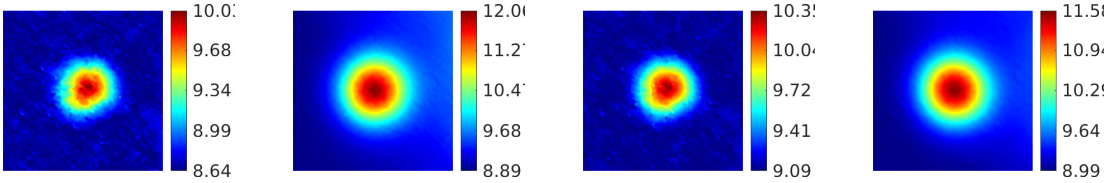

(a) $k_h = 1$, $\alpha_{div} = 0$, $\alpha_L = 0$ (b) $k_h = 3$, $\alpha_{div} = 0$, $\alpha_L = 0$ (c) $k_h = 1$, $\alpha_{div} = 100$, $\alpha_L = 10^{-4}$ (d) $k_h = 3$, $\alpha_{div} = 100$, $\alpha_L = 10^{-4}$

Figure 4.16: Reconstruction of μ, $\delta = 10^{-4}$

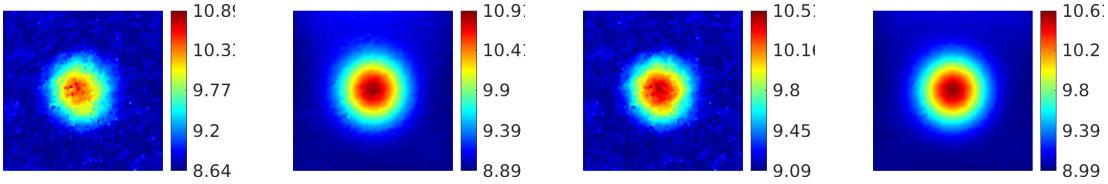

(a) $k_h = 1$, $\alpha_{div} = 0$, $\alpha_L = 0$ (b) $k_h = 3$, $\alpha_{div} = 0$, $\alpha_L = 0$ (c) $k_h = 1$, $\alpha_{div} = 100$, $\alpha_L = 10^{-4}$ (d) $k_h = 3$, $\alpha_{div} = 100$, $\alpha_L = 10^{-4}$

Figure 4.17: Reconstruction of λ, $\delta = 10^{-4}$

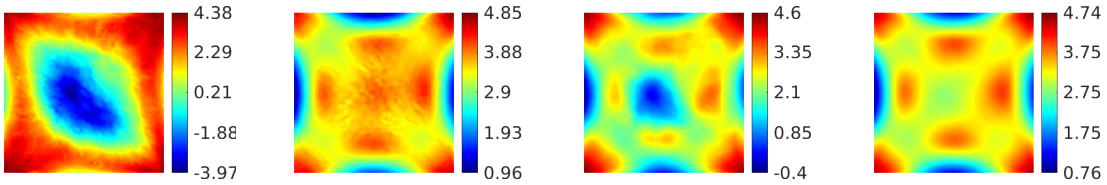

(a) $k_h = 1$, $\alpha_{div} = 0$, $\alpha_L = 0$ (b) $k_h = 3$, $\alpha_{div} = 0$, $\alpha_L = 0$ (c) $k_h = 1$, $\alpha_{div} = 100$, $\alpha_L = 10^{-4}$ (d) $k_h = 3$, $\alpha_{div} = 100$, $\alpha_L = 10^{-4}$

Figure 4.18: Ellipticity criteria

4.7 Conclusion

In this chapter, we have presented a new direct identification approach for the residual stress and the material parameters reconstruction. The approach is based on the variational formulation of the direct problem and it exploits only the internal data of a set of displacement measures. We have presented some stability results for a generalized initially-stress linear elastic material and particular model by different methods. Also, we have shown that only two displacement fields , fulfilling some mathematical restriction, are sufficient to the reconstruction of the residual stress field. Moreover, using only six perturbed displacement fields, we have reconstructed the residual stress field and the Lamé fields with good accuracy. A variety of numerical results are presented for both the residual stress reconstruction knowing the Lamé coefficients and the identification of all the material parameters : residual stress and the Lamé coefficients. Couple of regularization techniques are tested for both cases in the objective to analyze the parameters of the reconstruction approach on the quality and the accuracy of the results.

Chapter 5

XFEM and asymptotic analysis of the mechanical fields near a crack tip in an initially-stressed hyperelastic body

Contents

5.1 Introduction

It is well known that natural and manufactured materials and structures contain initial stress in their reference configuration. This initial stress field can be developed in the earth's crust due to processes such as various past tectonic events, in manufactured materials and mechanical parts during their fabrication and assembly, in composite materials and structures when they are manufactured, in soft tissue when growth and remodelling processes occur, in rock, etc. Here, the term initial stress shall be used in its general sense regardless of the origin of this initial stress field that verifies the equilibrium equation in the reference configuration with a no homogeneous static boundary condition (no zero surface loads). When this initial stress is accompanied by a pre-strain due to the applied load in the reference configuration, the term pre-stress is usually used. In the case of zero applied loads, the term residual stress is commonly adopted according to the definition of [Hoger 1986]. From a physical viewpoint, the initial stress can be a result of incompatible growth and/or plasticity deformation processes and then alters the mechanical properties and the stress distribution. This deformation incompatibility generates singularity due to stress concentration at the micro, meso and macro-scale. Other types of singularities are also present in structures like cracks, corners, voids, inclusions, and other material or geometrical imperfections. The problem here is that the combination of the initial stress and singularities effects can promote or prevent failure and alter the fracture mode by contributing to the crack-driving force. In contrast to metal-like materials, this problem is more complicated and challenging for rubber, rubber-like and soft tissue materials due to their geometrical and material nonlinearities. For example, the residual stress prevents the propagation of aortic dissection, which is a serious cardio-vascular disease and life-threatening event, by reducing stress gradient [Humphrey 2012, Wang 2017]. In contrast, residual stress promotes failure in bush mounting. These two examples, among others, show that residual stress can promote or prevent crack initiation and propagation in soft tissue and rubber. The investigation of fracture behaviours of the above presented problematics are relatively difficult and hence the analysis methods are multiplied: experimental [Drory 1988, Ohayon 2007, Creton 2016, Amabili 2019, Brunet 2019], theoretical [He 1994, Radayev 2001, Dal Corso 2008, Bigoni 2008] and numerical [Nagashima 2009,

Ebrahimi 2021].

Following these analyses, physical investigations and computational analysis using the finite element method (FEM) have shown that very high stress concentrations can arise in the region of cracks, edges, corners, and near-interface problems when the material characteristics are discontinuous [Martin Borret 1998]. In the mechanical community language, the associated problem is said to admit a singular stress which requires the development of crack initiation criteria. In fracture mechanics, the different crack initiation or propagation criteria are based on the stress field in the body and, therefore, a good knowledge of their analytical form is important. Furthermore, it is widely known that in the presence of stress singularities, the convergence rates of classical FEM decrease [Strang 1973]. Here, prior knowledge of the stress field can be exploited to improve algorithms by including particular singular functions in the FE-spaces [Strang 1973, Destuynder 1982, Moës 1999].

Thus, the purpose of this chapter is threefold. First, the academic paradigm three-dimensional boundary value problem (BVP) of an infinite initially-stressed hyperelastic cracked cylinder will be formulated. The aim is to give one issue of a generalization of the three-dimensional Linear Elastic Fracture Mechanics (LEFM) to hyperelasticity by superposing an in-plane transformation to an antiplane one. This is a particular "simpler" class of the three-dimensional initially-stressed crack problem with a simple initially-stressed hyperelastic potential which can elucidate the other "more complicated" class of problem. Secondly, the resolution of this BVP will be done with a neoHookean potential taking into account an initial constant stress. The elastostatic field results will be analyzed and differences with LEFM will be elucidated. Third, the XFEM formulation and numerical analysis will be realized. A convergence study will be carried out to show the contribution of the exploitation of such a method.

In linear elasticity, the Linear Fracture Elastic Mechanics (LEFM) based on the superposition principle gives us a three-dimensional analytical elastostatic field. A criticism and a review of the LEFM can be found in the excellent book of Bui [Bui 2007] in which some three-dimensional linear elastic problems were summarised. In the presence of initial stress and when its magnitude is sufficiently small, the principle of superposition can be used to provide a useful solution by adding the LEFM stress field to the initial stress field. Otherwise, the initial stress linear elastic models presented in chapter 2 should be used in a crack

boundary value problem. This BVP is resolved and analyzed by using three main methods: asymptotic development, complex variables and transform methods. Some valuable contributions are to be credited to [Parker 1982, Nazarenko 2000, Radayev 2001, Liu 2008, Barsoum 2009, Chaudhuri 2010, Chaudhuri 2012, Wu 2019]. For pre-stressed cracked solid and using the incremental formalism of Biot [Biot 1965, Biot 1973], the representations in the crack plane and antiplane of the incremental displacement and stress fields are given by [GrÁciun 1998, Zhou 2020, Guz 2013, Sadowski 2016, Craciun 2018].

Within the framework of finite deformation [Ogden 1997], in the past decades, only a few works have been focused on the analysis of the fully three-dimensional deformation and stress fields. This is due to the mathematics problem's tremendous complexity [Ogden 1997], which, in contrast to the planar problem, makes the boundary-value problem equations very nonlinear and difficult to solve analytically or numerically. A generalisation from a plane to a pseudo-plane deformation problem, with uniform axial extension [Rajagopal 1985, Hill 1986]. and non-uniform axial extension was conducted in [Saccomandi 2005]. Partial and exact solutions to some three-dimensional problems were done in a series of papers by Hill and his co-authors by exploiting the reciprocal equilibrium equations for particular hyperelastic potentials [Hill 1973, Hill 1989, Hill 2001]]. Coupling between antiplane and plane deformation fields in the boundary value problem was shown to exist for nonlinear hyperelastic potential, which makes it hard to resolve and the uncoupled governing equations hold only for the linear Neohookean material [Horgan 2003b].

Elastostatic fields near the crack front of a isotropic hyperelastic solid were first analysed by [Knowles 1974, Knowles 1973]for plane deformation, [Knowles 1983] for plane stress and [Knowles 1977a] for antiplane deformation hypothesis. Among other researchers, [Stephenson 1982] is to be credited to have clarified the local structure characteristic nature of the elastostatic fields near the crack tip of a generalised Mooney-Rivlin solid under plane deformation kinematic condition and mixed boundary conditions at infinity (Mode I and II). It was shown that the crack opens symmetrically, under Mode II conditions, contrary to the predictions of linear theory. In other words, the nonlinear global crack problem can not admit an antisymmetric solution. A review of this topic is presented by [Long 2015].

None of the aforementioned works took account of the possible existence of initial stress.

Hence, there is now a need to include initial stress to the constitutive model behaviour in concern in this chapter to model the hyperelastic material behaviour and also the effect of initial stresses. The response of initially-stressed materials has been modelled exploiting different approaches. One method is based on the modelling of the whole process that develops the initial stress by assuming a multiplicative decomposition of the deformation gradient, from the unstressed free configuration, into two contributions: a deformation describing the inelastic change of shape induced by the microstructural rearrangement of the matter and a deformation accounting for the elastic deformation of the body [Lee 1969, Rodriguez 1994, Skalak 1996, Du 2018]. Using the incremental deformation formalism [Biot 1965] where an infinitesimal deformation is superposed to a known initial finite deformation, the influence of pre-stress in continuum elastostatic fields has been analyzed for continuum boundary values problems by [Fung 1967, Destrade 2012a, Zidi 2000a, Zidi 2000b, Zidi 2001] and for singular boundary values problems (crack, inclusion, etc) by [Kurashige 1969, Kurashige 1971, Biot 1973, Dhaliwal 1979, Radi 2002, Dal Corso 2008, Bigoni 2008]. The second approach to modelling initial stresses is the so-called theory of initially-stressed materials in which the reference configuration is associated with the stressed one. Here, the strain energy density is assumed to depend on both the deformation (thanks to the objectivity principle) and on the initial stress field. In this second approach adopted in this work, the initial stress is a known field which can be determined from elastic wave speed [Man 1987, Shams 2011, Shams 2014] or by equilibrium equation and boundary conditions [Hoger 1986]. Some restrictions have been developed to ensure reasonable physical response of initially-stressed material: initial stress compatibility (ISC), initial stress symmetry (ISS) and initial stress reference independence (ISRI) [Shams 2011, Gower 2015, Gower 2017] (see chapter 2). The effect of initial stress (and residual stress) on elastostatic fields has been analyzed theoretically for continuum problems by [Merodio 2013b, Merodio 2016, Ciarletta 2016a, Ciarletta 2016b, Gower 2015, Gower 2017, Riccobelli 2018, Agosti 2018, Du 2018, Du 2019a, Du 2019b, Liu 2020a, Mukherjee 2021, Melnikov 2021]. To our knowledge, the singular boundary value problem associated with initially-stressed hyperelastic cracked solid is not theoretically analyzed apart from this thesis. However, it is to be noted that the effect of anisotropy on elastostatic fields near isotropic transverse hyperelastic cracked solid under plane stress assumption is analyzed in a series of papers [Liu 2020b, Liu 2021a, Liu 2021b].

The numerical analysis of crack problems has long been based on the theory of linear

elastic fracture mechanics coupled with the finite elements method (FEM). Nevertheless, FEM presents many drawbacks because its ability to detect singularities around the crack tip is very limited and requires fine mesh. To overcome these difficulties, many enriched finite element methods, and meshfree methods were introduced. The use of analytical enrichment functions to compute stress intensity factor was performed first by [Gifford Jr 1978]. [Babuška 1994] presented a method for elliptic boundary value problems with rough coefficients. In [Babuška 1997], they introduce a Generalized Finite Element Method named GFEM. They demonstrated that the use of an enrichment function obtained from an analytical solution improves the convergence rate of the finite element method. Later, [Belytschko 1999] and [Moës 1999] introduced the eXtended Finite Element Method, named XFEM, to treat crack problems numerically without remeshing. The analysis of standard XFEM [Stazi 2003] shows a reduction of the error level in spite of the decline of convergence rate compared to a classical finite element method. This convergence behaviour can be explained by the fact that the topological enrichment is applied only to the first layer of elements in the crack-tip.

Therefore, when the mesh is refined, the size of the zone of influence of the enrichment becomes negligible compared to the whole domain. To overcome this failure, geometrical enrichment is adopted by many authors [Stazi 2003, Laborde 2005] ; a fixed zone around the crack-tip is considered and an enrichment with crack-tip singular function is applied to all the degrees of freedom inside this zone. The analysis of this XFEM variant method shows the same behaviour as the classical XFEM regarding error. To affine this strategy [Chahine 2008] used a cut-off function to smooth the passage between enriched zone and non enriched zones. For mixed formulation enrichment with XFEM, the analysis performed by [Legrain 2008] for curved and straight interface for problems involving material inclusion and incompressible fracture problem leads to a stable mixed formulation with improved convergence rate. [Legrain 2008] used a standard XFEM method which disrupts the linear system conditioning.

Although the analysis of XFEM methods within a linear fracture mechanics frame is very developed as was mentioned, there are a few works that treat this method for nonlinear fracture mechanics in large deformations [Legrain 2005, Karoui 2014, Šuštarič 2014, Rashetnia 2015, Huynh 2019, Jansari 2019]. For compressible hyperelastic behaviour, the results of [Karoui 2014] with XFEM cut-off variant are relevant and analogous to linear

theory predictions for improving of numerical convergence and estimate errors, without degrading the linear system conditioning or increasing numerical problem size. For incompressible hyperelastic behaviour, [Legrain 2008] shows that the inf-sup condition is satisfied for the linearized problem. In [K. 2016], it was shown that this condition remains verified for large deformation.

In the following the second section is devoted to the global formulation of the crack boundary value problem. The third section shows the existence of an analogy between initially-stressed and unstressed material subjected to the same boundary conditions. Such analogy permits the simplification of the asymptotic resolution for both the plane and antiplane problems in the fourth section. Then the asymptotic expansion of the different mechanical fields will be discussed in multiple levels through the fifth section. Finally, the before last section is devoted to the numerical analysis of a plane cracked problem within an initially hyperelastic material using the XFEM method.

5.2 Formulation of the global crack problem

Let consider a body B composed by an homogeneous incompressible hyperelastic material body. The undeformed configuration, denoted by $\mathcal{B}_0$, is supposed to be an infinite cylinder whose generator is characterized by the vector $\vec{\mathcal{G}}$. Let $(\vec{E}_1, \vec{E}_2, \vec{E}_3)$ be the rectangular cartesian basis associated to the coordinates (X_1, X_2, X_3). The generator vector of the studied cylindrical body is supposed to be parallel to the vector $\vec{E}_3$ as it is illustrated in figure (5.1). Now, let Ω_0 denotes the cross section of the material body B in the reference configuration $\mathcal{B}_0$, so the latter can be defined as:

$$\mathcal{B}_0 = \{\vec{X} / \quad (X_1, X_2) \in \Omega_0, \quad -\infty < X_3 < +\infty\}. \tag{5.1}$$

The cross section Ω_0 in the undeformed configuration is containing a crack whose the tip is the origin of the cartesian coordinates and the crack faces are described locally by the cartesian coordinates as $(X_1 = 0, \quad X_1 \to 0^-)$ or by the polar coordinates as $(R \to 0, \quad \theta = \pm\pi)$ as it is shown in figure (5.2). In the reference configuration $\mathcal{B}_0$, the considered body B is subjected to an initial stress field denoted $\boldsymbol{\tau}$. The presence of a such internal stress has a significant effect on the intrinsic material response as it has been shown for the example of arteries [Holzapfel 2000]. As it is illustrated in [Hoger 1986, Hoger 1985], the initial stress $\boldsymbol{\tau}$, which is not necessarily associated with an elastic deformation, satisfies

in absence of volumetric density of forces the following equilibrium equation:

$$\mathrm{Div}\boldsymbol{\tau} = \vec{0}. \tag{5.2}$$

and the boundary condition:

$$\boldsymbol{\tau}.\vec{N} = \vec{t_\tau} \quad on \quad \partial\mathcal{B}_0, \tag{5.3}$$

where Div denotes the divergence operator relative to the cartesian coordinates of the reference configuration and $\vec{N}$ is the outward unit normal vector to the boundary of the region defined by the reference configuration $\mathcal{B}_0$, whereas the $\vec{t_\tau}$ denotes the imposed force vector. If $\vec{t_\tau}$ vanishes, the initial stress field is called residual stress: an equilibrated initial stress field in absence of all external loadings. Consider that the body B is subjected to a

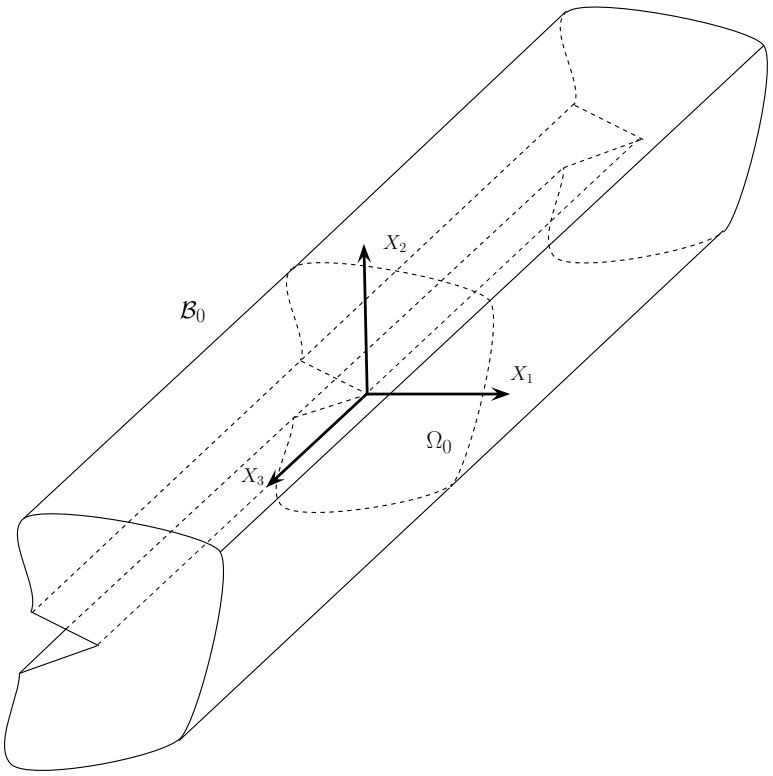

Figure 5.1: Cracked infinite cylinder.

deformation field denoted by $\vec{y}$ whose the associated displacement field is depending only

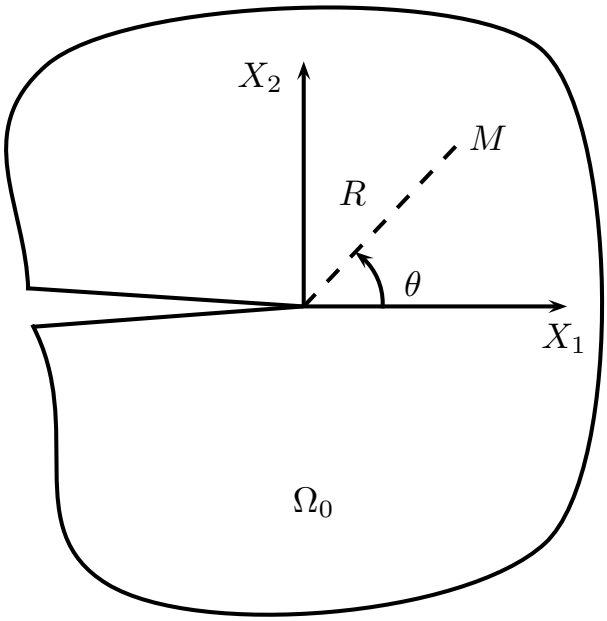

Figure 5.2: The cracked cross section Ω_0

on the the planar coordinates. Consequently, the mapping function $\vec{y}$ can be represented mathematically as:

$$\vec{y} = \chi(\vec{X}) = \begin{cases} y_1 = y_1(X_1, X_2) \\ y_2 = y_2(X_1, X_2) \\ y_3 = X_3 + u(X_1, X_2) \end{cases} \tag{5.4}$$

where $u(.,.)$ denotes the antiplane displacement. The deformation $\vec{y}$ represents a transformation for a coupled plane deformation with an antiplane shear. Hence the corresponding deformation gradient tensor field denoted by $\boldsymbol{F}$ becomes:

$$\boldsymbol{F} = \begin{bmatrix} y_{1,1} & y_{1,2} & 0 \\ y_{2,1} & y_{2,2} & 0 \\ y_{3,1} & y_{3,2} & 1 \end{bmatrix}, \tag{5.5}$$

with $y_{i,j} = \frac{\partial y_i}{\partial X_j}, \quad i,j \in \{1,2,3\}$. If we consider $\boldsymbol{F}^p$ and $\boldsymbol{F}^a$ the deformation gradient tensors relative respectively to plane and antiplane deformations which can be expressed

as:

$$\boldsymbol{F}^p = \begin{bmatrix} y_{1,1} & y_{1,2} & 0 \\ y_{2,1} & y_{2,2} & 0 \\ 0 & 0 & 1 \end{bmatrix}, \quad \boldsymbol{F}^a = \begin{bmatrix} 1 & 0 & 0 \\ 0 & 1 & 0 \\ y_{3,1} & y_{3,2} & 1 \end{bmatrix} \tag{5.6}$$

The deformation gradient tensor $\boldsymbol{F}$ can be expressed in function of the deformation gradient tensors $\boldsymbol{F}^p$ and $\boldsymbol{F}^a$ as the following:

$$\boldsymbol{F} = \boldsymbol{F}^p \boldsymbol{F}^a \neq \boldsymbol{F}^a \boldsymbol{F}^p \tag{5.7}$$

Hence the deformation field illustrated in equation (5.4) can be interpreted as a plane deformation field superimposed to an antiplane shear deformation. Since the incompressible constraint holds, the material supports only isochoric transformations, which is equivalent to:

$$J = \det(\boldsymbol{F}) = y_{1,1}y_{2,2} - y_{2,1}y_{1,2} = 1. \tag{5.8}$$

Now, we can define the left and right Cauchy-Green strain tensors as:

$$\boldsymbol{C} = \boldsymbol{F}^T \boldsymbol{F}, \quad \boldsymbol{B} = \boldsymbol{F}\boldsymbol{F}^T, \tag{5.9}$$

and by using the expression of the deformation gradient tensor in equation (5.5), the prior two measures of strain can be explicitly expressed as:

$$\boldsymbol{C} = \begin{bmatrix} (y_{1,1})^2 + (y_{2,1})^2 + (y_{3,1})^2 & y_{1,1}y_{1,2} + y_{2,1}y_{2,2} + y_{3,1}y_{3,2} & y_{3,1} \\ y_{1,1}y_{1,2} + y_{2,1}y_{2,2} + y_{3,1}y_{3,2} & (y_{1,2})^2 + (y_{2,2})^2 + (y_{3,2})^2 & y_{3,2} \\ y_{3,1} & y_{3,2} & 1 \end{bmatrix}, \tag{5.10}$$

$$\boldsymbol{B} = \begin{bmatrix} y_{1,1}^2 + y_{1,2}^2 & y_{1,1}y_{2,1} + y_{1,2}y_{2,2} & y_{1,1}y_{3,1} + y_{1,2}y_{3,2} \\ y_{1,1}y_{2,1} + y_{1,2}y_{2,2} & y_{2,1}^2 + y_{2,2}^2 & y_{2,1}y_{3,1} + y_{2,2}y_{3,2} \\ y_{1,1}y_{3,1} + y_{1,2}y_{3,2} & y_{2,1}y_{3,1} + y_{2,2}y_{3,2} & y_{3,1}^2 + y_{3,2}^2 + 1 \end{bmatrix} \tag{5.11}$$

Both the left and right Cauchy strain tensors share the same invariants which can be expressed as:

$$\begin{cases} I_1 & = \mathrm{tr}(\boldsymbol{C}) = 1 + (y_{1,1})^2 + (y_{1,2})^2 + (y_{2,1})^2 + (y_{2,2})^2 + (y_{3,1})^2 + (y_{3,2})^2 \\ & = |\nabla y_1|^2 + |\nabla y_2|^2 + |\nabla y_3|^2 \\ I_2 & = \frac{1}{2}((\mathrm{tr}(\boldsymbol{C}))^2 - \mathrm{tr}(\boldsymbol{C}^2)) = I_1 + (y_{1,1}y_{3,2} - y_{1,2}y_{3,1})^2 + (y_{2,1}y_{3,2} - y_{2,2}y_{3,1})^2 \\ I_3 & = 1. \end{cases} \tag{5.12}$$

Now, it is necessary to specify the constitutive model behaviour in concern with this chapter to model the elastic incompressible material behaviour and also the effect of initial stresses. The response of initially-stressed materials has been modelled exploiting two main approaches. The first one associates the residual stress to a non compatible deformation (initially-strained materials). This approach is based on a multiplicative decomposition of the deformation gradient, from the unstressed free configuration, into two contributions: a deformation describing the inelastic change of shape induced by the microstructural rearrangement of the matter and a deformation accounting for the elastic deformation of the body [Lee 1969, Rodriguez 1994]. Then using the virtual stress-free state concept [Johnson 1995, Johnson 1998], a hyperelastic constitutive law can be developed for initially-stressed materials. To do this, challenging calculations are needed and rarely yields analytic explicit hyperelastic models, unless great simplifications are assumed. The second approach to model initial stresses influence is the so-called theory of initially-stressed materials, in which the strain energy density is assumed to depend on both the deformation $\boldsymbol{C}$ (thanks to objectivity principle) and on the initial stress field $\boldsymbol{\tau}$, namely:

$$W = W(\boldsymbol{C}, \boldsymbol{\tau}) \tag{5.13}$$

This is an ideal way to overcome the technical difficulty of the first approach and this issue has been discussed by Hoger and her collaborators in [Johnson 1993, Johnson 1995, Johnson 1998]. Within this second approach which is adopted in this work, the development of a constitutive model of strain energy deformation does not need to distinguish between initial stress and residual stress [Merodio 2013b] which are known fields determined from elastic wave speed [Man 1987, Destrade 2013, Shams 2014] or by equilibrium equation and boundary conditions [Hoger 1986].

The first Piola-Kirchoff $\boldsymbol{S}$ and the Cauchy stress $\boldsymbol{\sigma}$ tensors can be deduced from the strain energy density respectively:

$$\boldsymbol{\sigma} = \frac{\partial W}{\partial \boldsymbol{F}}\boldsymbol{F} - p\mathbf{1}, \quad \boldsymbol{S} = \frac{\partial W}{\partial \boldsymbol{F}} - p\boldsymbol{F}^{-T}, \tag{5.14}$$

where p is the Lagrange multiplier associated to the incompressibility condition and $\mathbf{1}$ is the identity second order tensor. The initial stress field is defined to be the Cauchy stress tensor in the reference configuration which is equivalent to:

$$\boldsymbol{\sigma} = \boldsymbol{\tau}, \quad \text{if} \quad \boldsymbol{F} = \mathbf{1}. \tag{5.15}$$

The last relation represents the initial stress compatibility condition [Shams 2011, Gower 2015, Gower 2017] and imposes restrictions on the combination of the strain energy W and the initial stress $\boldsymbol{\tau}$. Other restrictions are developed to ensure reasonable physical response of initially-stressed material : initial stress symmetry (ISS) and initial stress reference independence (ISRI) [Gower 2015, Gower 2017] (see chapter 2).

As it was discussed in the second chapter that the presence of the initial stress $\boldsymbol{\tau}$ renders the material behaviour anisotropic, even if the material has no intrinsic anisotropy. Thus, the initial stress effect on the constitutive law is analogous to the fibre reinforced material behaviour. To more investigate this analogy, recall that the initial stress compatibility condition implies the initial stress tensor symmetry. Then, using the spectral theory, $\boldsymbol{\tau}$ can be presented as:

$$\boldsymbol{\tau} = \tau_1 \vec{L}_1 \otimes \vec{L}_1 + \tau_2 \vec{L}_2 \otimes \vec{L}_2 + \tau_3 \vec{L}_3 \otimes \vec{L}_3 \tag{5.16}$$

where τ_i is the eigenvalue associated to the eigenvector $\vec{L}_i$, $(i \in \{1,2,3\})$. The eigenvectors $(\vec{L}_1, \vec{L}_2, \vec{L}_3)$ constructs a direct orthonormal basis i.e

$$\begin{cases} \vec{L}_1 \otimes \vec{L}_1 + \vec{L}_2 \otimes \vec{L}_2 + \vec{L}_3 \otimes \vec{L}_3 = \mathbf{1}, \\ \vec{L}_i . \vec{L}_j = \delta_{ij}, \quad i,j \in \{1,2,3\} \end{cases} \tag{5.17}$$

where $\mathbf{1}$ denotes the identity tensor in three dimensions whereas δ is the Kronecker symbol.

Thus, the eigenvectors $\{\vec{L}_i, \quad i = 1..3\}$ of the initial stress $\boldsymbol{\tau}$ have a similar roles to the preferred directions of the fibre reinforced material and then induce anisotropy and gen-

erate invariants in the constitutive law which contribute to the independent variables in the functional dependence of W. This issue was discussed in details in chapter 2 with historically bibliographic references. Now, we assume that the material behaviour is initially isotropic in the natural configuration. Thus, the strain energy density is an isotropic functional of $\boldsymbol{C}$ and $\boldsymbol{\tau}$ and then it depends on the invariants of the tensors couple $(\boldsymbol{C}, \boldsymbol{\tau})$. This complete list of invariants is given by the invariants of $\boldsymbol{C}$:

$$I_1 = \mathrm{tr}(\boldsymbol{C}), \quad I_2 = \frac{1}{2}(\mathrm{tr}(\boldsymbol{C})^2 - \mathrm{tr}(\boldsymbol{C}^2), \quad I_3 = \det(\boldsymbol{C}), \tag{5.18}$$

and the invariants of initial stress $\boldsymbol{\tau}$:

$$I_1^\tau = \mathrm{tr}(\boldsymbol{\tau}), \quad I_2^\tau = \frac{1}{2}(\mathrm{tr}(\boldsymbol{\tau})^2 - \mathrm{tr}(\boldsymbol{\tau}^2), \quad I_3^\tau = \det(\boldsymbol{\tau}), \tag{5.19}$$

with the combined invariants of $\boldsymbol{C}$ and $\boldsymbol{\tau}$:

$$J_1 = \mathrm{tr}(\boldsymbol{C}\boldsymbol{\tau}), \quad J_2 = \mathrm{tr}(\boldsymbol{C}^2\boldsymbol{\tau}), \quad J_3 = \mathrm{tr}(\boldsymbol{C}\boldsymbol{\tau}^2), \quad J_1 = \mathrm{tr}(\boldsymbol{C}^2\boldsymbol{\tau}^2). \tag{5.20}$$

For an incompressible material, the strain energy density can be rewritten as:

$$W = W(I_1, I_2, I_1^\tau, I_2^\tau, I_3^\tau, J_1, J_2, J_3, J_4) \tag{5.21}$$

In the absence of the initial stress, the strain energy density W recovers the classical hyperelastic potential model where the determination of an explicit expression is a hard task [Saccomandi 2004]. Since the dependence of material properties on initial stress is not well understood [Gou 2014] and the experiments data to estimate residual stress are qualitative (for example from the opening angle method [Sigaeva 2019]) rather than quantitative, it is not reasonable to choose a very general constitutive law, i.e., a strain energy density that includes all invariants. Since one of the objectives of this chapter is to give analytical solution of the boundary value problem, a simple prototype of strain energy characterizing the hyperelastic behaviour of an initial stressed body based in a simple Neohookean isotropic energy function with an additional term that introduces initial stress is considered:

$$W = \frac{\mu}{2}(I_1 - 3) + \frac{1}{2}(J_1 - I_1^\tau) \tag{5.22}$$

where μ denotes the shear modulus for infinitesimal deformations in absence of the initial stress. The potential per unit of volume of the undeformed configuration introduced

in equation (5.22) is a simple potential that describes the influence of the initial stress on the hyperelastic behavior relative to the reference configuration. This strain energy density is widely used to illustrate the effect of initial stress on some boundary value problems. From an experimental viewpoint, a strain energy including one initial stress invariant is sufficient to model the effect of this residual stress on soft tissue (myocardium) behaviour [Wang 2014]. More complex forms of strain energy densities are introduced in [Shams 2011, Merodio 2013b, Shams 2014, Merodio 2016] to illustrate the effect of initial stress on some boundary value problems.

In the sake of problem's simplification, the strain energy in equation (5.22) is considered in the remainder of this chapter. Then, the related invariants can be explicitly expressed as:

$$\begin{cases} J_1 = \mathrm{tr}(\boldsymbol{C\tau}) & = \tau_{11}[(y_{1,1})^2 + (y_{2,1})^2 + (y_{3,1})^2] + \tau_{22}[(y_{1,2})^2 + (y_{2,2})^2 + (y_{3,2})^2] \\ & \quad +2\tau_{12}[y_{1,1}y_{1,2} + y_{2,1}y_{2,2} + y_{3,1}y_{3,2}] + 2\tau_{31}y_{3,1} + 2\tau_{32}y_{3,2} + \tau_{33} \\ I_1^{\tau} = \mathrm{tr}(\boldsymbol{\tau}) & = \tau_{11} + \tau_{22} + \tau_{33}. \end{cases} \tag{5.23}$$

where μ denotes the shear modulus for infinitesimal deformations in absence of the initial stress field. The potential per unit of volume of the undeformed configuration introduced in equation (5.22) is a simple potential that describes the influence of the initial stress field on the hyperelastic behavior relative to the reference configuration. When the initial stress field $\boldsymbol{\tau}$ vanishes, the strain energy density illustrated in equation (5.22) is reduced to the Neohookean potential.

Using equations (5.14,5.22), the first Piola Kirchhoff stress tensor can be defined as:

$$\boldsymbol{S} = \mu\boldsymbol{F} + \boldsymbol{F\tau} - p\boldsymbol{F}^{-T}, \tag{5.24}$$

Consequently, the Cauchy stress tensor can be explicitly presented as:

$$\boldsymbol{\sigma} = \boldsymbol{S}\boldsymbol{F}^T = \mu\boldsymbol{B} + \boldsymbol{F\tau}\boldsymbol{F}^T - p\mathbf{1} \tag{5.25}$$

Let consider the potential $\tilde{W}$ expressed as:

$$\tilde{W} = \frac{\mu_1}{2}(I_1 - 3) + \frac{\mu_2}{2}(I_2 - 3) + \frac{1}{2}(J_1 - I_1^{\tau}) \tag{5.26}$$

with $\mu = \mu_1 + \mu_2$. In absence of the initial stress field $\boldsymbol{\tau}$, the strain energy potential $\tilde{W}$ is reduced to the one of Mooney-Rivlin for incompressible materials. We notice in the case of pure plane deformation or pure antiplane shear deformation, the first Piola Kirchhoff stress tensor components are the same for the two potentials W and $\tilde{W}$. Thus for the case of pure plane deformation and pure antiplane shear deformation, the solutions of the boundary value problem relative to the strain energy densities in equation (5.22) and (5.26) are the same.

Hence, using equations (5.17-5.18) associated to the spectral form of $\boldsymbol{\tau}$, the previous expression of the strain energy mentioned in equation (5.22) becomes:

$$W = \frac{\mu + \tau_3}{2}(I_1 - 3) + \frac{\tau_1 - \tau_3}{2}[(\vec{L}_1.\boldsymbol{C}.\vec{L}_1) - 1] + \frac{\tau_2 - \tau_3}{2}[(\vec{L}_2.\boldsymbol{C}.\vec{L}_2) - 1]. \tag{5.27}$$

by the same way, the Cauchy stress tensor expression can be modified to:

$$\boldsymbol{\sigma} = (\mu + \tau_3)\boldsymbol{B} + (\tau_1 - \tau_3)\vec{l_1} \otimes \vec{l_1} + (\tau_2 - \tau_3)\vec{l_2} \otimes \vec{l_2} - p\mathbf{1} \tag{5.28}$$

with

$$\vec{l_i} = \boldsymbol{F}\vec{L}_i, \quad i \in \{1, 2\}. \tag{5.29}$$

Just by examining the strain energy potential and the Cauchy stress expressions, with the analogy of the anisotropic fibrous materials, the initial stress field $\boldsymbol{\tau}$ is source of anisotropic behaviour if the initial stress field is not reduced to a spherical tensor, and the eigenvectors of the initial stress field becomes analogous to fibers directions as it is enlightned in details in chapter 2 (section 2.5).

To ensure the existence and unicity of the static boundary values problem solution, the usual mathematical constraint that the strain energy density W must satisfy is the strong ellipticity condition, which can be expressed in the incompressible case as:

$$\vec{a} \otimes \vec{b} : \frac{\partial^2 W}{\partial \boldsymbol{F} \partial \boldsymbol{F}} : \vec{a} \otimes \vec{b} > 0, \forall \vec{a}, \vec{b}; \quad \vec{a}.\vec{b} = 0. \tag{5.30}$$

Consequently by considering the expression of the energy potential in equation (5.22), the strong ellipticity condition implies:

$$max(|\tau_1|, |\tau_2|, |\tau_3|) < \mu. \tag{5.31}$$

Using the explicit form of the deformation gradient in equation (5.5) and the first Piola Kirchhoff stress tensor expression in equation (5.24), the different components of the First Piola Kirchhoff stress tensor can be expanded as:

$$\begin{cases} S_{11} &= (\mu + \tau_{11})y_{1,1} + \tau_{12}y_{1,2} - py_{2,2}, \\ S_{12} &= (\mu + \tau_{22})y_{1,2} + \tau_{12}y_{1,1} + py_{2,1}, \\ S_{13} &= \tau_{13}y_{1,1} + \tau_{23}y_{1,2} + p(y_{3,1}y_{2,2} - y_{3,2}y_{2,1}), \\ S_{21} &= (\mu + \tau_{11})y_{2,1} + \tau_{12}y_{2,2} + py_{1,2}, \\ S_{22} &= (\mu + \tau_{22})y_{2,2} + \tau_{12}y_{2,1} - py_{1,1}, \\ S_{23} &= \tau_{13}y_{2,1} + \tau_{23}y_{2,2} + p(y_{3,2}y_{1,1} - y_{3,1}y_{1,2}), \\ S_{31} &= (\mu + \tau_{11})y_{3,1} + \tau_{12}y_{3,2} + \tau_{13}, \\ S_{32} &= (\mu + \tau_{22})y_{3,2} + \tau_{12}y_{3,1} + \tau_{23}, \\ S_{33} &= \mu + \tau_{33} + \tau_{13}y_{3,1} + \tau_{23}y_{3,2} - p. \end{cases} \tag{5.32}$$

The equilibrium equation in its static form and in absence of volumetric forces becomes:

$$\mathrm{Div}\boldsymbol{S} = \vec{0}. \tag{5.33}$$

where Div denotes the divergence operator related to the coordinates of the reference configuration $\mathcal{B}_0$. Considering the explicit form of the First Piola Kirchhoff stress tensor components, and supposing $\boldsymbol{\tau} = \boldsymbol{\tau}(X_1, X_2)$ (plane symmetry) the prior equilibrium equation is transformed into the three following partial differential equations:

$$\begin{cases} (\mu + \tau_{11})y_{1,11} + (\mu + \tau_{22})y_{1,22} + 2\tau_{12}y_{1,12} + p_{,2}y_{2,1} - p_{,1}y_{2,2} + p_{,3}[y_{3,1}y_{2,2} - y_{3,2}y_{2,1}] = 0, \\ (\mu + \tau_{11})y_{2,11} + (\mu + \tau_{22})y_{2,22} + 2\tau_{12}y_{2,12} + p_{,1}y_{1,2} - p_{,2}y_{1,1} + p_{,3}[y_{3,2}y_{1,1} - y_{3,1}y_{1,2}] = 0, \\ (\mu + \tau_{11})y_{3,11} + (\mu + \tau_{22})y_{3,22} + 2\tau_{12}y_{3,12} - p_{,3} = 0. \end{cases} \tag{5.34}$$

Since the antiplane displacement field depends only on the planar coordinates, and by using the third partial differential equation in the system of equations (5.34) related to the

equilibrium equation, then the Lagrange multiplier can be expressed in the following form:

$$p(X_1, X_2, X_3) = \alpha X_3 + q(X_1, X_2), \tag{5.35}$$

where α is a constant and $q(.,.)$ is a function depending on the planar coordinates X_1 and X_2. Now if we consider that the crack faces are free of traction then the local boundary condition near the crack tip is mathematically equivalent to:

$$\boldsymbol{S}(X_1 \to 0^-, X_2 = 0, X_3).\vec{E}_2 = \vec{0} \tag{5.36}$$

which can be expressed explicitly as:

$$S_{i2} = 0 \quad \text{if} \quad X_1 \to 0^-, \quad X_2 = 0, \quad i \in \{1, 2, 3\}. \tag{5.37}$$

We notice that in an incompressible initially-stressed hyperelastic material whose the strain energy is described by the potential in equation (5.22), a pure antiplane deformation can be supported only if the plane initial stress component of shear vanishes ($\tau_{12} = 0$), whereas the plane deformation holds only if $\tau_{32} = 0$.

If the above boundary conditions hold for every X_3, then using the incompressibility condition, the constant α vanishes and we can deduce:

$$p = p(X_1, X_2), \tag{5.38}$$

and consequently the plane and antiplane problems become completely decoupled both in the levels of equilibrium equations and boundary conditions. In the remainder of this chapter, the boundary value problem formulation will be simplified using multiple transformations and then an analogy with the same studied deformation for a Neohookean potential is derived.

Some remarks need now to be presented. First, the assumed transformation is clearly induced by the boundary conditions at the crack faces and at infinity. It was shown that this transformation is a superposition of two kinematical deformations: first an anti plane deformation which we superpose a plane deformation. The question here is : since the crack faces are traction-free, what is the loading scenario of the boundary conditions at infinity necessary to induce this transformation ? It is obvious that mixed in-plane mode

I and/or II loadings superposed to antiplane shear mode loading at infinity lead to this kinematical deformation. Similar deformation would, in general, be expected to occur due to an antiplane shear mode III loading at infinity since not all hyperelastic potentials can sustain antiplane deformation. Consequently, if antiplane kinematical deformation exists, particles will undergo a plane kinematic deformation for the majority of hyperelastic potentials. Also, the decoupling between the system of second order partial differential equations function of the unknowns inplane and antiplane transformations is due to the use of Neohookean hyperelastic initially-stressed potential. In fact, [Horgan 2003a] showed, in their study of the same problem with generalised Neohookean hyperelastic potential (without residual stress), that this conjecture holds for Neohookean material. One can affirm that the precedent result holds if and only if the material is Neohookean.

5.3 Analogy with NeoHookean potential

The objective of this section will be devoted to the simplification of the boundary value problem equations in order to put on spot the analagy of the same studied problem in the case of a standard Neo-Hookean potential. In the remainder of this section, the initial stress field $\boldsymbol{\tau}$ is supposed to be constant. Since the initial stress is auto-equilibrated stress field as it is illustrated through the equation (5.2), and both the Lagrange multiplier, the two planar components of the mapping function y_1 and y_2 and the antiplane displacement u are functions of the planar coordinates, then the equilibrium equation (5.33) is reduced to the following three scalar partial differential equations:

$$S_{i1,1} + S_{i2,2} = 0, \quad i \in \{1, 2, 3\}. \tag{5.39}$$

It is remarkable that only the planar components of the initial stress field are involved in the partial differential equations related to the equilibrium equation as it is illustrated in equation (5.34). That's why we will define the planar restriction of the initial stress field denoted by $\boldsymbol{\tau}_p$ and it can be explicited as:

$$\boldsymbol{\tau}_p = \begin{bmatrix} \tau_{11} & \tau_{12} \\ \tau_{12} & \tau_{22} \end{bmatrix} \tag{5.40}$$

The planar restriction of the initial stress field $\boldsymbol{\tau}_p$ is a symmetric tensor and hence, using the spectral theory, the tensor $\boldsymbol{\tau}_p$ can be expressed in the following spectral form:

$$\boldsymbol{\tau}_p = \tau_1^{(p)} \vec{L}_1^p \otimes \vec{L}_1^p + \tau_2^{(p)} \vec{L}_2^p \otimes \vec{L}_2^p, \tag{5.41}$$

where the basis defined through the principal vectors $(\vec{L}_1^{(p)}, \vec{L}_2^{(p)})$ is an orthonormal one, which is equivalent to:

$$\begin{cases} \vec{L}_1^p \otimes \vec{L}_1^p + \vec{L}_2^p \otimes \vec{L}_2^p = \mathbf{1}^p, \\ \vec{L}_i^p . \vec{L}_j^p = \delta_{ij}, \quad i,j \in \{1,2\}. \end{cases} \tag{5.42}$$

and with $\mathbf{1}^p$ denotes the planar identity tensor. The new orthonormal basis $(\vec{L}_1^p, \vec{L}_2^p, \vec{E}_3)$ can be seen as a rotation of the cartesian one by an angle ϕ in the plane (X_1, X_2) which implies that the eigenvectors of $\boldsymbol{\tau}_p$ can be expressed in the cartesian basis as:

$$\begin{cases} \vec{L}_1^p = \quad \cos(\phi)\vec{E}_1 + \sin(\phi)\vec{E}_2, \\ \vec{L}_2^p = \quad -\sin(\phi)\vec{E}_1 + \cos(\phi)\vec{E}_2, \end{cases} \tag{5.43}$$

Exploiting the expression of the eigenvectors in the cartesian basis illustrated through equation (5.43), the spectral form of the tensor $\boldsymbol{\tau}_p$ in equation (5.41) can be transformed to:

$$\begin{aligned} \boldsymbol{\tau}_p = {} & (\tau_1^{(p)} \cos^2(\phi) + \tau_2^{(p)} \sin^2(\phi))\vec{E}_1 \otimes \vec{E}_1 + (\tau_1^{(p)} \sin^2(\phi) + \tau_2^{(p)} \cos^2(\phi))\vec{E}_2 \otimes \vec{E}_2 \\ & + \frac{\tau_1^{(p)} - \tau_2^{(p)}}{2} \sin(2\phi)(\vec{E}_1 \otimes \vec{E}_2 + \vec{E}_2 \otimes \vec{E}_1) \end{aligned} \tag{5.44}$$

We notice that the expression of $\boldsymbol{\tau}_p$ is a π-periodic function of ϕ. If we can define $(\hat{X}_1, \hat{X}_2)$ as the new planar coordinates associated to the basis $(\vec{L}_1^p, \vec{L}_2^p)$, they can be expressed in function of the cartesian coordinates as:

$$\begin{cases} \hat{X}_1 \quad = cos(\phi)X_1 + \sin(\phi)X_2, \\ \hat{X}_2 \quad = -sin(\phi)X_1 + \cos(\phi)X_2. \end{cases} \tag{5.45}$$

In the same way, the planar and antiplane components of the vectorial mapping function can be obtained in the following way:

$$\begin{cases} \hat{y}_1 &= \vec{y}.\vec{L}_1^p = \cos(\phi)y_1 + \sin(\phi)y_2 \\ \hat{y}_2 &= \vec{y}.\vec{L}_2^p = -\sin(\phi)y_1 + \cos(\phi)y_2 \\ \hat{y}_3 &= y_3 \end{cases} \tag{5.46}$$

The latter transformation has an equivalent form in the polar coordinates which can be described as:

$$\begin{cases} \hat{R} = R \\ \hat{\theta} = \theta - \phi \end{cases} \tag{5.47}$$

where $(\hat{R}, \hat{\theta})$ are the polar coordinates associated to the cartesian coordinates $(\hat{X}_1, \hat{X}_2)$. The components of the first Piola Kirchoff stress tensor in the equilibrium equations can be now simplified in the new principal basis $(\vec{L}_1^p, \vec{L}_2^p, \vec{E}_3)$, so they can be presented as:

$$\begin{cases} \hat{S}_{11} &= \vec{L}_1^p.\boldsymbol{S}.\vec{L}_1^p &= (\mu + \tau_1^{(p)})\hat{y}_{1,\hat{1}} - p\hat{y}_{2,\hat{2}}, \\ \hat{S}_{12} &= \vec{L}_1^p.\boldsymbol{S}.\vec{L}_2^p &= (\mu + \tau_2^{(p)})\hat{y}_{1,\hat{2}} + p\hat{y}_{2,\hat{1}}, \\ \hat{S}_{13} &= \vec{L}_1^p.\boldsymbol{S}.\vec{E}_3 &= \hat{\tau}_{13}\hat{y}_{1,\hat{1}} + \hat{\tau}_{23}\hat{y}_{1,\hat{2}} + p(\hat{y}_{3,\hat{1}}\hat{y}_{2,\hat{2}} - \hat{y}_{3,\hat{2}}\hat{y}_{2,\hat{1}}), \\ \hat{S}_{21} &= \vec{L}_2^p.\boldsymbol{S}.\vec{L}_1^p &= (\mu + \tau_1^{(p)})\hat{y}_{2,\hat{1}} + p\hat{y}_{1,\hat{2}}, \\ \hat{S}_{22} &= \vec{L}_2^p.\boldsymbol{S}.\vec{L}_2^p &= (\mu + \tau_2^{(p)})\hat{y}_{2,\hat{2}} - p\hat{y}_{1,\hat{1}}, \\ \hat{S}_{23} &= \vec{L}_2^p.\boldsymbol{S}.\vec{E}_3 &= \hat{\tau}_{13}\hat{y}_{2,\hat{1}} + \hat{\tau}_{23}\hat{y}_{2,\hat{2}} + p(\hat{y}_{3,\hat{2}}\hat{y}_{1,\hat{1}} - \hat{y}_{3,\hat{1}}\hat{y}_{1,\hat{2}}), \\ \hat{S}_{31} &= \vec{E}_3.\boldsymbol{S}.\vec{L}_1^p &= (\mu + \tau_1^{(p)})\hat{y}_{3,\hat{1}} + \hat{\tau}_{13}, \\ \hat{S}_{32} &= \vec{E}_3.\boldsymbol{S}.\vec{L}_2^p &= (\mu + \tau_2^{(p)})\hat{y}_{3,\hat{2}} + \hat{\tau}_{23}, \\ \hat{S}_{33} &= \vec{E}_3.\boldsymbol{S}.\vec{E}_3 &= \mu + \hat{\tau}_{33} + \hat{\tau}_{13}\hat{y}_{3,\hat{1}} + \hat{\tau}_{23}\hat{y}_{3,\hat{2}} - p. \end{cases} \tag{5.48}$$

with

$$\cdot_{,\hat{i}} = \frac{\partial .}{\partial \hat{X}_i}, \quad i \in \{1, 2\} \tag{5.49}$$

and

$$\begin{cases} \hat{\tau}_{13} &= \cos(\phi)\tau_{13} + \sin(\phi)\tau_{23}, \\ \hat{\tau}_{23} &= -\sin(\phi)\tau_{13} + \cos(\phi)\tau_{23}, \\ \hat{\tau}_{33} &= \tau_{33}, \end{cases} \tag{5.50}$$

whereas the three partial differential equations relative to the equilibrium equation illuminated in equation (5.39) are transformed to:

$$\hat{S}_{i1,\hat{1}} + \hat{S}_{i2,\hat{2}} = 0, \quad i \in \{1,2,3\}. \tag{5.51}$$

Using the expressions of the different components of the First Piola Kirchhoff stress tensor components in the new basis $(\vec{L}_1^{(p)}, \vec{L}_2^{(p)}, \vec{E}_3)$ relative to the coordinate system $(\hat{X}_1, \hat{X}_2, X_3)$ as they are illustrated through equation (5.48), the prior equilibrium equations are transformed into explicit differential equations function of the mapping function components and the initial stress eigenvalues in the following way:

$$\begin{cases} (\mu + \tau_1^{(p)})\hat{y}_{1,\hat{1}\hat{1}} + (\mu + \tau_2^{(p)})\hat{y}_{1,\hat{2}\hat{2}} & = p_{,\hat{1}}\hat{y}_{2,\hat{2}} - p_{,\hat{2}}\hat{y}_{2,\hat{1}} \\ (\mu + \tau_1^{(p)})\hat{y}_{2,\hat{1}\hat{1}} + (\mu + \tau_2^{(p)})\hat{y}_{2,\hat{2}\hat{2}} & = p_{,\hat{2}}\hat{y}_{1,\hat{1}} - p_{,\hat{1}}\hat{y}_{1,\hat{2}}. \\ (\mu + \tau_1^{(p)})\hat{y}_{3,\hat{1}\hat{1}} + (\mu + \tau_2^{(p)})\hat{y}_{3,\hat{2}\hat{2}} & = 0. \end{cases} \tag{5.52}$$

Using the variable changements as it was mentioned in equations (5.45-5.46), the incompressibility condition in equation (5.8) becomes:

$$J = \hat{y}_{1,\hat{1}}\hat{y}_{2,\hat{2}} - \hat{y}_{1,\hat{2}}\hat{y}_{2,\hat{1}} = 1 \tag{5.53}$$

Exploiting the incompressibility condition illustrated through equation (5.53), and the previous partial differential equation related to the equilibrium of plane deformation are transformed to:

$$\hat{y}_{1,\hat{i}}[(\mu + \tau_1^{(p)})\hat{y}_{1,\hat{1}\hat{1}} + (\mu + \tau_2^{(p)})\hat{y}_{1,\hat{2}\hat{2}}] + \hat{y}_{2,\hat{i}}[(\mu + \tau_1^{(p)})\hat{y}_{2,\hat{1}\hat{1}} + (\mu + \tau_2^{(p)})\hat{y}_{2,\hat{2}\hat{2}}] = p_{,\hat{i}}, \quad i \in \{1,2\}. \tag{5.54}$$

Now, using the following transformation:

$$\begin{cases} \tilde{X}_1 = \xi^{-1}\hat{X}_1 \\ \tilde{X}_2 = \xi\hat{X}_2 \\ \tilde{X}_3 = X_3 \end{cases} \tag{5.55}$$

with

$$\begin{cases} \xi = (\dfrac{\mu + \tau_1^{(p)}}{\mu + \tau_2^{(p)}})^{\frac{1}{4}}, \\ \mu_{eq} = \sqrt{(\mu + \tau_1^{(p)})(\mu + \tau_2^{(p)})} \end{cases} \tag{5.56}$$

the equilibrium equation presented in equation (5.52) is equivalent to:

$$\begin{cases} \mu_{eq}[\hat{y}_{1,\hat{i}}\tilde{\Delta}\hat{y}_1 + \hat{y}_{2,\hat{i}}\tilde{\Delta}\hat{y}_2] &= p_{,\hat{i}}, \quad i \in \{1,2\}, \\ \mu_{eq}\tilde{\Delta}\hat{y}_3 &= 0, \end{cases} \tag{5.57}$$

with $\tilde{\Delta}$ denotes the Laplacian operator using the coordinates $(\tilde{X}_1, \tilde{X}_2)$ which is equivalent to:

$$\tilde{\Delta}. = \cdot_{,\tilde{1}\tilde{1}} + \cdot_{,\tilde{2}\tilde{2}}, \tag{5.58}$$

and consequently a similar equilibrium equation is finally obtained as the case of isotropic Neohookean plane-antiplane problem [Arfaoui 2018] with a set of suitable variables changements. This remark does not imply that the material behaviour is isotropic unless the initial stress field is spheric.

Using the polar coordinates $(\tilde{R}, \tilde{\theta})$ associated to the cartesian coordinates $(\tilde{X}_1, \tilde{X}_2)$ and which can be defined mathematically in relation to the previous polar coordinates $(\hat{R}, \hat{\theta})$ as:

$$\begin{cases} \tilde{R} &= \hat{R}g(\theta) \\ cos(\tilde{\theta}) &= (1/\xi)\dfrac{\cos(\hat{\theta})}{g(\theta)} \\ \sin(\tilde{\theta}) &= \xi\dfrac{\sin(\hat{\theta})}{g(\theta)}, \\ g(\theta) &= \sqrt{\xi^2\cos(\hat{\theta})^2 + (1/\xi)^2\sin(\hat{\theta})^2}. \end{cases} \tag{5.59}$$

then equation (5.57-1) related to the equilibrium equation for the plane deformaton can be expressed in terms of the polar coordinates like:

$$\begin{cases} p_{,\tilde{R}} &= \mu_{eq}(\hat{y}_{1,\tilde{R}}\tilde{\Delta}\hat{y}_1 + \hat{y}_{2,\tilde{R}}\tilde{\Delta}\hat{y}_2), \\ p_{,\tilde{\theta}} &= \mu_{eq}(\hat{y}_{1,\tilde{\theta}}\tilde{\Delta}\hat{y}_1 + \hat{y}_{2,\tilde{\theta}}\tilde{\Delta}\hat{y}_2). \end{cases} \tag{5.60}$$

Now, we will focus on the boundary conditions . Using the relation between the azimuthal angles $\hat{\theta}$ and θ through the equation (5.47), the angular crack position becomes characterized by $\hat{\theta} = \pm\pi - \phi$. Therefore the equations related to the local boundary conditions become:

$$cos(\phi)\hat{S}_{i2} + \sin(\phi)\hat{S}_{i1} = 0, \quad i \in \{1,2,3\}, \quad \text{if} \;\; \hat{R} \to 0, \quad \hat{\theta} = \pm\pi - \phi. \tag{5.61}$$

Now, using the expressions of the first Piola Kirchhoff stress tensor components through the system of equations (5.48) and the relation between the coordinates $(\tilde{X}_1, \tilde{X}_2)$ and $(\hat{X}_1, \hat{X}_2)$ illustrated by equation (5.55), then the above equation (5.61) describing the local boundary conditions can be explicitly shown as:

$$\begin{cases} sin(\phi)(\mu + \tau_1^{(p)})\xi\hat{y}_{1,\tilde{1}} + \cos(\phi)\dfrac{\mu + \tau_2^{(p)}}{\xi}\hat{y}_{1,\tilde{2}} = p[\sin(\phi)\xi\hat{y}_{2,\tilde{2}} - \dfrac{\cos(\phi)}{\xi}\hat{y}_{2,\tilde{1}}], & \text{if } \tilde{\theta} = \tilde{\omega}, \tilde{\omega} - 2\pi \\ sin(\phi)(\mu + \tau_1^{(p)})\xi\hat{y}_{2,\tilde{1}} + \cos(\phi)\dfrac{\mu + \tau_2^{(p)}}{\xi}\hat{y}_{2,\tilde{2}} = p[-\sin(\phi)\xi\hat{y}_{1,\tilde{2}} + \dfrac{\cos(\phi)}{\xi}\hat{y}_{1,\tilde{1}}], & \text{if } \tilde{\theta} = \tilde{\omega}, \tilde{\omega} - 2\pi \\ \sin(\phi)(\mu + \tau_1^{(p)})\xi\hat{y}_{3,\tilde{1}} + \cos(\phi)\dfrac{\mu + \tau_2^{(p)}}{\xi}\hat{y}_{3,\tilde{2}} = -\hat{\tau}_{23}, & \text{if } \tilde{\theta} = \tilde{\omega}, \tilde{\omega} - 2\pi \end{cases} \tag{5.62}$$

The incompressibility condition using the polar coordinates $(\tilde{R}, \tilde{\theta})$ is transformed to:

$$J = \frac{1}{\tilde{R}}[\hat{y}_{1,\tilde{R}}\hat{y}_{2,\tilde{\theta}} - \hat{y}_{1,\tilde{\theta}}\hat{y}_{2,\tilde{R}}] = 1 \tag{5.63}$$

The crack faces position can be characterized in the polar coordinates $(\tilde{R}, \tilde{\theta})$ by $\{\tilde{R} \to 0, \quad \tilde{\theta} = \tilde{\omega}, \;\; \tilde{\omega} - 2\pi\}$, where the angle $\tilde{\omega}$ is defined as:

$$\begin{cases} cos(\tilde{\omega}) & = -\frac{\cos(\phi)}{\xi\gamma}, \\ sin(\tilde{\omega}) & = \frac{\xi\sin(\phi)}{\gamma}, \\ \gamma & = \sqrt{\frac{1}{\xi^2}\cos^2(\phi) + \xi^2\sin^2(\phi)}, \end{cases} \tag{5.64}$$

Now if we consider the set of equations (5.45,5.47,5.55,5.64), then we get:

$$\begin{cases} \frac{\partial .}{\partial \tilde{X}_1} = \cos(\tilde{\omega})\frac{\partial .}{\partial \tilde{R}} - \frac{\sin(\tilde{\omega})}{\tilde{R}}\frac{\partial .}{\partial \tilde{\theta}}, & \text{if} \;\; \tilde{\theta} = \tilde{\omega}. \\ \frac{\partial .}{\partial \tilde{X}_2} = \sin(\tilde{\omega})\frac{\partial .}{\partial \tilde{R}} + \frac{\cos(\tilde{\omega})}{\tilde{R}}\frac{\partial .}{\partial \tilde{\theta}}, & \text{if} \;\; \tilde{\theta} = \tilde{\omega}. \end{cases} \tag{5.65}$$

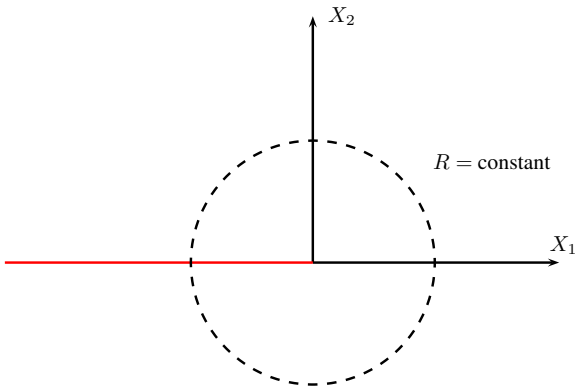

(a) Initial polar coordinates plane

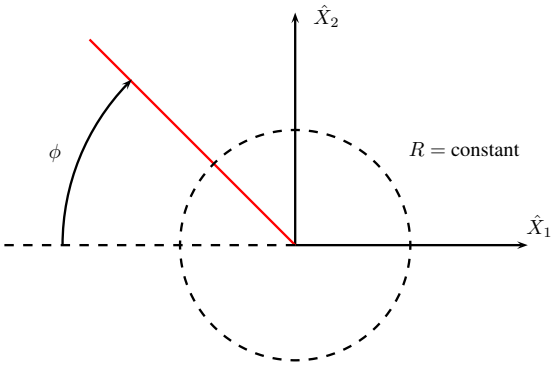

(b) First transformation

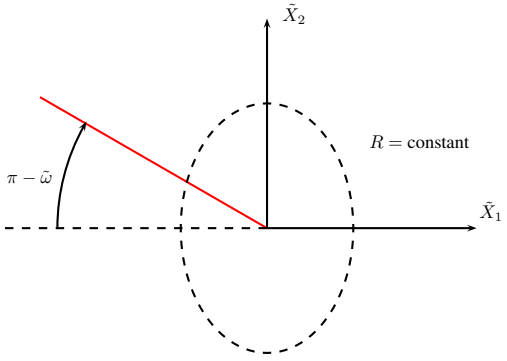

(c) Second transformation if $\xi < 1$

Figure 5.3: Different used transformations

which implies

$$\begin{cases} \xi \sin(\phi)\hat{y}_{i,\tilde{2}} - \frac{\cos(\phi)}{\xi}\hat{y}_{i,\tilde{1}} = \gamma \frac{\partial \hat{y}_i}{\partial \tilde{R}}, & \tilde{\theta} = \tilde{\omega}, \\ \xi \sin(\phi)\hat{y}_{i,\tilde{1}} + \frac{\cos(\phi)}{\xi}\hat{y}_{i,\tilde{2}} = -\frac{\gamma}{\tilde{R}} \frac{\partial \hat{y}_i}{\partial \tilde{\theta}}, & \tilde{\theta} = \tilde{\omega} \end{cases} \tag{5.66}$$

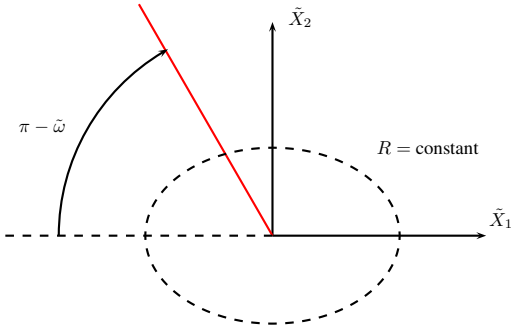

(d) Second transformation if $\xi > 1$

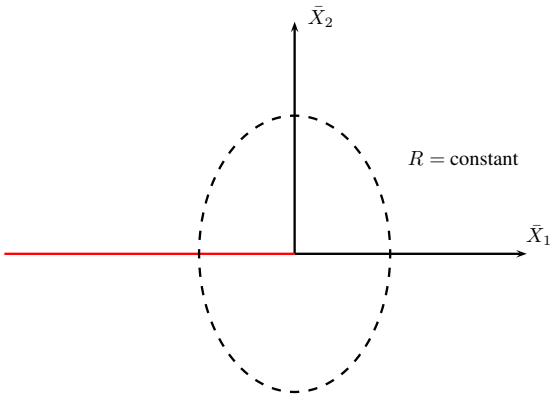

(e) Third transformation if $\xi < 1$

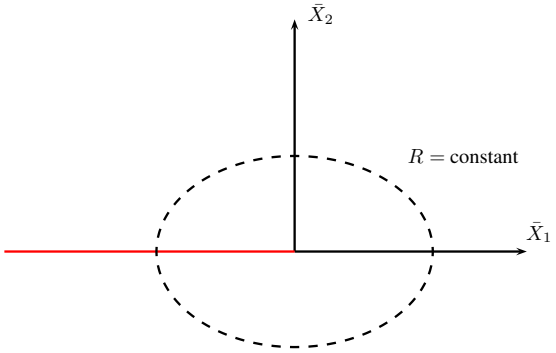

(f) Third transformation if $\xi > 1$

Figure 5.3: Different used transformations

Then the previous equations for the local boundary conditions (5.62) can be put in the polar coordinates $(\tilde{R}, \tilde{\theta})$ as:

$$\begin{cases} p & = \frac{\mu_{eq}}{\tilde{R}^2}[(\frac{\partial \hat{y}_1}{\partial \tilde{\theta}})^2 + (\frac{\partial \hat{y}_2}{\partial \tilde{\theta}})^2], \quad \tilde{R} \to 0, \quad \tilde{\theta} = \tilde{\omega}, \tilde{\omega} - 2\pi \\ 0 & = \frac{\mu_{eq}}{\tilde{R}}[\frac{\partial \hat{y}_1}{\partial \tilde{R}}\frac{\partial \hat{y}_1}{\partial \tilde{\theta}} + \frac{\partial \hat{y}_2}{\partial \tilde{R}}\frac{\partial \hat{y}_2}{\partial \tilde{\theta}}], \quad \tilde{R} \to 0, \tilde{\theta} = \tilde{\omega}, \tilde{\omega} - 2\pi, \\ \frac{\mu_{eq}}{\tilde{R}}\frac{\partial u}{\partial \tilde{\theta}} & = \beta, \quad \tilde{R} \to 0, \tilde{\theta} = \tilde{\omega}, \tilde{\omega} - 2\pi, \end{cases} \tag{5.67}$$

with

$$\beta = \frac{\tau_{23}}{\gamma} \tag{5.68}$$

It is remarkable that the obtained set of equilibrium equations and local boundary conditions are quasi-similar to the ones for a standard Neohookean incompressible material which are studied in (add reference here) considering the same transformation in equation (5.4) and the same local boundary conditions. The only difference between the boundary value problem related to the hyperelastic potential (5.22) and the one of classical incompressible Neohookean material is:

- the crack position for the initially-stressed potential in equation (5.22) is characterized by $\tilde{\theta} = \tilde{\omega},\ \ \tilde{\omega} - 2\pi$, whereas it is characterized by $\theta = \pm\pi$ for the classical studies dealing with the standard incompressible Neohookean potential

- the local boundary condition for the antiplane displacement field is homogenous for the classical NeoHookean potential, whereas it is not for the case of initially-stressed potential

To simplify the asymptotic resolution of the boundary value problem associated with the potential (5.22) and the transformation (5.4), a rotation of the polar coordinates can make the position of local boundary conditions the same for the two boundary values problems. Thus we define the new polar coordinates $(\bar{R}, \bar{\theta})$ as:

$$\begin{cases} \bar{R} = \tilde{R} \\ \bar{\theta} = \tilde{\theta} + \pi - \tilde{\omega} \end{cases} \tag{5.69}$$

The different transformations (or variables changes) enlightened in equations (5.47,5.59,5.69) can be graphically illustrated in figure (5.3). Using equation (5.69), the equilibrium equations expressed in the new set of the polar coordinates become:

$$\begin{cases} p_{,\bar{R}} & = \mu_{eq}(\hat{y}_{1,\bar{R}}\bar{\Delta}\hat{y}_1 + \hat{y}_{2,\bar{R}}\bar{\Delta}\hat{y}_2), \\ p_{,\bar{\theta}} & = \mu_{eq}(\hat{y}_{1,\bar{\theta}}\bar{\Delta}\hat{y}_1 + \hat{y}_{2,\bar{\theta}}\bar{\Delta}\hat{y}_2), \\ \mu_{eq}\bar{\Delta}u & = 0. \end{cases} \tag{5.70}$$

with the laplacian operator denoted by $\bar{\Delta}$ is defined as:

$$\bar{\Delta}. = \frac{\partial^2.}{\partial \bar{R}^2} + \frac{1}{\bar{R}}\frac{\partial.}{\partial \bar{R}} + \frac{1}{\bar{R}^2}\frac{\partial^2}{\partial \bar{\theta}^2} \tag{5.71}$$

whereas for the boundary conditions they can be expressed as:

$$\begin{cases} p & = \frac{\mu_{eq}}{\bar{R}^2}[(\frac{\partial \hat{y}_1}{\partial \theta})^2 + (\frac{\partial \hat{y}_2}{\partial \theta})^2], \quad \bar{R} \to 0, \quad \bar{\theta} = \pm\pi \\ 0 & = \frac{\mu_{eq}}{\bar{R}}[\frac{\partial \hat{y}_1}{\partial \bar{R}}\frac{\partial \hat{y}_1}{\partial \theta} + \frac{\partial \hat{y}_2}{\partial \bar{R}}\frac{\partial \hat{y}_2}{\partial \theta}], \quad \bar{R} \to 0, \bar{\theta} = \pm\pi, \\ \frac{\mu_{eq}}{\bar{R}}\frac{\partial u}{\partial \theta} & = \beta, \quad \bar{R} \to 0, \bar{\theta} = \pm\pi. \end{cases} \tag{5.72}$$

Since the partial differential equation associated to the antiplane displacement field $u(.,.)$ in terms of equilibrium equation and local boundary condition is linear, then the non-homogeneity in the local boundary condition can easily treated by expressing the antiplane solution as:

$$u = u_h + u_p, \tag{5.73}$$

where u_h is the homogenous solution and u_p is the particular one. Both u_p and u_h satisfy the equilibrium equation illustrated through the equation (5.70-3), whereas for the local boundary condition we have:

$$\begin{cases} \frac{\mu_{eq}}{\bar{R}}\frac{\partial u_h}{\partial \theta} & = 0, \quad \bar{R} \to 0, \bar{\theta} = \pm\pi, \\ \frac{\mu_{eq}}{\bar{R}}\frac{\partial u_p}{\partial \theta} & = \beta, \quad \bar{R} \to 0, \bar{\theta} = \pm\pi. \end{cases} \tag{5.74}$$

Finally, exploiting the the proposed transformations above, the plane-antiplane deformation problem within an incompressible initially-stressed hyperelastic material whose the material behaviour is described through the strain energy illustrated by equation (5.22), the differential equations for the equilibrium equations and the local boundary conditions becomes similar to the one of incompressible Neohookean material.

5.4 Asymptotic resolution

5.4.1 Plane deformation

The asymptotic analysis for plane deformations near a crack tip in incompressible isotropic homogeneous materials was studied by Stephensen in [Stephenson 1982] where a generalized Neohookean potential was adopted to characterize the hyperelastic behaviour. Such a

study was generalized in [Mansouri 2016, K. 2016] to the case of a wedge in an incompressible Neohookean bimaterial composite. These works also have permitted to investigate the logarithmic singularities which it has shown to appear only in particular cases. Besides, for a crack problem whose incompressible material behaviour is characterized by Neohookean potential, the logarithmic singularities vanishes as it was shown in [Mansouri 2016]. Hence, based on the works of [Stephenson 1982, Mansouri 2016] the analogy between the boundary value problem related to the transformation (5.4) (in particular the plane deformation when $u = 0$) with the potential of strain energy illustrated in equation (5.22) and the boundary value problem related to the same transformation field with the classical Neohookean potential, the asymptotic expansions of the planar vectorial mapping function components $\hat{y}_1$ and $\hat{y}_2$ become:

$$\hat{y}_k(\bar{R},\bar{\theta}) = \bar{R}^{m_1}\ U_k(\bar{\theta}) + \bar{R}^{m_2}\ V_k(\bar{\theta}) + \bar{R}^{m_3}\ W_k(\bar{\theta}) + \bar{R}^{m_4}\ Z_k(\bar{\theta}) + o(\bar{R}^{m_4}), \quad k \in \{1,2\} \tag{5.75}$$

with

$$\begin{cases} U_k(\bar{\theta}) & = a_k\ \ \sin(\frac{\bar{\theta}}{2}), \quad k \in \{1,2\} \\ V_1(\bar{\theta}) & = \frac{1}{a^2}[a_1\chi_1(\bar{\theta}) - a_2\psi_1(\bar{\theta})], \\ V_2(\bar{\theta}) & = \frac{1}{a^2}[a_2\chi_1(\bar{\theta}) + a_1\psi_1(\bar{\theta})], \\ W_1(\bar{\theta}) & = \frac{1}{a^2}[a_1\chi_2(\bar{\theta}) - a_2\psi_2(\bar{\theta})], \\ W_2(\bar{\theta}) & = \frac{1}{a^2}[a_2\chi_2(\bar{\theta}) + a_1\psi_2(\bar{\theta})], \\ Z_1(\bar{\theta}) & = \frac{1}{a^2}[a_1\chi_3(\bar{\theta}) - a_2\psi_3(\bar{\theta})], \\ Z_2(\bar{\theta}) & = \frac{1}{a^2}[a_2\chi_3(\bar{\theta}) + a_1\psi_3(\bar{\theta})], \\ a^2 & = a_1^2 + a_2^2 \end{cases} \tag{5.76}$$

where the functions $\psi_i, \quad \chi_i, \quad i \in \{1,2,3\}$ can be defined as:

$$\begin{cases} \psi_1(\bar{\theta}) & = b_2 \sin^2(\frac{\bar{\theta}}{2}), \\ \chi_1(\bar{\theta}) & = b_1 \cos(\bar{\theta}), \\ \psi_2(\bar{\theta}) & = c_2 \sin^3(\frac{\bar{\theta}}{2}) + \frac{2b_1b_2}{a^2} \sin(\frac{\bar{\theta}}{2}) - 4\sin^2(\frac{\bar{\theta}}{2})\cos(\frac{\bar{\theta}}{2}) - \frac{4}{3}\cos^2(\frac{\bar{\theta}}{2}), \\ \chi_2(\bar{\theta}) & = c_1 \sin(\frac{3\bar{\theta}}{2}) - \frac{b_2^2}{2a^2}\sin(\frac{\bar{\theta}}{2}), \\ \psi_3(\bar{\theta}) & = d_1 \sin^4(\frac{\bar{\theta}}{2}) + \frac{1}{a^2}(3b_1c_2 - \frac{b_2^3}{a^2} + \frac{8b_1^2b_2}{a^2} + 6b_2c_1)\sin^2(\frac{\bar{\theta}}{2}) \\ & \quad + \frac{b_1^2b_2}{a^4} - \frac{8b_1}{a^2}\cos(\frac{\bar{\theta}}{2})\sin^3(\frac{\bar{\theta}}{2}) - \frac{2b_1}{a^2}\cos^3(\frac{\bar{\theta}}{2})\sin(\frac{\bar{\theta}}{2}), \\ \chi_3(\bar{\theta}) & = \frac{b_2}{a^2}[2\sin(\bar{\theta}) - \sin(2\bar{\theta})] + d_2\cos(2\bar{\theta}) \\ & \quad + \frac{b_2}{a^2}[\frac{2b_1b_2}{a^2} + \frac{3c_2}{4}]\cos(\bar{\theta}) - \frac{b_2}{a^2}[\frac{7}{4}\frac{b_1b_2}{a^2} + \frac{9}{16}c_2] \end{cases}$$

and the power terms exponents are reduced to:

$$m_n = \frac{n}{2}, \quad n \in \{1,2,3,4\}. \tag{5.77}$$

In the other hand, the asymptotic expansion for the Lagrange multiplier p can be presented as in the following form:

$$p(\bar{R},\bar{\theta}) = \bar{R}^{l_1}P_1(\bar{\theta}) + \bar{R}^{l_2}P_2(\bar{\theta}) + o(\bar{R}^{l_2}) \tag{5.78}$$

where the functions P_1 and P_2 are defined as:

$$\begin{cases} P_1(\bar{\theta}) & = -\frac{2\mu_{eq}b_2}{a^2}\cos(\frac{\bar{\theta}}{2}), \\ P_2(\bar{\theta}) & = \frac{2\mu_{eq}}{a^2}[4 - 2 \quad \sin^2(\frac{\bar{\theta}}{2}) - (\frac{3c_2}{2} + \frac{5b_1b_2}{a^2})\sin(\bar{\theta})], \end{cases} \tag{5.79}$$

whereas the radial power terms exponents l_k can be presented as:

$$l_n = \frac{n}{2}, \quad n \in \{1,2\}. \tag{5.80}$$

By inverting the relations in equation (5.46), the components (y_1, y_2) of the deformation function can be expressed as:

$$\begin{cases} y_1 & = \cos(\phi)\hat{y}_1 - \sin(\phi)\hat{y}_2 \\ y_2 & = \sin(\phi)\hat{y}_1 + \cos(\phi)\hat{y}_2 \end{cases} \tag{5.81}$$

and by consequence, the asymptotic expansions for both the components y_1 and y_2 can be easily obtained.

5.4.2 Antiplane deformation

For harmonic problem, as it was discussed in [Grisvard 1992], the asymptotic expansion of the displacement field u will be in the following mathematical form:

$$u(\bar{R},\bar{\theta}) = \sum_{i=1}^{\infty} \bar{R}^{m_i}[U_i^a(\bar{\theta}) + log(\bar{R})V_i^a(\bar{\theta})]. \tag{5.82}$$

Since the partial differential problem associated to the antiplane displacement field $u(.,.)$ is linear, as it was mentioned above the complete solution for the antiplane displacement field can be the sum of an homogeneous and particular solution denoted subsequently as u_h and u_p. A simple solution that could be proposed as a particular solution can be on the form:

$$u_p(\bar{R},\bar{\theta}) = \frac{\beta}{\mu_{eq}}\bar{R}\sin(\bar{\theta}). \tag{5.83}$$

Using the asymptotic form in equation (5.82) and the equilibrium equation (5.70-3), leads to:

$$\begin{cases} m_i^2 V_i^a(\bar{\theta}) + V_i^{a\,''}(\bar{\theta}) = 0, \quad \forall i \in \mathbb{N}^*, \\ m_i^2 U_i^a(\bar{\theta}) + U_i^{a\,''}(\bar{\theta}) = -2m_i V_i^a(\bar{\theta}), \quad \forall i \in \mathbb{N}^*, \end{cases} \tag{5.84}$$

where the indexation "$.'$" stands for the derivation relative to the variable $\bar{\theta}$. Resolving the prior system of differential equations leads to the following solutions:

$$\begin{cases} V_i^a(\bar{\theta}) = A_i\cos(m_i\bar{\theta}) + B_i sin(m_i\bar{\theta}), \quad \forall i \in \mathbb{N}^* \\ U_i^a(\bar{\theta}) = C_i\cos(m_i\bar{\theta}) + D_i sin(m_i\bar{\theta}) - A_i m_i\bar{\theta}\sin(m_i\bar{\theta}) + \frac{B_i m_i\bar{\theta} - A_i}{m_i}\cos(m_i\bar{\theta}), \quad \forall i \in \mathbb{N}^*. \end{cases} \tag{5.85}$$

Now, exploiting the boundary conditions through the equation (5.74-1) and by separating the logarithmic, we get:

$$\begin{cases} V_i^{a\,'}(\bar{\theta} = \pm\pi) = 0, \quad \forall i \in \mathbb{N}^* \\ U_i^{a\,'}(\bar{\theta} = \pm\pi) = 0, \quad \forall i \in \mathbb{N}^*. \end{cases} \tag{5.86}$$

Bearing in mind the explicit form of the functions U_i^a and V_i^a illustrated through the equation (5.85), the boundary conditions illustrated in equation (5.92) are equivalent to:

$$\begin{cases} -m_i A_i \sin(m_i\pi) + m_i B_i \cos(m_i\pi) = 0, \quad \forall i \in \mathbb{N}^* \\ \ \ m_i A_i \sin(m_i\pi) + m_i B_i \cos(m_i\pi) = 0, \quad \forall i \in \mathbb{N}^* \\ -m_i C_i \sin(m_i\pi) - B_i m_i \pi \sin(m_i\pi) + [m_i D_i + B_i]\cos(m_i\pi) - A_i m_i \pi \cos(m_i\pi) = 0, \quad \forall i \in \mathbb{N}^* \\ m_i C_i \sin(m_i\pi) - B_i m_i \pi \sin(m_i\pi) + [m_i D_i + B_i]\cos(m_i\pi) + A_i m_i \pi \cos(m_i\pi) = 0, \quad \forall i \in \mathbb{N}^*. \end{cases} \tag{5.87}$$

Thus a necessary and sufficient condition for the non vanishing of the azimuthal functions V_i^a related to the logarithmic terms is:

$$m_i = \frac{i}{2}, \quad \forall i \in \mathbb{N}^*. \tag{5.88}$$

which leads to:

$$A_{2k+1} = 0, \quad B_{ki} = 0, \quad \forall k \in \mathbb{N}. \tag{5.89}$$

Using the expression of the power terms m_i in the last equation (5.99), then the boundary conditions related to the U_i^a functions leads to:

$$D_{2k} = A_{2k} = 0, \quad C_{2k+1} = B_{2k+1} = 0, \quad \forall k \in \mathbb{N}, \tag{5.90}$$

which implies the vanishing of the functions V_i^a which is in contrast with the hypothesis made in the beginning of the asymptotic resolution. Therefore, the logarithmic terms can not be present in the asymptotic expansion of the antiplane displacement field. Now, by the same way as it was done above, the asymptotic expansion related to the homogenous solution u_h is reduced to:

$$u(\bar{R}, \bar{\theta}) = \sum_{i=1}^{\infty} \bar{R}^{m_i} U_i^a(\bar{\theta}), \tag{5.91}$$

with

$$\begin{cases} U_i^a(\bar{\theta}) = C_i \cos(m_i\bar{\theta}) + D_i \sin(m_i\bar{\theta}), \quad \forall i \in \mathbb{N}^*, \\ m_i = \frac{i}{2}, \quad \forall i \in \mathbb{N}^*. \end{cases} \tag{5.92}$$

Finally, using the linearity of the antiplane problem, the asymptotic expansion for the antiplane displacement field can be presented as:

$$u(\tilde{R},\tilde{\theta}) = \frac{\beta}{\mu_{eq}}\bar{R}\sin(\bar{\theta}) + \sum_{i=0}^{\infty}\bar{R}^{m_{2i+1}}D_{2i+1}\sin(m_{2i+1}\bar{\theta}) + \sum_{i=1}^{\infty}\bar{R}^{m_{2i}}C_{2i}\cos(m_{2i}\bar{\theta}). \tag{5.93}$$

5.5 Discussion of the asymptotic results

The formulation studied above for an incompressible initially-stressed Neohookean is made with an only assumption that the initial stress field is constant. If we suppose that the initial stress tensor is a pressure field which means:

$$\boldsymbol{\tau} = p_0\mathbf{1} \tag{5.94}$$

Then both the first Piola Kirchhoff and the Cauchy stress tensor can be expressed as:

$$\boldsymbol{S} = \mu_{eq}\boldsymbol{F} - p\boldsymbol{F}^{-T}, \quad \boldsymbol{\sigma} = \mu_{eq}\boldsymbol{B} - p\mathbf{1}. \tag{5.95}$$

with

$$\mu_{eq} = \mu + p_0 \tag{5.96}$$

In other words, in the case of a spherical initial stress field, the mechanical behaviour of the initially-stressed hyperelastic material described by the potential in equation (5.22) is equivalent to an incompressible Neohookean hyperelastic material where the shear modulus is replaced by the equivalent modulus μ_{eq}. Since the initial stress field is spheric then the parameters related to it and introduced in the asymptotic expansion becomes: $\xi = 1$ whereas ϕ is undetermined. By consequence the asymptotic expansions, derived above for the coupled plane-antiplane deformations, becomes reduced to the classical ones for a hyperelastic incompressible Neohookean material which was studied in many works [Stephenson 1982, Arfaoui 2018, Mansouri 2016, Grine 2019].

In the remainder of this chapter the initial stress is considered on its general form. Now, if we consider a superimposed rigid rotation to the mapping vectorial function $\vec{y}$, then the

resulted deformation function $\vec{y}^*$ can be expressed as:

$$\vec{y}^* = \boldsymbol{Q}\vec{y} \tag{5.97}$$

where $\boldsymbol{Q}$ is an orthogonal tensor (i.e $\boldsymbol{Q}\boldsymbol{Q}^T = \boldsymbol{Q}^T\boldsymbol{Q} = \mathbf{1}$) and it can be seen as a deformation gradient tensor associated to a rigid rotation. Consequently, the derived deformation gradient tensor associated to $\vec{y}^*$ becomes:

$$\boldsymbol{F}^* = \nabla_{\vec{X}}\vec{y}^* = \boldsymbol{Q}\boldsymbol{F} \tag{5.98}$$

whereas the first Piola-Kirchhoff and the Cauchy stress tensor associated to the two deformations functions $\vec{y}$ and $\vec{y}^*$ can be expressed as:

$$\boldsymbol{S}^* = \boldsymbol{Q}\boldsymbol{S}, \quad \boldsymbol{\sigma}^* = \boldsymbol{Q}\boldsymbol{\sigma}\boldsymbol{Q}^T. \tag{5.99}$$

Considering the local boundary condition related to the traction-free of crack faces and illustrated through equation (5.36), then it is clear that the first Piola Kirchhoff stress tensor $\boldsymbol{S}^*$ associated to the superimposed rigid rotation $\boldsymbol{Q}$, satisfies also the same equilibrium equations and local boundary conditions since:

$$\begin{cases} \mathrm{Div}\boldsymbol{S}^* = \mathrm{Div}(\boldsymbol{Q}\boldsymbol{S}) = \boldsymbol{Q}\mathrm{Div}\boldsymbol{S} = \boldsymbol{Q}.\vec{0} = \vec{0}, \\ \boldsymbol{S}^*.\vec{E}_2 = \boldsymbol{Q}\boldsymbol{S}.\vec{E}_2 = \boldsymbol{Q}.\vec{0} = \vec{0}, \quad \text{if} X_2 = 0, \quad X_1 \to 0^-. \end{cases} \tag{5.100}$$

Thus, if $(\vec{y}, \boldsymbol{\sigma})$ are the solution of the boundary value problem (considering the equilibrium equation and the local boundary conditions) then $(\vec{y}^* = \boldsymbol{Q}\vec{y}, \boldsymbol{\sigma}^* = \boldsymbol{Q}\boldsymbol{\sigma}\boldsymbol{Q}^T)$ are also a solution.

To analyze the complicated form of the asymptotic expansion associated to the deformation components, it is convenient to consider a superimposed rigid rotation to the mapping vectorial function as it was done by Stephensen in [Stephenson 1982] for the isotropic incompressible NeoHookean plane problem. In fact, the rigid rotation $\boldsymbol{Q}$ can be interpreted as a change of the observer to spot on the crack rotation or just a simple modification of the constant parameters to get a simple appropriate solution without any effective rotation. Both interpretations can be exploited here to simplify the analysis of the asymptotic form of the transformation field. In fact, the choice of $\boldsymbol{Q}$ is purely motivated by the idea of having deformation components with different orders and by consequence the crack faces

opening in the deformed configuration can be clearly discussed.

For the boundary value problem treated in this chapter, the considered superimposed rotation will be in the following form:

$$\boldsymbol{Q} = \boldsymbol{Q}_2\boldsymbol{Q}_1 \tag{5.101}$$

with

$$\boldsymbol{Q}_1 = \begin{bmatrix} \frac{a_2}{a} & -\frac{a_1}{a} & 0 \\ \frac{a_1}{a} & \frac{a_1}{a} & 0 \\ 0 & 0 & 1 \end{bmatrix}, \quad \boldsymbol{Q}_2 = \begin{bmatrix} \cos(\phi) & -\sin(\phi) & 0 \\ \sin(\phi) & \cos(\phi) & 0 \\ 0 & 0 & 1 \end{bmatrix}, \tag{5.102}$$

where the coefficients a_1 and a_2 are arbitrary constants and they are involved in the asymptotic form of the plane deformation components illustrated in equation (5.76). It is important to notice that the parameter a cannot vanish because from the beginning of the asymptotic resolution for the plane problem, the works in the literature dealing with such problem (mentioned above) have excluded the vanishing of the first term of the transformation field components. Hence the singularity of the rotation tensor $\boldsymbol{Q}_1$ is avoided. Since $\boldsymbol{Q}_1$ is an orthogonal tensor, it can be associated to a rotation of an angle ψ, which implies:

$$\boldsymbol{Q}_1 = \begin{bmatrix} \cos(\psi) & -\sin(\psi) & 0 \\ \sin(\psi) & \cos(\psi) & 0 \\ 0 & 0 & 1 \end{bmatrix} \tag{5.103}$$

and consequently the relation between the rotation angle ψ and the coefficients (a_1, a_2) as:

$$\sin(\psi) = \frac{a_2}{a}, \quad \cos(\psi) = \frac{a_1}{a} \tag{5.104}$$

Now, exploiting the representation of the rotation tensors $\boldsymbol{Q}_1$ and $\boldsymbol{Q}_2$ in equations (5.99-5.100), then the resulting tensor of rigid rotation $\boldsymbol{Q}$ defined in equation (5.98) can be expressed in the following form:

$$\boldsymbol{Q} = \begin{bmatrix} \cos(\psi+\phi) & -\sin(\psi+\phi) & 0 \\ \sin(\psi+\phi) & \cos(\psi+\phi) & 0 \\ 0 & 0 & 1 \end{bmatrix} \tag{5.105}$$

In the case of unstressed Neohookean material, the crack rotation is induced only by the boundary conditions so far from the crack-tip. Although, in the case of initially-stressed material studied here, the crack rotation is a result of two factors: the so-far boundary conditions and the initial stress field itself. Such influence of the initial stress filed can be divided in two parts:

- an explicit influence through the spectral angle ϕ based on the rotation tensor $\boldsymbol{Q}_2$.
- an implicit influence based on the rotation tensor $\boldsymbol{Q}_1$, since the so-far boundary conditions effect on the crack rotation is related to the strain energy potential which depends itself on the initial stress field $\boldsymbol{\tau}$.

5.5.1 Discussion of the deformation near the crack front

Now, considering the asymptotic expansion of the boundary value problem solution presented in the above sections, the deformation components after the rigid motion described by the tensor $\boldsymbol{Q}$, can be approximated by the following asymptotic expansions:

$$\left\{\begin{array}{ll} y_1^* & = -\frac{1}{a}\bar{R}\psi_1(\bar{\theta}) - \frac{1}{a}\bar{R}^{\frac{3}{2}}\psi_2(\bar{\theta}) + o(R^{\frac{3}{2}}), \\ y_2^* & = a\bar{R}^{\frac{1}{2}}U(\bar{\theta}) + \frac{1}{a}\bar{R}\chi_1(\bar{\theta}) + \frac{1}{a}\bar{R}^{\frac{3}{2}}\chi_2(\bar{\theta}) + o(R^{\frac{3}{2}}), \\ y_3^* & = a_3\bar{R}^{\frac{1}{2}}U(\bar{\theta}) + \bar{R}[b_3\sin(\bar{\theta}) + c_3\cos(\bar{\theta})] + d_3\bar{R}^{\frac{3}{2}}\sin(\frac{3\bar{\theta}}{2}) + o(R^{\frac{3}{2}}). \end{array}\right. \tag{5.106}$$

At the crack faces the components y_1^*, y_2^* and y_3^* are reduced to:

$$\left\{\begin{array}{ll} y_1^*(\bar{R},\bar{\theta}=\pi) & = -\frac{b_2}{a}\bar{R} - \frac{1}{a^2}[c_2a + 2b_1b_2]\bar{R}^{\frac{3}{2}} + o(R^{\frac{3}{2}}), \\ y_2^*(\bar{R},\bar{\theta}=\pi) & = a\bar{R}^{\frac{1}{2}} + o(R^{\frac{1}{2}}), \\ y_3^*(\bar{R},\bar{\theta}=\pi) & = a_3\bar{R}^{\frac{1}{2}} - c_3\bar{R} - d_3\bar{R}^{\frac{3}{2}} + o(R^{\frac{3}{2}}). \end{array}\right. \tag{5.107}$$

$$\left\{\begin{array}{ll} y_1^*(\bar{R},\bar{\theta}=-\pi) & = -\frac{b_2}{a}\bar{R} + \frac{1}{a^2}[c_2a + 2b_1b_2]\bar{R}^{\frac{3}{2}} + o(R^{\frac{3}{2}}), \\ y_2^*(\bar{R},\bar{\theta}=-\pi) & = -a\bar{R}^{\frac{1}{2}} + o(R^{\frac{1}{2}}), \\ y_3^*(\bar{R},\bar{\theta}=-\pi) & = -a_3\bar{R}^{\frac{1}{2}} - c_3\bar{R} + d_3\bar{R}^{\frac{3}{2}} + o(R^{\frac{3}{2}}). \end{array}\right. \tag{5.108}$$

To simplify the analysis of the crack opening shape, we will restrict the analysis in the first place for the plane deformation. Bearing in mind the plane transformation field components at the level of the crack faces described above in equations (5.107-5.108) and

considering the case where $b_2 \neq 0$ we deduce:

$$y_1^*(\bar{R}, \bar{\theta} = \pm\pi) = -\frac{b_2}{a^3}(y_2^*(\bar{R}, \bar{\theta} = \pm\pi))^2 + o((y_2^*(\bar{R}, \bar{\theta} = \pm\pi))^2), \quad \text{with} \begin{cases} y_2^* \geq 0 \text{ if } \theta = \pi \\ y_2^* \leq 0 \text{ if } \theta = -\pi \end{cases} \tag{5.109}$$

This description shows that the crack faces are transformed into two arcs of the same parabola with a vertical tangent at the crack tip. The concavity of the deforemed crack faces is determined by the sign of the unknown constant b_2, where it is convex if $b_2 < 0$ and concave if $b_2 > 0$ as it is illustrated in figure (5.4-a). In case where $b_2 = 0$, we can deduce

$$y_1^*(\bar{R}, \bar{\theta} = \pm\pi) = \pm\frac{c_2}{a^4}(y_2^*(\bar{R}, \bar{\theta} = \pm\pi))^2 + o((y_2^*(\bar{R}, \bar{\theta} = \pm\pi))^2), \quad \text{with} \begin{cases} y_2^* \geq 0 \text{ if } \theta = \pi \\ y_2^* \leq 0 \text{ if } \theta = -\pi \end{cases} \tag{5.110}$$

The mathematical description of the latter approximation, shows that every crack face is transformed to a parabolic arc. Although the deformed crack faces share the same vertical tangent at the crack tip, they have different concavity. Consequently, the crack faces are transformed into a **S-shaped** curve as it is shown in figure (5.4-c). Finally, if we consider $b_2 = c_2 = 0$, the mathematical characterization of the deformed crack faces in the plane of the cross section Ω_0 is reduced to:

$$y_1^*(\bar{R}, \bar{\theta} = \pm\pi) = -\frac{d_1}{a^3}(y_2^*(\bar{R}, \bar{\theta} = \pm\pi))^2 + o((y_2^*(\bar{R}, \bar{\theta} = \pm\pi))^2), \quad \text{with} \begin{cases} y_2^* \geq 0 \text{ if } \theta = \pi \\ y_2^* \leq 0 \text{ if } \theta = -\pi \end{cases} \tag{5.111}$$

In this case, the deformed crack faces have a parabolic-like shape as the case for $b_2 \neq 0$ but with faster growing form and with a vertical tangent at the crack tip as it is illustrated through figure (5.4-b).

Now, in the following the deformed crack shape will be discussed in the case of pure antiplane deformation. In this case, the asymptotic approximation for the components y_3^*

and y_1^* at the level of the crack faces become:

$$\begin{cases} y_1(R,\pi) = -R \\ y_3(R,\pi) = \sum_{i=0}^{\infty} \bar{R}^{m_{2i+1}} D_{2i+1}(-1)^i + \sum_{i=1}^{\infty} \bar{R}^{m_{2i}} C_{2i}(-1)^i \end{cases} \tag{5.112}$$

$$\begin{cases} y_1(R,-\pi) = -R \\ y_3(R,-\pi) = -\sum_{i=0}^{\infty} \bar{R}^{m_{2i+1}} D_{2i+1}(-1)^i + \sum_{i=1}^{\infty} \bar{R}^{m_{2i}} C_{2i}(-1)^i \end{cases} \tag{5.113}$$

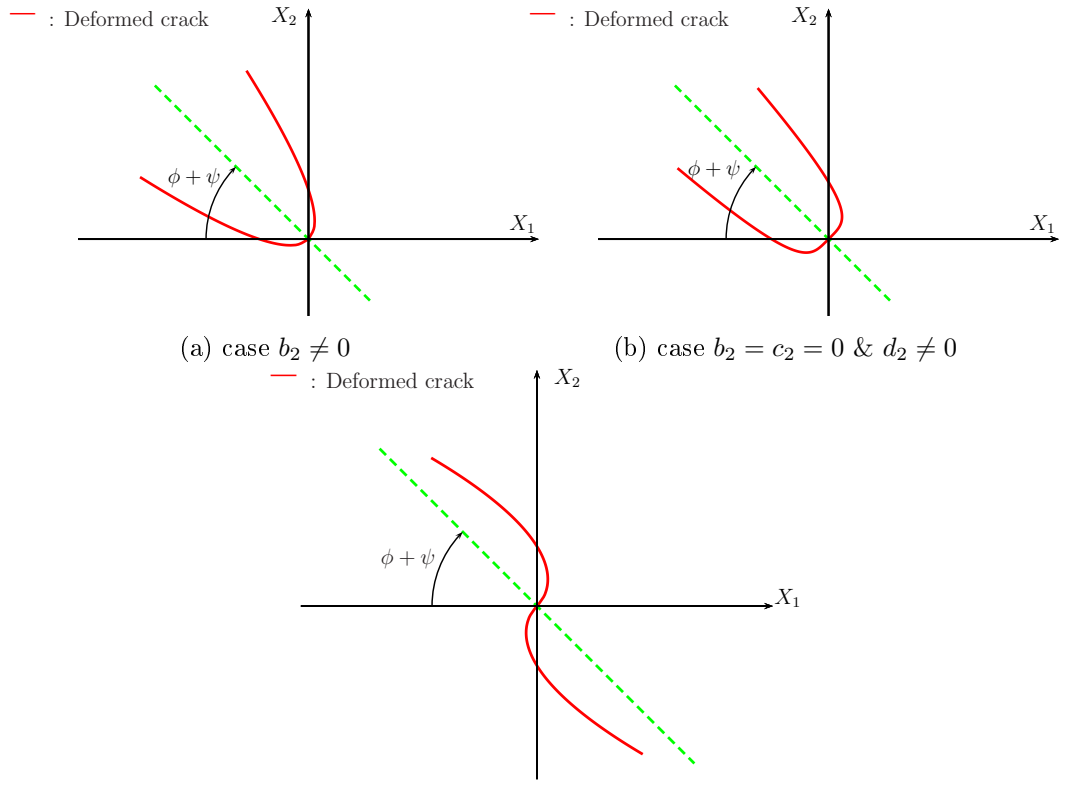

(a) case $b_2 \neq 0$

(b) case $b_2 = c_2 = 0$ & $d_2 \neq 0$

(c) case $b_2 = 0$ & $c_2 \neq 0$

Figure 5.4: Deformed crack shapes in the case of planar deformation

In fact, we can sort the class of the graphical representation of the deformed crack faces into two cases. the first class is if the first non-vanishing order related to the antiplane

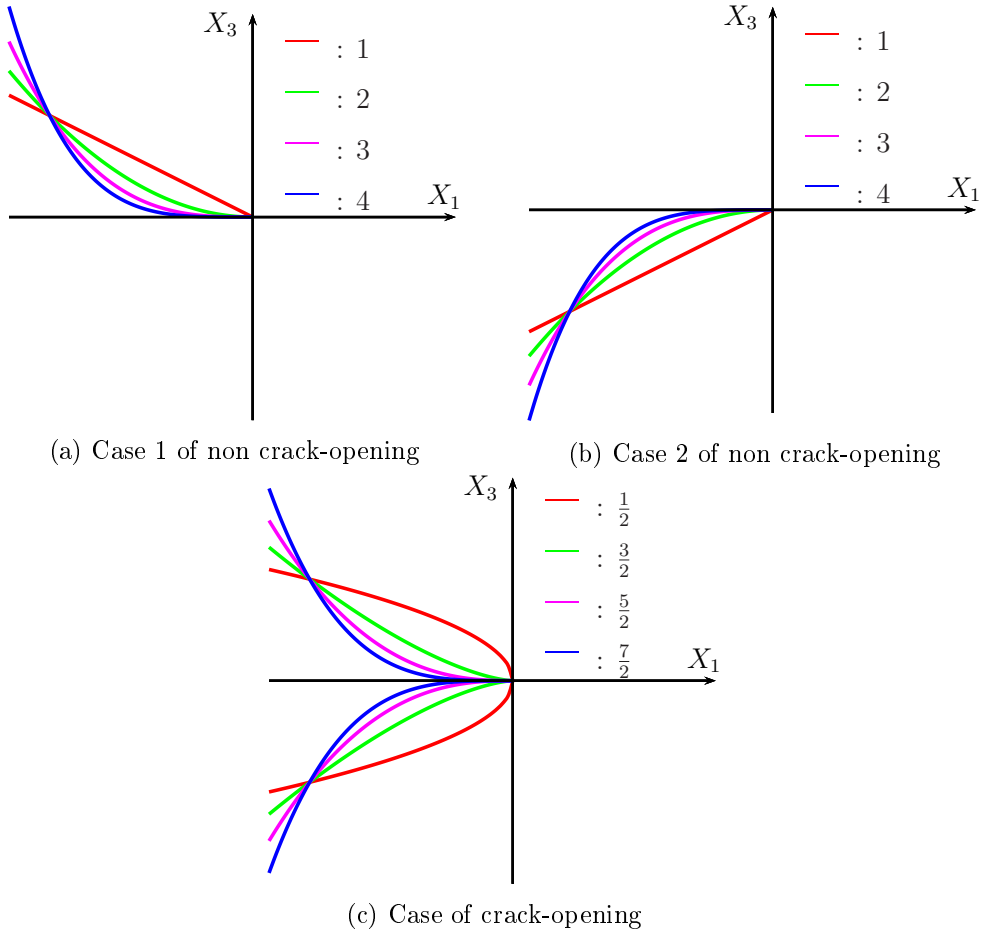

(a) Case 1 of non crack-opening

(b) Case 2 of non crack-opening

(c) Case of crack-opening

Figure 5.5: Deformed crack shapes in the case of antiplane deformation

deformation component is corresponding to the power term m_{2i_0+1} which is equivalent to:

$$\begin{cases} y_1(R,\pm\pi) = -R \\ y_3(R,\pm\pi) = \pm\bar{R}^{m_{2i_0+1}} D_{2i_0+1}(-1)^i + o(\bar{R}^{m_{2i_0+1}}) \end{cases} \tag{5.114}$$

which leads to:

$$y_3(R,\pm\pi) = \pm(-1)^i \gamma^{m_{2i+1}} D_{2i+1}(-y_1(R,\pm\pi))^{m_{2i+1}} + o(\bar{R}^{m_{2i+1}}) \tag{5.115}$$

In this first class two possible situations are possible:

- if $i_0 = 0$ then the geometrical shape of the crack faces is a parabola whose the axis is aligned with X_1-axis, which eludes the opening of the crack in the X_3 direction (see figure (5.5-c)).

- if $i_0 > 0$, then each crack-face is transformed into a different parabolic-arc whose the axis is aligned with the X_3-axis. in such case the crack has the intention to be closed in the vicinity of the crack-tip (see figure (5.5-c)).

The second class of the deformed crack faces is characterized by a first asymptotic term of the antiplane component y_3 related to the power term m_{2i_0} which is equivalent to:

$$\begin{cases} y_1(R, \pm\pi) = -R \\ y_3(R, \pm\pi) = \bar{R}^{m_{2i_0}} C_{2i_0} (-1)^i + o(\bar{R}^{m_{2i_0}}) \end{cases} \tag{5.116}$$

which implies:

$$y_3(R, \pm\pi) = (-1)^i \gamma^{m_{2i_0}} C_{2i_0} (-y_1(R, \pm\pi))^{m_{2i_0}} + o(\bar{R}^{m_{2i_0}}) \tag{5.117}$$

In this case the crack faces are transformed into the same shape which can be a simple straight line (if $i_0 = 1$) or parabolic-like shape (if $i_0 > 1$) as it is illustrated in figures (5.5-a) and (5.5-b).

The transformation studied here and illuminated through equation (5.4), is an antiplane deformation followed by a plane deformation as it was illustrated through equation (5.7). Hence, in the case of couple plane-antiplane deformation, the deformed crack shape can be deduced as a combination of plane deformation of the antiplane deformed shape. We present here some examples for different three-dimensional deformed crack shapes illustrated in the table of figures (5.1).

Table 5.1: Examples of three-dimensional deformed crack shapes.

Planar deformed crack	Antiplanar deformed crack	three-dimensional deformed crack

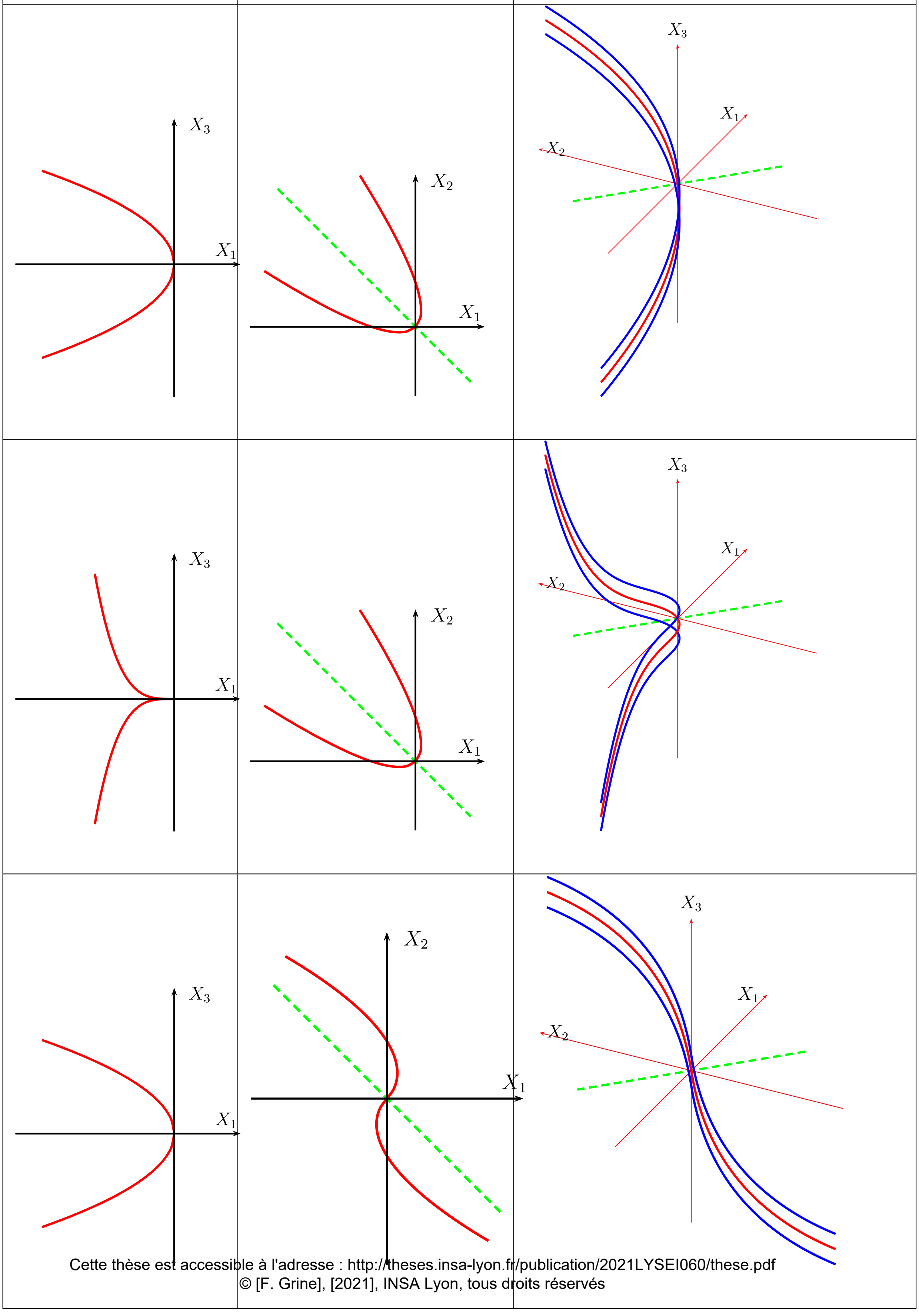

In the objective to simplify the analysis of the asymptotic results, we will rewrite the quantities g and γ (defined above in equations (5.59-4,5.64-3)) as functions parametrized by the coefficients ϕ and ξ and we will define new function f_0 as the following:

$$\begin{cases} g(\xi,\phi;\theta) & = \sqrt{\frac{1}{\xi^2}\cos^2(\theta-\phi)+\xi^2\sin^2(\theta-\phi)}, \\ \gamma(\xi,\phi) & = g(\xi,\phi;\pi), \\ f_0(\xi,\phi;\theta) & = cos(\bar{\theta}). \end{cases} \tag{5.118}$$

Such parametrization of the previous functions will be omitted unless it is necessary. Using the set of equations (5.47,5.59,5.64,5.69), we can derive:

$$sin(\bar{\theta}) = \frac{\sin(\theta)}{g(\theta)\gamma} \tag{5.119}$$

Since $\theta, \bar{\theta} \in [-\pi, \pi]$, exploiting equations (5.118-5.119) we can deduce that the variables θ and $\bar{\theta}$ have the same sign. Thus, with some trigonometric properties we can deduce:

$$\begin{cases} sin(\frac{\bar{\theta}}{2}) & = \sqrt{\frac{1-cos(\bar{\theta})}{2}}sign(\theta), \quad \forall\theta \in]-\pi \;\; \pi[, \\ cos(\frac{\bar{\theta}}{2}) & = \sqrt{\frac{1-cos(\bar{\theta})}{2}}, \quad \forall\theta \in]-\pi \;\; \pi[. \end{cases} \tag{5.120}$$

Now, we can express the azimuthal function related to the first order of the component y_1^* of the deformation field as:

$$f_1(\xi,\phi;\theta) = (\frac{1}{\xi^2}\cos^2(\hat{\theta})+\xi^2\sin^2(\hat{\theta}))^{\frac{1}{4}} \quad \sin(\frac{\bar{\theta}}{2}) = g(\xi,\phi;\theta)^{\frac{1}{2}}\sqrt{\frac{1-f_0(\xi,\phi;\theta)}{2}}sign(\theta) \tag{5.121}$$

Focusing on the functions f_0, g and γ, we can derive the following properties:

- if we interchange the order of the eigenvalues $(\tau_1^{(p)}, \tau_2^{(p)})$ as it is illustrated in figure (5.6), we derive the following mathematical property:

$$\begin{cases} g(\xi,\phi;\theta) & = g(\frac{1}{\xi},\phi+\frac{\pi}{2};\theta), \\ f_0(\xi,\phi;\theta) & = f_0(\frac{1}{\xi},\phi+\frac{\pi}{2};\theta), \\ \gamma(\xi,\phi) & = \gamma(\frac{1}{\xi},\phi+\frac{\pi}{2}). \end{cases} \tag{5.122}$$

- if we made a π-rotation around the X_1-axis (crack direction), as it is enlightened in

figure (5.7), it implies:

$$\begin{cases} g(\xi, \frac{\pi}{4}; \theta) & = g(\frac{1}{\xi}, \frac{\pi}{4}; -\theta), \\ \gamma(\xi, \frac{\pi}{4}) & = \gamma(\frac{1}{\xi}, \frac{\pi}{4}), \\ f_0(\xi, \frac{\pi}{4}; \theta) & = f_0(\frac{1}{\xi}, \frac{\pi}{4}; -\theta). \end{cases} \tag{5.123}$$

Exploiting the prior mathematical properties, the first azimuthal function of the component y_1^* satisfies:

$$f_1(\xi, \phi; \theta) = f_1(\frac{1}{\xi}, \phi + \frac{\pi}{2}; \theta) \tag{5.124}$$

In the case where $\phi = 0$, the vertical deformation to the crack plane y_2^* (respectively the aligned deformation to the crack faces y_1^*) is impair (respectively is pair), and hence the first order of the deformation field represent a deformation solution of the mode-I type. Focusing on the figure (5.8-a) and bearing in mind the property presented through equation (5.122), in case where one of the eigenvector of the planar initial stress field $\boldsymbol{\tau}_p$ is aligned with crack direction (i.e $\phi = \dfrac{k\pi}{2}, \ \ k \in \mathbb{Z}$), the vertical transformation to the crack plane y_2^* reaches its maximum at the level of the crack faces if the eigenvalue associated to eigenvector orthogonal to the crack faces is greater than the other one (i.e $\xi < 1$ if $\phi = 0$). In other words, in this case, the crack opening is maximum of the vertical displacement near the crack tip. But, in the contrary case where the maximum of the eigenvalues is related to the eigenvector is parallel to the crack faces direction, the maximum of vertical deformation to the crack plane is not reached an azimuthal direction different to the crack faces, and which depends on the initial stress field $\boldsymbol{\tau}_p$ through the parameters ξ and ϕ as it is illustrated in the set of figures (5.8).

To simplify the previous assertainment, let us suppose that the crack is only subjected to an initial stress field orthogonal to the crack faces ($\phi = 0, \tau_1^{(p)} = 0, \tau_2^{(p)} \neq 0$). If the initial stress field is of tensile nature ($\tau_2^{(p)} > 0 \rightarrow \xi < 1$) (respectively compressive nature ($\tau_<^{(p)} 0 \ \rightarrow \ \xi \ > \ 1$)) then the crack opening increases (respectively decreases) compared to the unstressed case ($\xi = 1$) as it is illustrated in figures (5.8-a,5.9-a). Such a result is coherent with what is usually "believed" in the literature about the influence of the residual stress nature on crack problems. When the residual stress is of compressive nature, it participates in the closing of the crack or at least limits the influence of the so-far loading in the crack opening which brakes the crack propagation. Although, if the

residual stress is of tensile nature, it participates in the increasing of the crack opening and hence it promotes the crack propagation.

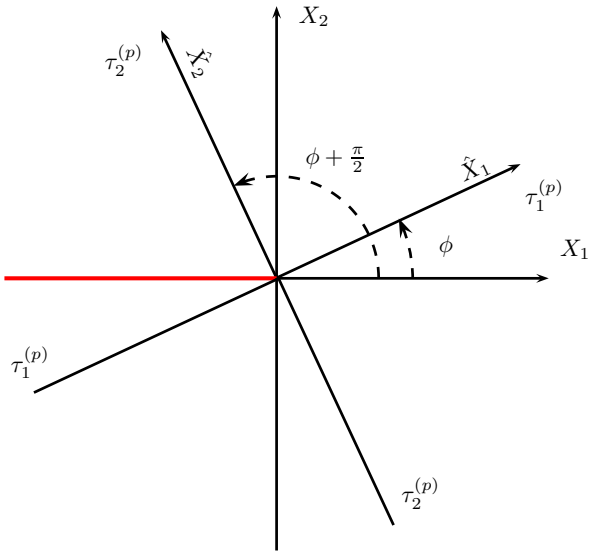

Figure 5.6: Graphical representation of equation (5.122)

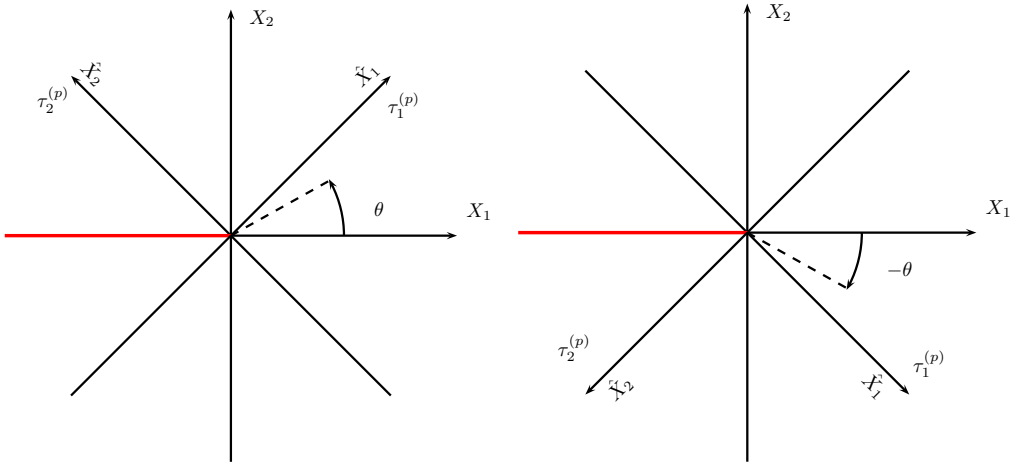

Figure 5.7: Graphical interpretation of equation (5.123): If the cross section in the left figure is subjected to a rotation around the X_1-axis by an angle π it turns to the one represented in the right figure.

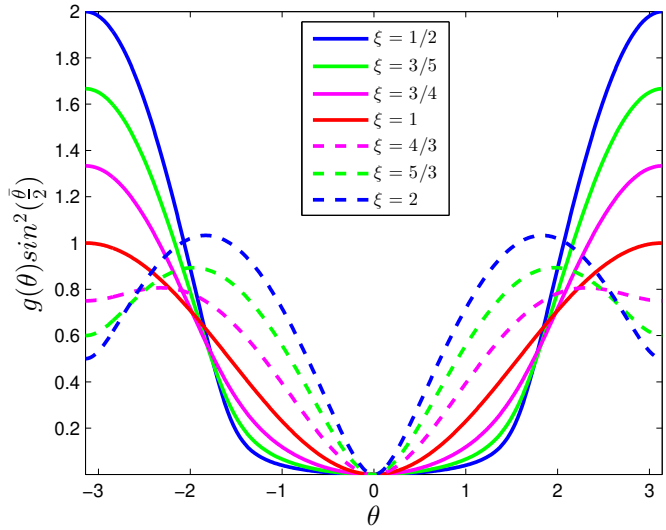

(a) $\phi = 0$

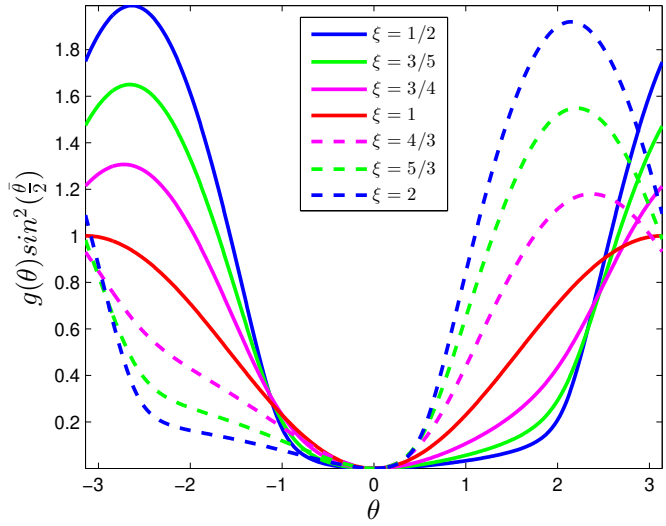

(b) $\phi = \frac{\pi}{6}$

Figure 5.8: $g(\theta)\sin^2(\frac{\theta}{2})$: the first asymptotic term of y_1^* function of the azimuthal variable θ

It is remarkable that when the eigenvectors of the initial stress field $\boldsymbol{\tau}_p$ is not aligned with the crack faces, the vertical and the horizontal deformations reaches its maximum

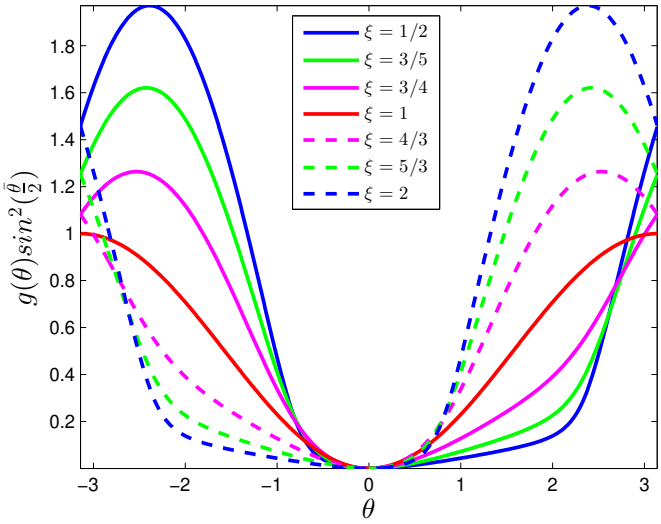

(c) $\phi = \frac{\pi}{4}$

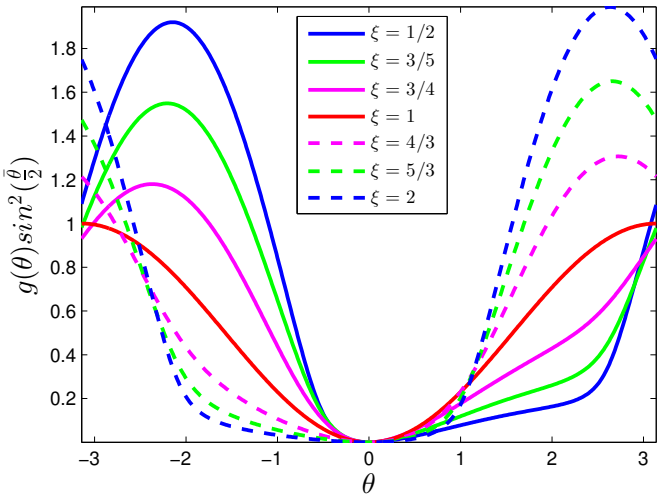

(d) $\phi = \frac{\pi}{3}$

Figure 5.8: $g(\theta)\sin^2(\frac{\bar{\theta}}{2})$: the first asymptotic term of y_1^* function of the azimuthal variable θ

in absolute value in one direction near the crack tip different of those of the crack faces as it is illustrated in figures (5.8-5.9). Focusing on the figures (5.8-5.9), it seems that the initial stress field creates a sort of perturbation of the deformation field relatively to the

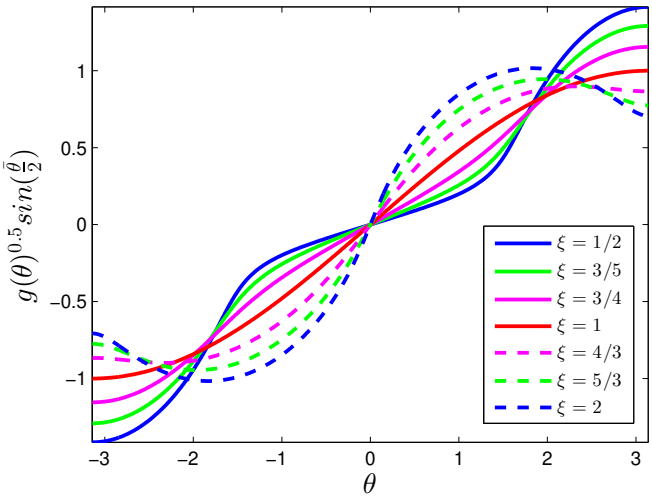

(a) $\phi = 0$

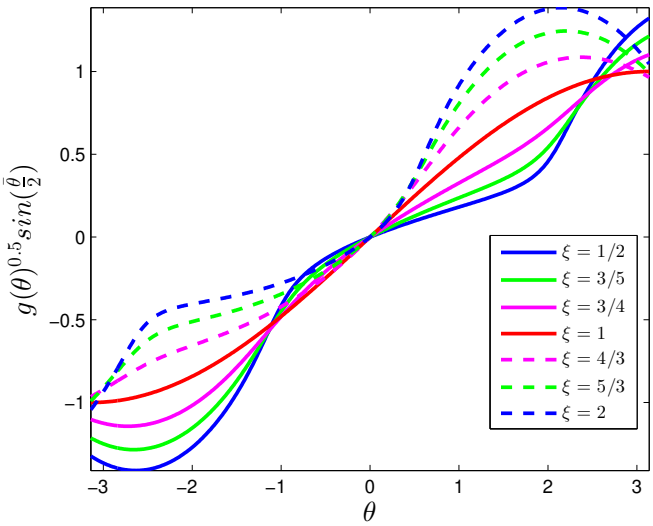

(b) $\phi = \frac{\pi}{6}$

Figure 5.9: $g(\theta)^{\frac{1}{2}} \sin(\frac{\bar{\theta}}{2})$: the first asymptotic term of y_2^* function of the azimuthal variable θ

deformation field of the unstressed materials: if the initial stress increases the level of the deformation field in one region it decreases it in another one.

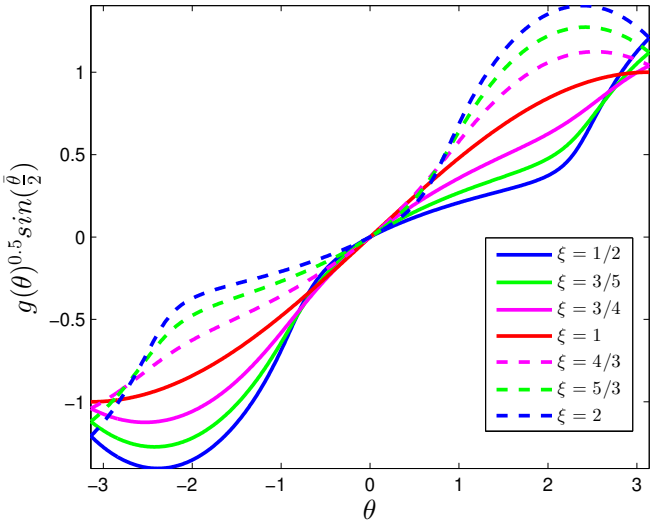

(c) $\phi = \frac{\pi}{4}$

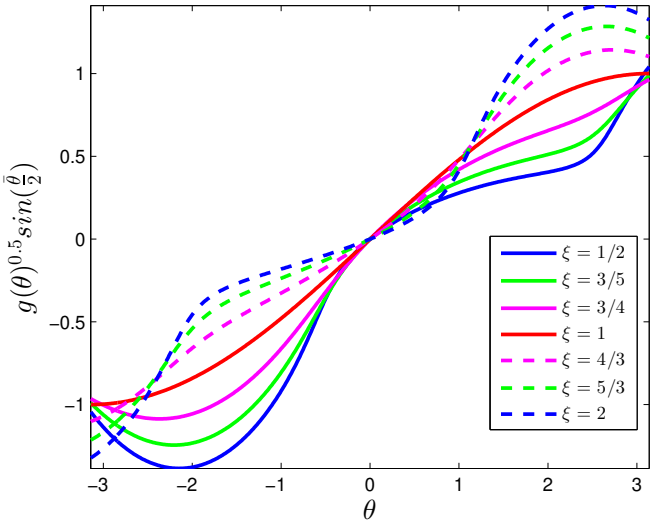

(d) $\phi = \frac{\pi}{3}$

Figure 5.9: $g(\theta)^{\frac{1}{2}} \sin(\frac{\bar{\theta}}{2})$: the first asymptotic term of y_2^* function of the azimuthal variable θ

If ($\phi \neq \frac{k\pi}{2}, \quad k \in \mathbb{Z}$), in another words if the eigenvectors of the initial stress field $\boldsymbol{\tau}_p$ is not aligned with the crack direction, then if one eigenvalue $\tau_i^{(p)}$ becomes of com-

pressie nature and it increases in amplitude then the deformation field of the non-cracked half plane normal to the corresponding eigenvector $\vec{L}_j^p$ $(j \neq i)$ decreases in amplitude. In such case this half plane looks like it is pinned (see appendix E).

If $\phi = 0$, then if $\xi \to \infty$, the orthogonal eigenvalue decreases to be of compressive nature, the half plane normal to the other eigenvector becomes like a pinned one (see appendix E). Whereas, if $\xi \to 0$, the crack opening becomes weaker and weaker compared to the deformation in the rest of the cross section, which looks like a buckling effect (see appendix E).

5.5.2 Discussion of the stress field near the crack front

Now, exploiting the asymptotic approximation of the deformation field subjected to the rigid rotation as it is illustrated in equations (5.101-5.102), and bearing in mind the explicit form of the first Piola Kirchhoff stress in (5.32) and the relation between it and the Cauchy stress field in equation (5.25) , then the different Cauchy stress components $\hat{\sigma}_{ij}$ which can be presented as:

$$\begin{cases} \hat{\sigma}_{11} &= \mu_{eq}[(\hat{y}_{1,\tilde{1}})^2 + (\hat{y}_{1,\tilde{2}})^2] - p, \\ \hat{\sigma}_{12} &= \mu_{eq}[\hat{y}_{1,\tilde{1}}\hat{y}_{2,\tilde{1}} + \hat{y}_{1,\tilde{2}}\hat{y}_{2,\tilde{2}}], \\ \hat{\sigma}_{22} &= \mu_{eq}[(\hat{y}_{2,\tilde{1}})^2 + (\hat{y}_{2,\tilde{2}})^2] - p, \\ \hat{\sigma}_{13} &= \mu_{eq}[\hat{y}_{1,\tilde{1}}\hat{y}_{3,\tilde{1}} + \hat{y}_{1,\tilde{2}}\hat{y}_{3,\tilde{2}}] + p[\hat{y}_{3,\tilde{1}}\hat{y}_{2,\tilde{2}} - \hat{y}_{3,\tilde{2}}\hat{y}_{2,\tilde{1}}] + \frac{\hat{\tau}_{13}}{\xi}\hat{y}_{1,\tilde{1}} + \hat{\tau}_{23}\xi\hat{y}_{1,\tilde{2}}, \\ \hat{\sigma}_{23} &= \mu_{eq}[\hat{y}_{2,\tilde{1}}\hat{y}_{3,\tilde{1}} + \hat{y}_{2,\tilde{2}}\hat{y}_{3,\tilde{2}}] + p[\hat{y}_{3,\tilde{2}}\hat{y}_{1,\tilde{1}} - \hat{y}_{3,\tilde{1}}\hat{y}_{1,\tilde{2}}] + \frac{\hat{\tau}_{13}}{\xi}\hat{y}_{2,\tilde{1}} + \hat{\tau}_{23}\xi\hat{y}_{2,\tilde{2}}, \\ \hat{\sigma}_{33} &= \mu_{eq}[(\hat{y}_{3,\tilde{1}})^2 + (\hat{y}_{3,\tilde{2}})^2] + 2\frac{\hat{\tau}_{13}}{\xi}\hat{y}_{3,\tilde{1}} + 2\hat{\tau}_{23}\xi\hat{y}_{3,\tilde{2}} + \mu + \hat{\tau}_{33} - p. \end{cases} \tag{5.125}$$

implies the following asymptotic expansions for the Cauchy stress $\boldsymbol{\sigma}^*$ components in the rotated basis used for the analysis:

$$\left\{\begin{array}{ll}
\sigma^*_{11} &= \frac{\mu_{eq}b_2^2}{a^2}\sin^2(\frac{\bar\theta}{2}) + o(1), \quad \forall\bar\theta \neq 0,\\
\sigma^*_{11} &= \frac{\mu_{eq}b_2}{6a}\bar R^{\frac12} + o(\bar R^{\frac12}), \quad \text{if} \;\; \bar\theta = 0,\\
\sigma^*_{22} &= \frac{\mu_{eq}a^2}{4}\bar R^{-1} - \mu_{eq}b_1\bar R^{-\frac12}\sin(\frac{\bar\theta}{2}) + o(\bar R^{-\frac12}),\\
\sigma^*_{12} &= -\frac{\mu_{eq}b_2}{2}\bar R^{-\frac12}\sin(\frac{\bar\theta}{2}) + o(\bar R^{-\frac12}), \quad \forall\bar\theta \neq 0,\\
\sigma^*_{12} &= -\frac{\mu_{eq}b_1b_2}{2a^2} + o(1), \quad \text{if} \;\; \bar\theta = 0,\\
\sigma^*_{13} &= -\frac{\mu_{eq}b_2a_3}{2a}\bar R^{-\frac12}\sin(\frac{\bar\theta}{2}) + o(\bar R^{-\frac12}), \quad \forall\bar\theta \neq 0,\\
\sigma^*_{13} &= -\frac{\mu_{eq}b_2}{2a^3}(2a^3c_3 - 2ab_1 + b_1) + o(1), \quad \text{if} \;\; \bar\theta = 0,\\
\sigma^*_{23} &= \frac{\mu_{eq}a_3}{4}\bar R^{-1} + \bar R^{-\frac12}[\alpha^{(23)}_{11}\cos(\frac{\bar\theta}{2}) + \alpha^{(23)}_{12}\sin(\frac{\bar\theta}{2})] + \alpha^{(23)}_{21}\cos^2(\frac{\bar\theta}{2}) + \alpha^{(23)}_{22} + o(1),\\
\sigma^*_{33} &= \frac{\mu_{eq}a_3^2}{4}\bar R^{-1} + \bar R^{-\frac12}[\alpha^{(33)}_{11}\cos(\frac{\bar\theta}{2}) + \alpha^{(33)}_{12}\sin(\frac{\bar\theta}{2})] + \alpha^{(33)}_{21}\cos^2(\frac{\bar\theta}{2}) + \alpha^{(33)}_{22} + o(1).
\end{array}\right. \tag{5.126}$$

with

$$\left\{\begin{array}{ll}
\alpha^{(23)}_{11} &= \frac{a}{2}(\mu_{eq}b_3 + \hat\tau_{23}\xi)\\
\alpha^{(23)}_{12} &= -\frac{1}{2a\xi}[\mu_{eq}\xi(a^2c_3 + a_3b_1) + \hat\tau_{13}a^2]\\
\alpha^{(23)}_{21} &= \frac{\mu_{eq}}{4a^3}[6a^4 + 6a^2a_3c_1 + a_3b_2^2]\\
\alpha^{(23)}_{22} &= -\frac{1}{8a^3\xi}[-\mu_{eq}\xi(6a^4 + 2a^2(3a_3c_1 - 4b_1c_3) + 3a_3b_2^2) + 8a^2b_1\hat\tau_{13}]\\
\alpha^{(33)}_{11} &= a_3(\mu_{eq}b_3 + \xi\hat\tau_{23})\\
\alpha^{(33)}_{12} &= -\frac{a_3}{\xi}(\mu_{eq}c_3\xi + \hat\tau_{13})\\
\alpha^{(33)}_{21} &= 3\mu_{eq}a_3\\
\alpha^{(33)}_{22} &= \frac{1}{4\xi}[8\hat\tau_{23}\xi^2b_3 + (4b_3^2 + 4c_3^2 - 6a_3 + 4)\mu_{eq}\xi + 4\hat\tau_{33}\xi + 8\hat\tau_{13}c_3].
\end{array}\right. \tag{5.127}$$

Discussing merely the form of the stress Cauchy components shows, that unlike the case of linear elasticity [Seweryn 1996], they have different radial and azimuthal terms. Also the singular orders depend on the azimuthal direction (see the example of the components σ^*_{11}, σ^*_{12} and σ^*_{13}). In the case of plane deformations, the component σ^*_{22} is most singular component, which means the material element near the crack tip is essentially subjected to a uniaxial traction loading in the first order in the direction of X^*_2-axis. Hence such a fact permits the planar opening of the crack regardless of the amplitude or the nature of the boundary conditions so at infinity (so far from the crack tip). As in the case of the deformations components, the initial stress field creates a sort of perturbation around the unstressed solution for the azimuthal function associated with the different

Cauchy stress components (see figures (5.10-12)). For plane deformations, in the case of unstressed Neohookean material, only the shear and normal components σ^*_{12} and σ^*_{22} are singular. Whereas in the case of an initially-stressed material, we have the antiplane shear component σ^*_{23} as an extra singular term due to the coupling generated due to the antiplane initial stress shear components τ_{13} and τ_{23}.

In the case of pure antiplane deformation, the antiplane axial stress components σ^*_{33} dominates and the most singular radial term is R^{-1}. In other terms, the material element near the crack tip under an antiplane deformation is subjected to an out-of-plane tensile loading. Only σ^*_{32} and σ^*_{33} are the singular stress components related to the antiplane deformation. If we focus on the coupled plane-antiplane deformations, only the stress components σ^*_{22} , σ^*_{32} and σ^*_{33} dominate through the singular radial term R^{-1}. This implies that the material element in the vicinity of the crack tip is subjected to a triaxial loading of bi-axial tensile coupled to a plane shear. The triaxial deformation leads to the singular behaviour for all the shear stress components.

When one of the eigenvectors of the initial stress field $\boldsymbol{\tau}_p$ is aligned with crack faces, the most singular term of the plane shear is impair function of the azimuthal planar coordinate. If $\xi \geq 1$, then the maximum of planar shear component of the stress field is reached at the crack faces, whereas in the opposite case, the maximum is reached in azimuthal direction different of those of the crack faces and depends on both the parameters ξ and ϕ as it is illustrated in figure (5.15-a). In addition, if $\phi \neq \dfrac{k\pi}{2}, \quad k \in \mathbb{Z}$, the singular term associated to the Cauchy stress component σ^*_{12} is reached in position different of those of the crack faces and it depends on the spectral parameters (ξ, ϕ) as it is enlightened in figures (5.11-b-c-d).

5.5.3 Discussion of the strain energy near the crack front

Considering the strain energy expression as it is illustrated in equation (5.22) and taking into account the asymptotic expansion of the displacement field illuminated through equations (5.75-5.77), then the asymptotic expansion of the strain energy becomes:

$$W = \frac{\mu_{eq}}{2}(a^2 + a_3^2)\bar{R}^{-1} + o(R^{-1}). \tag{5.128}$$

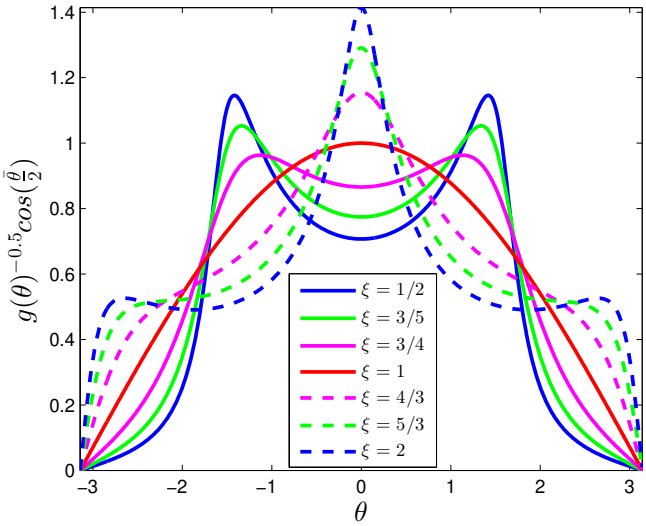

(a) $\phi = 0$

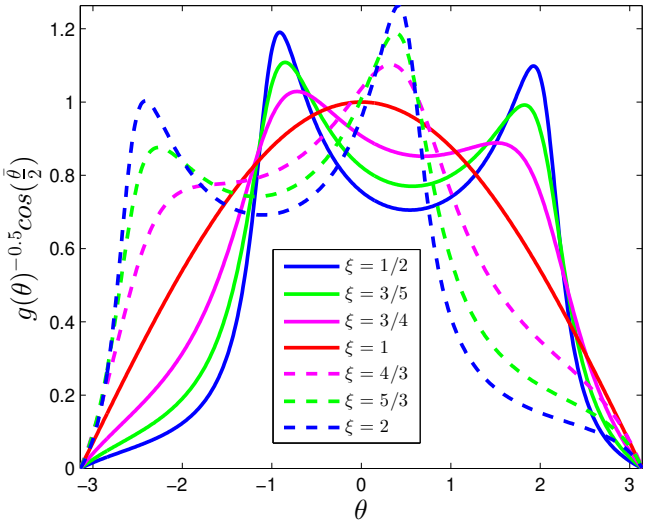

(b) $\phi = \frac{\pi}{6}$

Figure 5.10: $g(\theta)^{-\frac{1}{2}}\cos(\frac{\bar{\theta}}{2})$: the first asymptotic term of σ^*_{23} (in the case of pure plane deformation and $\hat{\tau}_{23} \neq 0$) function of the azimuthal variable θ

Considering the function $g(.,.;.)$, it is remarkable that the strain energy is maximal (respectively minimal) in the direction relative to the eigenvector related to the maximal (re-

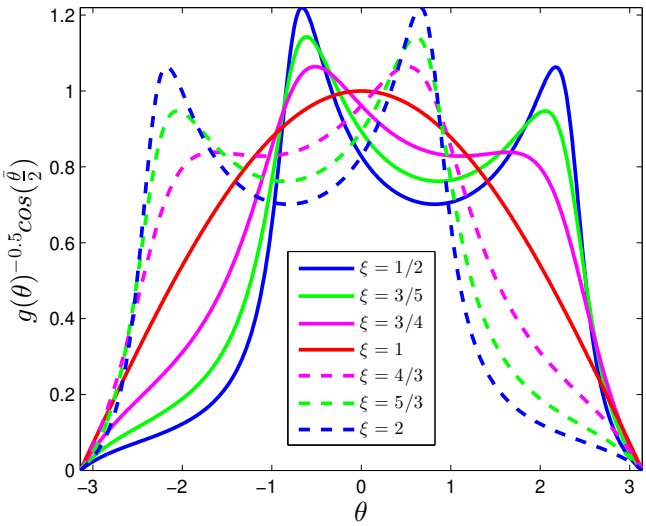

(c) $\phi = \frac{\pi}{4}$

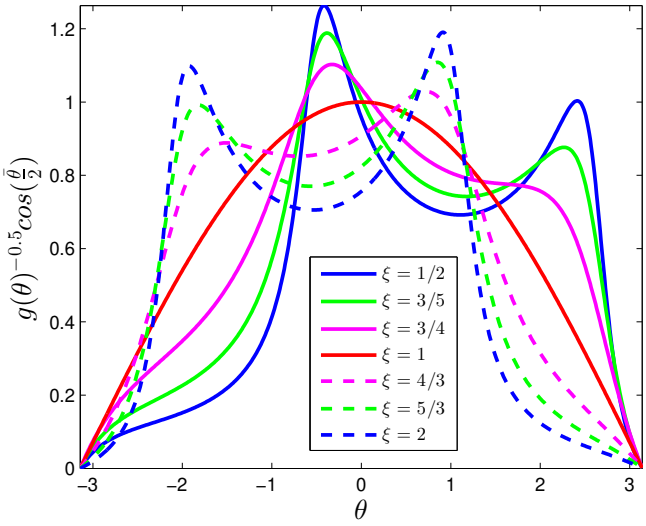

(d) $\phi = \frac{\pi}{3}$

Figure 5.10: $g(\theta)^{-\frac{1}{2}}\cos(\frac{\bar{\theta}}{2})$: the first asymptotic term of σ^*_{23} (in the case of pure plane deformation and $\hat{\tau}_{23} \neq 0$) function of the azimuthal variable θ

spectively the minimal) eigenvalues of the planar initial stress field $\boldsymbol{\tau}_p$ as it is highlighted in figure (5.12). Since the strain energy density is involved in the J-integral calculation

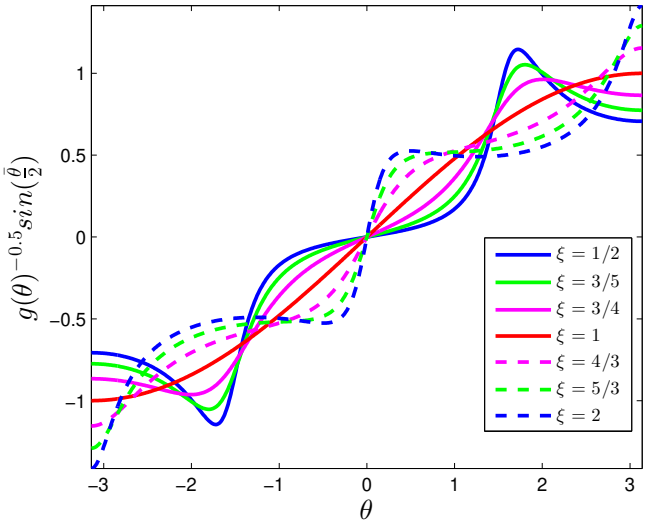

(a) $\phi = 0$

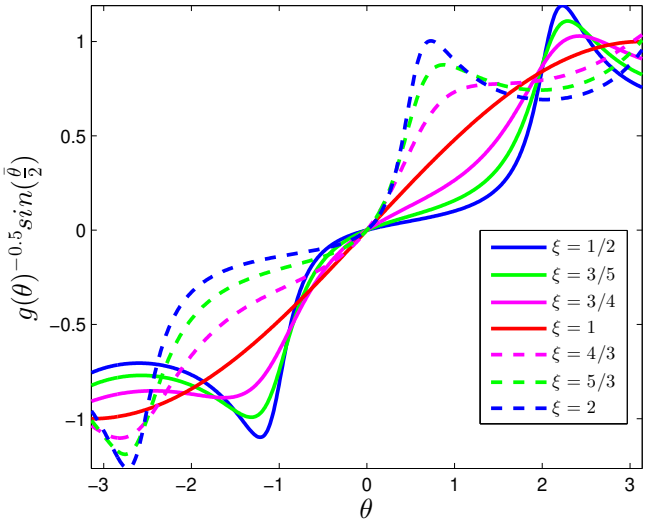

(b) $\phi = \frac{\pi}{6}$

Figure 5.11: $g(\theta)^{-\frac{1}{2}}\sin(\frac{\bar{\theta}}{2})$: the first asymptotic term of σ^*_{23} (in the case of pure plane deformation and $\hat{\tau}_{13} \neq 0$) function of the azimuthal variable θ

and by consequence it influences the propagation and initiation of cracks.

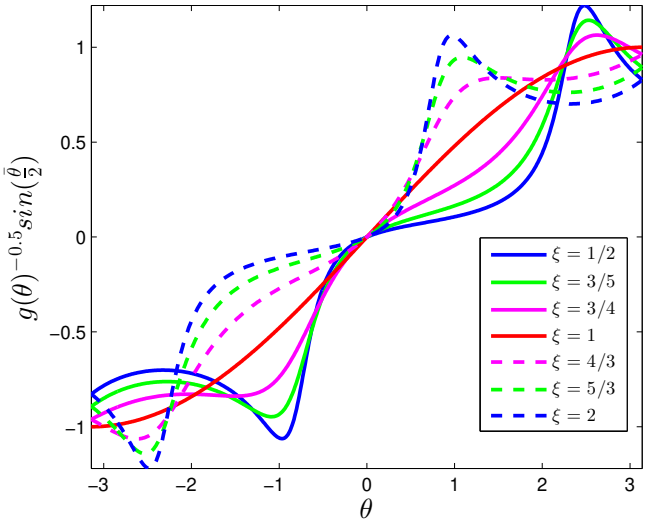

(c) $\phi = \frac{\pi}{4}$

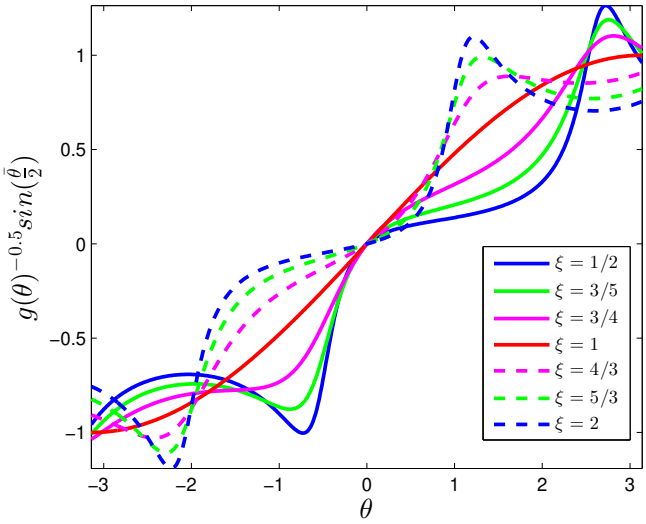

(d) $\phi = \frac{\pi}{3}$

Figure 5.11: $g(\theta)^{-\frac{1}{2}}\sin(\frac{\bar{\theta}}{2})$: the first asymptotic term of σ^*_{23} (in the case of pure plane deformation and $\hat{\tau}_{13} \neq 0$) function of the azimuthal variable θ

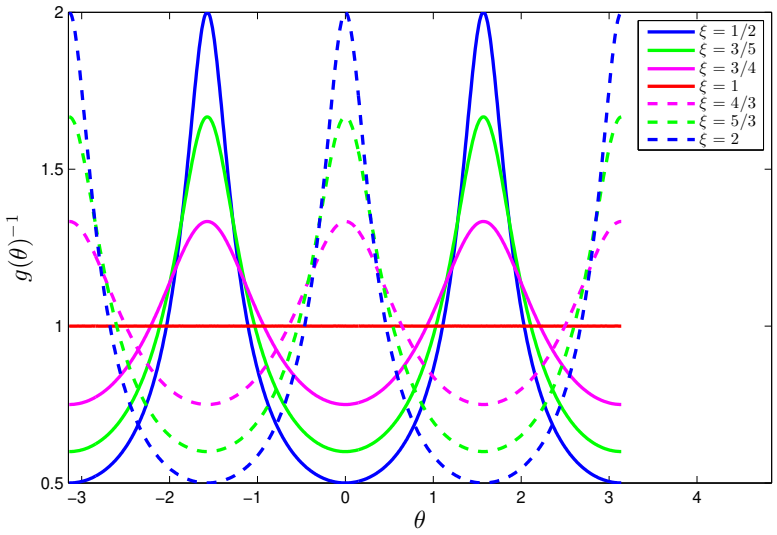

Figure 5.12: $g(\theta)^{-1}$, $\phi = 0$: the first asymptotic term of the Cauchy stress components σ^*_{22}, σ^*_{23}, σ^*_{33} and the strain energy density W function of the azimuthal variable θ

5.6 Numerical analysis of a cracked initially-stressed material

5.6.1 Strong form of the problem

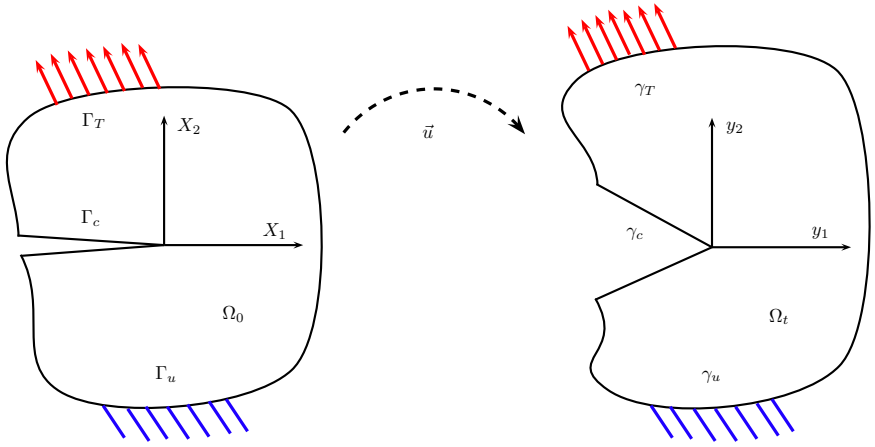

Figure 5.13: Kinematic and boundary conditions.

To develop the numerical model for a cracked initially-stressed material based on the

XFEM approach, let us represent the boundary value problem in a brief way. First of all, to simplify the numerical analysis, we consider a plane problem, where the solid body is homogeneous incompressible material containing a crack. The reference configuration is denoted by Ω_0 where the solid body is subjected to an equilibrated initial stress field. Whereas the deformed configuration will be denoted by Ω_t as it is illustrated through figure (5.13). Let us consider $\vec{u}$ as 2-dimensional displacement field and p as the Lagrange multiplier related to the incompressibility condition. Both $\vec{u}$ and p are the solution of the studied boundary value problem. The boundary of the of both the reference and deformed configurations will be partitioned in three parts: the crack faces represented by (Γ_c, γ_c), the boundary region for Neumann condition far from the crack faces (Γ_T, γ_T) and the boundary region for Dirichlet conditions (Γ_d, γ_d). The mathematical representation of the boundary value problem can be divided in three sets of equations: where the first set of representation is related to the deformed configuration (Euleurian formulation)

$$\begin{cases} \text{div}\boldsymbol{\sigma} = \vec{0}, \quad \text{in} \ \ \omega_t, \\ \boldsymbol{\sigma}.\vec{n} = \vec{t}_d, \quad \text{on} \ \ \gamma_T, \\ \vec{u} = \vec{u}_d, \quad \text{on} \ \ \gamma_u \\ \boldsymbol{\sigma}.\vec{n} = \vec{0}, \quad \text{on} \ \ \gamma \backslash (\gamma_T \cup \gamma_u), \\ \boldsymbol{\sigma} = \mu \boldsymbol{B} + \boldsymbol{F}\boldsymbol{\tau}\boldsymbol{F}^T - p\mathbf{1}, \\ \det(\boldsymbol{F}) = 1. \end{cases} \tag{5.129}$$

the second set is devoted to Lagrangian formulation (relatively to the reference configuration)

$$\begin{cases} \text{Div}\boldsymbol{S} = \vec{0}, \quad \text{in} \ \ \Omega_0, \\ \boldsymbol{S}.\vec{N} = \vec{t}_d, \quad \text{on} \ \ \Gamma_T, \\ \vec{u} = \vec{u}_d, \quad \text{on} \ \ \Gamma_u \\ \boldsymbol{S}.\vec{N} = \vec{0}, \quad \text{on} \ \ \Gamma \backslash (\Gamma_T \cup \Gamma_u), \\ \boldsymbol{S} = \mu \boldsymbol{F} + \boldsymbol{F}\boldsymbol{\tau} - p\boldsymbol{F}^{-T}, \\ \det(\boldsymbol{F}) = 1. \end{cases} \tag{5.130}$$

whereas the last set is dedicated to the equilibrium of the initial stress field defined on the reference configuration

$$\begin{cases} \text{Div}\boldsymbol{\tau} = \vec{0}, \quad \text{in} \ \ \Omega_0, \\ \boldsymbol{\tau}.\vec{N} = \vec{t}_0, \quad \text{on} \ \ \Gamma. \end{cases} \tag{5.131}$$

5.6.2 Variational formulation and discretization of the problem

The variational formulation of the boundary value problem is usually referred to as the weak formulation or in a more physical interpretation as the virtual work formulation. In the objective to elaborate the variational formulation, in absence of volumetric forces and in the scope of static deformations, the internal energy $\mathcal{P}$ in the material body can be modeled through the following integral form:

$$\mathcal{P} = \int_{\Omega_0} W(\mathbf{1} + \boldsymbol{\nabla}\vec{u}) \;\; d\Omega_0 - \int_{\Gamma} \vec{t}.\vec{u} d\Gamma \tag{5.132}$$

where $\vec{t}$ denotes the force vector to what the material body is subjected in the refernce configuration on the boundary Γ. The displacement field solution of the boundary value problem minimizes the stored energy $\mathcal{P}$. The incompressible behavior is equivalent to the fact that the material supports only isochoric deformation. Such internal constraint can be represented through the following condition:

$$\Psi^{inc}(J) = 0 \tag{5.133}$$

where Ψ^{inc} is a sufficiently smooth function. Hence, taking account of the incompressibility condition, the displacement field $\vec{u}$ minimize the modified potential $\mathcal{P}^*$ which can be expressed as:

$$\mathcal{P}^* = \int_{\Omega_0} W(\mathbf{1} + \boldsymbol{\nabla}\vec{u}) \;\; d\Omega_0 - \int_{\Gamma} \vec{t}.\vec{u} d\Gamma - \int_{\Omega_0} p\Psi^{inc}(\det(\mathbf{1} + \boldsymbol{\nabla}\vec{u}))d\Omega_0 \tag{5.134}$$

By consequence, if we consider a 2-dimensional vector field $\vec{v}$ that will be denoted as a virtual displacement field, then the displacement field $\vec{u}$ solution of the boundary value problem satisfies:

$$\int_{\Omega_0} \frac{\partial W}{\partial \boldsymbol{F}}(\mathbf{1} + \boldsymbol{\nabla}\vec{u}) : \boldsymbol{\nabla}\vec{v} \;\; d\Omega_0 - \int_{\Omega_0} p\frac{\partial \Psi^{inc}}{\partial \boldsymbol{F}} \; (\det(\mathbf{1} + \boldsymbol{\nabla}\vec{u})) : \boldsymbol{\nabla}\vec{v} d\Omega_0 = \int_{\Gamma_T} \vec{t}_d.\vec{v} d\Gamma, \quad \forall \vec{v} \in \mathbb{V}, \tag{5.135}$$

where $\mathbb{V}$ denotes the space of virtual displacement field and it can be defined as:

$$\mathbb{V} = \{\vec{v} \in \mathbb{W}^{s_1,s_2}(\Omega_0), \quad | \quad \vec{v}_{|\Gamma_u} = \vec{0}\}, \tag{5.136}$$

with $\mathbb{W}^{\cdots}(\Omega_0)$ denotes the Sobolov space defined on the domain of the reference configuration Ω_0 whereas s_1 and s_2 depend on the strain energy and the regularity of the virtual displacement fields. Similarly, the weak variational formulation of the incompressibility condition can be presented as:

$$\int_{\Omega_0} \Psi^{inc}(\det(\mathbf{1}+\boldsymbol{\nabla}\vec{u}))\ \ q\ \ d\Omega_0 = 0, \quad \forall \vec{q} \in \mathbb{Q} \tag{5.137}$$

where $\mathbb{Q}$ denotes the space of virtual Lagrange multiplier and it is defined as:

$$\mathbb{Q} = \{\vec{v} \in \mathbb{W}^{0,s^*}(\Omega_0)\} \tag{5.138}$$

where s^* characterize the regularity of the virtual Lagrange multipliers. We notice that the Lagrange multiplier p depends on the function Ψ^{inc} choice. For the numerical resolution of the variational formulation highlighted in equations (5.155,5.156), a linearization procedure has to be made. Let us defined the increments of displacement field and the Lagrange multiplier as the following:

$$\vec{u} = \vec{u}_0 + \delta\vec{u}, \quad p = p_0 + \delta p \tag{5.139}$$

where the indexation $\vec{u}_0$ and p_0 denote reference values for the described boundary value problem solutions. Thus with sufficiently small variations for the $\vec{u}$ and p ($||\delta\vec{u}|| << 1$, $|\delta p| << 1$) result of a small variation of the external loading ($|||\delta\vec{t}| << 1$ and $|||\delta\vec{u}_d| << 1$), the linearization of both the compressible part of first Piola Kirchhoff stress tensor and the incompressibility potential can be presented as:

$$\frac{\partial W}{\partial \boldsymbol{F}}(\mathbf{1}+\vec{u}) = \frac{\partial W}{\partial \boldsymbol{F}}(\mathbf{1}+\boldsymbol{\nabla}\vec{u}_0) + \frac{\partial^2 W}{\partial \boldsymbol{F}\partial \boldsymbol{F}}(\mathbf{1}+\boldsymbol{\nabla}\vec{u}_0) : \boldsymbol{\nabla}\vec{\delta u} + o(\boldsymbol{\nabla}\vec{\delta u}). \tag{5.140}$$

$$\Psi^{inc}(J(\mathbf{1}+\boldsymbol{\nabla}\vec{u})) = \Psi(J(\mathbf{1}+\boldsymbol{\nabla}\vec{u}_0)) + < D(\Psi^{inc}(J(\mathbf{1}+\boldsymbol{\nabla}\vec{u})))(\vec{u}_0), \boldsymbol{\nabla}\vec{\delta u} > + o(\boldsymbol{\nabla}\vec{\delta u}). \tag{5.141}$$

To ensure the coherence between the expression of the first Piola Kirchhoff stress tensor in equation (5.24) and the variational formulation in equation (5.155), the function Ψ^{inc} representing the incompressibility constraint must satisfy:

$$\Psi^{inc}(J) = J - 1. \tag{5.142}$$

Hence, the linearization of the weak formulation of the boundary value problem can be presented in the following equations:

$$a_L(\delta\vec{u},\vec{v}) + b_L(\delta p,\vec{v}) = \mathcal{R}_u(\vec{v}), \quad \forall\vec{v}\in\mathbb{V} \tag{5.143}$$

$$b_L(q,\delta\vec{u}) = \mathcal{R}_p(q), \quad \forall\vec{q}\in\mathbb{Q} \tag{5.144}$$

with the linearized form of the bilinear operator $a(.,.)$ and the mixed operator $b(.,.)$ can be explicitly presented as:

$$a_L(\delta\vec{u},\vec{v}) = \int_{\Omega_0}[\frac{\partial^2 W}{\partial\boldsymbol{F}\partial\boldsymbol{F}}(\mathbf{1}+\boldsymbol{\nabla}\vec{u}_0):\boldsymbol{\nabla}\delta\vec{u}]:\boldsymbol{\nabla}\vec{v}\ \ d\Omega_0 + \int_{\Omega_0} p_0[\boldsymbol{F}_0^{-T}(\boldsymbol{\nabla}\delta\vec{u})^T\boldsymbol{F}_0^{-T}]:\boldsymbol{\nabla}\vec{v}\ \ d\Omega_0. \tag{5.145}$$

$$b_L(\delta p,\vec{v}) = -\int_{\Omega_0}\delta p\boldsymbol{F}_0^{-T}:\boldsymbol{\nabla}\vec{v}\ \ d\Omega_0, \tag{5.146}$$

whereas the residual terms for both the energy balance and the weak formulation of the incompressibility condition become:

$$\mathcal{R}_u(\vec{v}) = \int_{\Omega_0}\vec{t}.\vec{v}d\Omega_0 - \int_{\Omega_0}\frac{\partial W}{\partial\boldsymbol{F}}(\boldsymbol{F}_0):\boldsymbol{\nabla}\vec{v}\ \ d\Omega_0 + \int_{\Omega_0} p_0\boldsymbol{F}_0^{-T}:\boldsymbol{\nabla}\vec{v}\ \ d\Omega_0, \tag{5.147}$$

$$\mathcal{R}_p(\vec{u}) = \int_{\Omega_0} q(\det(\boldsymbol{F}_0)-1)\ \ d\Omega_0, \tag{5.148}$$

bearing in mind

$$\boldsymbol{F}_0 = \mathbf{1}+\boldsymbol{\nabla}\vec{u}_0. \tag{5.149}$$

5.6.3 Inf-Sup condition

The mixed formulations, based barely on their nomination, are some formulations usually, at least in mechanics, involving the displacement or the velocity fields and some extra fields related to some internal constraints. In the scope of mechanics of solids, the mixed formulation is usually referred to the formulations treating the case of quasi-incompressible or incompressible materials, where the formulation is a function of the displacement field and an extra scalar field. The latter scalar field denotes the pressure field in the case of quasi-incompressible material, whereas it is denoted as the Lagrange multiplier when the incompressibility constraint is considered. Unlike classical formulation based only on the displacement field, the convergence of mixed formulation relies not only on the coercivity

condition (a weak-equivalent condition to ellipticity of the partial differential equation in the case of static problems) but also on stability criterion. To fulfill these requirements, Ladyzhenskaya, Brezzi and Babuska in [Ladyzhenskaya 1969, Babuška 1973, Brezzi 1974] have established the Inf-sup condition which is also referred as the LBB condition in relation with the names of authors contributing to the development of this condition. In the scope of linear elasticity, the inf-sup condition can be presented as:

$$Sup_{\substack{q\in\mathbb{Q}\\ q\neq 0}} \; Inf_{\substack{\vec{u}\in\mathbb{V}\\ \vec{u}\neq\vec{0}}} \frac{\int_{\Omega_0} q \;\; \mathrm{Div}\vec{u} \;\; d\Omega_0}{||q||_{\mathbb{Q}} \;\; ||v||_{\mathbb{V}}} > \beta_0 > 0 \tag{5.150}$$

where β_0 is a constant independent of the solution $\vec{u}$, whereas $||.||_{\mathbb{V}}$ and $||.||_{\mathbb{Q}}$ are two norms associated respectively to the spaces $\mathbb{V}$ and $\mathbb{Q}$. This condition was generalized to the case of mixed problems in hyperelasticity by Le Tallec in [Le Tallec 1982]. If we consider the function $b(\vec{u}, p)$ as the weak form of the incompressibility condition, then inf-sup condition can be formulated as:

$$Sup_{\substack{q\in\mathbb{Q}\\ q\neq 0}} \; Inf_{\vec{u}\in\mathbb{V},\;\; \vec{u}\neq\vec{0}} \frac{< \frac{dB}{d\vec{v}}(\vec{u}.\vec{v}, q >}{||q||_{\mathbb{Q}} \;\; ||v||_{\mathbb{V}}} > \beta_0 > 0 \tag{5.151}$$

with

$$b(\vec{u}, p) =< B(\vec{u}), p > \tag{5.152}$$

where $< ., . >$ denotes the duality pairing. Since the Inf-Sup condition is difficult to verify analytically to every formulation, Chapelle and Bathe have proposed in [Chapelle 1993] a numerical test to check the inf-sup condition based on the analysis of the algebraic discrete form related to the weak formulation. To perform the stability check, the tangent matrix has to be evaluated in every iteration. The discrete form of the weak linearized formulation enlightened through equations (5.163-5.164) can be presented at a chosen iteration n as:

$$\begin{bmatrix} \boldsymbol{A}_n & \boldsymbol{B}_n^T \\ \boldsymbol{B}_n & \mathbf{0} \end{bmatrix} \begin{bmatrix} U_n \\ P_n \end{bmatrix} = \begin{bmatrix} R_n^u \\ R_n^p \end{bmatrix} \tag{5.153}$$

Now, let us define the rigidity matrix $\boldsymbol{K}$ and the mass matrix $\boldsymbol{T}$ defined as:

$$\begin{cases} V^T \boldsymbol{K} U = \int_\Omega \boldsymbol{\nabla}\vec{u} : \boldsymbol{\nabla}\vec{v} d\Omega, \\ Q^T \boldsymbol{T} P = \int_\Omega qp d\Omega, \end{cases} \tag{5.154}$$

where (U, V) and (P, Q) are the vectors representing the discrete form of the displacement variables $(\vec{u}, \vec{v})$ and the Lagrange multiplier variables (p, q) respectively.

Considering the following eigenvalue problem:

$$\boldsymbol{G}X = \lambda \boldsymbol{K}X \tag{5.155}$$

then the inf-sup criteria illustrated in equation (5.171) is equivalent to $\beta_{stab} = \min \sqrt{\lambda} > 0$.

5.6.4 Extended finite element method

The development of the modeling tools have played an important role in the characterization of the materials behaviour with a good accuray. But such advances in the physical behaviour of complex structures lead to the resolution of complex partial differential equations related to the considered boundary value problem. That is why the finite element method is considered as one of the necessary numerical tools to study mechanical problems. However, the FEM is facing new difficulties arising from the new challenges related to the evolution of engineering requirements. In fact, it has been shown that material or mechanical discontinuities can be the source of singular phenomena. Classically, a mesh refinement near the region of the singular behaviour source is the usual solution to treat such cases. When the dynamic character of the mechanical problem is pointed out, then the region of singular behaviour may change and the mesh refinement has to be updated which increases the cost of the mechanical problem resolution. Introduced by Moes Dolbow and Belytshko in [Moës 2002, Moës 1999] to avoid the mesh refinement near a crack tip, the eXtended Finite Element Method is considered as a powerful tool to treat singular problems. The XFEM was developed later in [Stolarska 2001a] based on a technique to represent the crack geometry using level set functions which enables a coupling between the geometrical representation of the crack and the mesh. The XFEM can incorporate not only analytical functions like the ones issued of asymptotic analysis for many physical problems, but also accurate numerical solutions as enrichment functions. The enrichment functions characterize the local behaviour related to the studied singular phenomenon, which enhance the accuracy of the mechanical problem solution without using mesh-refinement techniques. Since the XFEM was originally used for crack problems, there is no surprise that there are many works studying the singular behaviour of the mechanical fields near a crack tip, we can cite [Sukumar 2008, Sukumar 2000, Areias 2005, Belytschko 2001, Chahine 2008, Duflot 2008, Legrain 2005].

The use of XFEM is not restricted for crack problems, it was applied for different mechanical problems with different singular natures, like the analysis of dislocation and discontinuity interfaces [Ventura 2005, Belytschko 2007], holes and dislocations [Sukumar 2001], fluid mechanics and fluid-structure interaction [Chessa 2003a, Gerstenberger 2008, Zilian 2008]. To have an overview of the different applications of XFEM, we suggest the different surveys in [Fries 2010, Belytschko 2009, Abdelaziz 2008].

5.6.4.1 Discrete formulation of the XFEM method

Before discussing the XFEM formulation, the finite element approximation of weak formulation illustrated through equations (5.155,5.157), can be derived by replacing of the virtual spaces $\mathbb{V}$ and $\mathbb{Q}$ by finite dimensional subspaces $\mathbb{V}^h$ and $\mathbb{Q}^h$ defined on the geometrical approximation of the domain Ω using meshing elements. Hence the approximated finite element solutions will be denoted by $\vec{u}^h$ and p^h.

The concept of XFEM is to exploit the partition of unity with the addition of chosen enrichment functions to better describe and fit the crack influence on the mechanical fields behaviour. Focusing on cracked problems, the enrichment functions are usually divided into two sets. The first set contains the heaviside function to point out the displacement or the Lagrange multiplier jump across the crack faces. Whereas, the second one is a set of singular functions to better represent the singular stress or strain fields near the crack tip. The singular enrichment functions can be refined numerical solutions or some analytical approximations for the two unknowns of the boundary value problem $(\vec{u}, p)$. Hence, the approximated solutions $(\vec{u}^h, p^h)$will be decomposed into two quantities: one inherited from the classical finite element method exploiting Lagrange shape functions (denoted by $(\vec{u}^{fem}, p^{fem})$) and a second part using a set of enrichment functions (denoted by $(\vec{u}^{enr}, p^{enr})$). Such formulation can be mathematically described as:

$$\begin{cases} \vec{u}^h = \vec{u}^{fem} + \vec{u}^{enr}, \quad \vec{u}^{fem} \in \mathbb{V}^{fem}, \quad \vec{u}^{enr} \in \mathbb{V}^{enr}, \\ p^h = p^{fem} + p^{enr}, \quad p^{fem} \in \mathbb{Q}^{fem}, \quad p^{enr} \in \mathbb{Q}^{enr} \end{cases} \tag{5.156}$$

with $\mathbb{V}^{fem}$ and $\mathbb{Q}^{fem}$ are the classical finite element space for the displacement and the Lagrange multiplier respectively. On the other hand, $\mathbb{V}^{enr}$ and $\mathbb{Q}^{enr}$ are 2 enrichment

spaces which can be defined as:

$$\mathbb{V}_u^{enr} = \{\vec{e}_u^h, \quad \vec{e}_u^h = \sum_{i\in\mathcal{I}_\mathcal{H}} \vec{t}_{(i)}^u H_i \phi_i^u + \sum_{i\in\mathcal{I}_\mathcal{C}} \sum_{j=1}^{N_u^{enr}} \vec{s}_{(ij)}^u F_j^u \phi_i^u\} \tag{5.157}$$

$$\mathbb{V}_p^{enr} = \{e_p^h, \quad e_p^h = \sum_{i\in\mathcal{I}_\mathcal{H}} t_{(i)}^p H_i \phi_i^p + \sum_{i\in\mathcal{I}_\mathcal{C}} \sum_{j=1}^{N_p^{enr}} s_{(ij)}^u F_j^p \phi_i^p\} \tag{5.158}$$

where

- $\{\phi_i^u\}_{i=1}^{N_u^{dof}}$ and $\{\phi_i^p\}_{i=1}^{N_p^{dof}}$ denote the classical Lagrange polynomial shape functions associated respectively to the finite element approximated solutions $\vec{u}^{fem}$ and p^{fem},

- $\mathcal{I}_\mathcal{H}$: is the set of degrees of freedom enriched by the Heaviside function,

- $\mathcal{I}_\mathcal{C}$: is the set of degrees of freedom enriched by the crack-tip (or singular) enrichment functions.

- $\{F\}_{j=1}^{N_u^{enr}}$ denotes the set of singular enrichment functions.

- H denotes the Heaviside function which can be defined as:

$$H = \begin{cases} 1 \text{ for } (\vec{X} - \vec{X}_c).\vec{N} \\ -1 \text{ elsewhere} \end{cases} \tag{5.159}$$

  where $\vec{N}$ denotes the outward normal to the crack faces and $\vec{X}_c$ denotes the crack tip position.

Considering the decomposition of the boundary value problem solutions in equation (5.176), then the resulting XFEM spaces $\mathbb{V}^h$ and $\mathbb{Q}^h$ can be expressed as direct sum of the finite element and the enriched subspaces as:

$$\mathbb{V}^h = \mathbb{V}^{fem} \oplus \mathbb{V}^{enr} \tag{5.160}$$

$$\mathbb{Q}_X^h = \mathbb{Q}^{fem} \oplus \mathbb{Q}^{enr} \tag{5.161}$$

Thus the XFEM solutions will be in the following mathematical forms:

$$\vec{u}^h = \sum_{i=1}^{N_u^{dof}} \vec{t}^u_{(i)} \phi^u_i + \sum_{i \in \mathcal{I}_\mathcal{H}} \vec{t}^u_{(i)} H \phi^u_i + \sum_{i \in \mathcal{I}_\mathcal{C}} \sum_{j=1}^{N_u^{enr}} \vec{s}^u_{(ij)} F^u_j \phi^u_i \} \tag{5.162}$$

$$p^h = \sum_{i=1}^{N_u^{dof}} t^p_{(i)} \phi^p_i + \sum_{i \in \mathcal{I}_\mathcal{H}} t^p_{(i)} H \phi^p_i + \sum_{i \in \mathcal{I}_\mathcal{C}} \sum_{j=1}^{N_p^{enr}} s^u_{(ij)} F^p_j \phi^p_i \} \tag{5.163}$$

Moreover, the Heaviside enrichment concerns only the nodes associated to the mesh elements completely cut by the crack. In the classical XFEM approach, only the mesh elements containing the crack tip are enriched by the set of singular functions. Such choice reduces the number of nodes affected by the singular enrichment and leads to a poor computational accuracy as it is shown in [Chessa 2003b]. As a remedy for this limitation, [Béchet 2005] proposed to enrich a fixed area around the crack tip which can be characterized by a radius denoted as R^{enr}. The whole strategy of nodes enrichment can be presented in a simple way via figure (5.14).

5.6.4.2 Levelset method

In the case of XFEM, The geometrical representation of the crack shape is based on the level set method. To our knowledge, this concept is introduced for the first time in [Osher 1988] to trail moving interfaces. In the case of cracked domain, [Stolarska 2001b] proposed the use of multiple scalar functions to represent the crack geometry. Focusing on the case of cracked plane body, the crack can be defined using two level set functions ϕ and ψ as:

$$\begin{cases} \phi(\vec{X}) = 0 \text{ and } \psi(\vec{X}) < 0 \Leftrightarrow \vec{X} \in \Gamma_c \\ \phi(\vec{X}) = 0 \text{ and } \psi(\vec{X}) = 0 \Leftrightarrow \vec{X} = \vec{X}_c. \end{cases} \tag{5.164}$$

To better understand the geometrical representation of the crack in the case of plane geometry we invite the reader to see figure (5.15). Based on the levelset concept, the Heaviside function can be simplified to:

$$H(\vec{X}) = \text{sign}(\phi(\vec{X})). \tag{5.165}$$

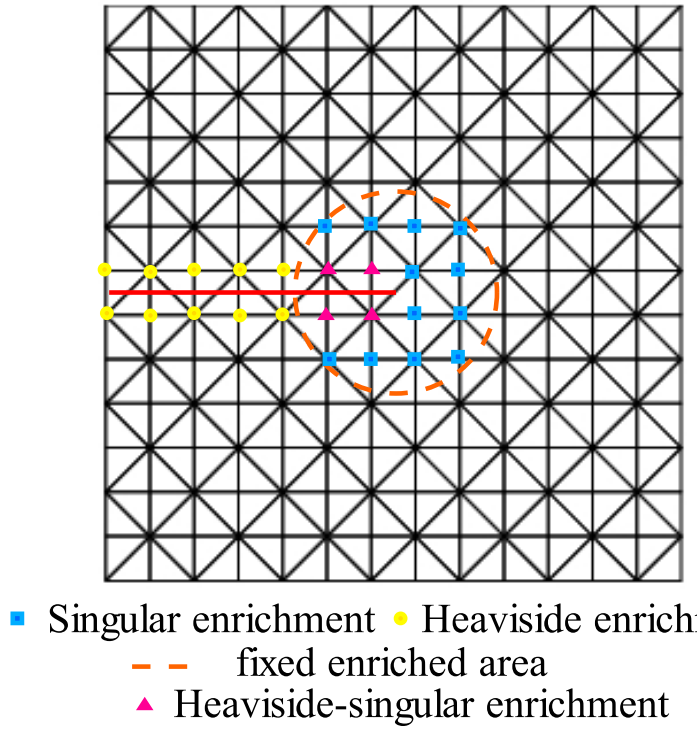

Figure 5.14: XFEM with fixed enriched area

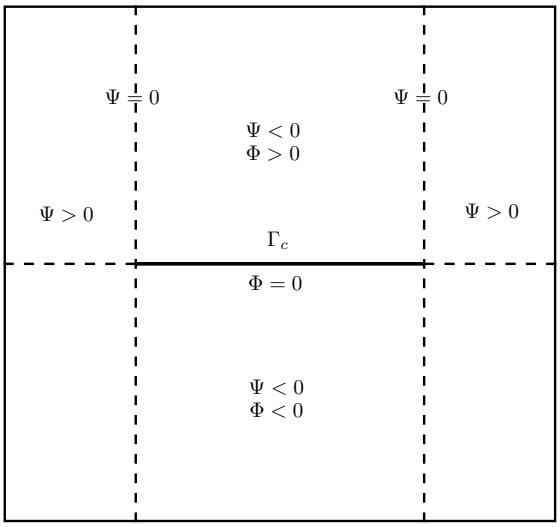

Figure 5.15: Level set functions for cracked domain

5.6.5 Numerical analysis

For the numerical analysis, we consider a non cracked square domain $\bar{\Omega} = [-0.5 \quad 0.5] \times [0.5 \quad 0.5]$. The geometrical crack shape Γ_c can be characterized by $\Gamma_c = \{X_1 \in [-0.5 \quad 0], \quad X_2 = 0\}$. For the sake of simplification, we have considered a simple uniform tangential initial stress field which is equivalent to:

$$\tau_1 \neq 0, \quad \tau_2 = 0, \quad \phi = 0. \tag{5.166}$$

which implies that the crack faces are traction-free. The boundary conditions are chosen to be as the ones for a simple tensile test in absence of crack (see figure (5.16)). To avoid any mesh-arising problems, the domain $\bar{\Omega}$ is uniformly meshed using triangular elements. For the sake of parametric analysis, multiple finite elements are used and

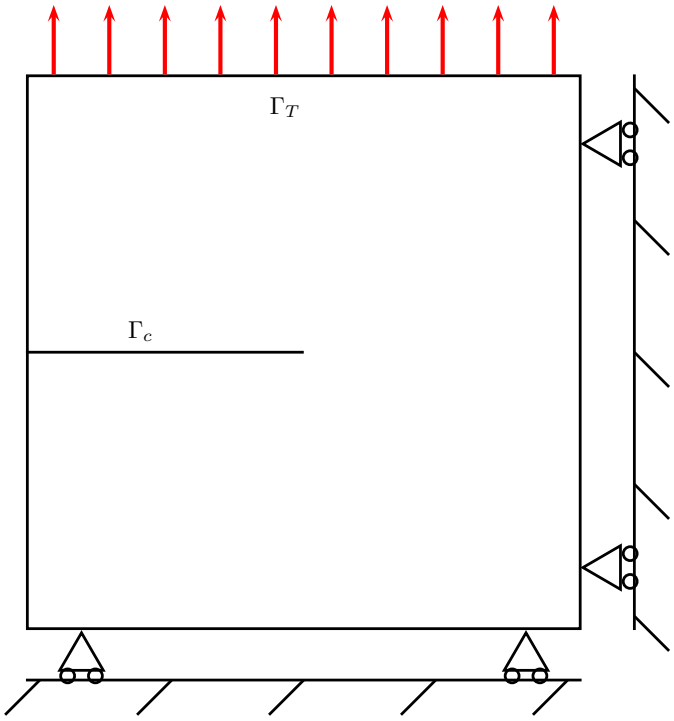

Figure 5.16: Boundary conditions for the boundary value problem used for the numerical test

different choices for the singular enrichment functions are considered. In analogy with the different works done in the context of mixed crack problems, a set of three different

elements formulations are considered: P_2/P_1, P_2/P_0 and P_1^+/P_1. The stability of the latter elements are proved within the scope of finite element method in [Brezzi 2012] and numerically in the scope of cracked problems using the extended finite element method within [Nicaise 2011, Amdouni 2012]. The objective here is to test the limit of such finite elements in the scope of finite transformation and in the presence of an initial stress field. Let define $\mathcal{F}^u$ and $\mathcal{F}^p$ as the sets of crack-tip enrichment functions for the displacement and the Lagrange multiplier fields. Then, the different discussed choices for the crack-tip enrichment functions can be presented as:

- case U2P0: we have exploited the second order of the asymptotic expansion for the displacement field without singular enrichment of the Lagrange multiplier which is equivalent to: $\mathcal{F}^u = \{F_1^u, F_2^u\}$, $\mathcal{F}^p = \emptyset$.
- case U2P1: The second order asymptotic expansion for the displacement field and the first order asymptotic expansion for the Lagrange multiplier are considered which implies $\mathcal{F}^u = \{F_1^u, F_2^u\}$, $\mathcal{F}^p = \{F_1^p\}$.
- case U7P3: the third order of the asymptotic expansion for the displacement field and the second order of the asymptotic expansion for the Lagrange multiplier are considered which justifies the following set of singular enrichment functions sets $\mathcal{F}^u = \{F_1^u, \ldots, F_7^u\}$, $\mathcal{F}^p = \{F_1^p, \ldots, F_3^p\}$.

where the different crack-tip enrichment functions mentioned above can be expressed as:

$$\begin{cases} F_1^u(\bar{R},\bar{\theta}) = \bar{R}^{\frac{1}{2}}\sin(\frac{\bar{\theta}}{2}), \quad F_2^u(\bar{R},\bar{\theta}) = \bar{R}\sin^2(\frac{\bar{\theta}}{2})\}, \quad F_3^u(\bar{R},\bar{\theta}) = \bar{R}^{\frac{3}{2}}\sin^3(\frac{\bar{\theta}}{2}), \\ F_4^u(\bar{R},\bar{\theta}) = \bar{R}^{\frac{3}{2}}\sin(\frac{\bar{\theta}}{2}), \quad F_5^u(\bar{R},\bar{\theta}) = \bar{R}^{\frac{3}{2}}\sin(\frac{3\bar{\theta}}{2}), \quad F_6^u(\bar{R},\bar{\theta}) = \bar{R}^{\frac{3}{2}}\sin^2(\frac{\bar{\theta}}{2})\cos(\frac{\bar{\theta}}{2}), \\ F_7^u(\bar{R},\bar{\theta}) = \bar{R}^{\frac{3}{2}}\cos^3(\frac{\bar{\theta}}{2}), \end{cases} \tag{5.167}$$

and

$$F_1^p(\bar{R},\bar{\theta}) = \bar{R}^{\frac{1}{2}}\cos(\frac{\bar{\theta}}{2}), \quad F_2^p(\bar{R},\bar{\theta}) = \bar{R}\sin^2(\frac{\bar{\theta}}{2}), \quad F_3^p(\bar{R},\bar{\theta}) = \bar{R}\cos^2(\frac{\bar{\theta}}{2}). \tag{5.168}$$

For the size of the singular enrichment area, $R^{enr} = 0.1$ is considered for the cases UP0 and U2P1. Whereas, the radius of this enriched area is reduced to $R^{enr} = 0.05$ to ensure the convergence of the XFEM solution in the case of the most refined mesh considered

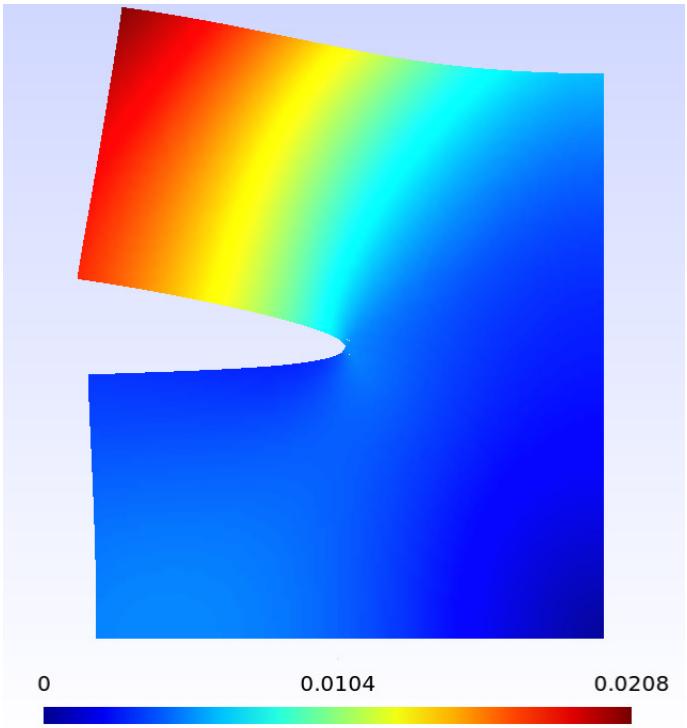

Figure 5.17: XFEM-numerical solution for the displacement field (U7P3-enrichment)

(for the calulation of the reference solutions). In figures (5.17) and (5.18), we present the numerical solution for the boundary value problem using the XFEm method using the enrichment functions relative to the U7P3 case.

5.6.6 Stability results

Based on the evolution of the eigenvalue parameter β_{stab} in function of the mesh size as it is presented in figure (5.19-d), we can affirm that in the case of the finite element method the different elements formulations (P_2/P_1, P_2/P_0 and P_1^+/P_1), are stable at least for the case of our numerical solution. However in the case of extended finite element method, the stability of the numerical formulation seems to be dependent not only on the degree of elements interpolation but also the set of employed crack-tip enrichment functions. If

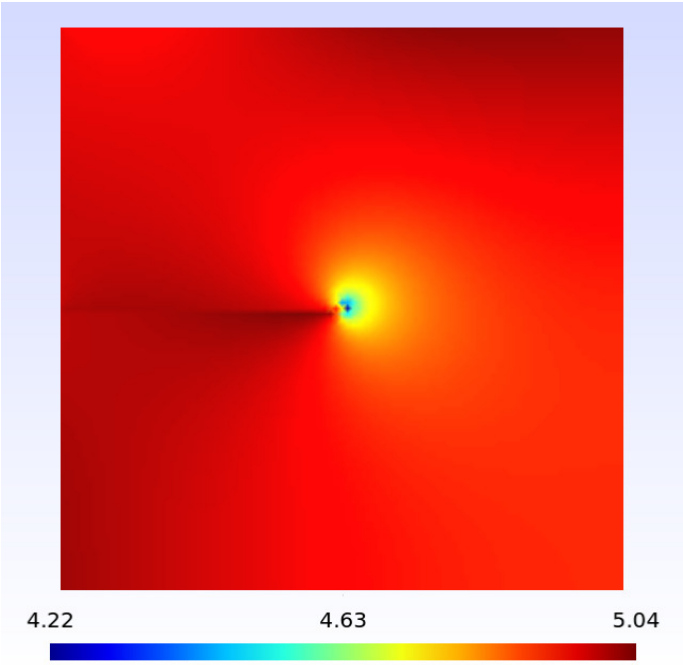

Figure 5.18: XFEM-numerical solution for the Lagrange multiplier (U7P3-enrichment)

we take the example of the U2P0 enrichment case, it is clear that β_{stab} is alternating and decreasing with the mesh size h for the three interpolation cases (see figure (5.20-d)). Thus we can conclude, for all the tested elements in the case of U2P0 enrichment situation, the extended finite element method is completely unstable. Whereas, in the case of Lagrange multiplier enrichment whether U7P3 or U2P1, the XFEM method is stable and the stability degree increases with the number of used crack-tip functions as it is illustrated in figures (5.21-d) and (5.22-d).

5.6.7 Convergence results

In this section a convergence study will be performed to the different element formulations and the enrichment cases. To do that, two error measures are considered for the displacement field (L_2 and H_1 norms) and one single error measure for the Lagrange multiplier field (L_2-norm).

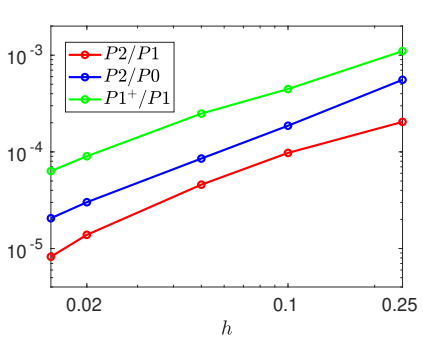

(a) L_2-norm error of the displacement field function of the mesh size h

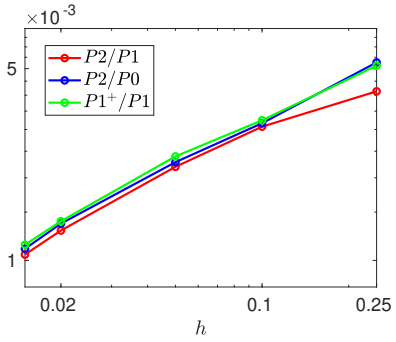

(b) H_1-norm error of the displacement field function of the mesh size h

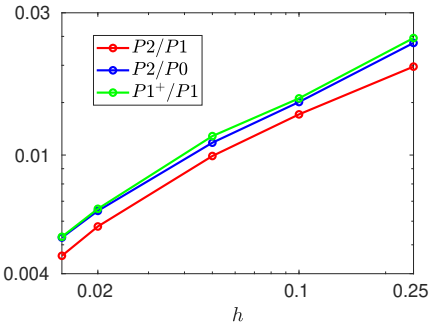

(c) L_2-norm error of the Lagrange multiplier function of the mesh size h

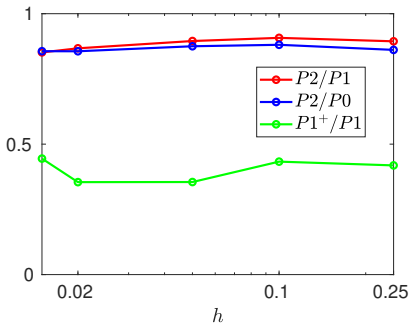

(d) β_{stab} function of the mesh size h

Figure 5.19: numerical results of the FEM model

Convergence rate \ Element formulation	P_2/P_1	P_2/P_0	P_1^+/P_1
L_2-error convergence rate for $\vec{u}$	1.2903	1.1534	1.0363
H_1-error convergence rate for $\vec{u}$	0.5648	0.5517	0.5535
L_2-error convergence rate for p	0.5729	0.5509	0.5659

Table 5.2: Convergence rates in the FEM case

Since it is difficult to have an analytical solution for the complicated nonlinear boundary value problem, a refined numerical solution will be computed for every enrichment case and element formulation to be considered as a reference to perform the different error measures.

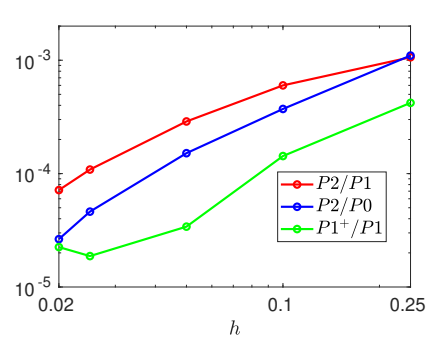

(a) L_2-norm error of the displacement field function of the mesh size h

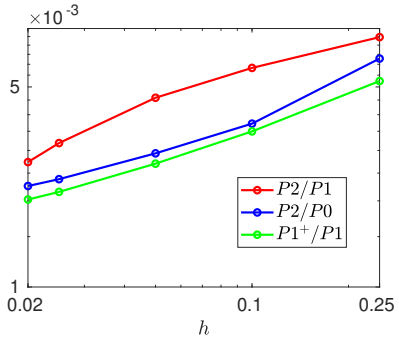

(b) H_1-norm error of the displacement field function of the mesh size h

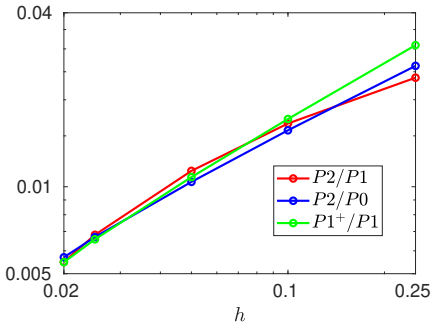

(c) L_2-norm error of the Lagrange multiplier function of the mesh size h

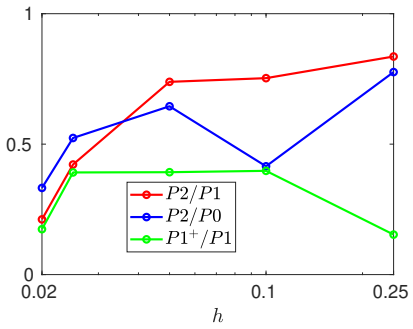

(d) β_{stab} function of the mesh size h

Figure 5.20: numerical results of the XFEM model with U2P0 enrichment

FEM formulation / Convergence rate	P_2/P_1	P_2/P_0	P_1^+/P_1
L_2-error convergence rate for $\vec{u}$	1.3118	1.6212	1.1849
H_1-error convergence rate for $\vec{u}$	0.4692	0.3128	0.3414
L_2-error convergence rate for p	0.6812	0.6263	0.7061

Table 5.3: Convergence rates in the XFEM case with $U2P0$-enrichment

In the scope of linear incompressible or compressible elasticity, it has been shown that the XFEM method is stable and leads to an optimal convergence rate [Nicaise 2011, Amdouni 2012]. If we take the example of single crack-tip enrichment for the displacement field and the Lagrange multiplier then the convergence rate for the different considered formulations is enhanced and can be presented in table (5.6)

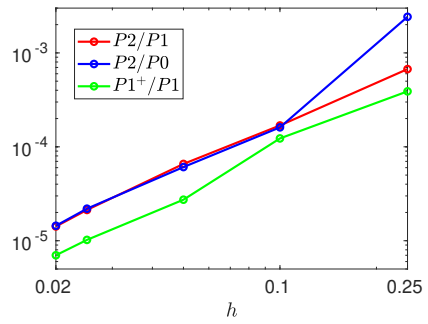

(a) L_2-norm error of the displacement field function of the mesh size h

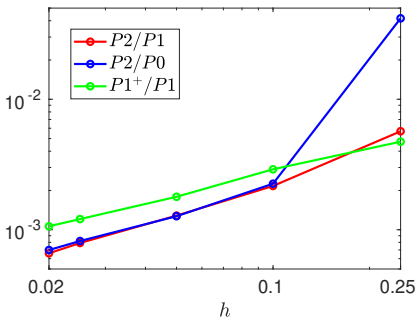

(b) H_1-norm error of the displacement field function of the mesh size h

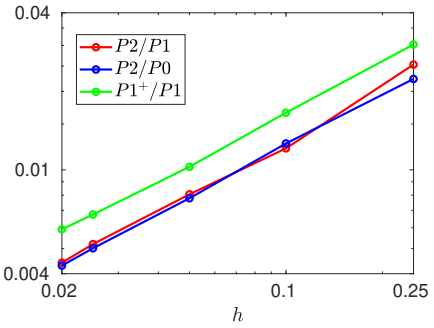

(c) L_2-norm error of the Lagrange multiplier function of the mesh size h

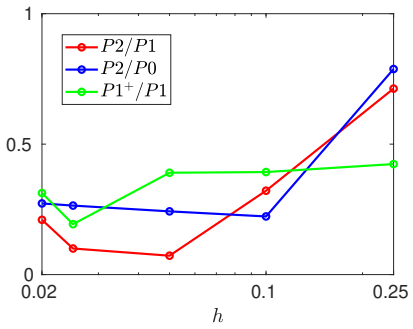

(d) λ_{stab} function of the mesh size h

Figure 5.21: numerical results of the XFEM model with U2P1 enrichment

FEM formulation / Convergence rate	P_2/P_1	P_2/P_0	P_1^+/P_1
L_2-error convergence rate for $\vec{u}$	1.5381	1.4840	1.4715
H_1-error convergence rate for $\vec{u}$	0.7316	0.7182	0.6209
L_2-error convergence rate for p	0.6242	0.6659	0.6381

Table 5.4: Convergence rates in the XFEM case with $U2P1$-enrichment

[Amdouni 2012]: Although, in the scope of finite transformation, the above convergence rates can not be guaranteed. To our knowledge, the only work which has done a convergence study for mixed formulation in the scope of finite transformation is [K. 2016] where a plane crack problem in an incompressible NeoHookean hyperelastic material is analyzed. To point out the usefulness of the XFEM method, the obtained convergence

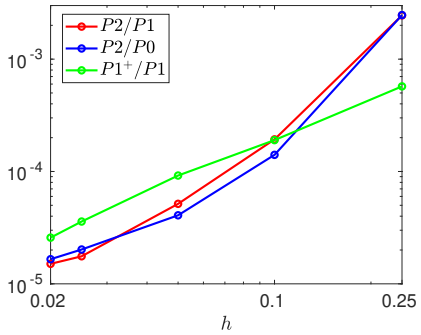

(a) L_2-norm error of the displacement field function of the mesh size h

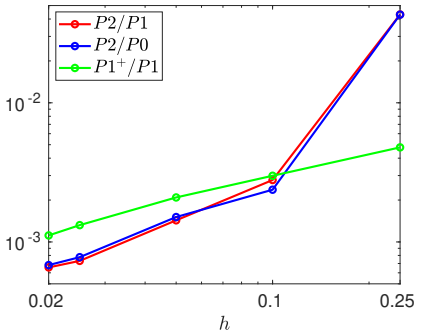

(b) H_1-norm error of the displacement field function of the mesh size h

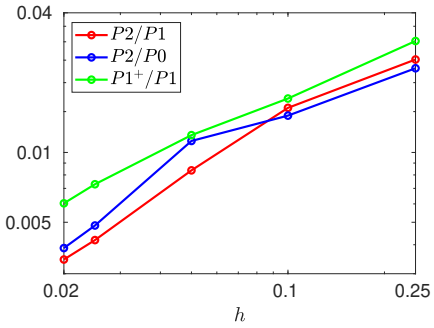

(c) L_2-norm error of the Lagrange multiplier function of the mesh size h

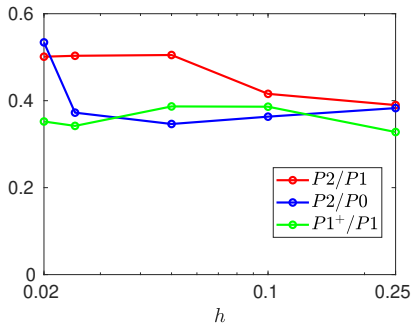

(d) β_{stab} function of the mesh size h

Figure 5.22: numerical results of the XFEM model with U7P3 enrichment

FEM formulation / Convergence rate	P_2/P_1	P_2/P_0	P_1^+/P_1
L_2-error convergence rate for $\vec{u}$	1.6108	1.3117	1.2458
H_1-error convergence rate for $\vec{u}$	0.9192	0.7996	0.6133
L_2-error convergence rate for p	0.9442	0.8502	0.6455

Table 5.5: Convergence rates in the XFEM case with $U7P3$-enrichment

rates for the different scenarios can be compared to those using the FEM method (see figure (5.19) and table (5.2)).

Focusing on figure (5.20) it seem that the formulation P_1^+/P_1 gives more accurate

Convergence rate \ Formulation	P_2/P_1	P_2/P_0	P_1^+/P_1
L_2-error convergence rate for $\vec{u}$	3	2	2
H_1-error convergence rate for $\vec{u}$	1.5	1	1
L_2-error convergence rate for p	1.5	1	1

Table 5.6: Convergence rates in the XFEM case with first order enrichment in the scope of incompressible linear elasticity

solutions than (P_2/P_1) which confirms in another way the instability of the XFEM method in the U2P0 enrichment. Hence, even if the convergence rate is slightly better than the FEM case as it is illustrated in tables (5.1,5.3) at least for the P_2/P_0 considering the L_2-norm error measure relative to the displacement field, such result is not reliable. Focusing on the tables (5.4-5.5)it is clear that the convergence rates are enhanced compared to those using the FEM method. Also, more enriched functions are considered, slightly better are the convergence rates.

5.7 Conclusions

This chapter was dedicated to the analysis of the initial stress field influence on the mechanical fields near a crack tip through an incompressible hyperelastic material. We have shown that the asymptotic expansion of the different mechanical fields are functions of the eigenvectors orientation relative to the crack plane and also a weighting parameter relating the shear modulus and the eigenvalues of the initial stress field. A comparison between the initially-stressed and the unstressed materials has been done through the different asymptotic expansions, and we have shown that the initial stress field can contribute to the rotation of the crack and it has an influence on the crack opening. Finally, based on the asymptotic expansion of the displacement field, a set of enrichment shape functions were chosen to be exploited using the Extended Finite Element Method (XFEM) for the numerical analysis of this singular problem. A convergence and stability studies have been done to point out the influence of multiple parameters (different elements formulations and different chosen enrichment functions) on the stability and the convergence rates.

Chapter 6

The anti-plane shear elasto-static fields near a crack terminating at an isotropic hyperelastic bi-material interface

Contents

6.1 Introduction

Nowadays, reinforced rubber, rubber-like materials and structures are in increasing use in different industrial products and engineering applications. In fact, it is well known that the junction between rubber or rubber-like elastomeric materials and other materials with different rigidities is usually used to improve the stiffness of their design. As an example, the reinforcement of a rubber matrix by transverse fibers has been known to enhance the

toughness of the composite, to impede eventually crack propagation in the matrix and stop it on the interface rather than grow it into uncracked matrix. However, such coupling causes stress concentration due to the material and/or geometric discontinuities which can affect the product strength.

In this work, a crack terminating at a bi-material interface with arbitrary angles is taken as a geometrical model. The bi-material is composed by two incompressible isotropic Neo-Hookean hyperelastic materials. The anti-plane shear is considered due to its simplicity compared to other types of transformations. Such transformation is not simple as it may look [Destrade 2012b] and it is still a subject of research in the scope of non-linear elasticity [Pucci 2015b]. From historical point of view, the theory of continuum mechanics is used to model the mechanical fields concentration due to cracks presence with singular elastostatic fileds: strain and stress.

In linear elasticity, the boundary value problem of the two-dimensional multimaterial wedges or junctions is governed by partial differential equations with Neumann and/or Dirichlet boundary conditions. Its singular nature is well established in [Grisvard 1992] and was analyzed by three methods: asymptotic expansion, complex variables and transform methods. It was shown that the general solution of the linear boundary value problems corresponding is an asymptotic development composed by a linear combination of a power and logarithm types singularities. The unknowns of this asymptotic expansion are considered as eigenvalues (exponent orders) and eigenfunctions. The plane strain or stress formulation was treated theoretically in [Zak 1963, Bogy 1971a, Bogy 1971b, Cook 1972, Erdogan 1973, Fenner 1976, Pinsan 1991, Wang 1994, Tzuchiang 1998, Chen 2003, Lin 1997], numerically in [Lin 1976, Ahmad 1991, Meguid 1985] and experimentally in [Wang 1993, Chen 1996]. It was shown that oscillatory singularity in the elastostatic fields can occur except for a crack perpendicular to an interface. The case of an anti-plane shear transformation was analyzed in [Erdogan 1974, Fenner 1976, Chen 2012, Hu 2013, Wang 1996, Chien-Ching 1990] and no oscillatory singularity in the elastostatic fields occurs (see reviews in [Sinclair 2004a, Sinclair 2004b, Paggi 2008] and the associated references).

The plasticity aspect at a crack tip has been given by Rice in [Rice 1966, Rice 1967] for anti-plane problem and by Hutchinson in [Hutchinson 1968], Rice and Rosengren

in [Rice 1968] for plane problem. It was shown that the asymptotic development is made by a power-type singularity. After that, few papers have been dedicated to solve the crack terminating at bi-material interface problem: in plane strain or stress by [Chao 1993, Romeo 1994, Delfin 1995, Yu 1997, Banerjee 2004] and in anti-plane transformation by [Li 1996]. The Linear Elastic Fracture Mechanics (LEFM) and the Elasto-Plastic Fracture Mechanics (EPFM) approaches described below played a prominent role in the investigation and comprehension of the crack, defect and singular problems. However, these approaches are based on the kinematic assumption of small deformations which is in contradiction with the induced unbounded strain field deduced.

Within the framework of finite deformations, in the past five decades, only few works have been focused on the analysis of the strain and stress fields around a crack, notch, defect... This is due to the complexity of the mathematical problem, as it is illustrated in [Ogden 1997] which makes the boundary-value problem equations highly nonlinear and very difficult to solve analytically or even numerically. We note that Wong and Shield in [Wong 1969] carried the first analysis of an infinite Neo-Hookean sheet containing a finite crack.

In the early 1970s, Knowles and Sternberg in [Knowles 1973, Knowles 1974] analyzed the asymptotic deformation field near the tip of a mode-I plane strain crack for generalized Blatz-Ko compressible hyperelastic solids. Their analysis of the crack problem within the framework of nonlinear elasticity is considered as a fundamental work. Later, Knowles in [Knowles 1977a] performed a mode III local crack analysis for generalized Neo-Hookean incompressible hyperelastic material. This class of hyperelastic potential, depending only on the deformation's first invariant, is capable to sustain nonhomogeneous anti-plane shear transformation as it is demonstrated in [Knowles 1976]. Some necessary and sufficient mathematical conditions, restricted the hyperelastic potential form, are given by Knowles in [Knowles 1976, Knowles 1977b] for incompressible and compressible materials to admit non-trivial states of anti-plane shear, (see [Horgan 1995a] for a review and more references).

To the best of our knowledge, the first analysis of the interface crack of hyperelastic bi-material junction is studied by Knowles and Sternberg in [Knowles 1983]. In two fundamental papers of Herrmann [Herrmann 1989, Herrmann 1992], it was shown the existence of multiple second order asymptotic forms for elastostatic fields for the compress-

ible generalised Blatz-Ko hyperelastic bi-material interface crack. Other interesting works on the topic using analytical asymptotic expansion, numerical and/or experimental investigations were done by: [Knauss 1970, Ravichandran 1989, Gao 1994, Geubelle 1994a, Geubelle 1994b, Geubelle 1995, Ru 1997b, Ru 2002, Krishnan 2009, Lengyel 2014] (see [Gao 2008, Long 2015] for a review and references). The more complicated crack terminating at bi-material interface problem with arbitrary angles was analyzed in [Shanyi 1994] and [Ru 1997a] for a crack perpendicular to interface. All the previous contributions done with different hyperelastic potentials and the plane deformation or stress hypothesis have shown no oscillatory singular behaviour (except in [Krishnan 2009]).

In this chapter, the second section is dedicated to the problem formulation for an anti-plane transformation. The third section focuses on the asymptotic solution of the equilibrium equation for different special geometrical configurations. Finally an investigation on the presence of logarithmic singularities is made to justify the asymptotic form used in the third section.

6.2 Formulation of the anti-plane problem

Consider a solid body C in the form of an infinite cylinder. Let $\mathcal{C}$ the region of three-space occupied by the considered solid body in the initial configuration. $\mathcal{C}$ is characterized by a cross section Ω and a generator vector $\vec{\mathcal{G}}$ as illustrated in figure (6.1). Now, we define the Cartesian basis $(\vec{E}_1\ ,\ \vec{E}_2\ ,\ \vec{E}_3)$ which is tied to the undeformed configuration of C relative to the coordinates $(X_1,\ X_2,\ X_3)$. The generator vector $\vec{\mathcal{G}}$ is chosen to be parallel to $\vec{E}_3$. The cylinder is composed of two isotropic incompressible hyperelastic materials, perfectly bonded to each others. A crack is present in the way to split one of the two material sectors into two different parts. So that we can divide the domain $\mathcal{C}$ into three distinct regions: $\mathcal{C}_k = \{\vec{X}, (X_1, X_2) \in \Omega_k, -\infty < X_3 < +\infty\}, \quad k \in \{1,2,3\}$, where $\vec{X}$ denotes the position of each material particle in the undeformed configuration. Let Ω_k be the associated cross section to the region $\mathcal{C}_k$ with $k \in \{1,2,3\}$. $\{\Omega_k, \quad k \in \{1,2,3\}\}$ is a set of wedge angular sectors defined in the cross section Ω as:
$\Omega_1 = \{(R,\Theta), \omega^U \leq \Theta \leq \pi\}$
$\Omega_2 = \{(R,\Theta), \omega^L \leq \Theta \leq \omega^U\}$, $0 < \omega^U - \omega^L < 2\pi$ with $\omega^L < \omega^U$
$\Omega_3 = \Omega \backslash \{\Omega_2 U \Omega_1\}$
(R,Θ) are the polar coordiantes for every material point in Ω. With respect to the above conditions on ω^U and ω^L, these two angles are to typify a feature of a bi-material

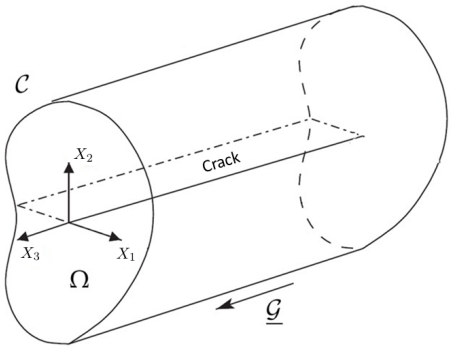

Figure 6.1: Studied body in 3D representation

configuartions as it is described in the figure (6.2). The parts $\mathcal{C}_1$ and $\mathcal{C}_3$ are made of the same material which is different from the material of the part $\mathcal{C}_3$ (figure (6.2)).

Now, the body C is subjected to a prescribed transformation $\mathcal{F}$ which can outline the anti-plane shear transformation near the crack tip. Mathematically, $\mathcal{F}$ can be described as:

$$\vec{x} = \vec{\mathcal{F}}(vecX) = \begin{cases} x_1 = X_1, \\ x_2 = X_2, \\ x_3 = X_3 + u(X_1, X_2), \end{cases} \tag{6.1}$$

where, X_i and x_i $i \in \{1, 2, 3\}$ are the components of the vectors $\vec{X}$ and $\vec{x}$ in the Cartesian basis relied respectively to the undeformed configuration and the deformed one. $u(.,.)$ represents the anti-plane shear displacement which must be at least twice continuously differentiable. The gradient of the $\mathcal{F}$ transformation, denoted as $\boldsymbol{F}$, can be written as:

$$[\boldsymbol{F}]_{ij} = [\boldsymbol{\nabla}\vec{x}]_{ij} = \frac{\partial x_i}{\partial X_j} = x_{i,j}, \quad on \quad each \quad \mathcal{C}_k; \quad i, j, k \in \{1, 2, 3\}. \tag{6.2}$$

Using the form of the anti-plane transformation in equation (6.1) and the definition of the gradient transformation in (2), the matrix form of $\boldsymbol{F}$ is concluded as:

$$[\boldsymbol{F}] = \begin{bmatrix} 1 & 0 & 0 \\ 0 & 1 & 0 \\ u_{,1} & u_{,2} & 1 \end{bmatrix}. \tag{6.3}$$

To describe the state of the deformation related to the transformation $\vec{\mathcal{F}}$, one measure of

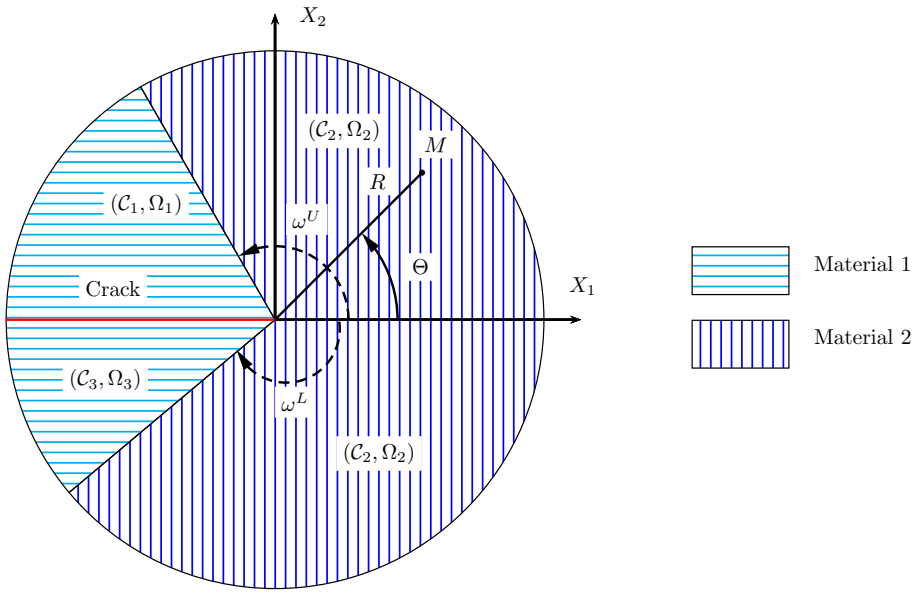

Figure 6.2: Bi-material section

strain can be the *left Cauchy-Green tensor* $\boldsymbol{B}$ that can be expressed as:

$$\boldsymbol{B} = \boldsymbol{F} \ \ \boldsymbol{F}^T = \begin{bmatrix} 1 & 0 & u_{,1} \\ 0 & 1 & u_{,2} \\ u_{,1} & u_{,2} & 1 + |\vec{\nabla} u|^2 \end{bmatrix}. \tag{6.4}$$

$|.|$ denotes the Cartesian norm of a vector, and the notation $.^T$ is used to represent the transpose operator. The incompressibility condition indicates the preserving of the local elementary volume during the governed transformation. It is equivalent to:

$$J = \det(\boldsymbol{F}) = 1, \tag{6.5}$$

where $\det(.)$ denotes the determinant operator. The previous condition is automatically verified in the case of simple anti-plane transformation as it is explicitly formulated in (1), without adding any additional conditions on the form of the unknown displacement field. The hyperelastic behaviour of each part of the cylinder $\mathcal{C}$ can be elucidated using an energy potential form $\mathcal{W}$. Using the isotropy of each part of the bi-material composite, the potential $\mathcal{W}$ depends only on the first two invariants of the *left Cauchy-Green tensor*.

Hence, we derive:

$$\mathcal{W} = \mathcal{W}(I_1, I_2), \tag{6.6}$$

where

$$I_1 = \mathrm{tr}(\boldsymbol{B}) = 3 + |\vec{\nabla} u|^2, \tag{6.7}$$

$$I_2 = \frac{1}{2}(\mathrm{tr}(\boldsymbol{B})^2 - \mathrm{tr}(\boldsymbol{B}^2)) = 3 + |\vec{\nabla} u|^2. \tag{6.8}$$

Here, we consider the Neo-Hookean potential expressed as:

$$\mathcal{W}(I_1) = \frac{\mu_k}{2}(I_1 - 3), \quad \mu_k > 0, \quad on \ \ each \ \ \mathcal{C}_k, \quad k \in \{1, 2, 3\}. \tag{6.9}$$

μ_k is a positive coefficient denoting the shear modulus of each material for infinitesimal deformations. The above potential is a result of the statistical mechanics using a Gaussian distribution [Boyce 2000]. Since the domains $\mathcal{C}_1$ and $\mathcal{C}_3$ are composed by the same material, we have $\mu_1 = \mu_3 \neq \mu_2$. The indexations $(.^{(k)})$ or $(._k)$, unless they are necessary, will be omitted to lighten the following mathematical expressions. We define also the dimensionless parameter $\delta = \frac{1-\frac{\mu_1}{\mu_2}}{1+\frac{\mu_1}{\mu_2}}$, function of the relative rigidity ratio $\frac{\mu_1}{\mu_2}$, which will play a crucial role in analyzing the singular behaviour as it will be shown later. We remark that this dimensionless parameter δ takes values in $]-1 \ \ 1[$ when the rigidity ratio $\frac{\mu_1}{\mu_2}$ belongs to $]0 \ \ +\infty[$. Thus, δ takes into account all material combinations. The state of the stress field can be represented using the *first Piola Kirchhoff tensor* related to the energy potential by:

$$\boldsymbol{S} = \frac{\partial \mathcal{W}}{\partial \boldsymbol{F}} - p\boldsymbol{F}^{-T}, \tag{6.10}$$

where p is the *Lagrange multiplier* field resulting from the incompressibility condition. To have a better physical interpretation of the stress field, we use the *Cauchy stress tensor* developed as:

$$\boldsymbol{\sigma} = \boldsymbol{S} \ \ \boldsymbol{F}^T = \frac{\partial \mathcal{W}}{\partial \boldsymbol{F}} \boldsymbol{F}^T - p\mathbf{1}. \tag{6.11}$$

1 is the identity second-order tensor. If we consider the Neo-Hookean behaviour we can expand the formulation of both *first Piola-Kirchhoff* and *Cauchy* stress tensors as:

$$S_{\alpha\beta} = \sigma_{\alpha\beta} = \zeta_{\alpha\beta}(\mu - p), \quad \alpha, \beta \in \{1, 2\}, \tag{6.12}$$

$$S_{\alpha 3} = p u_{,\alpha}, \tag{6.13}$$

$$S_{3\alpha} = \sigma_{3\alpha} = \mu u_{,\alpha}, \tag{6.14}$$

$$S_{33} = \mu - p \neq \sigma_{33} = \mu(1 + |\nabla u|^2) - p. \tag{6.15}$$

ζ denotes the Kronecker delta function. Unlike the case of linear elasticity theory, the axial component of *Cauchy* stress tensor σ_{33} can not vanish. The sufficient condition for the cylinder's equilibrium using the material coordinates in the undeformed configuration is:

$$\mathrm{Div}(\boldsymbol{S}) = \vec{0}, \tag{6.16}$$

where Div(.) is the divergence operator relative to the coordinates of the initial configuration. Using the expanded form of the *first Piola Kirchhoff stress tensor* illustrated in equations (6.12-6.15) and the transformation's gradient in the matrix form (3) added to the equilibrium equation (6.16), we obtain:

$$[\mu - p]_{,\alpha} + p_{,3} u_{,\alpha} = 0, \quad \alpha \in \{1, 2\}, \tag{6.17}$$

$$\mu \Delta u = p_{,3}. \tag{6.18}$$

$\Delta(.)$ denotes the *Laplace differential operator*. Here, we have 3 differential equations (6.17-6.18) governing 2 unknown fields. To have a non-trivial solution, in [Knowles 1976] we can find the sufficient conditions which must be satisfied by the energy potential. In our case, using the energy potential in (9), a non trivial solution is guaranteed based on the results mentioned by Knowles in [Knowles 1976]. Using the displacement's independence of X_3 and combining the equations (6.17-6.18), we can prove the linearity of the *Lagrange multiplier* p relative to the third coordinate X_3:

$$p(X_1, X_2, X_3) = dX_3 + p_0(X_1, X_2). \tag{6.19}$$

d is an unknown constant. The local boundary conditions when $R \to 0$ is chosen to have a traction-free crack faces. These conditions are translated mathematically into:

$$\boldsymbol{S}(X_1 < 0, X_2 = \pm 0).\vec{N}(X_1 < 0, X_2 = \pm 0) = 0. \tag{6.20}$$

$\vec{N}$ is the unit outward normal vector defined in the initial configuration. Since the materials are perfectly bonded, the continuity of the force vector and the displacement field through the two interfaces between the two considered materials leads to:

$$[|u(R, \Theta = \omega^{(l)})|] = 0, \tag{6.21}$$

$$[|\boldsymbol{S}(R, \Theta = \omega^{(l)})|]\vec{N}(R, \Theta = \omega^{(l)}) = 0, \quad l \in \{U, L\}. \tag{6.22}$$

$[|.|]$ refers to the discontinuity operator. Exploiting the previous equation of boundary conditions in (6.20), the interface conditions mentioned in equations (6.21-6.22) and the form of the *first Piola Kirchhoff tensor* in the equations (6.12-6.15), we can deduce:

$$d = 0, \tag{6.23}$$

$$p = \mu. \tag{6.24}$$

Finally, the formulation of the anti-plane shear transformation as it is described above, can be summarized by the following boundary value problem:

$$\Delta u = 0, \tag{6.25}$$

$$u^{(k^*)}_{,\Theta}(R, \Theta = \pm\pi) = 0, \quad k^* \in \{1, 3\}, \tag{6.26}$$

$$[|u(R, \Theta = \omega^{(l)})|] = 0, \quad l \in \{U, L\}, \tag{6.27}$$

$$[|\mu u_{,\Theta}(R, \Theta = \omega^{(l)})|] = 0. \tag{6.28}$$

6.3 Asymptotic solution

In the literature, there are so many studies focusing on the solution of elastostatic problems using the asymptotic method. The general form proposed in [Kondrat'ev 1967] and [Costabel 1982], as it is illustrated in [Yosibash 2011], for the equation (6.25) is:

$$u(R, \Theta) = \sum_{i}^{I} \sum_{j}^{J} R^{m_i} (log(R))^{n_j} \psi_{ij}(\Theta) \ , \quad m_i \in \mathbb{C}, \quad n_j \in \mathbb{N}, \tag{6.29}$$

where I and J are two chosen integers. In the case where m_i is a complex numbrer, the singularity can be in the type $O(R^{\xi_i} exp(i_c \eta_i log(R))(log(R))^{n_j})$ ($i_c^2 = -1$), where ξ_i and η_i denote respectivelly the real and the imaginary part of m_i. When m_i has non-null imaginary part, the radial oscillation of the displacement field can be pointed out. In this case, the stress field seems to have no physical behaviour. Thus to preclude this non physical solution, we will suppose in the following that all m_i are real cofficients. For the case of cracked configuration, based on many works on such case as the one of [Grisvard 1992] and [Li 2000], it seems that the logarithmic singularities are absent in the displacement expansion. In the opposite way, in the linear elastic theory, many works of Bogy [Bogy 1970, Bogy 1971a, Bogy 1971b] demonstrated the appearance of the logarithmic power singularities under some material and geometrical conditions for the case of homogeneous and bi-material composite. We can use the method established by Dempsey and Sinclair 1979 [Dempsey 1979] exploited in the scope of linear elasticity to investigate the presence of logarithmic singularities. Although their concept was used for linear elastic problems, it can be used here since we have a harmonic problem to be solved. Their idea comes from the fact that the differential operator in the equilibrium equation is linear and independent of the singularity power coefficient m. Thus, if $u(.,.)$ is a solution of equations (6.25-6.28), then $\frac{\partial u}{\partial m}$ must be a solution also. The originality of the study of Dempsey and Sinclair, is the inspection of the logarithmic singularities based on the equations of power singularities. In other words, this technique, which will be discussed in details in the following, makes possible the inquire of the logarithmic singularities without introducing the logarithmic form in the asymptotic expression of the displacement field. This lightens the algebraic system to solve leading to the eigenvalues equation and reduces it by half. Knowing all these advantages of this method, the new asymptotic expansion of the displacement unknown function $u(.,.)$ can be formulated as:

$$u(R,\Theta) = \sum_{i=1}^{N} R^{m_i} \psi_i(\Theta) + u_{reg}(R,\Theta). \tag{6.30}$$

As presented in [Yosibash 2011], $u_{reg}(.,.)$ is the regularized part of the displacement field and N is the number of the effective orders contributing to the singular form of the stress fields, where $0 < m_1 < m_2 < ... < m_N$. Inserting the asymptotic form of the anti-plane

displacement field in the equilibrium equation, it will be transformed into:

$$u(R,\Theta) = \sum_{i=1}^{N} R^{m_i}[A_i cos(m_i\Theta) + B_i sin(m_i\Theta)] + o(R^{m_N}). \tag{6.31}$$

$o(R^{m_N})$ denotes a negligible function compared to R^{m_N} when $R \to 0$. Then, the outspread of *Cauchy stress tensor* asymptotic form becomes:

$$\sigma_{\alpha\beta} = 0, \quad (\alpha,\beta) \in \{1,2\}, \tag{6.32}$$

$$\sigma_{13} = \mu \sum_{i=1}^{N} m_i R^{m_i-1}(A_i cos((m_i-1)\Theta) + B_i sin((m_i-1)\Theta)) + o(R^{m_N-1}), \tag{6.33}$$

$$\sigma_{23} = \mu \sum_{i=1}^{N} m_i R^{m_i-1}(-A_i sin((m_i-1)\Theta) + B_i cos((m_i-1)\Theta)) + o(R^{m_N-1}), \tag{6.34}$$

$$\sigma_{33} = \mu \sum_{i=1}^{N} {m_i}^2 R^{2(m_i-1)}({A_i}^2+{B_i}^2) + 2\mu \sum_{i=1}^{N-1}\sum_{j=i+1}^{N} m_i m_j R^{m_i+m_j-2}\{(A_iA_j+B_iB_j)cos((m_i-m_j)\Theta) + (B_iA_j - A_iB_j)sin((m_i-m_j)\Theta)\} + o(R^{2m_N-2}). \tag{6.35}$$

As a result of the displacement field's continuity and using of equation (6.27), the exponent parameters are independent of the position of any considered material particle. In other way, we may write:

$$m_i^{(k)} = m_i, \quad \forall i, \quad k \in \{1,2,3\}. \tag{6.36}$$

The traction free conditions and the continuity of both the force vector and the displacement $u(.,.)$ expressed in equations (6.26-6.28) lead to:

$$\mu_1(-A_i^{(1)}sin(m_i\omega^U) + B_i^{(1)}cos(m_i\omega^U)) = \mu_2(-A_i^{(2)}sin(m_i\omega^U) + B_i^{(2)}cos(m_i\omega^U)), \tag{6.37}$$

$$\mu_1(-A_i^{(3)}sin(m_i\omega^L) + B_i^{(3)}cos(m_i\omega^L)) = \mu_2(-A_i^{(2)}sin(m_i\omega^L) + B_i^{(2)}cos(m_i\omega^L)), \tag{6.38}$$

$$\mu_1(-A_i^{(1)}sin(m_i\pi) + B_i^{(1)}cos(m_i\pi)) = 0, \tag{6.39}$$

$$\mu_1(A_i^{(3)}sin(m_i\pi) + B_i^{(3)}cos(m_i\pi)) = 0, \tag{6.40}$$

$$A_i^{(1)}cos(m_i\omega^U) + B_i^{(1)}sin(m_i\omega^U) = A_i^{(2)}cos(m_i\omega^U) + B_i^{(2)}sin(m_i\omega^U), \tag{6.41}$$

$$A_i^{(3)}cos(m_i\omega^L) + B_i^{(3)}sin(m_i\omega^L) = A_i^{(2)}cos(m_i\omega^L) + B_i^{(2)}sin(m_i\omega^L). \tag{6.42}$$

The algebraic form of the previous equations can be on the from $MV = 0$, where M is a 6-by-6 matrix and V is a column vector by 6 lines regrouping all the unknown constants for every order. To have a non trivial solution for the harmonic problem taking into account the conditions (26-28), one sufficient condition governing the singularity power coefficients m_i is:

$$D = \det(M) = 0, \tag{6.43}$$

which can explicitly expressed as:

$$sin(2m_i\pi) + \delta sin(2m_i\omega^U) - \delta sin(2m_i\omega^L) - \delta^2 sin(2m_i(\omega^L + \pi - \omega^U)) = 0, \tag{6.44}$$

with $\delta = \frac{1-\frac{\mu_1}{\mu_2}}{1+\frac{\mu_1}{\mu_2}} = \frac{\mu_2-\mu_1}{\mu_2+\mu_1}$ is a dimensionless parameter defined in section 2 which is function of the rigidity ratio $\frac{\mu_1}{\mu_2}$. It is clear that δ is a decreasing function of the relative ratio of rigidity $\frac{\mu_1}{\mu_2}$. Therefore, δ can be seen as a relative measure of the rigidity gap between the two considered materials. The eigenvalues equation governing the singularity exponents $\{m_i\}_i$ for a wide range of geometrical and material configurations is a function of geometrical angles (ω^U, ω^L) and the dimensionless material parameter δ. In other words, the parameters $\{m_i\}_i$ are the exponents of the radial terms in the displacement asymptotic expansion. These parameters evaluate how much singular are the asymptotic terms of the different *Cauchy stress tensor* components (rate of divergence when $R \to 0$). It is diffuclt to have analytical solutions for equation (6.44) for every value of δ, ω^U and ω^L. That is why, we will discuss the numerical solutions for three particular geometrical configurations

as it is shown in figure (6.3):

- $\omega^L = 0$,
- $\omega^U = -\omega^L$,
- $\omega^U - \omega^L = \pi$.

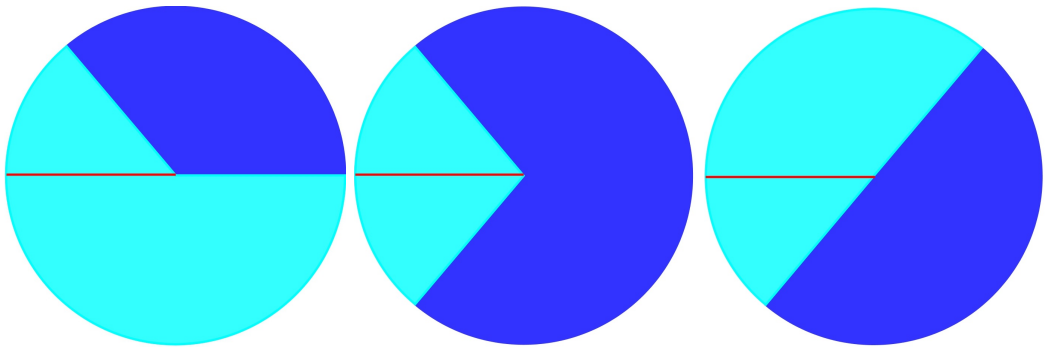

(a) Case $\omega^L = 0$ (b) Case $\omega^U = -\omega^L$ (c) Case $\omega^U - \omega^L = \pi$

Figure 6.3: Different cases to be treated

The singular terms of the *Cauchy stress tensor* are different from component to another. For the σ_{13} and σ_{23} (see equations (6.33-6.34)), the singularity source is derived from the terms R^{m_i-1}. Although, the singularity of the σ_{33} is a result of the terms R^{2m_i-2} and $R^{m_i+m_j-2}$. Then, it is clear that in all cases, σ_{33} is the most singular among the *Cauchy stress tensor* components. Thus, we extract from this remark that in the case of an anti-plane transformation, every material particle locally in the vicinity of the crack tip is essentially in state of tensile in the $\vec{E}_3$ direction.

We will focus, in the following analysis for the different cases treated here, on the behaviour of the different combinations of the m_i, eigenvalues equation solutions, relative to the clearance δ of the bi-material composite and the angular variables describing such a particular configuration.

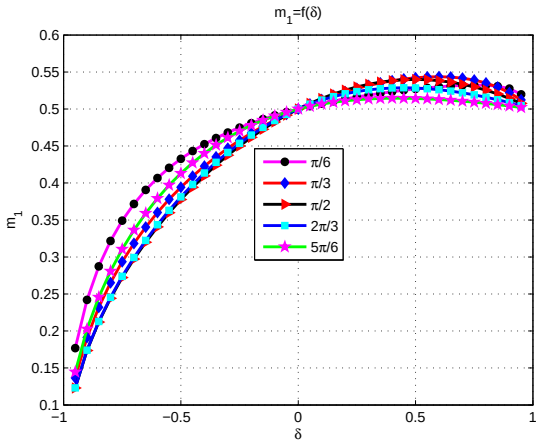

Figure 6.4: Case $\omega^L = 0$: $m_1 = f(\delta)$

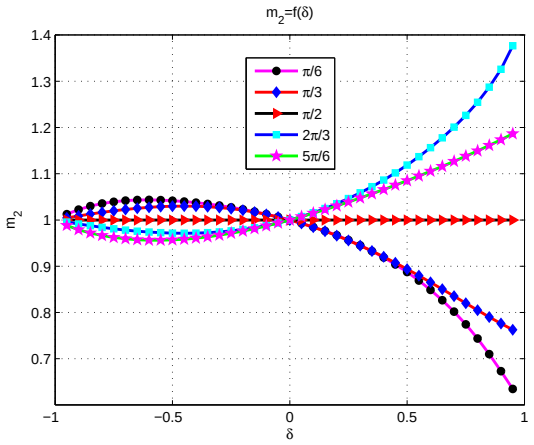

Figure 6.5: Case $\omega^L = 0$: $m_2 = f(\delta)$

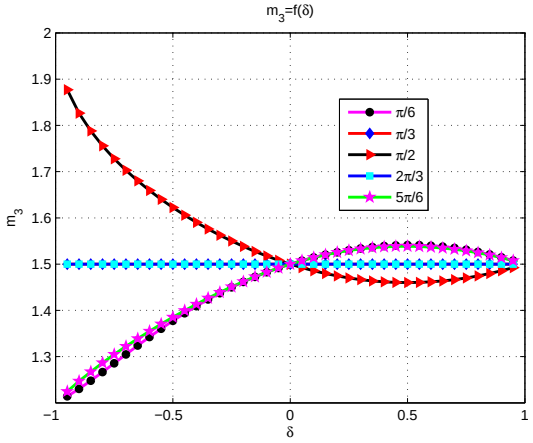

Figure 6.6: Case $\omega^L = 0$: $m_3 = f(\delta)$

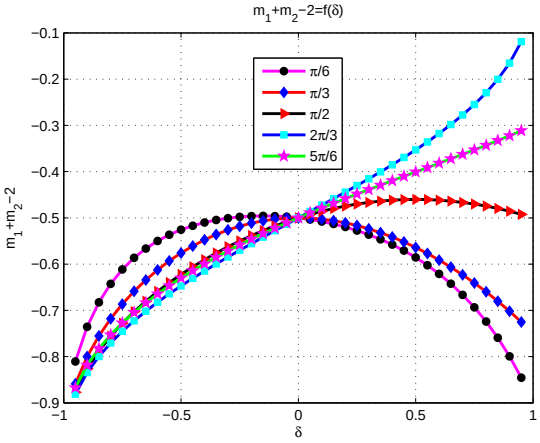

Figure 6.7: Case $\omega^L = 0$: $m_1 + m_2 - 2 = f(\delta)$

6.3.1 Configuration $\omega^L = 0$

In this instance where $\omega^L = 0$, the bi-material composite can be seen as an assembly of an homogenous half plane part bonded to a composite half plane. For every value of ω^U varying in $]0 \ \ \pi[$, the eigenvalues equation leading to the singularity orders becomes:

$$sin(2m\pi) + \delta sin(2m\omega^U) - \delta^2 sin(2m(\pi - \omega^U)) = 0, \quad -1 < \delta < 1, \quad \omega^U \in]0 \ \ \pi[. \tag{6.45}$$

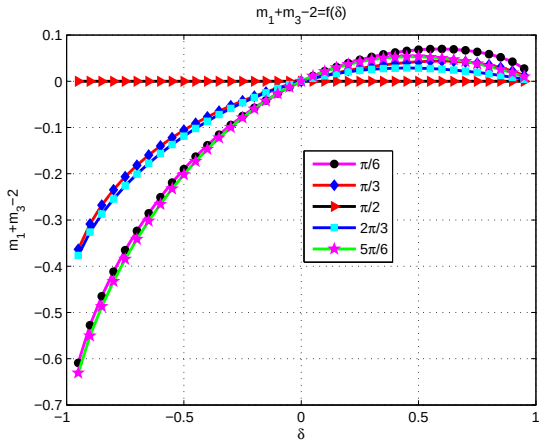

Figure 6.8: Case $\omega^L = 0$: $m_1 + m_3 - 2 = f(\delta)$

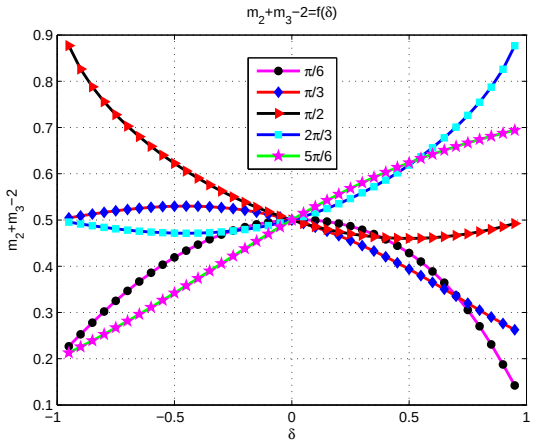

Figure 6.9: Case $\omega^L = 0$: $m_2 + m_3 - 2 = f(\delta)$

The existence of one solution to equation (6.45) in]0 1[is assured as it is shown in figure (6.4). Otherwise, it may have more than one admissible solution (at most 2 solutions in the gap]0 1[). To have the second singularity order in the interval]0 1[, one sufficient condition needs to be verified: in the upper-half cylinder, the part which is more rigid has to have the smallest angular sector. In the case where $\delta > 0$ (respectively $\delta < 0$), first order coefficient m_1 (respectively m_2) seems to not vary so much near the value $m_1 = \frac{1}{2}$ (repectively $m_2 = 1$) as it is illustrated in figure (6.4) (respectively figure (6.5)). Though, the first order power's coefficient m_1 collapses drastically when the first material becomes more rigid than the second one ($\mu_1 > \mu_2$). We notice here the independence of the bi-material composition, for the solutions $m_2 = 1$ for $\omega^U = \frac{\pi}{2}$ and $m_3 = \frac{3}{2}$ for both $\omega^U = \frac{\pi}{3}$ and $\omega^U = \frac{2\pi}{3}$. The fact of independence of the material composition for some solutions of the eigenvalues equation might be not surprising, since Ru in [Ru 1997b] found the same thing for special cases to some orders for a different geometrical configuration than ours. Whatever the rigidity or the geometrical distribution of the materials constituting the cylinder C, taking into account the assumption $\omega^L = 0$, the term $R^{m_1+m_2-2}$ is always singular (see figure (6.7)). However, the term $R^{m_1+m_3-2}$ contributes to the singularity of the component σ_{33} in one condition, when the first material is more rigid than the second one ($\mu_1 > \mu_2$) (see figure (6.8)). We notice in this case, that the terms R^{m_3-1} (see figure (6.6)), R^{2m_3-2} and $R^{m_3+m_2-2}$ (see figure (6.9)) are non singular for every material combination.

As a conclusion for this particular geometrical configuration, to outline the singular form of the shear components of the *Cauchy stress tensor*, we need at most the two first terms of the displacement asymptotic form, and only the first term in the case where the big part of the upper angular sector is the most rigid. As to the axial component σ_{33}, the singular behaviour can be illustrated using between 2 and 3 first terms of equation (6.31), and in the case where the first material is softer than the second one ($\mu_1 < \mu_2$), only the two first order are needed.

6.3.2 Configuration $\omega^U = -\omega^L$

This configuration is characterized by an assembly of two homogeneous equal-angle wedges : a V-notch and totally fractured one. Assuming $\omega^U = -\omega^L = \omega$, $\omega \in]0 \ \ \pi[$, we derive as equation to resolve:

$$sin(2m\pi) + 2\delta sin(2m\omega) - \delta^2 sin(2m(\pi - 2\omega)) = 0, \quad -1 < \delta < 1, \omega \in]0 \ \ \pi[. \tag{6.46}$$

We have proved numerically the following results:

$$m_1(\omega, \delta) = m_1(\pi - \omega, \delta), \tag{6.47}$$

$$m_2(\omega, \delta) = m_2(\pi - \omega, -\delta), \tag{6.48}$$

$$m_3(\omega, \delta) = m_3(\pi - \omega, \delta). \tag{6.49}$$

As it is illustrated in figure (6.10), the solution m_1 is increasing monotonically with the clearance variable δ. As the case described before, it is always guaranteed to have one solution in the gap $]0 \ \ 1[$. To have the second one in this gap, the sector that has an acute angle has to be the most rigid one as it is presented in figure (6.11). It is remarkable that when the first material is more rigid than the second one ($\mu_1 > \mu_2$), for any fixed value of δ, m_1 is maximal at $\omega = \frac{\pi}{2}$ (see figure (6.10)). In the other case m_1 is minimal at $\omega = \frac{\pi}{2}$ (see figure (6.10)). The singularity of the terms $\{R^{m_1+m_2-2}, R^{m_1+m_3-2}\}$ can be affirmative whenever $\delta < 0$ (see figures (6.13) and (6.14)). Whereas, for all material combinations in this case, the terms R^{m_3-1}, R^{2m_3-2} and $R^{m_3+m_2-2}$, found in the expressions of the different stress components, become non singular (see figures (6.12) and (6.15)).
As found below, we remark that the solutions $m_2 = 1$ for $\omega^U = \frac{\pi}{2}$ and $m_3 = \frac{3}{2}$ for the couple $\omega^U = \frac{\pi}{3}$ and $\omega^U = \frac{2\pi}{3}$ are independent of the material composition for this special geometrical configuration.

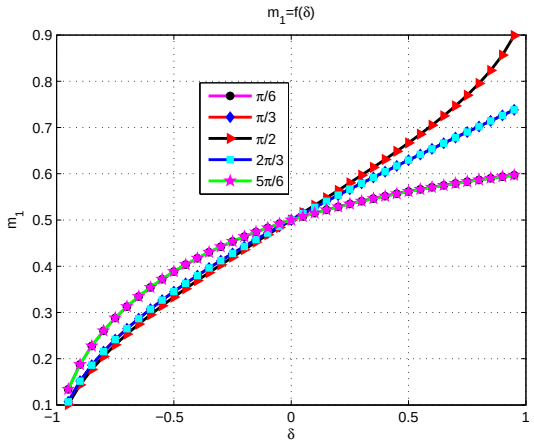

Figure 6.10: Case $\omega^U = -\omega^L$: $m_1 = f(\delta)$

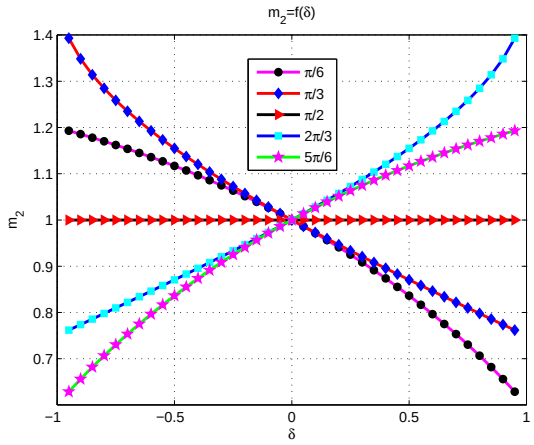

Figure 6.11: Case $\omega^U = -\omega^L$: $m_2 = f(\delta)$

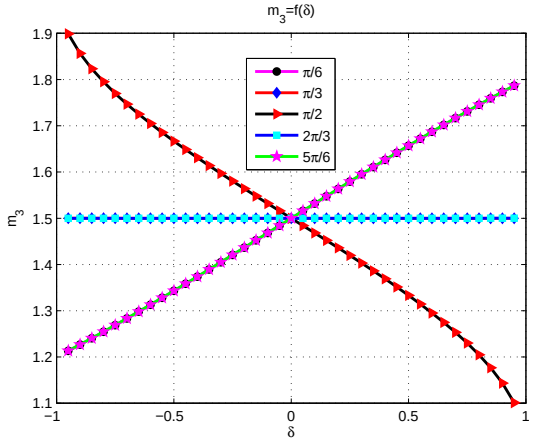

Figure 6.12: Case $\omega^U = -\omega^L$: $m_3 = f(\delta)$

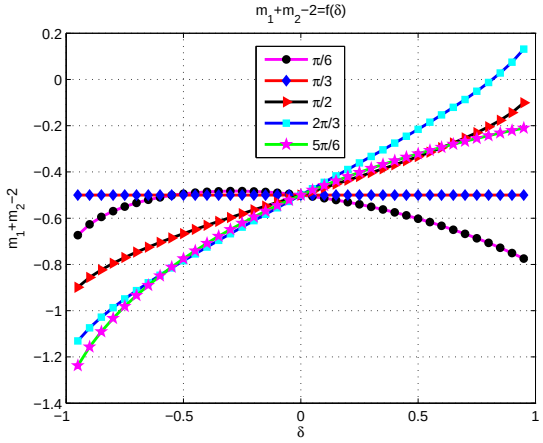

Figure 6.13: Case $\omega^U = -\omega^L$: $m_1 + m_2 - 2 = f(\delta)$

In this configuration, the singular terms of the *Cauchy stress tensor* σ_{13} and σ_{23} can be well pictured using the two first orders of the asymptotic form of diplacement field $u(.)$. When the big part of the upper-half cylinder becomes the most rigid one, the first order will be sufficient. For the component σ_{33}, to highlight it singular behaviour, the first three terms in the asymptotic form of the anti-plane displacement are needed at most. When the second material is more rigid than the first one ($\mu_2 > \mu_1$) we need at most the first two orders.

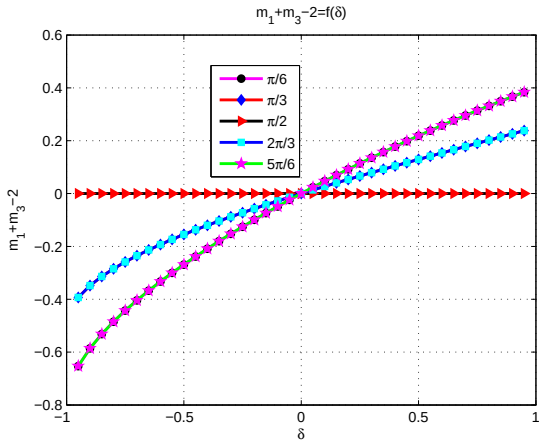

Figure 6.14: Case $\omega^U = -\omega^L$: $m_1 + m_3 - 2 = f(\delta)$

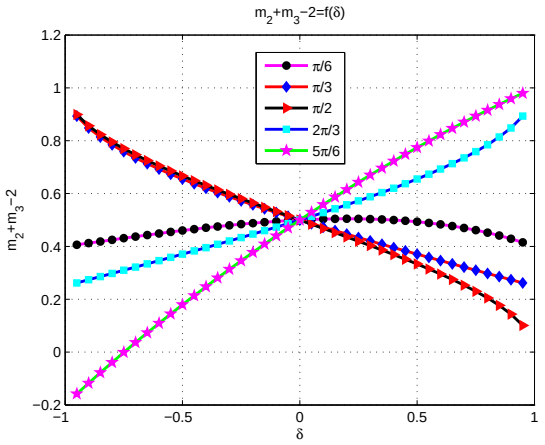

Figure 6.15: Case $\omega^U = -\omega^L$: $m_2 + m_3 - 2 = f(\delta)$

6.3.3 Configuration $\omega^U - \omega^L = \pi$

Here the geometrical state of the domain studied may be divided in two homogenous half-plane structures: a totaly fractured one bonded to the other structure. The geometrical distribution of the two materials is defined by $\omega^U - \omega^L = \pi$, $\omega^U = \omega \quad \in]0 \;\; \pi[$, that is why the eigenvalues equation can be remodeled to:

$$sin(2m\pi) + \delta sin(2m\omega) + \delta sin(2m(\pi - \omega)) = 0, \quad -1 < \delta < 1, \quad \omega \in]0 \;\; \pi[. \tag{6.50}$$

In this case, we have verified numerically, that the first and the third solutions (m_1 & m_3) for equation (6.50) are the same as the previous configuration where $\omega^U = -\omega^L$. It is clear here, that the second order power's coefficient $m_2 = 1$ is independent of δ and ω values. The mixed terms which are considered source of singular behaviour are reduced to only the terms $R^{m_1+m_3-2}$ in the condition where δ is strictly negative and $R^{m_1+m_2-2}$ (see figures (6.13) and (6.14)).

The first term of the anti-plane displacement's asymptotic form is sufficient to feature the singular behaviour of the shear components of the *Cauchy stress tensor*. However, we need the first between 2 and 3 terms to outline the same thing of the axial component σ_{33}. The third term is only needed when the second material is the most rigid one ($\mu_2 > \mu_1$) and $\omega^U \neq \frac{\pi}{2}$.

6.4 Investigation of the logarithmic singularities

The remark expressed in the presentation of Dempsey and Sinclair work can be reformulated here to be: if $u(.,.)$ is a solution of the differential equations (6.25-6.28), then the derivative of the solution u with respect to the singularity power's coefficient m holds as a solution whatever the order of the derivative operator. So if we choose in the beginning for the displacement field a singular form type of $O(R^m)$, by derivation we can investigate the presence of the singularities having the form $O(R^m log(R))$. By repeating the same process, the asymptotic form postulated in equation (6.30), can be exploited to inquiry the presence of singular forms in the type of $O(R^m(log(R))^n)$. Since it is demonstrated in [Grisvard 1992], that the only possible logarithmic singular form for the stress field in the case of harmonic problem, as in our case, is $(R^m log(R))$. So, our analysis requires the use of the presented method for once. Remarking the linearity of equations (6.25-6.28) describing the solution for the material configuration as it is presented above, we can use the final result as it is mentioned in [Dempsey 1979]: the singular form of the stress field can include $O(R^{m_i} log(R))$ in one condition, if m_i is a solution of the following system:

$$\begin{cases} MV = 0, \\ \frac{\partial M}{\partial m} V + M \frac{\partial V}{\partial m} = 0. \end{cases} \tag{6.51}$$

These two conditions are equivalent to:

$$D(m_i) = \frac{\partial D}{\partial m}(m_i) = ... = \frac{\partial^{(6-s)} D}{\partial m^{(6-s)}}(m_i) = 0, \tag{6.52}$$

where s denotes the rank of the matrix M. The previous investigations for the research of the m_i solution of the eigenvalues equation was carried out using the dichothomy method ensuring a scale of accuracy in the order of $error = O(10^{-15})$. In this stage, to seek the possibility of logarithmic singularities, a *Matlab* script is used to automate the whole process. For the matrix rank calculation, the *Matlab* "rank" function [Matlab R2012a User Guide 2012] was used. The algorithm used in *Matlab* is based on the singular values decompositions SVD which implies the following decomposition for the M matrix:

$$M = KYE, \tag{6.53}$$

where K and E are 6-by-6 orthogonal matrices, and Y is a positive diagonal matrix. And so the rank of the matrix M becomes the number of non-null diagonal terms of the matrix Y. In every case of the three geometrical configurations, for each value of ω^U or ω^L and δ, we seek the solutions of the eigenvalues equation (6.44), followed by the calculation of the matrix M rank. Then, we need to verify that the solution of equation (6.44) satisfies the relation (6.52). Consequently, we discovered that the singularity of the stress field can not be in the form of $O(R^m log(R))$ in the three cases studied above (see the added materials related to this paper), which justifies the used asymptotic form for the analysis in the third section.

6.5 Conclusion

In the present chapter, we have examined a particular geometrical configuration for a bi-material composite in the case of anti-plane shear transformation for a simple potential (Neo-Hookean). Based on the work of Dempsey and Sinclair in the scope of linear elasticity, their method is used here in the scope of large deformations to study the presence of logarithmic singularities. We proove in the case of Neo-hookean cylinder subjected to anti-plane transformation, that the only asymptotic singular form for the stress field, for the particular cases treated here, are just power form singularities $O(R^m)$. At most, the first three asymptotic terms are needed to highlight the singular behaviour of the *Cauchy stress* field in the vicinity of the crack tip. The power terms of the asymptotic form of the displacement field depend only on the parameters describing the geometrical distribution of the two materials and the gap of rigidity between the different sectors.

General conclusion and outlook

This thesis focuses on the analysis of initially-stressed materials in multiple scopes. Based on theory of invariants and some results of tensors algebra, this PhD presents in a new rigorous way some classical theoritical results related to the modeling of initially-stressed materials. Also a general explicit constitutive relation for initially-stressed linear elastic materials is established. Moreover, the anisotropy generated by the initial stress presence is discussed in analogy with the constitutive formulations used to describe fibrous materials behaviour. Also, a formulation for the plane deformations is performed generalizing the concept of Airy stress function.

Since the anisotropy is an essential element to study initially-stressed materials, a part of this PhD is devoted to study the anisotropic influence on some singular and regular boundary value problems. Indeed, in studying the basic constitutive models of elasticity with residual stresses, we have pointed out a certain âĂİequivalenceâĂİ of this theory with the constitutive equations of transverse isotropic or orthotropic materials. By going deep in such a topic, and focusing on the class of isotropic transverse materials, we have realized the possibility to exploit some particularities of these materials to couple various deformation modes in a clever way. This fact suggests using anisotropy to design some elastic machines which can couple different kinematic or deformation modes.

In general, the global anisotropic material can be seen locally as the junction of two or more separate isotropic material bodies. Hence, to study the anisotropic effect on the scope of singular problems, we have considered a cracked hyperelastic bi-material composite subjected to an antiplane deformation. An asymptotic analysis is performed to identify the sufficient orders contributing to the singular form of the Cauchy stress static fields. This study leads to the absence of logarithmic singularities, and to the fact that the exponent parameters of the singular terms depend on the geometrical configuration of the rigidity distribution of the bi-material composite.

Since the initial stress field is considered as a predefined parameter, the identification of such an internal field is an essential task for the characterization of initially-stressed materials. Two stability estimates are derived: the first one concerns the identification of all the material parameters for a generalized initially-stressed linear elastic material,

whereas the second one is dedicated to the residual stress reconstruction in the case of a relatively simple model. Also, a direct method is used for the identification of the residual stress and the material parameters using multiple noisy full-field displacement data. Different techniques of regularization are adopted, and an analysis of the different parameters influencing the quality of the reconstructed fields is carried out.

Furthermore, a special attention is dedicated to the analysis of the initial stress field influence on the mechanical fields near a crack tip through an incompressible hyperelastic material. We have shown that the asymptotic expansion of the different mechanical fields are functions of the eigenvectors orientation relative to the crack plane and also a weighting parameter relating the shear modulus and the eigenvalues of the initial stress field. A comparison between the initially-stressed and the unstressed materials has been done through the different asymptotic expansions, and we have shown that the initial stress field can contribute to the rotation of the crack and it has an influence on the crack opening. Finally, based on the asymptotic expansion of the displacement field, a set of enrichment shape functions are chosen to be exploited using the Extended Finite Element Method (XFEM) method for the numerical analysis of this singular problem. A convergence and stability studies have been done to point out the influence of different numerical formulations on the convergence rate and the stability of the numerical results.

This Phd work can be completed by the generalization of the different constitutive formulations for the initially-stressed and initially-strained hyperelastic materials to take account of the inner anisotropy and more complex behaviors (plasticity, viscosity ...). Moreover, for the analysis of singular problems, a non-constant initial stress can be considered to point out in particular the influence of the residual stress class on the same boundary value problem. Also, different boundary conditions can be chosen. On the numerical level, more XFEM formulations can be tested in the objective to enhance the stability and the converce rate of the numerical solutions. Focusing on the identification part, the presented approach can be tested and ameliorated for more complex models. Also, the same work can be adapted for experimental data.

Appendix A: Investigation of the logarithmic singularities

Based on the approach explained in the section 4, here we present the related materials for the investigation on the logarithmic singularities. In fact, we show here the derivative of the eigenvalues equation $\frac{\partial D}{\partial m}(m_i)$ function of δ and ω, $i \in \{1, 2, 3\}$, where m_i are the first three solutions for the eigenvalues equation D. It is remarkable from the accompanying figures (from matlab) that $\frac{\partial D}{\partial m}(m_i)$ can not be null for any value of δ and ω, which confirms the absence of logarithmic singularities in the asymptotic expansion of the displacement field. We note also that you can find the 3d matlab figures accompanied to this manuscript.

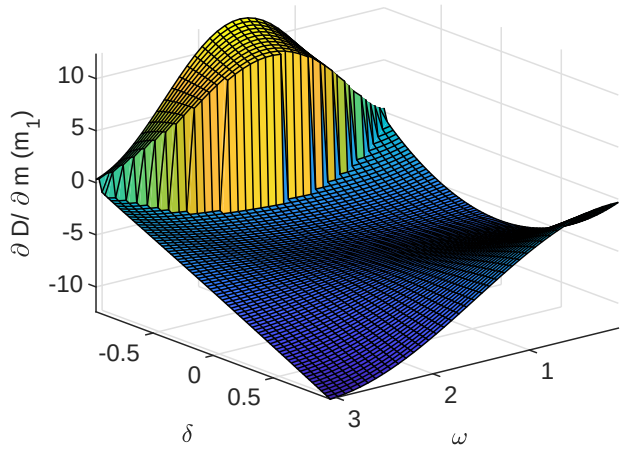

Figure A.1: Case $\omega^L = 0$: $\frac{dD}{dm}(m_1) = f(\delta, \omega)$

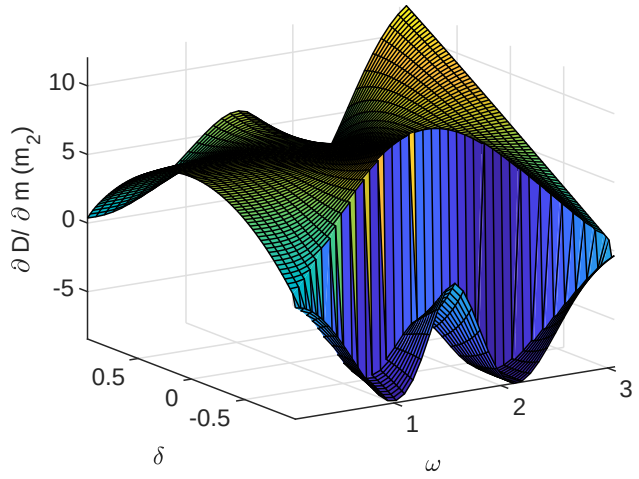

Figure A.2: Case $\omega^L = 0$: $\frac{dD}{dm}(m_2) = f(\delta, \omega)$

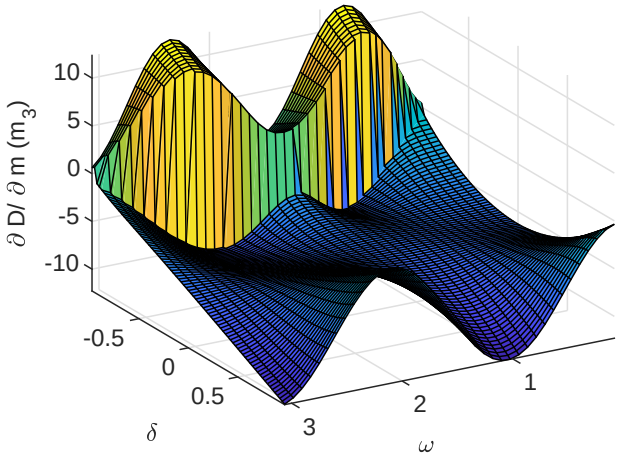

Figure A.3: Case $\omega^L = 0$: $\frac{dD}{dm}(m_3) = f(\delta, \omega)$

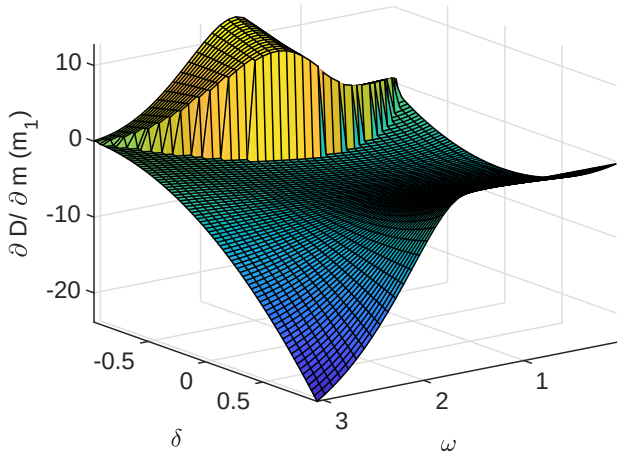

Figure A.4: Case $\omega^U = -\omega^L$: $\frac{dD}{dm}(m_1) = f(\delta, \omega)$

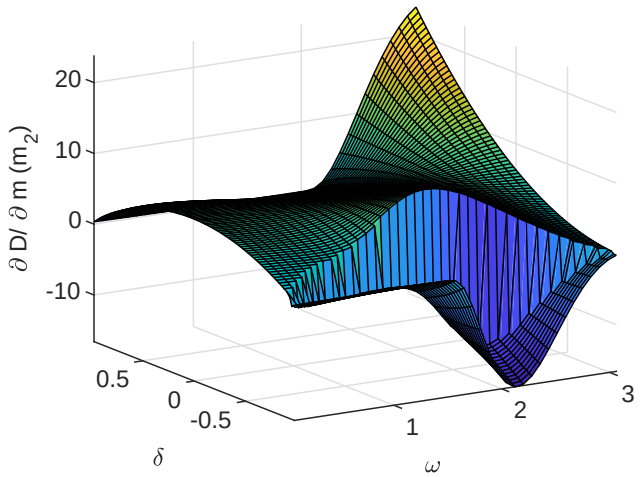

Figure A.5: Case $\omega^U = -\omega^L$: $\frac{dD}{dm}(m_2) = f(\delta, \omega)$

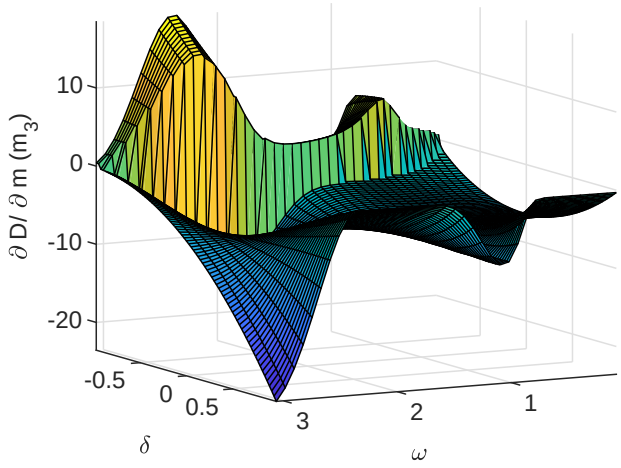

Figure A.6: Case $\omega^U = -\omega^L$: $\frac{dD}{dm}(m_3) = f(\delta, \omega)$

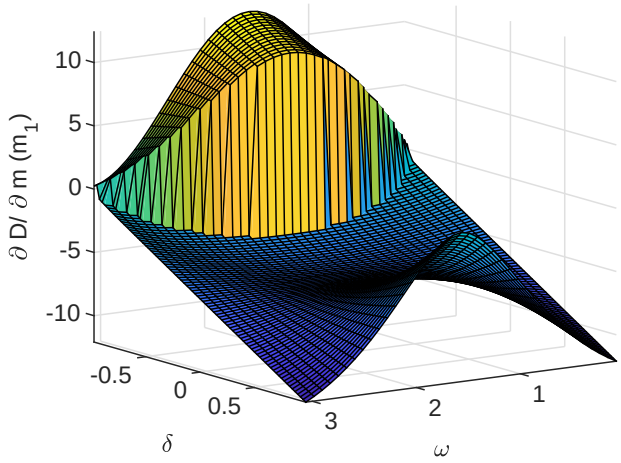

Figure A.7: Case $\omega^U - \omega^L = \pi$: $\frac{dD}{dm}(m_1) = f(\delta, \omega)$

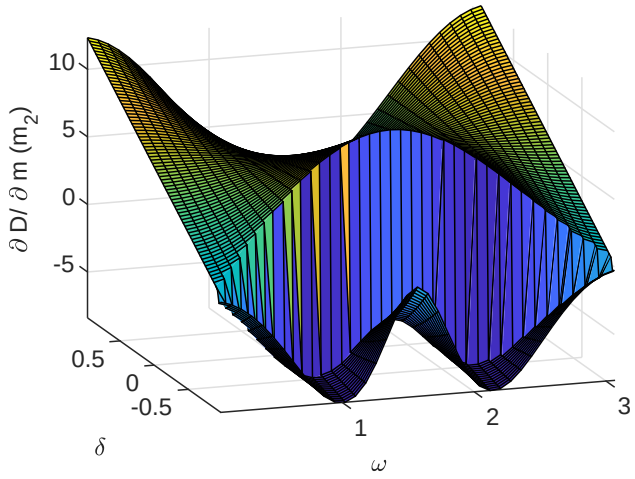

Figure A.8: Case $\omega^U - \omega^L = \pi$: $\frac{dD}{dm}(m_2) = f(\delta, \omega)$

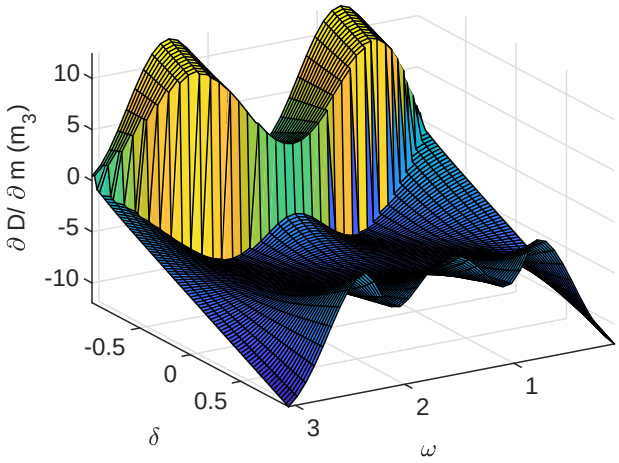

Figure A.9: Case $\omega^U - \omega^L = \pi$: $\frac{dD}{dm}(m_3) = f(\delta, \omega)$

Appendix B

Moment Optimisation

The explicit form of the fifth order polynomial equation in the M_r^2 unknown used in section 5 is given by:

$$b_5 M_r^{10} + b_4 M_r^8 + b_3 M_r^6 + b_2 M_r^4 + b_1 M_r^2 + b_0 = 0, \tag{B.1}$$

where

$$b_5 = -6(\hat{\mu}-1)^2[1+\hat{\mu}^2+(-(1/2)\hat{\beta}-2)\hat{\mu}]\hat{\beta}^2,$$

$$\begin{aligned} b_4 = {} & 8(\hat{\mu}-1)\{\hat{\mu}^4+(\hat{\beta}-4)\hat{\mu}^3+ \\ & -[(3/4)\hat{\beta}^2+3\hat{\beta}-6]\hat{\mu}^2+[(7/8)\hat{\beta}^2+3\hat{\beta}]\hat{\mu}-\hat{\beta}+1\}\hat{\beta}, \end{aligned}$$

$$\begin{aligned} b_3 = {} & 2(\hat{\mu}-1)\{\hat{\beta}^2\hat{\mu}^2+3\hat{\beta}\hat{\mu}^3-10\hat{\mu}^4-2\hat{\beta}^2\hat{\mu}+ \\ & -3\hat{\beta}\hat{\mu}^2+34\hat{\mu}^3-2\hat{\beta}\hat{\mu}-42\hat{\mu}^2+2\hat{\beta}+22\hat{\mu}-4\}\hat{\beta}, \end{aligned}$$

$$\begin{aligned} b_2 = {} & (16\hat{\beta}+8)\hat{\mu}^5-(12\hat{\beta}^2+70\hat{\beta}+40)\hat{\mu}^4+(2\hat{\beta}^3+29\hat{\beta}^2+122\hat{\beta}+80)\hat{\mu}^3+ \\ & -(\hat{\beta}^3+26\hat{\beta}^2+106\hat{\beta}+80)\hat{\mu}^2+(9\hat{\beta}^2+46\hat{\beta}+40)\hat{\mu}-8\hat{\beta}-8, \end{aligned}$$

$$\begin{aligned} b_1 = {} & -4\{1+\hat{\mu}^2-[(1/2)\hat{\beta}+2]\hat{\mu}\}\{1/2+(\hat{\beta}+3)\hat{\mu}^3+ \\ & -[(1/2)\hat{\beta}^2+3\hat{\beta}+11/2]\hat{\mu}^2+2\hat{\mu}\}, \end{aligned}$$

$$b_0 = (\hat{\beta}\hat{\mu}-2\hat{\mu}^2+4\hat{\mu}-2)(\hat{\beta}\hat{\mu}-2\hat{\mu}^2+3\hat{\mu}-1)\hat{\mu}.$$

Appendix C

Relations between invariants in case of 2 families of fibers in hyperelastic material

C.1 I_9 function of the rest of invariants

Let $\vec{M}_1$ and $\vec{M}_2$ denote the characteristic vectors to the fibers directions in the reference configuration. Hence, if the material body is considered to have a hyperelastic behaviour, then based on the theory of invariants developed by Boehler and Spencer in [Boehler 1987b], the strain energy W is expressed in terms of the following invariants:

$$I_1 = tr(\boldsymbol{C}), \quad I_2 = \frac{1}{2}(I_1^2 - tr(\boldsymbol{C}^2)), \quad I_3 = det(\boldsymbol{C}), \tag{C.1}$$

$$I_4 = \vec{M}_1.\boldsymbol{C}.\vec{M}_1, \quad I_5 = \vec{M}_1.\boldsymbol{C}^2.\vec{M}_1, \quad I_6 = \vec{M}_2.\boldsymbol{C}.\vec{M}_2, \tag{C.2}$$

$$I_7 = \vec{M}_2.\boldsymbol{C}^2.\vec{M}_2, \quad I_8 = \vec{M}_1.\boldsymbol{C}.\vec{M}_2, \quad I_9 = \vec{M}_1.\boldsymbol{C}^2.\vec{M}_2, \quad I_{10} = \vec{M}_1.\vec{M}_2. \tag{C.3}$$

I_8, I_9 and I_{10} are usually denoted as semi-invariants because they depend of the vectors orientation for both $\vec{M}_1$ and $\vec{M}_2$. Thus to avoid this problem, the dependence of the energy potential W of the semi-invariants has to be through the following quantities:

$$I_8: \ \tilde{I}_{81} = I_{10}I_8 = (\vec{M}_1.\boldsymbol{C}.\vec{M}_2)(\vec{M}_1.\vec{M}_2), \quad \tilde{I}_{82} = I_8^2 = (\vec{M}_1.\boldsymbol{C}.\vec{M}_2)^2. \tag{C.4}$$

$$I_9: \ \tilde{I}_{91} = I_{10}I_9 = (\vec{M}_1.\boldsymbol{C}^2.\vec{M}_2)(\vec{M}_1.\vec{M}_2), \quad \tilde{I}_{92} = I_9^2 = (\vec{M}_1.\boldsymbol{C}.\vec{M}_2)^2. \tag{C.5}$$

$$I_{10}: \ \tilde{I}_{10} = I_{10}^2 = (\vec{M}_1.\vec{M}_2)^2. \tag{C.6}$$

Using the spectral theory, the Cauchy-Green strain tensor $\boldsymbol{C}$ can be put in the following form:

$$\boldsymbol{C} = \lambda_1^2\vec{u}_1 \otimes \vec{u}_1 + \lambda_2^2\vec{u}_2 \otimes \vec{u}_2 + \lambda_3^2\vec{u}_3 \otimes \vec{u}_3 \tag{C.7}$$

with λ_i denotes the principal strech relative to the principal vector $\vec{u}_i$. The vectors $(\vec{u}_1, \vec{u}_2, \vec{u}_3)$ constructs an orthonormal basis verifying:

$$\vec{u}_1 \otimes \vec{u}_1 + \vec{u}_2 \otimes \vec{u}_2 + \vec{u}_3 \otimes \vec{u}_3 = \mathbf{1}, \tag{C.8}$$

$$\vec{u}_i.\vec{u}_j = \delta_{ij}, \quad i,j \in \{1,2,3\}, \tag{C.9}$$

where δ_{ij} denotes the Kronecker operator. Using equations (C.9-C.9), the spectral form of the Cauchy-Green strain tensor becomes:

$$\boldsymbol{C} = (\lambda_1^2 - \lambda_3^2)\vec{u}_1 \otimes \vec{u}_1 + (\lambda_2^2 - \lambda_3^2)\vec{u}_2 \otimes \vec{u}_2 + \lambda_3^2\mathbf{1} \tag{C.10}$$

Now exploiting the spectral form of the $\boldsymbol{C}$ in equation (C.10) and the fact that $\vec{M}_1$ and $\vec{M}_2$ are two unit vectors, the above invariants are transformed to:

$$I_1 = \lambda_1^2 + \lambda_2^2 + \lambda_3^2, \tag{C.11}$$

$$I_2 = \lambda_1^2\lambda_2^2 + \lambda_1^2\lambda_3^2 + \lambda_2^2\lambda_3^2, \tag{C.12}$$

$$I_3 = \lambda_1^2\lambda_2^2\lambda_3^2, \tag{C.13}$$

$$I_4 = (\lambda_1^2 - \lambda_3^2)M_{11}^2 + (\lambda_2^2 - \lambda_3^2)M_{12}^2 + \lambda_3^2, \tag{C.14}$$

$$I_5 = (\lambda_1^4 - \lambda_3^4)M_{11}^2 + (\lambda_2^4 - \lambda_3^4)M_{12}^2 + \lambda_3^4, \tag{C.15}$$

$$I_6 = (\lambda_1^2 - \lambda_3^2)M_{21}^2 + (\lambda_2^2 - \lambda_3^2)M_{22}^2 + \lambda_3^2, \tag{C.16}$$

$$I_7 = (\lambda_1^4 - \lambda_3^4)M_{21}^2 + (\lambda_2^4 - \lambda_3^4)M_{22}^2 + \lambda_3^4, \tag{C.17}$$

$$I_8 = (\lambda_1^2 - \lambda_3^2)M_{21}M_{11} + (\lambda_2^2 - \lambda_3^2)M_{22}M_{12} + \lambda_3^2(\vec{M}_1.\vec{M}_2), \tag{C.18}$$

$$I_9 = (\lambda_1^4 - \lambda_3^4)M_{21}M_{11} + (\lambda_2^4 - \lambda_3^4)M_{22}M_{12} + \lambda_3^4(\vec{M}_1.\vec{M}_2), \tag{C.19}$$

whereas for the quantities defined above relative to the semi-invariants, they can be written as:

$$\begin{aligned}\tilde{I}_{81} &= M_{11}^2M_{21}^2\lambda_1^2 + \xi_1\lambda_2^2 + M_{12}^2M_{22}^2\lambda_2^2 + (1-M_{11}^2-M_{12}^2)(1-M_{21}^2-M_{22}^2)\lambda_3^2 \\ &\quad + \lambda_1^2\xi_1 + \lambda_1^2\xi_2 + \lambda_2^2\xi_3 + \lambda_3^2\xi_2 + \lambda_3^2\xi_3, \end{aligned} \tag{C.20}$$

$$\begin{aligned}\tilde{I}_{82} &= M_{11}^2M_{21}^2\lambda_1^4 + M_{12}^2M_{22}^2\lambda_2^4 + (1-M_{11}^2-M_{12}^2)(1-M_{21}^2-M_{22}^2)\lambda_3^4 \\ &\quad + 2\lambda_1^2\lambda_2^2\xi_1 + 2\lambda_1^2\lambda_3^2\xi_2 + 2\lambda_2^2\lambda_3^2\xi_3, \end{aligned} \tag{C.21}$$

$$\begin{aligned}\tilde{I}_{91} &= M_{11}^2M_{21}^2\lambda_1^4 + M_{12}^2M_{22}^2\lambda_2^4 + (1-M_{11}^2-M_{12}^2)(1-M_{21}^2-M_{22}^2)\lambda_3^4 \\ &\quad + \lambda_1^4\xi_1 + \lambda_1^4\xi_2 + \lambda_2^4\xi_1 + \lambda_2^4\xi_3 + \lambda_3^4\xi_2 + \lambda_3^4\xi_3, \end{aligned} \tag{C.22}$$

$$\begin{aligned}\tilde{I}_{92} &= M_{11}^2M_{21}^2\lambda_1^8 + M_{12}^2M_{22}^2\lambda_2^8 + (1-M_{11}^2-M_{12}^2)(1-M_{21}^2-M_{22}^2)\lambda_3^8 \\ &\quad + 2\lambda_1^4\lambda_2^4\xi_1 + 2\lambda_1^4\lambda_3^4\xi_2 + 2\lambda_2^4\lambda_3^4\xi_3, \end{aligned} \tag{C.23}$$

$$\tilde{I}_{10} = M_{11}^2M_{21}^2 + M_{12}^2M_{22}^2 + (1-M_{11}^2-M_{12}^2)(1-M_{21}^2-M_{22}^2) + 2\xi_1 + 2\xi_2 + 2\xi_3. \tag{C.24}$$

with

$$\xi_1 = M_{11}M_{12}M_{21}M_{22}, \tag{C.25}$$

$$\xi_1 = M_{11}M_{13}M_{21}M_{23}, \tag{C.26}$$

$$\xi_1 = M_{12}M_{13}M_{22}M_{23}. \tag{C.27}$$

Now, using the 4 equations (C.14-C.17), the quantities $(M_{11}^2, M_{12}^2, M_{21}^2, M_{22}^2)$ can be deduced in function of the principal streches $(\lambda_1, \lambda_2, \lambda_3)$ and the invariants (I_4, I_5, I_6, I_7). Exploiting the prior expressions $(M_{11}^2, M_{12}^2, M_{21}^2, M_{22}^2)$, then the set of equations (C.20,C.21,C.24) can be seen as a system of equations whose the unknowns are (ξ_1, ξ_2, ξ_3) which can be derived from both the invariants $(I_4, I_5, I_6, I_7, \tilde{I}_{81}, \tilde{I}_{82}, \tilde{I}_{10})$ and the principal streches $(\lambda_1, \lambda_2, \lambda_3)$. Consequentely, if the resulted equations relying the above quantities to the different invariants are injected into the equations (C.22-C.23), it implies:

$$2\tilde{I}_{91} = 2(\vec{M}_1.\vec{M}_2)I_9 = (1-(\vec{M}_1.\vec{M}_2)^2)I_2 + (2I_8(\vec{M}_1.\vec{M}_2) - I_4 - I_6)I_1 + I_6I_4 - I_8^2 + I_5 + I_7. \tag{C.28}$$

$$\tilde{I}_{92} = I_9^2 = I_7I_5 - (I_6I_4 - I_8^2)I_2 + (I_4 + I_6 - 2I_8(\vec{M}_1.\vec{M}_2))I_3. \tag{C.29}$$

C.2 I_8 function of the rest of invariants in case of orthogonal fibers

When the two families of the fibers presented in the reference configuration are orthogonal i.e

$$I_{10} = \vec{M}_1.\vec{M}_2 = 0 \tag{C.30}$$

which can be transformed to:

$$M_{11}^2 M_{21}^2 + M_{12}^2 M_{22}^2 + 2\xi_1 = (1 - M_{11}^2 - M_{12}^2)(1 - M_{21}^2 - M_{22}^2). \tag{C.31}$$

The invaraints $(I_1, I_2, I_3, I_4, I_5, I_6, I_7)$ keep the same expressions as they are mentioned in the equations (C.11-C.17),. Althought, the quantities defined relaive to the semi-invaraint I_8 become:

$$\begin{aligned}\tilde{I}_{82} &= M_{11}^2 M_{21}^2 \lambda_1^4 - 2M_{11}^2 M_{21}^2 \lambda_1^2 \lambda_3^2 + M_{11}^2 M_{21}^2 \lambda_3^4 + M_{12}^2 M_{22}^2 \lambda_2^4 - 2M_{12}^2 M_{22}^2 \lambda_2^2 \lambda_3^2 \\ &\quad + M_{12}^2 M_{22}^2 \lambda_3^4 + 2\xi_1(\lambda_1^2 \lambda_2^2 - \lambda_1^2 \lambda_3^2 - \lambda_2^2 \lambda_3^2 + \lambda_3^4) \qquad \text{(C.32)} \\ \tilde{I}_{81} &= 0. \qquad \text{(C.33)}\end{aligned}$$

Following the same approach as it is done in the general case in the above section, the quantities $(\vec{M}_{11}^2, \vec{M}_{12}^2, \vec{M}_{21}^2, \vec{M}_{22}^2)$ can be deduced from equations (C.14-C.17). Furthermore, the variable ξ_1 can derived from the equation (C.31). Therefore, all the different varaible relied to the vectors $\vec{M}_1$ and $\vec{M}_2$ can be expressed in function of the different invaraints and by consequence the only non vanishing invariant $\tilde{I}_{82}$ relied to the semi-invariant I_8 can be presented in function of the different involved invaraints as:

$$\tilde{I}_{82} = I_8^2 = I_6 I_4 - I_1(I_6 + I_4) + I_2 + I_5 + I_7. \tag{C.34}$$

Appendix D

Dimension of the space $\mathcal{V}(\mathbb{R})$ in chapter 4

Consider $\{\boldsymbol{A}^{(ij)}\}$ and $\{\boldsymbol{B}^{(mn)}\}$ the canonical bases of $S_6(\mathbb{R})$ and $S_3(\mathbb{R})$ respectively where every matrix $\boldsymbol{A}^{(ij)}$ can be defined as:

$$[\boldsymbol{A}^{(ij)}]_{kl} = \begin{cases} \delta_{ik}\delta_{jl} + \delta_{jk}\delta_{il} \text{ , if } i \neq j, \\ \delta_{ik}\delta_{il} \text{ , if } i = j \end{cases} \quad , \quad [\boldsymbol{B}^{(mn)}]_{kl} = \begin{cases} \delta_{mk}\delta_{nl} + \delta_{nk}\delta_{ml} \text{ , if } m \neq n, \\ \delta_{mk}\delta_{nl} \text{ , if } m = n \end{cases} \quad , \quad m, n = 1..3, \tag{D.1}$$

As illustrated in chapter 4, we can construct a family of matrices that spanned the space $\mathcal{V}(\mathbb{R})$ in the following way:

$$\mathcal{M} = \{\boldsymbol{M}_{S\sigma}\boldsymbol{A}^{(ij)}\boldsymbol{M}_{S\sigma}^{T}, \quad i, j = 1..6\} \cup \{\begin{bmatrix} \boldsymbol{B}^{(mn)} & \boldsymbol{0} & \boldsymbol{0} \\ \boldsymbol{0} & \boldsymbol{B}^{(mn)} & \boldsymbol{0} \\ \boldsymbol{0} & \boldsymbol{0} & \boldsymbol{B}^{(mn)} \end{bmatrix}, \quad m, n = 1..3\} \tag{D.2}$$

It is clear that the set $\mathcal{M}$ contains 27 matrices (27=21+6). We intend to prove that the family $\mathcal{M}$ is linearly independent and hence we can conclude that $\dim(\mathcal{V}(\mathbb{R})) = 27$.

Let us define the function $\mathcal{F}$ which transforms a symmetric $N \times N$ matrix into a $N!$ vector. In fact the operator F will regroup all the major diagonals one after one from the biggest to the smallest one. It is clear that the operator $\mathcal{F}$ is bijective. To understand the definition of this operator let us take 3×3-matrix $\boldsymbol{A}$ which can be explicitly presented as:

$$\boldsymbol{A} = \begin{bmatrix} a_{11} & a_{12} & a_{13} \\ a_{12} & a_{22} & a_{23} \\ a_{13} & a_{23} & a_{33} \end{bmatrix} \tag{D.3}$$

then we can deduce:

$$\mathcal{F}(\boldsymbol{A}) = \begin{bmatrix} a_{11} & a_{22} & a_{33} & a_{12} & a_{23} & a_{13} \end{bmatrix}^T \tag{D.4}$$

Consequently, if we denote by $\boldsymbol{M}$ the matrix defined as the linear operator related to the restriction of the operator $\mathcal{F}$ on the space $\mathcal{V}(\mathcal{R})$, then it can be explicitly presented as:

$$\boldsymbol{M} = \begin{bmatrix} \mathcal{F}(\boldsymbol{E}_1) & \dots & \mathcal{F}(\boldsymbol{E}_{27}) \end{bmatrix} \tag{D.5}$$

where $\{\boldsymbol{E}_k\}_{k=1}^{27}$ are the matrices of the set $\mathcal{M}$. Due to the cumbersome calculations, the matrix M has been constructed numerically and using the the module *numpy.linalg* in *Python*, we have derived that the $\text{rank}(\boldsymbol{M}) = 27$. Thus, using the bijectivity of $\mathcal{F}$, we can conclude that $\dim(\mathcal{V}(\mathbb{R})) = 27$.

Appendix E

Asymptotic expansion terms on the limit of ellipticity condition

E.1 Case1: $\xi \to 0$

if $\cos(\phi) = 0$

$$g(\theta)\sin^2(\frac{\bar{\theta}}{2}) = \begin{cases} o(\xi), & \text{if} \quad \cos(\hat{\theta}) = 0, \\ \frac{|\sin(\hat{\theta})|}{2\xi} + \mathcal{O}(\xi), & \text{if} \quad \cos(\hat{\theta}) \neq 0 \end{cases} \tag{E.1}$$

if $\cos(\phi) \neq 0$

$$g(\theta)\sin^2(\frac{\bar{\theta}}{2}) = \begin{cases} o(\xi), & \text{if} \quad \cos(\hat{\theta}) = 0, \\ \frac{|\cos(\hat{\theta})|}{2\xi}[1 - \frac{\cos(\phi)\cos(\hat{\theta})}{|\cos(\phi)\cos(\hat{\theta})|}] + \mathcal{O}(\xi^3), & \text{if} \quad \cos(\hat{\theta}) \neq 0 \end{cases} \tag{E.2}$$

E.2 Case2: $\xi \to +\infty$

if $\sin(\phi) = 0$

$$g(\theta)\sin^2(\frac{\bar{\theta}}{2}) = \begin{cases} o(\xi^{-1}), & \text{if} \quad \sin(\hat{\theta}) = 0, \\ \frac{\xi|\cos(\hat{\theta})|}{2} + \mathcal{O}(\xi^{-1}), & \text{if} \quad \sin(\hat{\theta}) \neq 0 \end{cases} \tag{E.3}$$

if $\cos(\phi) \neq 0$

$$g(\theta)\sin^2(\frac{\bar{\theta}}{2}) = \begin{cases} o(\xi^{-1}), & \text{if} \quad \sin(\hat{\theta}) = 0, \\ \frac{\xi|\sin(\hat{\theta})|}{2}[1 + \frac{\sin(\phi)\sin(\hat{\theta})}{|\sin(\phi)\sin(\hat{\theta})|}] + \mathcal{O}(\xi^{-3}), & \text{if} \quad \sin(\hat{\theta}) \neq 0 \end{cases} \tag{E.4}$$

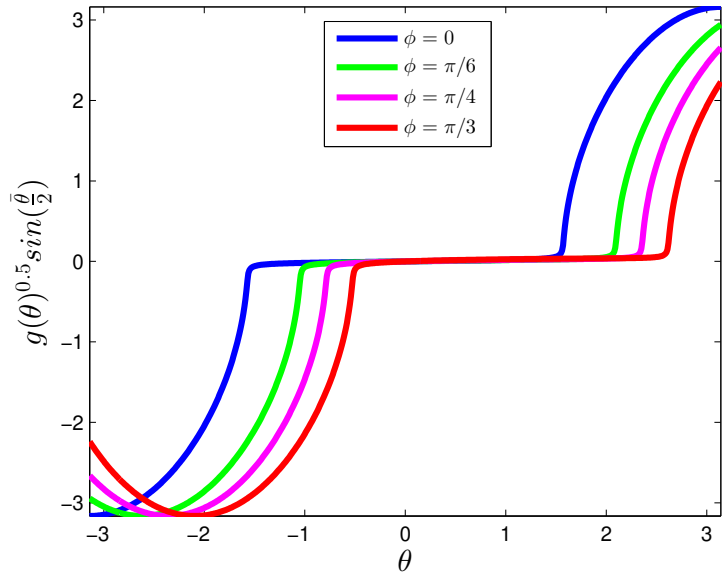

(a) $g^{\frac{1}{2}}(\theta)\sin(\frac{\bar{\theta}}{2})$

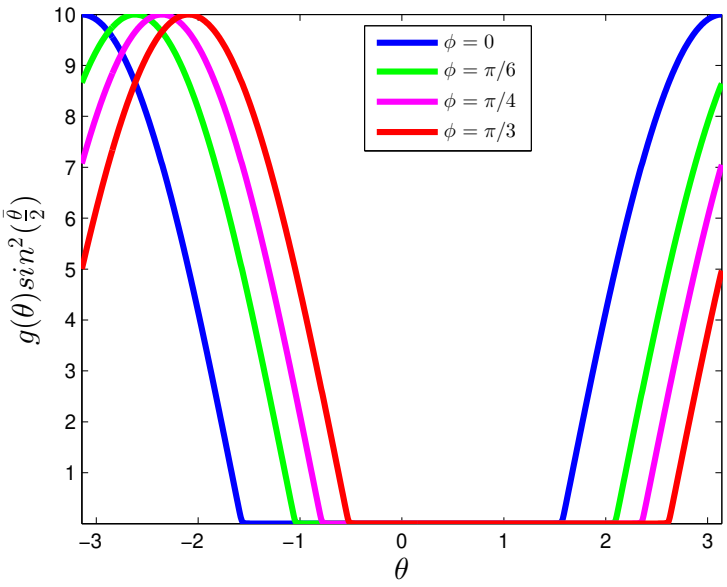

(b) $g(\theta)\sin^2(\frac{\bar{\theta}}{2})$

Figure E.1: Limit case when $\xi \to 0$

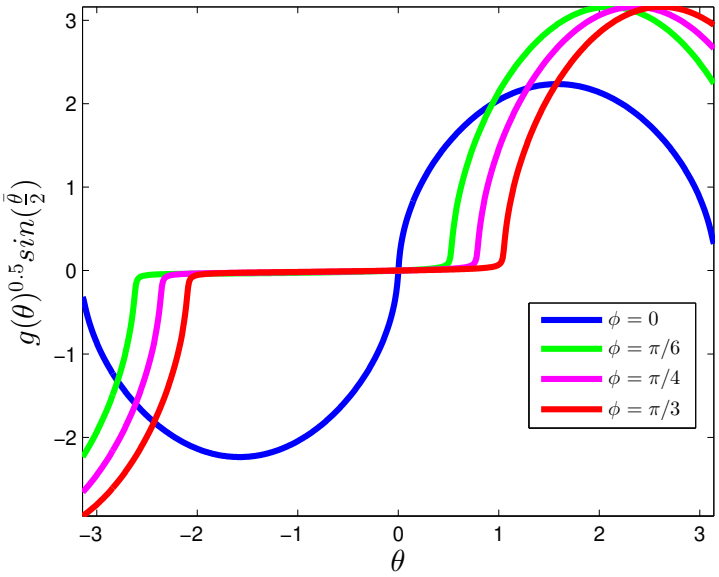

(a) $g^{\frac{1}{2}}(\theta)\sin(\frac{\bar{\theta}}{2})$

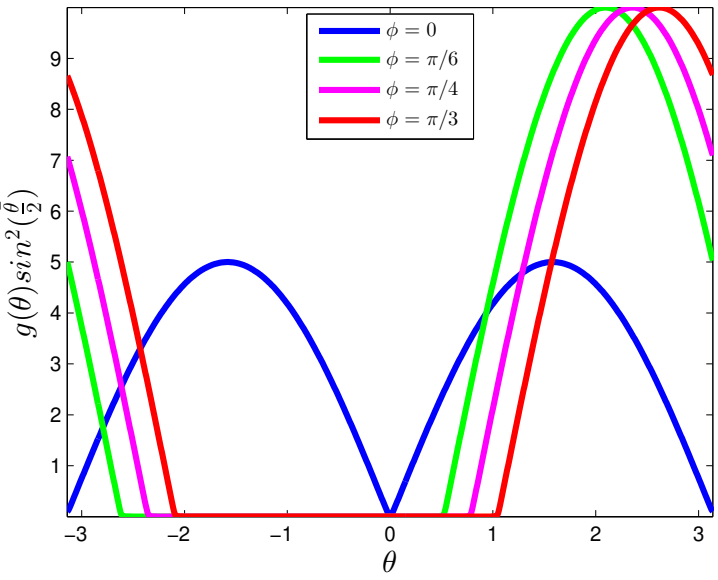

(b) $g(\theta)\sin^2(\frac{\bar{\theta}}{2})$

Figure E.2: Limit case when $\xi \to +\infty$

Bibliography

[Abdelaziz 2008] Yazid Abdelaziz and Abdelmadjid Hamouine. *A survey of the extended finite element.* Computers & structures, vol. 86, no. 11-12, pages 1141–1151, 2008. 190

[Agosti 2018] Abramo Agosti, Artur L Gower and Pasquale Ciarletta. *The constitutive relations of initially stressed incompressible Mooney-Rivlin materials.* Mechanics Research Communications, vol. 93, pages 4–10, 2018. 2, 5, 133

[Ahmad 1991] Jalees Ahmad. *A micromechanics analysis of cracks in unidirectional fiber composites.* ASME, Transactions, Journal of Applied Mechanics, vol. 58, pages 964–972, 1991. 206

[Amabili 2019] Marco Amabili, Prabakaran Balasubramanian, Isabella Bozzo, Ivan D Breslavsky and Giovanni Ferrari. *Layer-specific hyperelastic and viscoelastic characterization of human descending thoracic aortas.* Journal of the mechanical behavior of biomedical materials, vol. 99, pages 27–46, 2019. 130

[Amar 2005] Martine Ben Amar and Alain Goriely. *Growth and instability in elastic tissues.* Journal of the Mechanics and Physics of Solids, vol. 53, no. 10, pages 2284–2319, 2005. 2

[Amdouni 2012] Saber Amdouni, Khalil Mansouri, Yves Renard, Makrem Arfaoui and Maher Moakher. *Numerical convergence and stability of mixed formulation with X-FEM cut-off.* European Journal of Computational Mechanics, vol. 21, no. 3-6, pages 160–173, 2012. 195, 199, 200

[Areias 2005] Pedro MA Areias and Ted Belytschko. *Analysis of three-dimensional crack initiation and propagation using the extended finite element method.* International journal for numerical methods in engineering, vol. 63, no. 5, pages 760–788, 2005. 189

[Arfaoui 2018] Makrem Arfaoui, Mohamed Trifa, Khalil Mansouri, Amine Karoui and Yves Renard. *Three-dimensional singular elastostatic fields in a cracked Neo-Hookean hyperelastic solid.* International Journal of Engineering Science, vol. 128, pages 1–11, 2018. 150, 160

[Atkin 2005] Raymond John Atkin and Norman Fox. An introduction to the theory of elasticity. Courier Corporation, 2005. 68

[Babuška 1973] Ivo Babuška. *The finite element method with Lagrangian multipliers.* Numerische Mathematik, vol. 20, no. 3, pages 179–192, 1973. 188

[Babuška 1994] Ivo Babuška, Gabriel Caloz and John E Osborn. *Special finite element methods for a class of second order elliptic problems with rough coefficients.* SIAM Journal on Numerical Analysis, vol. 31, no. 4, pages 945–981, 1994. 134

[Babuška 1997] Ivo Babuška and Jens M Melenk. *The partition of unity method.* International journal for numerical methods in engineering, vol. 40, no. 4, pages 727–758, 1997. 134

[Bal 2014] Guillaume Bal, Cédric Bellis, Sébastien Imperiale and François Monard. *Reconstruction of constitutive parameters in isotropic linear elasticity from noisy full-field measurements.* Inverse Problems, vol. 30, no. 12, page 125004, 2014. 108, 111, 115

[Bal 2015] Guillaume Bal, François Monard and Gunther Uhlmann. *Reconstruction of a fully anisotropic elasticity tensor from knowledge of displacement fields.* SIAM Journal on Applied Mathematics, vol. 75, no. 5, pages 2214–2231, 2015. 96, 98, 99, 100

[Ballard 1994] P Ballard and A Constantinescu. *On the inversion of subsurface residual stresses from surface stress measurements.* Journal of the Mechanics and Physics of Solids, vol. 42, no. 11, pages 1767–1787, 1994. 90

[Banerjee 2004] Anuradha Banerjee and JW Hancock. *The role of constraint in the fields of a crack normal to the interface between elastically and plastically mismatched solids.* Journal of the Mechanics and Physics of Solids, vol. 52, no. 5, pages 1093–1108, 2004. 207

[Barnett 1997] DM Barnett and HOK Kirchner. *A proof of the equivalence of the Stroh and Lekhnitskii sextic equations for plane anisotropic elastostatics.* Philosophical Magazine A, vol. 76, no. 1, pages 231–239, 1997. 66

[Barsoum 2009] Zuheir Barsoum and Imad Barsoum. *Residual stress effects on fatigue life of welded structures using LEFM.* Engineering failure analysis, vol. 16, no. 1, pages 449–467, 2009. 132

[Béchet 2005] Éric Béchet, Hans Minnebo, Nicolas Moës and Bertrand Burgardt. *Improved implementation and robustness study of the X-FEM for stress analysis around cracks.* International journal for numerical methods in engineering, vol. 64, no. 8, pages 1033–1056, 2005. 192

[Belytschko 1999] Ted Belytschko and Tom Black. *Elastic crack growth in finite elements with minimal remeshing.* International journal for numerical methods in engineering, vol. 45, no. 5, pages 601–620, 1999. 134

[Belytschko 2001] Ted Belytschko, Nicolas Moës, Shuji Usui and Chandu Parimi. *Arbitrary discontinuities in finite elements.* International Journal for Numerical Methods in Engineering, vol. 50, no. 4, pages 993–1013, 2001. 189

[Belytschko 2007] Ted Belytschko and Robert Gracie. *On XFEM applications to dislocations and interfaces.* International Journal of Plasticity, vol. 23, no. 10-11, pages 1721–1738, 2007. 190

[Belytschko 2009] Ted Belytschko, Robert Gracie and Giulio Ventura. *A review of extended/generalized finite element methods for material modeling.* Modelling and Simulation in Materials Science and Engineering, vol. 17, no. 4, page 043001, 2009. 190

[Bigoni 2008] Davide Bigoni, Francesco Dal Corso and Massimiliano Gei. *The stress concentration near a rigid line inclusion in a prestressed, elastic material. Part II.: Implications on shear band nucleation, growth and energy release rate.* Journal of the Mechanics and Physics of Solids, vol. 56, no. 3, pages 839–857, 2008. 130, 133

[Biot 1965] Maurice A Biot and Jacques E Romain. *Mechanics of Incremental Deformations.* Physics Today, vol. 18, no. 11, page 68, 1965. 3, 132, 133

[Biot 1973] Maurice A Biot. *Nonlinear effect of initial stress on crack propagation between similar and dissimilar orthotropic media.* Quarterly of Applied Mathematics, vol. 30, no. 4, pages 379–406, 1973. 132, 133

[Blatz 1962] Paul J Blatz and William L Ko. *Application of finite elastic theory to the deformation of rubbery materials.* Transactions of the Society of Rheology, vol. 6, no. 1, pages 223–252, 1962. 24

[Blouin 1989] F Blouin and A Cardou. *A study of helically reinforced cylinders under axially symmetric loads and application to strand mathematical modelling.* International journal of solids and structures, vol. 25, no. 2, pages 189–200, 1989. 67

[Boehler 1987a] Jean-Paul Boehler and Jean-Paul Boehler. Applications of tensor functions in solid mechanics, volume 292. Springer, 1987. 21, 43

[Boehler 1987b] Jean-Paul Boehler and Jean-Paul Boehler. Applications of tensor functions in solid mechanics, volume 292. Springer, 1987. 55, 235

[Bogy 1970] D. B. Bogy. *On the problem of edge-bonded elastic quarter-planes loaded at the boundary.* International Journal of Solids and Structures, vol. 6, no. 9, pages 1287–1313, 1970. 214

[Bogy 1971a] D. B. Bogy. *Two edge-bonded elastic wedges of different materials and wedge angles under surface tractions.* Journal of Applied Mechanics, vol. 38, no. 2, pages 377–386, 1971. 206, 214

[Bogy 1971b] D. B. Bogy and K. C. Wang. *Stress singularities at interface corners in bonded dissimilar isotropic elastic materials.* International Journal of Solids and Structures, vol. 7, no. 8, pages 993–1005, 1971. 206, 214

[Bonnet 2005] Marc Bonnet and Andrei Constantinescu. *Inverse problems in elasticity.* Inverse problems, vol. 21, no. 2, page R1, 2005. 90

[Boyce 2000] Mary C Boyce and Ellen M Arruda. *Constitutive models of rubber elasticity: a review.* Rubber Chemistry and Technology, vol. 73, no. 3, pages 504–523, 2000. 211

[Brezzi 1974] Franco Brezzi. *On the existence, uniqueness and approximation of saddle-point problems arising from Lagrangian multipliers.* Publications mathématiques et informatique de Rennes, no. S4, pages 1–26, 1974. 188

[Brezzi 2012] Franco Brezzi and Michel Fortin. Mixed and hybrid finite element methods, volume 15. Springer Science & Business Media, 2012. 195

[Brunet 2019] J Brunet, B Pierrat, E Maire, J Adrien and P Badel. *A combined experimental-numerical lamellar-scale approach of tensile rupture in arterial medial tissue using X-ray tomography.* Journal of the mechanical behavior of biomedical materials, vol. 95, pages 116–123, 2019. 130

[Bui 2007] Huy Duong Bui. Fracture mechanics: inverse problems and solutions, volume 139. Springer Science & Business Media, 2007. 4, 90, 131

[Bui 2011] Huy Duong Bui. Imaging the cheops pyramid, volume 182. Springer Science & Business Media, 2011. 1

[Bustamante 2015] R Bustamante and KR Rajagopal. *Solutions of some boundary value problems for a new class of elastic bodies undergoing small strains. Comparison with the predictions of the classical theory of linearized elasticity: Part I. Problems with cylindrical symmetry.* Acta Mechanica, vol. 226, no. 6, pages 1815–1838, 2015. 38

[Bustamante 2016] R Bustamante, O Orellana, R Meneses and KR Rajagopal. *Large deformations of a new class of incompressible elastic bodies.* Zeitschrift für angewandte Mathematik und Physik, vol. 67, no. 3, page 47, 2016. 38

[Bustamante 2018] R Bustamante and KR Rajagopal. *Modelling residual stresses in elastic bodies described by implicit constitutive relations.* International Journal of Non-Linear Mechanics, vol. 105, pages 113–129, 2018. 38

[Cardamone 2009] L Cardamone, A Valentin, JF Eberth and JD Humphrey. *Origin of axial prestretch and residual stress in arteries.* Biomechanics and modeling in mechanobiology, vol. 8, no. 6, page 431, 2009. 1, 37

[Chahine 2008] Elie Chahine, Patrick Laborde and Yves Renard. *Crack tip enrichment in the XFEM using a cutoff function.* International journal for numerical methods in engineering, vol. 75, no. 6, pages 629–646, 2008. 134, 189

[Chao 1993] Y J Chao, MA Sutton and R Wu. *Determination of the asymptotic crack tip fields for a crack perpendicular to an interface between elastic-plastic materials.* Acta Mechanica, vol. 100, no. 1, pages 13–36, 1993. 207

[Chapelle 1993] Dominique Chapelle and Klaus-Jürgen Bathe. *The inf-sup test.* Computers & structures, vol. 47, no. 4-5, pages 537–545, 1993. 188

[Chaudhuri 2010] Reaz A Chaudhuri. *On three-dimensional singular stress/residual stress fields at the front of a crack/anticrack in an orthotropic/orthorhombic plate under anti-plane shear loading.* Composite structures, vol. 92, no. 8, pages 1977–1984, 2010. 132

[Chaudhuri 2012] Reaz A Chaudhuri. *Three-dimensional singular stress/residual stress fields at crack/anticrack fronts in monoclinic plates under antiplane shear loading.* Engineering Fracture Mechanics, vol. 87, pages 16–35, 2012. 132

[Chen 1996] J T Chen and W C Wang. *Experimental analysis of an arbitrarily inclined semiinfinite crack terminated at the bimaterial interface.* Experimental Mechanics, vol. 36, no. 1, pages 7–16, 1996. 206

[Chen 2003] SH Chen, TC Wang and Sharon Kao-Walter. *A crack perpendicular to the bimaterial interface in finite solid.* International Journal of Solids and Structures, vol. 40, no. 11, pages 2731–2755, 2003. 206

[Chen 2012] Chih Hao Chen, Chein Lee Wang and Chun Chih Kuo. *Solutions for antiplane problems of a composite material with a crack terminating at the interface.* Archive of Applied Mechanics, vol. 82, no. 9, pages 1233–1250, 2012. 206

[Chessa 2003a] Jack Chessa and Ted Belytschko. *An extended finite element method for two-phase fluids.* J. Appl. Mech., vol. 70, no. 1, pages 10–17, 2003. 190

[Chessa 2003b] Jack Chessa, Hongwu Wang and Ted Belytschko. *On the construction of blending elements for local partition of unity enriched finite elements.* International Journal for Numerical Methods in Engineering, vol. 57, no. 7, pages 1015–1038, 2003. 192

[Chien-Ching 1990] Ma Chien-Ching and Hour Bao-Luh. *Antiplane problems in composite anisotropic materials with an inclined crack terminating at a bimaterial interface.* International Journal of Solids and Structures, vol. 26, no. 12, pages 1387–1400, 1990. 206

[Chuong 1986] Cheng-Jen Chuong and Yuan-Cheng Fung. *Residual stress in arteries.* In Frontiers in biomechanics, pages 117–129. Springer, 1986. 2

[Ciarletta 2016a] Pasquale Ciarletta, Michel Destrade and Artur L Gower. *On residual stresses and homeostasis: an elastic theory of functional adaptation in living matter.* Scientific reports, vol. 6, no. 1, pages 1–8, 2016. 2, 5, 133

[Ciarletta 2016b] Pasquale Ciarletta, Michel Destrade, Artur L Gower and Matteo Taffetani. *Morphology of residually stressed tubular tissues: Beyond the elastic multiplicative decomposition.* Journal of the Mechanics and Physics of Solids, vol. 90, pages 242–253, 2016. 5, 133

[Coleman 1964] Bernard D Coleman and Walter Noll. *Material symmetry and thermostatic inequalities in finite elastic deformations.* Archive for Rational Mechanics and Analysis, vol. 15, no. 2, pages 87–111, 1964. 3, 37, 41, 50

[Cook 1972] TS Cook and F Erdogan. *Stresses in bonded materials with a crack perpendicular to the interface.* International Journal of Engineering Science, vol. 10, no. 8, pages 677–697, 1972. 206

[Costabel 1982] Martin Costabel and Ernst Stephan. Curvature terms in the asymptotic expansions for solutions of boundary integral equations on curved polygons. Techn. Hochsch., Fachbereich Mathematik, 1982. 213

[Costello 1997] George A Costello. Theory of wire rope. Springer Science & Business Media, 1997. 68

[Craciun 2018] EM Craciun, M Marin and A Rabaea. *Anti-plane crack in human bone. I. Mathematical modelling.* ANALELE STIINTIFICE ALE UNIVERSITATII OVIDIUS CONSTANTA-SERIA MATEMATICA, vol. 26, no. 1, pages 81–90, 2018. 132

[Creton 2016] Costantino Creton and Matteo Ciccotti. *Fracture and adhesion of soft materials: a review.* Reports on Progress in Physics, vol. 79, no. 4, page 046601, 2016. 130

[Crossley 2003] JA Crossley, AH England and AJM Spencer. *Bending and flexure of cylindrically monoclinic elastic cylinders.* International journal of solids and structures, vol. 40, no. 25, pages 6999–7013, 2003. 67

[Dal Corso 2008] Francesco Dal Corso, Davide Bigoni and Massimiliano Gei. *The stress concentration near a rigid line inclusion in a prestressed, elastic material. part i.: Full-field solution and asymptotics.* Journal of the Mechanics and Physics of Solids, vol. 56, no. 3, pages 815–838, 2008. 130, 133

[Delfin 1995] P Delfin, Jens Gunnars and P Stárhle. *Effect of elastic mismatch on the growth of a crack initially terminated at an interface in elastic plastic bimaterials.* Fatigue & Fracture of Engineering Materials & Structures, vol. 18, no. 10, pages 1201–1212, 1995. 207

[Dempsey 1979] J. P. Dempsey and G. B. Sinclair. *On the stress singularities in the plane elasticity of the composite wedge.* Journal of Elasticity, vol. 9, no. 4, pages 373–391, oct 1979. 214, 223

[Deng 2008] Dean Deng and Hidekazu Murakawa. *Prediction of welding distortion and residual stress in a thin plate butt-welded joint.* Computational Materials Science, vol. 43, no. 2, pages 353–365, 2008. 36

[Destrade 2012a] Michel Destrade, Yi Liu, Jeremiah G Murphy and Ghassan S Kassab. *Uniform transmural strain in pre-stressed arteries occurs at physiological pressure.* Journal of theoretical biology, vol. 303, pages 93–97, 2012. 133

[Destrade 2012b] Michel Destrade, Jerry G Murphy and Giuseppe Saccomandi. *Simple shear is not so simple.* International Journal of Non-Linear Mechanics, vol. 47, no. 2, pages 210–214, 2012. 206

[Destrade 2013] Michel Destrade and Ray W Ogden. *On stress-dependent elastic moduli and wave speeds.* The IMA Journal of Applied Mathematics, vol. 78, no. 5, pages 965–997, 2013. 139

[Destuynder 1982] P Destuynder, M Djaoua and S Lescure. *A new method for calculating stress intensity factors.* Strojnicky Cas., vol. 33, no. 4, pages 395–400, 1982. 131

[Dhaliwal 1979] Ranjit S Dhaliwal and Brij Mohan Singh. *Plane-strain problem of two coplanar cracks in an initially stressed neo-Hookean elastic layer.* Quarterly of Applied Mathematics, vol. 36, no. 4, pages 361–376, 1979. 133

[Drory 1988] Michael David Drory, Michael D Thouless and Anthony G Evans. *On the decohesion of residually stressed thin films.* Acta metallurgica, vol. 36, no. 8, pages 2019–2028, 1988. 130

[Du 2018] Yangkun Du, Chaofeng Lü, Weiqiu Chen and Michel Destrade. *Modified multiplicative decomposition model for tissue growth: Beyond the initial stress-free state.* Journal of the Mechanics and Physics of Solids, vol. 118, pages 133–151, 2018. 5, 133

[Du 2019a] Yangkun Du, Chaofeng Lü, Michel Destrade and Weiqiu Chen. *Influence of initial residual stress on growth and pattern creation for a layered aorta.* Scientific reports, vol. 9, no. 1, pages 1–9, 2019. 5, 133

[Du 2019b] Yangkun Du, Chaofeng Lü, Congshan Liu, Zilong Han, Jian Li, Weiqiu Chen, Shaoxing Qu and Michel Destrade. *Prescribing patterns in growing tubular soft*

matter by initial residual stress. Soft matter, vol. 15, no. 42, pages 8468–8474, 2019. 5, 133

[Duan 2010] Benchun Duan. *Role of initial stress rotations in rupture dynamics and ground motion: A case study with implications for the Wenchuan earthquake.* Journal of Geophysical Research: Solid Earth, vol. 115, no. B5, 2010. 1

[Duflot 2008] Marc Duflot. *The extended finite element method in thermoelastic fracture mechanics.* International Journal for Numerical Methods in Engineering, vol. 74, no. 5, pages 827–847, 2008. 189

[Dunham 2003] Eric M Dunham, Pascal Favreau and JM Carlson. *A supershear transition mechanism for cracks.* Science, vol. 299, no. 5612, pages 1557–1559, 2003. 1

[Ebrahimi 2021] S Hamed Ebrahimi. *Residual stress effects on crack-tip stress singularity in XFEM fracture analysis.* European Journal of Mechanics-A/Solids, vol. 86, page 104191, 2021. 131

[Erdogan 1973] Fazil Erdogan and V Biricikoglu. *Two bonded half planes with a crack going through the interface.* International Journal of Engineering Science, vol. 11, no. 7, pages 745–766, 1973. 206

[Erdogan 1974] Fi Erdogan and TS Cook. *Antiplane shear crack terminating at and going through a bimaterial interface.* International Journal of Fracture, vol. 10, no. 2, pages 227–240, 1974. 206

[Faghidian 2012] SA Faghidian, Dev Goudar, GH Farrahi and David J Smith. *Measurement, analysis and reconstruction of residual stresses.* The Journal of Strain Analysis for Engineering Design, vol. 47, no. 4, pages 254–264, 2012. 90

[Faghidian 2014] S Ali Faghidian. *A smoothed inverse eigenstrain method for reconstruction of the regularized residual fields.* International Journal of Solids and Structures, vol. 51, no. 25-26, pages 4427–4434, 2014. 4, 90

[Fenner 1976] DN Fenner. *Stress singularities in composite materials with an arbitrarily oriented crack meeting an interface.* International Journal of Fracture, vol. 12, no. 5, pages 705–721, 1976. 206

[Finger 1983] Larry W Finger. *Physical properties of crystals, their representation by tensors and matrices.* Eos, Transactions American Geophysical Union, vol. 64, no. 45, pages 643–643, 1983. 66

[Forte 1996] Sandra Forte and Maurizio Vianello. *Symmetry classes for elasticity tensors.* Journal of Elasticity, vol. 43, no. 2, pages 81–108, 1996. 66

[Friedman 1970] M Friedman and JM Logan. *Influence of residual elastic strain on the orientation of experimental fractures in three quartzose sandstones.* Journal of Geophysical Research, vol. 75, no. 2, pages 387–405, 1970. 36

[Fries 2010] Thomas-Peter Fries and Ted Belytschko. *The extended/generalized finite element method: an overview of the method and its applications.* International journal for numerical methods in engineering, vol. 84, no. 3, pages 253–304, 2010. 190

[Fung 1967] YC Fung. *Elasticity of soft tissues in simple elongation.* American Journal of Physiology-Legacy Content, vol. 213, no. 6, pages 1532–1544, 1967. 133

[Fung 1991] YC Fung. *What are the residual stresses doing in our blood vessels?* Annals of biomedical engineering, vol. 19, no. 3, pages 237–249, 1991. 36, 37

[Gao 1994] YC Gao and ZF Shi. *Large strain field near an interface crack tip.* International Journal of Fracture, vol. 69, no. 3, pages 269–279, 1994. 208

[Gao 2008] Yu Chen Gao, Ming Jin and Guan Suo Dui. *Stresses, singularities, and a complementary energy principle for large strain elasticity.* Applied Mechanics Reviews, vol. 61, no. 3, page 030801, 2008. 208

[Gerstenberger 2008] Axel Gerstenberger and Wolfgang A Wall. *An extended finite element method/Lagrange multiplier based approach for fluid–structure interaction.* Computer Methods in Applied Mechanics and Engineering, vol. 197, no. 19-20, pages 1699–1714, 2008. 190

[Geubelle 1994a] Philippe H Geubelle and Wolfgang G Knauss. *Finite strains at the tip of a crack in a sheet of hyperelastic material: I. Homogeneous case.* Journal of Elasticity, vol. 35, no. 1, pages 61–98, 1994. 208

[Geubelle 1994b] Philippe H Geubelle and Wolfgang G Knauss. *Finite strains at the tip of a crack in a sheet of hyperelastic material: II. Special bimaterial cases.* Journal of Elasticity, vol. 35, no. 1, pages 99–137, 1994. 208

[Geubelle 1995] Philippe H Geubelle. *Finite deformation effects in homogeneous and interfacial fracture.* International Journal of Solids and Structures, vol. 32, no. 6-7, pages 1003–1016, 1995. 208

[Gifford Jr 1978] L Nash Gifford Jr and Peter D Hilton. *Stress intensity factors by enriched finite elements.* Engineering Fracture Mechanics, vol. 10, no. 3, pages 485–496, 1978. 134

[Gou 2014] Kun Gou and Jay R Walton. *Reconstruction of nonuniform residual stress for soft hyperelastic tissue via inverse spectral techniques.* International Journal of Engineering Science, vol. 82, pages 46–73, 2014. 4, 141

[Gower 2015] AL Gower, Pasquale Ciarletta and M Destrade. *Initial stress symmetry and its applications in elasticity.* Proceedings of the Royal Society A: Mathematical, Physical and Engineering Sciences, vol. 471, no. 2183, page 20150448, 2015. 4, 5, 38, 46, 47, 90, 133, 140

[Gower 2017] Artur L Gower, Tom Shearer and Pasquale Ciarletta. *A new restriction for initially stressed elastic solids.* The Quarterly Journal of Mechanics and Applied Mathematics, vol. 70, no. 4, pages 455–478, 2017. 4, 5, 38, 47, 49, 55, 56, 90, 133, 140

[GrÁciun 1998] EM GrÁciun and Eugen Soós. *Interaction of two unequal cracks in a prestressed fiber reinforced composite.* International journal of fracture, vol. 94, no. 2, pages 137–159, 1998. 132

[Grine 2019] Fahmi Grine, Mohamed Trifa, Makrem Arfaoui, Yamen Maalej and Yves Renard. *The anti-plane shear elasto-static fields near a crack terminating at an isotropic hyperelastic bi-material interface.* Mathematics and Mechanics of Solids, vol. 24, no. 9, pages 2914–2930, 2019. 160

[Grisvard 1992] Pierre Grisvard. *Singularities in boundary value problems, Recherches en Mathématiques Appliquées [Research in Applied Mathematics], vol. 22*, 1992. 158, 206, 214, 223

[Gurtin 1972] ME Gurtin. *The Linear Theory of Elasticity in Handbuch der Physik, Vol. VIa/2; C. Truesdell.* Springer-Verlag, vol. 1, page 296, 1972. 66

[Gurtin 1982] Morton E Gurtin. An introduction to continuum mechanics. Academic press, 1982. 3, 53

[Guz 2002] Aleksandr Nikolaevich Guz. *Elastic waves in bodies with initial (residual) stresses.* International Applied Mechanics, vol. 38, no. 1, pages 23–59, 2002. 36

[Guz 2013] Aleksandr Nikolaevich Guz. Fundamentals of the three-dimensional theory of stability of deformable bodies. Springer Science & Business Media, 2013. 132

[Hadamard 1903] Jacques Hadamard. Leçons sur la propagation des ondes et les équations de l'hydrodynamique. A. Hermann, 1903. 3

[Hauk 1997] Viktor Hauk. Structural and residual stress analysis by nondestructive methods: Evaluation-application-assessment. Elsevier, 1997. 44

[Haupt 1992] Peter Haupt, Yih-Hsing Pao and Kolumban Hutter. *Theory of incremental motion in a body with initial elasto-plastic deformation.* Journal of elasticity, vol. 28, no. 3, pages 193–221, 1992. 2

[He 1994] Ming Yuan He, Anthony G Evans and John W Hutchinson. *Crack deflection at an interface between dissimilar elastic materials: role of residual stresses.* International Journal of Solids and Structures, vol. 31, no. 24, pages 3443–3455, 1994. 130

[Herrmann 1989] JM Herrmann. *An asymptotic analysis of finite deformations near the tip of an interface-crack.* Journal of Elasticity, vol. 21, no. 3, pages 227–269, 1989. 207

[Herrmann 1992] JM Herrmann. *An asymptotic analysis of finite deformations near the tip of an interface-crack: Part II.* Journal of Elasticity, vol. 29, no. 3, pages 203–241, 1992. 207

[Hill 1973] James M Hill. *Partial solutions of finite elasticity-three dimensional deformations.* Zeitschrift für angewandte Mathematik und Physik ZAMP, vol. 24, no. 4, pages 609–618, 1973. 132

[Hill 1986] James M Hill and RT Shield. *On pseudo-plane deformations for the neo-Hookean material.* Zeitschrift für angewandte Mathematik und Physik ZAMP, vol. 37, no. 1, pages 104–113, 1986. 132

[Hill 1989] James M Hill and Alexander I Lee. *Partial three dimensional deformations for the perfectly elastic Mooney material.* Zeitschrift für angewandte Mathematik und Physik ZAMP, vol. 40, no. 1, pages 128–132, 1989. 132

[Hill 2001] James M Hill. *A review of partial solutions of finite elasticity and their applications.* International journal of non-linear mechanics, vol. 36, no. 3, pages 447–463, 2001. 132

[Hoger 1985] Anne Hoger. *On the residual stress possible in an elastic body with material symmetry.* Archive for Rational Mechanics and Analysis, vol. 88, no. 3, pages 271–289, 1985. 3, 37, 50, 53, 135

[Hoger 1986] Anne Hoger. *On the determination of residual stress in an elastic body.* Journal of Elasticity, vol. 16, no. 3, pages 303–324, 1986. 1, 3, 4, 37, 41, 54, 90, 91, 105, 130, 133, 135, 139

[Hoger 1993a] Anne Hoger. *The constitutive equation for finite deformations of a transversely isotropic hyperelastic material with residual stress.* Journal of elasticity, vol. 33, no. 2, pages 107–118, 1993. 3, 38

[Hoger 1993b] Anne Hoger. *Residual stress in an elastic body: a theory for small strains and arbitrary rotations.* Journal of Elasticity, vol. 31, no. 1, pages 1–24, 1993. 3, 37

[Hoger 1994] Anne Hoger. *Positive definiteness of the elasticity tensor of a residually stressed material.* Journal of elasticity, vol. 36, no. 3, pages 201–226, 1994. 3

[Hoger 1997] Anne Hoger. *Virtual configurations and constitutive equations for residually stressed bodies with material symmetry.* Journal of Elasticity, vol. 48, no. 2, pages 125–144, 1997. 2, 38

[Holzapfel 2000] Gerhard A Holzapfel, Thomas C Gasser and Ray W Ogden. *A new constitutive framework for arterial wall mechanics and a comparative study of material models.* Journal of elasticity and the physical science of solids, vol. 61, no. 1-3, pages 1–48, 2000. 27, 135

[Holzapfel 2014] Gerhard A Holzapfel and Ray W Ogden. Biomechanics of soft tissue in cardiovascular systems, volume 441. Springer, 2014. 36

[Holzhausen 1979] Gary R Holzhausen and Arvid M Johnson. *The concept of residual stress in rock.* Tectonophysics, vol. 58, no. 3-4, pages 237–267, 1979. 36

[HORGAN 1994] CO HORGAN and KL MILLER. *Antiplane shear deformations for homogeneous and inhomogeneous anisotropic linearly elastic solids.* Journal of applied mechanics, vol. 61, no. 1, pages 23–29, 1994. 66

[Horgan 1995a] CO Horgan. *Anti-plane shear deformations in linear and nonlinear solid mechanics.* SIAM review, vol. 37, no. 1, pages 53–81, 1995. 207

[Horgan 1995b] Cornelius O Horgan. *Anti-plane shear deformations in linear and nonlinear solid mechanics.* SIAM review, vol. 37, no. 1, pages 53–81, 1995. 67, 70

[Horgan 1996] CO Horgan and SC Baxter. *Effects of curvilinear anisotropy on radially symmetric stresses in anisotropic linearly elastic solids.* Journal of elasticity, vol. 42, no. 1, pages 31–48, 1996. 66

[Horgan 2003a] Cornelius O Horgan and Giuseppe Saccomandi. *Helical shear for hardening generalized neo-Hookean elastic materials.* Mathematics and Mechanics of Solids, vol. 8, no. 5, pages 539–559, 2003. 68, 146

[Horgan 2003b] Cornelius O Horgan and Giuseppe Saccomandi. *Superposition of generalized plane strain on anti-plane shear deformations in isotropic incompressible hyperelastic materials.* Journal of elasticity, vol. 73, no. 1, pages 221–235, 2003. 132

[Hu 2013] Xiaofei Hu and Weian Yao. *Stress singularity analysis of multi-material wedges under antiplane deformation.* Acta Mechanica Solida Sinica, vol. 26, no. 2, pages 151–160, 2013. 206

[Hughes 1983] Thomas JR Hughes and JE Marsden. Mathematical foundations of elasticity. Citeseer, 1983. 96

[Humphrey 1987] JD Humphrey and FC Yin. *A new constitutive formulation for characterizing the mechanical behavior of soft tissues.* Biophysical journal, vol. 52, no. 4, pages 563–570, 1987. 27

[Humphrey 2012] Jay D Humphrey and Gerhard A Holzapfel. *Mechanics, mechanobiology, and modeling of human abdominal aorta and aneurysms.* Journal of biomechanics, vol. 45, no. 5, pages 805–814, 2012. 1, 130

[Huntley 1996] Hugh E Huntley, Alan S Wineman and KR Rajagopal. *Chemorheological relaxation, residual stress, and permanent set arising in radial deformation of elas-*

tomeric hollow spheres. Mathematics and Mechanics of Solids, vol. 1, no. 3, pages 267–299, 1996. 1

[Hutchinson 1968] JW Hutchinson. *Plastic stress and strain fields at a crack tip.* Journal of the Mechanics and Physics of Solids, vol. 16, no. 5, pages 337–342, 1968. 206

[Huynh 2019] Hai D Huynh, Phuong Tran, Xiaoying Zhuang and Hung Nguyen-Xuan. *An extended polygonal finite element method for large deformation fracture analysis.* Engineering Fracture Mechanics, vol. 209, pages 344–368, 2019. 134

[Isakov 2007] Victor Isakov, Jenn-Nan Wang and Masahiro Yamamoto. *Uniqueness and stability of determining the residual stress by one measurement.* Communications in Partial Differential Equations, vol. 32, no. 5, pages 833–848, 2007. 4, 90

[Isakov 2008] Victor Isakov, Jenn-Nan Wang and Masahiro Yamamoto. *An inverse problem for a dynamical Lamé system with residual stress.* SIAM journal on mathematical analysis, vol. 39, no. 4, pages 1328–1343, 2008. 4, 90

[Ivanov 2005] Sergei A Ivanov, Chi-Sing Man and Gen Nakamura. *Recovery of residual stress in a vertically heterogeneous elastic medium.* IMA journal of applied mathematics, vol. 70, no. 1, pages 129–146, 2005. 4, 90

[Jansari 2019] Chintan Jansari, Sundararajan Natarajan, Lars Beex and Krishna Kannan. *Adaptive smoothed stable extended finite element method for weak discontinuities for finite elasticity.* European Journal of Mechanics-A/Solids, vol. 78, page 103824, 2019. 134

[Johnson 1993] Byron E Johnson and Anne Hoger. *The dependence of the elasticity tensor on residual stress.* Journal of Elasticity, vol. 33, no. 2, pages 145–165, 1993. 3, 37, 139

[Johnson 1995] Byron E Johnson and Anne Hoger. *The use of a virtual configuration in formulating constitutive equations for residually stressed elastic materials.* Journal of Elasticity, vol. 41, no. 3, pages 177–215, 1995. 2, 3, 38, 44, 46, 139

[Johnson 1998] BE Johnson and A Hoger. *The use of strain energy to quantify the effect of residual stress on mechanical behavior.* Mathematics and Mechanics of Solids, vol. 3, no. 4, pages 447–470, 1998. 2, 139

[Jun 2010] Tea-Sung Jun and Alexander M Korsunsky. *Evaluation of residual stresses and strains using the eigenstrain reconstruction method.* International Journal of Solids and Structures, vol. 47, no. 13, pages 1678–1686, 2010. 90

[K. 2016] Mansouri K. *On some mechanical and numerical singular problems in incompressible isotropic hyperelastic cracked solids.* PhD thesis, National Engineering School of Tunis, 2016. 135, 156, 200

[Karoui 2014] A Karoui, K Mansouri, Y Renard and M Arfaoui. *The extended finite element method for cracked hyperelastic materials: a convergence study.* International Journal for Numerical Methods in Engineering, vol. 100, no. 3, pages 222–242, 2014. 134

[Knauss 1970] WG Knauss. *An observation of crack propagation in anti-plane shear.* International Journal of Fracture, vol. 6, no. 2, pages 183–187, 1970. 208

[Knowles 1973] James K Knowles and Eli Sternberg. *An asymptotic finite-deformation analysis of the elastostatic field near the tip of a crack.* Journal of Elasticity, vol. 3, no. 2, pages 67–107, 1973. 132, 207

[Knowles 1974] James K Knowles and Eli Sternberg. *Finite-deformation analysis of the elastostatic field near the tip of a crack: Reconsideration and higher-order results.* Journal of Elasticity, vol. 4, no. 3, pages 201–233, 1974. 132, 207

[Knowles 1976] James K Knowles. *On finite anti-plane shear for imcompressible elastic materials.* The Journal of the Australian Mathematical Society. Series B. Applied Mathematics, vol. 19, no. 04, pages 400–415, 1976. 207, 212

[Knowles 1977a] James K Knowles. *The finite anti-plane shear field near the tip of a crack for a class of incompressible elastic solids.* International Journal of Fracture, vol. 13, no. 5, pages 611–639, 1977. 132, 207

[Knowles 1977b] James K Knowles. *A note on anti-plane shear for compressible materials in finite elastostatics.* Journal of the Australian Mathematical Society. Series B. Applied Mathematics, vol. 20, no. 01, pages 1–7, 1977. 207

[Knowles 1983] JK Knowles and Eli Sternberg. *Large deformations near a tip of an interface-crack between two Neo-Hookean sheets.* Journal of Elasticity, vol. 13, no. 3, pages 257–293, 1983. 132, 207

[Kondrat'ev 1967] Vladimir Aleksandrovich Kondrat'ev. *Boundary value problems for elliptic equations in domains with conical or angular points.* Trudy Moskovskogo Matematicheskogo Obshchestva, vol. 16, pages 209–292, 1967. 213

[Korsunsky 2007] Alexander M Korsunsky and Gabriel M Regino. *Residual Elastic Strains in Autofrettaged Tubes: Variational Analysis by the Eigenstrain Finite Element Method.* Journal of Applied Mechanics, vol. 74, no. 4, page 717, 2007. 90

[Krishnan 2009] VR Krishnan and C Y Hui. *Finite strain stress fields near the tip of an interface crack between a soft incompressible elastic material and a rigid substrate.* The European Physical Journal E: Soft Matter and Biological Physics, vol. 29, no. 1, pages 61–72, 2009. 208

[Kurashige 1969] Mo Kurashige. *Circular Crack Problem for Initialy Stressed Neo-Hookean Solid.* ZAMM-Journal of Applied Mathematics and Mechanics/Zeitschrift für Angewandte Mathematik und Mechanik, vol. 49, no. 11, pages 671–678, 1969. 133

[Kurashige 1971] M Kurashige. *Two-dimensional Crack Problem for Initially Stressed Neo-Hookean Solid.* ZAMM-Journal of Applied Mathematics and Mechanics/Zeitschrift für Angewandte Mathematik und Mechanik, vol. 51, no. 2, pages 145–147, 1971. 133

[Laborde 2005] Patrick Laborde, Julien Pommier, Yves Renard and Michel Salaün. *High-order extended finite element method for cracked domains.* International Journal for Numerical Methods in Engineering, vol. 64, no. 3, pages 354–381, 2005. 134

[Ladyzhenskaya 1969] Olga Aleksandrovna Ladyzhenskaya. The mathematical theory of viscous incompressible flow, volume 2. Gordon and Breach New York, 1969. 188

[Le Tallec 1982] Patrick Le Tallec. *Existence and approximation results for nonlinear mixed problems: application to incompressible finite elasticity.* Numerische Mathematik, vol. 38, no. 3, pages 365–382, 1982. 188

[Lee 1969] EH Lee. *Elastic-Plastic Deformation at Finite Strains.* Journal of Applied Mechanics, vol. 36, no. 1, page 1, 1969. 2, 133, 139

[Legrain 2005] Grégory Legrain, Nicolas Moes and Erwan Verron. *Stress analysis around crack tips in finite strain problems using the extended finite element method.* International Journal for Numerical Methods in Engineering, vol. 63, no. 2, pages 290–314, 2005. 134, 189

[Legrain 2008] Grégory Legrain, Nicolas Moës and Antonio Huerta. *Stability of incompressible formulations enriched with X-FEM.* Computer Methods in Applied Mechanics and Engineering, vol. 197, no. 21-24, pages 1835–1849, 2008. 134, 135

[Lekhnitskii 1950] SG Lekhnitskii. *Theory of Elasticity of an Anisotropic Elastic Body. Gostekhizdat, Moscow (in Russian). Theory of Elasticity of an Anisotropic Elastic Body*, 1950. 66

[Lekhnitskii 1963] SG Lekhnitskii, SW Tsai and T Cheron. *Anisotropic plates Gordon and Breach Science Publishers New York.* NY, USA, 1963. 66

[Lengyel 2014] TH Lengyel, Rong Long and P Schiavone. *Effect of interfacial slippage on the near-tip fields of an interface crack between a soft elastomer and a rigid substrate.* In Proc. R. Soc. A, volume 470, page 20140497. The Royal Society, 2014. 208

[Li 1996] J Li and XB Zhang. *Elastic-plastic analysis of an arbitrarily-oriented mode III crack touching an interface.* International Journal of Fracture, vol. 80, no. 4, pages 311–337, 1996. 207

[Li 2000] Zi Cai Li and Tzon Tzer Lu. *Singularities and treatments of elliptic boundary value problems.* Mathematical and Computer Modelling, vol. 31, no. 8-9, pages 97–145, 2000. 214

[Lin 1976] KY Lin and JW Mar. *Finite element analysis of stress intensity factors for cracks at a bi-material interface.* International Journal of Fracture, vol. 12, no. 4, pages 521–531, 1976. 206

[Lin 1997] YY Lin and JC Sung. *Singularities of an inclined crack terminating at an anisotropic bimaterial interface.* International Journal of Solids and Structures, vol. 34, no. 28, pages 3727–3754, 1997. 206

[Lin 2003] Ching-Lung Lin and Jenn-Nan Wang. *Uniqueness in inverse problems for an elasticity system with residual stress by a single measurement.* Inverse Problems, vol. 19, no. 4, page 807, 2003. 90

[Liu 2008] J Liu, ZL Zhang and B Nyhus. *Residual stress induced crack tip constraint.* Engineering Fracture Mechanics, vol. 75, no. 14, pages 4151–4166, 2008. 132

[Liu 2020a] Congshan Liu, Yangkun Du, Chaofeng Lü and Weiqiu Chen. *Growth and patterns of residually stressed core–shell soft sphere.* International Journal of Non-Linear Mechanics, vol. 127, page 103594, 2020. 5, 133

[Liu 2020b] Yin Liu and Brian Moran. *Large deformation near a crack tip in a fiber-reinforced neo-Hookean sheet.* Journal of the Mechanics and Physics of Solids, vol. 143, page 104049, 2020. 5, 133

[Liu 2021a] Yin Liu and Brian Moran. *Crack tip fields in a neo-Hookean sheet reinforced by nonlinear fibers.* Journal of the Mechanics and Physics of Solids, vol. 152, page 104406, 2021. 133

[Liu 2021b] Yin Liu and Brian Moran. *Effects of multiple families of nonlinear fibers on finite deformation near a crack tip in a neo-Hookean sheet.* European Journal of Mechanics-A/Solids, page 104324, 2021. 133

[Long 2015] Rong Long and Chung Yuen Hui. *Crack tip fields in soft elastic solids subjected to large quasi-static deformationâĂŤA review.* Extreme Mechanics Letters, vol. 4, pages 131–155, 2015. 132, 208

[Love 2013] Augustus Edward Hough Love. A treatise on the mathematical theory of elasticity. Cambridge university press, 2013. 3

[Man 1987] Chi-Sing Man and WY Lu. *Towards an acoustoelastic theory for measurement of residual stress.* Journal of Elasticity, vol. 17, no. 2, pages 159–182, 1987. 4, 90, 133, 139

[Man 1994] Chi-Sing Man and Donald E Carlson. *On the traction problem of dead loading in linear elasticity with initial stress.* Archive for rational mechanics and analysis, vol. 128, no. 3, pages 223–247, 1994. 4, 90

[Man 1998] Chi-Sing Man. *Hartig's law and linear elasticity with initial stress.* Inverse Problems, vol. 14, no. 2, page 313, 1998. 54, 57

[Mansouri 2016] Khalil Mansouri, Makrem Arfaoui, Mohamed Trifa, Hedi Hassis and Yves Renard. *Singular elastostatic fields near the notch vertex of a Mooney–Rivlin hyper-elastic body.* International Journal of Solids and Structures, vol. 80, pages 532–544, 2016. 156, 160

[Marlow 1992] Randall Scot Marlow. *On the stress in an internally constrained elastic material.* Journal of Elasticity, vol. 27, no. 2, pages 97–131, 1992. 37

[Marsden 1994] Jerrold E Marsden and Thomas JR Hughes. Mathematical foundations of elasticity. Courier Corporation, 1994. 69

[Martin Borret 1998] Guy Martin Borret. *Sur la propagation de fissure dans les caoutchoucs synthetiques.* PhD thesis, Palaiseau, Ecole polytechnique, 1998. 131

[Matlab R2012a User Guide 2012] Matlab R2012a User Guide. *The Mathworks Inc*, 2012. 223

[Meguid 1985] SA Meguid, Mingan Tan and ZH Zhu. *Analysis of cracks perpendicular to bimaterial interfaces using a novel finite element.* International Journal of Fracture, vol. 73, no. 1, pages 1–23, 1985. 206

[Melnikov 2021] Andrey Melnikov, Ray W Ogden, Luis Dorfmann and José Merodio. *Bifurcation analysis of elastic residually-stressed circular cylindrical tubes.* International Journal of Solids and Structures, vol. 226, page 111062, 2021. 5, 133

[Merodio 2013a] José Merodio, Ray W Ogden and Javier Rodríguez. *The influence of residual stress on finite deformation elastic response.* International Journal of Non-Linear Mechanics, vol. 56, pages 43–49, 2013. 5

[Merodio 2013b] José Merodio, Ray W Ogden and Javier Rodríguez. *The influence of residual stress on finite deformation elastic response.* International Journal of Non-Linear Mechanics, vol. 56, pages 43–49, 2013. 133, 139, 142

[Merodio 2016] José Merodio and Ray W Ogden. *Extension, inflation and torsion of a residually stressed circular cylindrical tube.* Continuum Mechanics and Thermodynamics, vol. 28, no. 1-2, pages 157–174, 2016. 5, 133, 142

[Moës 1999] Nicolas Moës, John Dolbow and Ted Belytschko. *A finite element method for crack growth without remeshing.* International journal for numerical methods in engineering, vol. 46, no. 1, pages 131–150, 1999. 131, 134, 189

[Moës 2002] Nicolas Moës and Ted Belytschko. *X-FEM, de nouvelles frontières pour les éléments finis.* Revue européenne des Eléments, vol. 11, no. 2-4, pages 305–318, 2002. 189

[Monard 2011] Francois Monard and Guillaume Bal. *Inverse diffusion problems with redundant internal information.* arXiv preprint arXiv:1106.4277, 2011. 111

[Monard 2013] François Monard and Guillaume Bal. *Inverse anisotropic conductivity from power densities in dimension nâĽě 3.* Communications in Partial Differential Equations, vol. 38, no. 7, pages 1183–1207, 2013. 98

[Morgan 1966] AJA Morgan. *Some properties of media defined by constitutive equations in implicit form.* International Journal of Engineering Science, vol. 4, no. 2, pages 155–178, 1966. 38

[Mukherjee 2021] S Mukherjee and AK Mandal. *A generalized strain energy function using fractional powers: Application to isotropy, transverse isotropy, orthotropy, and residual stress symmetry.* International Journal of Non-Linear Mechanics, vol. 128, page 103617, 2021. 5, 133

[Nagashima 2009] Toshio Nagashima and Naoki Miura. *Crack analysis in residual stress field by X-FEM.* Journal of Computational Science and Technology, vol. 3, no. 1, pages 136–147, 2009. 131

[Nazarenko 2000] VM Nazarenko, VL Bogdanov and H Altenbach. *Influence of initial stress on fracture of a halfspace containing a penny-shaped crack under radial shear.* International journal of fracture, vol. 104, no. 3, pages 273–287, 2000. 132

[Nelson 1982] DV Nelson. *Effects of residual stress on fatigue crack propagation.* In Residual stress effects in fatigue. ASTM International, 1982. 36

[Nicaise 2011] Serge Nicaise, Yves Renard and Elie Chahine. *Optimal convergence analysis for the extended finite element method.* International Journal for Numerical Methods in Engineering, vol. 86, no. 4-5, pages 528–548, 2011. 195, 199

[Ogden 1997] Raymond W Ogden. Non-linear elastic deformations. Courier Corporation, 1997. 4, 132, 207

[Ohayon 2007] Jacques Ohayon, Olivier Dubreuil, Philippe Tracqui, Simon Le Floc'h, Gilles Rioufol, Lara Chalabreysse, Françoise Thivolet, Roderic I Pettigrew and Gérard Finet. *Influence of residual stress/strain on the biomechanical stability of vulnerable coronary plaques: potential impact for evaluating the risk of plaque rupture.* American Journal of Physiology-Heart and Circulatory Physiology, vol. 293, no. 3, pages H1987–H1996, 2007. 130

[Osher 1988] Stanley Osher and James A Sethian. *Fronts propagating with curvature-dependent speed: Algorithms based on Hamilton-Jacobi formulations.* Journal of computational physics, vol. 79, no. 1, pages 12–49, 1988. 192

[Paggi 2008] Marco Paggi and Alberto Carpinteri. *On the stress singularities at multimaterial interfaces and related analogies with fluid dynamics and diffusion.* Applied Mechanics Reviews, vol. 61, no. 2, page 020801, 2008. 206

[Parker 1982] AP Parker. *Stress intensity factors, crack profiles, and fatigue crack growth rates in residual stress fields.* In Residual stress effects in fatigue. ASTM International, 1982. 132

[Pinsan 1991] Cheng Pinsan and Duan Zhuping. *Singular behaviour and asymptotic stress field of a crack terminating at a bimaterial interface.* Acta Mechanica Sinica, vol. 7, no. 4, pages 342–343, 1991. 206

[Poynting 1909] John Henry Poynting. *On pressure perpendicular to the shear planes in finite pure shears, and on the lengthening of loaded wires when twisted.* Proceedings of the Royal Society of London. Series A, Containing Papers of a Mathematical and Physical Character, vol. 82, no. 557, pages 546–559, 1909. 68

[Pucci 2013a] E Pucci and G Saccomandi. *Secondary motions associated with anti-plane shear in nonlinear isotropic elasticity.* The Quarterly Journal of Mechanics and Applied Mathematics, vol. 66, no. 2, pages 221–239, 2013. 80

[Pucci 2013b] Edvige Pucci and Giuseppe Saccomandi. *The anti-plane shear problem in nonlinear elasticity revisited.* Journal of Elasticity, vol. 113, no. 2, pages 167–177, 2013. 67

[Pucci 2015a] Edvige Pucci, KR Rajagopal and Giuseppe Saccomandi. *On the determination of semi-inverse solutions of nonlinear Cauchy elasticity: The not so simple case of anti-plane shear*. International Journal of Engineering Science, vol. 88, pages 3–14, 2015. 67

[Pucci 2015b] Edvige Pucci, KR Rajagopal and Giuseppe Saccomandi. *On the determination of semi-inverse solutions of nonlinear Cauchy elasticity: The not so simple case of anti-plane shear*. International Journal of Engineering Science, vol. 88, pages 3–14, 2015. 206

[Rachele 2003] Lizabeth V. Rachele. *Uniqueness in Inverse Problems for Elastic Media with Residual Stress.* Communications in Partial Differential Equations, vol. 28, no. 11-12, pages 1787–1806, 2003. 4, 90

[Radayev 2001] YN Radayev and LV Stepanova. *On the effect of the residual stresses on the crack opening displacement in a cracked sheet.* International journal of fracture, vol. 107, no. 4, pages 329–360, 2001. 130, 132

[Radi 2002] Enrico Radi, Davide Bigoni and Domenico Capuani. *Effects of pre-stress on crack-tip fields in elastic, incompressible solids.* International journal of solids and structures, vol. 39, no. 15, pages 3971–3996, 2002. 133

[Rajagopal 1985] Kumbakonam R Rajagopal and Alan S Wineman. *New exact solutions in non-linear elasticity.* International journal of engineering science, vol. 23, no. 2, pages 217–234, 1985. 132

[Rajagopal 1992] Kumbakonam R Rajagopal and Alan S Wineman. *A constitutive equation for nonlinear solids which undergo deformation induced microstructural changes.* International Journal of Plasticity, vol. 8, no. 4, pages 385–395, 1992. 1

[Rajagopal 1998] KR Rajagopal and AR Srinivasa. *Mechanics of the inelastic behavior of materialsâĂŤPart 1, theoretical underpinnings.* International Journal of Plasticity, vol. 14, no. 10-11, pages 945–967, 1998. 2

[Rajagopal 2003] Kumbakonam R Rajagopal. *On implicit constitutive theories.* Applications of Mathematics, vol. 48, no. 4, pages 279–319, 2003. 38

[Rashetnia 2015] R Rashetnia and S Mohammadi. *Finite strain fracture analysis using the extended finite element method with new set of enrichment functions.* International Journal for Numerical Methods in Engineering, vol. 102, no. 6, pages 1316–1351, 2015. 134

[Ravichandran 1989] G Ravichandran and WG Knauss. *A finite elastostatic analysis of bimaterial interface cracks.* International Journal of Fracture, vol. 39, no. 1-3, pages 235–253, 1989. 208

[Riccobelli 2018] Davide Riccobelli and Pasquale Ciarletta. *Shape transitions in a soft incompressible sphere with residual stresses.* Mathematics and Mechanics of Solids, vol. 23, no. 12, pages 1507–1524, 2018. 5, 133

[Riccobelli 2019] Davide Riccobelli, Abramo Agosti and Pasquale Ciarletta. *On the existence of elastic minimizers for initially stressed materials.* Philosophical Transactions of the Royal Society A, vol. 377, no. 2144, page 20180074, 2019. 4

[Rice 1966] James R Rice. *Contained plastic deformation near cracks and notches under longitudinal shear.* International Journal of Fracture, vol. 2, no. 2, pages 426–447, 1966. 206

[Rice 1967] JR Rice. *Stresses Due to a Sharp Notch in a Work-Hardening Elastic-Plastic Material Loaded by Longitudinal Shear.* Journal of Applied Mechanics, vol. 34, page 287, 1967. 206

[Rice 1968] JRa Rice and Gl F Rosengren. *Plane strain deformation near a crack tip in a power-law hardening material.* Journal of the Mechanics and Physics of Solids, vol. 16, no. 1, pages 1–12, 1968. 207

[Roberts 2003] Peter M Roberts, Igor B Esipov and Ernest L Majer. *Elastic wave stimulation of oil reservoirs: Promising EOR technology?* The Leading Edge, vol. 22, no. 5, pages 448–453, 2003. 36

[Robertson 1997] Robert L Robertson. *Boundary identifiability of residual stress via the Dirichlet to Neumann map.* Inverse Problems, vol. 13, no. 4, page 1107, 1997. 55, 90

[Robertson 1998] Robert L Robertson. *Determining residual stress from boundary measurements: a linearized approach.* Journal of Elasticity, vol. 52, no. 1, page 63, 1998. 58, 90, 105, 106

[Rodriguez 1994] Edward K Rodriguez, Anne Hoger and Andrew D McCulloch. *Stress-dependent finite growth in soft elastic tissues.* Journal of biomechanics, vol. 27, no. 4, pages 455–467, 1994. 2, 133, 139

[Romeo 1994] Alberto Romeo and Roberto Ballarini. *The influence of elastic mismatch on the size of the plastic zone of a crack terminating at a brittle-ductile interface.* International Journal of Fracture, vol. 65, no. 2, pages 183–196, 1994. 207

[Ru 1997a] Chong Qing Ru. *Finite strain singular field near the tip of a crack terminating at a material interface.* Mathematics and Mechanics of Solids, vol. 2, no. 1, pages 49–73, 1997. 208

[Ru 1997b] CQ Ru. *Finite deformations at the vertex of a bi-material wedge.* International Journal of Fracture, vol. 84, no. 4, pages 325–358, 1997. 208, 219

[Ru 2002] CQ Ru. *On complex-variable formulation for finite plane elastostatics of harmonic materials.* Acta Mechanica, vol. 156, no. 3, pages 219–234, 2002. 208

[Saccomandi 2004] Giuseppe Saccomandi. *Phenomenology of rubber-like materials.* Mechanics and thermomechanics of rubberlike solids, pages 91–134, 2004. 4, 141

[Saccomandi 2005] Giuseppe Saccomandi. *Some generalized pseudo-plane deformations for the neo-Hookean material.* IMA journal of applied mathematics, vol. 70, no. 4, pages 550–563, 2005. 132

[Sadowski 2016] T Sadowski, EM Craciun, A Răbâea and L Marsavina. *Mathematical modeling of three equal collinear cracks in an orthotropic solid.* Meccanica, vol. 51, no. 2, pages 329–339, 2016. 132

[Saravanan 2008] U Saravanan. *Representation for stress from a stressed reference configuration.* International journal of engineering science, vol. 46, no. 11, pages 1063–1076, 2008. 2

[Savage 1986] William Z Savage and Henri S Swolfs. *Tectonic and gravitational stress in long symmetric ridges and valleys.* Journal of Geophysical Research: Solid Earth, vol. 91, no. B3, pages 3677–3685, 1986. 36

[Sburlati 1992] Roberta Sburlati. *On universal solutions in initially stressed bodies.* Journal of elasticity, vol. 27, no. 1, pages 85–96, 1992. 4, 90

[Seweryn 1996] Andrzej Seweryn and Krzysztof Molski. *Elastic stress singularities and corresponding generalized stress intensity factors for angular corners under various boundary conditions.* Engineering Fracture Mechanics, vol. 55, no. 4, pages 529–556, 1996. 177

[Shams 2011] Moniba Shams, Michel Destrade and Ray W Ogden. *Initial stresses in elastic solids: constitutive laws and acoustoelasticity.* Wave Motion, vol. 48, no. 7, pages 552–567, 2011. 4, 41, 43, 133, 140, 142

[Shams 2014] Moniba Shams and Ray W Ogden. *On Rayleigh-type surface waves in an initially stressed incompressible elastic solid.* The IMA Journal of Applied Mathematics, vol. 79, no. 2, pages 360–376, 2014. 38, 133, 139, 142

[Shanyi 1994] Du Shanyi, Shi Zhifei and Wu Linzhi. *A transverse crack tip field in bimaterial.* Acta Mechanica Sinica, vol. 10, no. 3, pages 267–272, 1994. 208

[Sigaeva 2019] Taisiya Sigaeva, Michel Destrade and Elena S Di Martino. *Multi-sector approximation method for arteries: the residual stresses of circumferential rings with non-trivial openings.* Journal of the Royal Society Interface, vol. 16, no. 156, page 20190023, 2019. 141

[Sinclair 2004a] GB Sinclair. *Stress singularities in classical elasticityâĂŤII: Asymptotic identification.* Applied Mechanics Reviews, vol. 57, no. 5, pages 385–439, 2004. 206

[Sinclair 2004b] Glenn B Sinclair. *Stress singularities in classical elasticity–I: Removal, interpretation, and analysis.* Applied Mechanics Reviews, vol. 57, no. 4, pages 251–298, 2004. 206

[Skalak 1996] Richard Skalak, Stephen Zargaryan, Rakesh K Jain, Paolo A Netti and Anne Hoger. *Compatibility and the genesis of residual stress by volumetric growth.* Journal of mathematical biology, vol. 34, no. 8, pages 889–914, 1996. 133

[Spencer 1971] AJM Spencer. *Continuum physics.* In Theory of invariants, volume 1. Academic Press New York, 1971. 43

[Spencer 1984a] Anthony James Merrill Spencer. *Constitutive theory for strongly anisotropic solids.* In Continuum theory of the mechanics of fibre-reinforced composites, pages 1–32. Springer, 1984. 31

[Spencer 1984b] Anthony James Merrill Spencer. *Constitutive theory for strongly anisotropic solids.* In Continuum theory of the mechanics of fibre-reinforced composites, pages 1–32. Springer, 1984. 69

[Stazi 2003] FL Stazi, Elisa Budyn, Jack Chessa and Ted Belytschko. *An extended finite element method with higher-order elements for curved cracks.* Computational Mechanics, vol. 31, no. 1, pages 38–48, 2003. 134

[Stephenson 1982] Rodney A Stephenson. *The equilibrium field near the tip of a crack for finite plane strain of incompressible elastic materials.* Journal of Elasticity, vol. 12, no. 1, pages 65–99, 1982. 132, 155, 156, 160, 161

[Stolarska 2001a] M Stolarska, David L Chopp, Nicolas Moës and Ted Belytschko. *Modelling crack growth by level sets in the extended finite element method.* International

journal for numerical methods in Engineering, vol. 51, no. 8, pages 943–960, 2001. 189

[Stolarska 2001b] M Stolarska, David L Chopp, Nicolas Moës and Ted Belytschko. *Modelling crack growth by level sets in the extended finite element method.* International journal for numerical methods in Engineering, vol. 51, no. 8, pages 943–960, 2001. 192

[Strang 1973] Gilbert Strang and George J Fix. *An analysis of the finite element method(Book- An analysis of the finite element method.).* Englewood Cliffs, N. J., Prentice-Hall, Inc., 1973. 318 p, 1973. 131

[Stroh 1958] AN Stroh. *Dislocations and cracks in anisotropic elasticity.* Philosophical magazine, vol. 3, no. 30, pages 625–646, 1958. 66

[Stroh 1962] AN Stroh. *Steady state problems in anisotropic elasticity.* Journal of Mathematics and Physics, vol. 41, no. 1-4, pages 77–103, 1962. 66

[Sukumar 2000] Natarajan Sukumar, Nicolas Moës, Brian Moran and Ted Belytschko. *Extended finite element method for three-dimensional crack modelling.* International journal for numerical methods in engineering, vol. 48, no. 11, pages 1549–1570, 2000. 189

[Sukumar 2001] Natarajan Sukumar, David L Chopp, Nicolas Moës and Ted Belytschko. *Modeling holes and inclusions by level sets in the extended finite-element method.* Computer methods in applied mechanics and engineering, vol. 190, no. 46-47, pages 6183–6200, 2001. 190

[Sukumar 2008] Nsu Sukumar, David L Chopp, Eric Béchet and N Moës. *Three-dimensional non-planar crack growth by a coupled extended finite element and fast marching method.* International journal for numerical methods in engineering, vol. 76, no. 5, pages 727–748, 2008. 189

[Šuštarič 2014] Primož Šuštarič, Mariana RR Seabra, Jose MA Cesar de Sa and Tomaž Rodič. *Sensitivity analysis based crack propagation criterion for compressible and (near) incompressible hyperelastic materials.* Finite Elements in Analysis and Design, vol. 82, pages 1–15, 2014. 134

[Ting 1996a] TCT Ting. *Pressuring, shearing, torsion and extension of a circular tube or bar of cylindrically anisotropic material.* Proceedings of the Royal Society of London. Series A: Mathematical, Physical and Engineering Sciences, vol. 452, no. 1954, pages 2397–2421, 1996. 66

[Ting 1996b] TCT Ting and CO Horgan. *Anisotropic Elasticity: Theory and Applications.* Journal of Applied Mechanics, vol. 63, no. 4, page 1056, 1996. 66, 67

[Ting 2000] TCT Ting. *Recent developments in anisotropic elasticity.* International Journal of Solids and Structures, vol. 37, no. 1-2, pages 401–409, 2000. 66

[Tings 1999] TCT Tings. *New solutions to pressuring, shearing, torsion and extension of a cylindrically anisotropic elastic circular tube or bar.* Proceedings of the Royal Society of London. Series A: Mathematical, Physical and Engineering Sciences, vol. 455, no. 1989, pages 3527–3542, 1999. 66

[Tolstoy 1982] I Tolstoy. *On elastic waves in prestressed solids.* Journal of Geophysical Research: Solid Earth, vol. 87, no. B8, pages 6823–6827, 1982. 36

[Treuting 1951] RG Treuting and WT Read Jr. *A mechanical determination of biaxial residual stress in sheet materials.* Journal of Applied Physics, vol. 22, no. 2, pages 130–134, 1951. 36

[Truesdell 1952] Clifford Truesdell. *The mechanical foundations of elasticity and fluid dynamics.* Journal of Rational Mechanics and Analysis, vol. 1, pages 125–300, 1952. 1, 3, 5

[Truesdell 2004] Clifford Truesdell and Walter Noll. *The non-linear field theories of mechanics.* In The non-linear field theories of mechanics, pages 1–579. Springer, 2004. 3

[Truesdell 2012] Clifford Truesdell. The elements of continuum mechanics: Lectures given in august-september 1965 for the department of mechanical and aerospace engineering syracuse university syracuse, new york. Springer Science & Business Media, 2012. 3

[Tzuchiang 1998] Wang Tzuchiang and Per Ståhle. *A crack perpendicular to and terminating at a bimaterial interface.* Acta Mechanica Sinica, vol. 14, no. 1, pages 27–36, 1998. 206

[Vannucci 2018] Paolo Vannucci. *Basic Concepts on Anisotropy*. In Anisotropic Elasticity, pages 1–17. Springer, 2018. 66

[Ventura 2005] Giulio Ventura, B Moran and T Belytschko. *Dislocations by partition of unity*. International Journal for Numerical Methods in Engineering, vol. 62, no. 11, pages 1463–1487, 2005. 190

[Wang 1993] WC Wang and JT Chen. *Theoretical and experimental re-examination of a crack perpendicular to and terminating at the bimaterial interface*. The Journal of Strain Analysis for Engineering Design, vol. 28, no. 1, pages 53–61, 1993. 206

[Wang 1994] Wei Chung Wang and Jin Tzaih Chen. *Singularities of an arbitrarily inclined semi-infinite crack meeting a bimaterial interface*. Engineering Fracture Mechanics, vol. 49, no. 5, pages 671–680, 1994. 206

[Wang 1996] XD Wang and SA Meguid. *On the general treatment of an oblique crack near a bimaterial interface under antiplane loading*. International Journal of Solids and Structures, vol. 33, no. 17, pages 2485–2500, 1996. 206

[Wang 2014] HM Wang, XY Luo, H Gao, RW Ogden, BE Griffith, C Berry and TJ Wang. *A modified Holzapfel-Ogden law for a residually stressed finite strain model of the human left ventricle in diastole*. Biomechanics and modeling in mechanobiology, vol. 13, no. 1, pages 99–113, 2014. 142

[Wang 2017] Lei Wang, Steven M Roper, Nicholas A Hill and Xiaoyu Luo. *Propagation of dissection in a residually-stressed artery model*. Biomechanics and modeling in mechanobiology, vol. 16, no. 1, pages 139–149, 2017. 1, 130

[Wineman 1990] AS Wineman and KR Rajagopal. *On a constitutive theory for materials undergoing microstructural changes*. Arch. Mech, vol. 42, no. 1, pages 53–75, 1990. 1

[Withers 2001] Philip J Withers and HKDH Bhadeshia. *Residual stress. Part 2–Nature and origins*. Materials science and technology, vol. 17, no. 4, pages 366–375, 2001. 36

[Wong 1969] Felix S Wong and Richard T Shield. *Large plane deformations of thin elastic sheets of neo-Hookean material*. Zeitschrift für angewandte Mathematik und Physik (ZAMP), vol. 20, no. 2, pages 176–199, 1969. 207

[Wu 2019] G Wu, CJ Aird and MJ Pavier. *The effect of residual stress on a centre-cracked plate under uniaxial loading.* International Journal of Fracture, vol. 219, no. 1, pages 101–121, 2019. 132

[Yosibash 2011] Zohar Yosibash. Singularities in elliptic boundary value problems and elasticity and their connection with failure initiation, volume 37. Springer Science & Business Media, 2011. 213, 214

[Yu 1997] Hongrong Yu, Yong Li Wu and Guochen Li. *Plane strain asymptotic fields for cracks terminating at the interface between elastic and pressure-sensitive dilatant materials.* International Journal of Fracture, vol. 86, no. 4, pages 343–360, 1997. 207

[Zak 1963] AR Zak and ML Williams. *Crack Point Stress Singularities at a Bi-Material Interface.* Journal of Applied Mechanics, vol. 30, page 142, 1963. 206

[Zhou 2020] Sha-Xu Zhou and Xian-Fang Li. *Full incremental elastic field induced by a mode-I crack in a prestressed orthotropic material.* Engineering Fracture Mechanics, vol. 235, page 107070, 2020. 132

[Zidi 2000a] M Zidi. *Azimuthal shearing and torsion of a compressible hyperelastic and prestressed tube.* International journal of non-linear mechanics, vol. 35, no. 2, pages 201–209, 2000. 133

[Zidi 2000b] M Zidi. *Combined torsion, circular and axial shearing of a compressible hyperelastic and prestressed tube.* J. Appl. Mech., vol. 67, no. 1, pages 33–40, 2000. 133

[Zidi 2001] M Zidi. *Effects of a prestress on a reinforced, nonlinearly elastic and compressible tube subjected to combined deformations.* International journal of solids and structures, vol. 38, no. 26-27, pages 4657–4669, 2001. 133

[Zilian 2008] Andreas Zilian and Antoine Legay. *The enriched space–time finite element method (EST) for simultaneous solution of fluid–structure interaction.* International Journal for Numerical Methods in Engineering, vol. 75, no. 3, pages 305–334, 2008. 190

[ZP 1971] ZP BAZANT ZP. *A correlation study of formulations of incremental deformation and stability of continuous bodies.* Journal of Applied Mechanics, Transactions ASME, vol. 38, no. 4, pages 919–928, 1971. 4, 37, 90